Control of disseminated breast cancer cell dormancy in the bone marrow by TGFβ2 and BMP4 signaling

Emma Risson

N°d'ordre NNT :
2022LYSE1100

THESE de DOCTORAT DE L'UNIVERSITE DE LYON
opérée au sein de
l'Université Claude Bernard Lyon 1

École Doctorale N° 340
(ED Biologie Moléculaire Intégrative et Cellulaire)

Spécialité de doctorat : Cancérologie
Discipline : Biologie moléculaire et cellulaire

Soutenue publiquement le 05/07/2022, par :
Emma RISSON

Control of Disseminated Breast Cancer Cell Dormancy in the Bone Marrow by TGFβ2 and BMP4 Signaling

---

Devant le jury composé de :

VALCOURT, Ulrich	Professeur des Universités	Président
MECHTA-GRIGORIOU, Fatima	Directrice de Recherche	Rapporteure
QUESNEL, Bruno	Professeur des Universités – Praticien Hospitalier	Rapporteur
AGUIRRE-GHISO, Julio	Professeur	Examinateur
BAILLY, Sabine	Directrice de Recherche	Examinatrice
CASTETS, Marie	Chargée de Recherche	Examinatrice
JUIN, Philippe	Directeur de Recherche	Examinateur
MAGUER-SATTA, Véronique	Directrice de Recherche	Directrice de thèse

UNIVERSITE CLAUDE BERNARD - LYON 1

Président de l'Université	**M. le Professeur Frédéric FLEURY**
Président du Conseil Académique	M. le Professeur Hamda BEN HADID
Vice-président du Conseil d'Administration	M. le Professeur Didier REVEL
Vice-président du Conseil Formation et Vie Universitaire	M. le Professeur Philippe CHEVALIER
Vice-président de la Commission Recherche	M. Fabrice VALLÉE
Directrice Générale des Services	Mme Dominique MARCHAND

COMPOSANTES SANTE

Faculté de Médecine Lyon Est – Claude Bernard	Directeur : M. le Professeur G.RODE
Faculté de Médecine et de Maïeutique Lyon Sud – Charles Mérieux	Directeur : Mme la Professeure C. BURILLON
Faculté d'Odontologie	Directeur : M. le Professeur D. BOURGEOIS
Institut des Sciences Pharmaceutiques et Biologiques	Directeur : Mme la Professeure C. VINCIGUERRA
Institut des Sciences et Techniques de la Réadaptation	Directeur : M. X. PERROT
Département de formation et Centre de Recherche en Biologie Humaine	Directeur : Mme la Professeure A-M. SCHOTT

COMPOSANTES ET DEPARTEMENTS DE SCIENCES ET TECHNOLOGIE

Faculté des Sciences et Technologies	Directeur : M. F. DE MARCHI
Département Biologie	Directeur : M. le Professeur F. THEVENARD
Département Chimie Biochimie	Directeur : Mme C. FELIX
Département GEP	Directeur : M. Hassan HAMMOURI
Département Informatique	Directeur : M. le Professeur S. AKKOUCHE
Département Mathématiques	Directeur : M. le Professeur G. TOMANOV
Département Mécanique	Directeur : M. le Professeur H. BEN HADID
Département Physique	Directeur : M. le Professeur J-C PLENET
UFR Sciences et Techniques des Activités Physiques et Sportives	Directeur : M. Y.VANPOULLE
Observatoire des Sciences de l'Univers de Lyon	Directeur : M. B. GUIDERDONI
Polytech Lyon	Directeur : M. le Professeur E.PERRIN
Ecole Supérieure de Chimie Physique Electronique	Directeur : M. G. PIGNAULT
Institut Universitaire de Technologie de Lyon 1	Directeur : M. le Professeur C. VITON
Ecole Supérieure du Professorat et de l'Education	Directeur : M. le Professeur A. MOUGNIOTTE
Institut de Science Financière et d'Assurances	Directeur : M. N. LEBOISNE

ACKNOWLEDGMENTS

Les remerciements seront inclus dans la dernière version de ce manuscrit.

FOREWORD

When I started my studies at the Faculté de Médecine Lyon-Est, I also had the aim to train in basic scientific research. I succeeded in accessing the MD-PhD programs of the “ENS de Lyon - Université de Lyon” and of the “École de l’INSERM Lilianne Bettencourt”. After my master’s internship in Julio Aguirre-Ghiso’s lab, the creation of an exciting collaboration and project between Julio Aguirre-Ghiso and Véronique Maguer Satta led me to continue as a PhD student. I spent half of my PhD in each laboratory to better understand disseminated breast cancer cell dormancy regulation in the bone marrow.
I will introduce this project with three chapters: “Breast Cancer”, “Cancer Cell Dormancy” and “The TGFβ and BMP Family”. I have kept this introduction short to focus on the discussion and perspectives of this project.

The results that I obtained during this project led to the redaction of a paper that is soon to be submitted. Some preliminary experiments in continuation of the project will also be presented in a second result part.

> **Risson E**, Guyot B, Moindrot L, Jeanpierre S, , Lefort S, Nobre AR, Aguirre-Ghiso JA, Maguer-Satta V: **Heterogeneity of breast cancer cell dormancy in the bone marrow is co-regulated by TGFB2 and BMP4**.
> *In preparation*, 2022.

Intense scientific discussion on the development of our collaborative project led to the publication of a review of the recent scientific literature on cancer dormancy (Appendix 1).

> **Risson E***, Nobre AR*, Maguer-Satta V, Aguirre-Ghiso JA: **The current paradigm and challenges ahead for the dormancy of disseminated tumor cells**.
> *Nature Cancer* 2020, doi: 10.1038/s43018-020-0088-5.

During my PhD I also had the incredible opportunity to be mentored by and collaborate with Ana Rita Nobre, another PhD student in Pr. Aguirre-Ghiso's laboratory, leading to two publications.

The first project I participated in functionalized the role of TGFβ2 secretion by mesenchymal stem cells in cancer dormancy induction. I mainly contributed to this project by performing *in vivo* experiments and their analysis and taking charge of mice colony maintenance (Appendix 2).

> Nobre AR, **Risson E**, Singh DK, Di Martino JS, Cheung JF, Wang J, Johnson J, Russnes HG, Bravo-Cordero JJ, Birbrair A, Bjorn Naume, Mohamad Azhar, Paul S. Frenette and Julio A. Aguirre-Ghiso: **Bone marrow NG2$^+$/Nestin$^+$ mesenchymal stem cells drive DTC dormancy via TGF-β2**. *Nature Cancer* 2021, doi:10.1038/s43018-021-00179-8.

The second project I participated in identified a major regulator of early disseminated tumor cell dormancy programs. I contributed to this project by initiating a discussion and collaboration with Pr. Cristina Curtis (Stanford, USA) and Dr. Jose Seoane (VHIO, Spain) to validate our findings with molecular signatures from tumors of breast cancer patients (Appendix 3).

> Nobre AR , Dalla E , Yang J , Huang X , Wullkopf L , **Risson E**, Razghandi P , Lopez-Anton M , Zheng W , Seoane JA , Curtis C , Kenigsberg E , Wang J, Aguirre-Ghiso JA: **Single-cell analysis of early disseminated cancer cells identifies ZFP281 and a mesenchymal-like dormancy program as a barrier to metastasis.**
> *Under review, Nature Cell Biology 2022.*

I am also a co-author of a publication of another ongoing project in Dr. Maguer-Satta's laboratory, which defines the role of CD10 in aggressive cancer stem cells. I participated in this project by analyzing single-cell RNAseq data.

> Guyot B, Clément F, Drouet Y, **Risson E**, Schmidt X, Delay E, Treilleux I, Foy JP, Jeanpierre S, Thomas E, Kielbassa K, Tonon L, Zhu HH, Saintigny P, Gao WQ, Fouchardière A, Tirode F, Viari A, Blay JY, Maguer-Satta V: **CD10 defines stem cells features and the molecular identity of aggressive cancer cells.**
> *In preparation, 2022*

My PhD was also affected by the ongoing SARS-CoV-2 pandemic. While New York City was in lockdown in spring 2020, I joined “The Sinai Immunology Review Project” coordinated by Pr. Miriam Merad (Mount Sinai, USA) to review the increasing amount of pre-preprints published on MedXriv and BioXriv every day. This important group effort led to the redaction of an extremely needed review of our accumulated knowledge on SARS-CoV-2 in June 2020 (Appendix 5), where I was in charge of the part on neutralizing antibodies as COVID-19 treatment:

> Vabret N., …, **Risson E.**, …, Merad M., Samstein R.M., The Sinai Immunology Review Project, et al. : **Immunology of COVID-19: Current State of the Science**.
> *Immunity* 2020, doi: 10.1016/j.immuni.2020.05.002

My CV (Appendix 6) summarizes other accomplishments of my PhD (grant writing, teaching, mentoring, science communication). After this surprising, fruitful, and intense doctorate, I am now going back to medical school in September 2022 at the Faculté de Médecine Lyon-Est. These 4 years of my curriculum dedicated to basic scientific research will bring many advantages to my future clinical practice. I am deeply committed to facilitating discussions and collaborations between clinicians and scientists, as I am convinced that these interactions are what lead to therapeutic breakthroughs for patients.

TABLE OF CONTENTS

LIST OF FIGURES

MAIN ABBREVIATIONS

BCP: biphasic calcium phosphate

BM: bone marrow

BMP: bone morphogenetic protein

BMPR : bone morphogenetic protein receptor

CDK: cyclin dependent kinase

CTGF: connective tissue growth factor

DALY: disability-adjuster life years

DTC: disseminated tumor cell

EMT: epithelial to mesenchymal transition

ER: Estrogen receptor

ERK: extracellular signal-regulated kinases

GAS6: growth arrest specific 6

HER2: human epidermal growth factor 2

HNSCC: head and neck squamous cell carcinoma

HSC: hematopoietic stem cell

MSC: mesenchymal stem cell

MRD: minimal residual disease

NETs: nuclear extra-cellular traps

NR2F1: nuclear receptor subfamily 2 group F member 1

NSC: neural stem cell

PR: progesterone receptor

qNSC : quiescent neural stem cell

SEER: surveillance epidemiology and end results

TGFβ: transforming growth factor β

TGFβR: transforming growth factor β receptor

UPR: unfolded protein response

scRNAseq : single-cell RNA sequencing

INTRODUCTION

BREAST CANCER

I. Clinical characteristics

A) General Incidence & Mortality

Breast cancer has the highest incidence and mortality of all women's cancers, according to World Health Organization (WHO) 2020 reports (Sung et al., 2021). In 2020 alone, 2.3 million women were diagnosed with breast cancer and 685 000 died globally. These numbers are expected to continue increasing, especially in countries with low Human Development Index (HDI), where incidence is estimated to increase by more than 100%, and mortality by 99% by 2040 (**Figure 1**). In countries with a very high HDI, such as western Europe, the incidence is expected to increase by 18% and mortality by 30%. Breast cancer has a high economic cost and adverse effects of treatment, impact on fertility, and an important fear of relapse among patients (Sun et al., 2019) (Yang et al., 2018), leading to reduced disability-adjusted life years (DALYs) (Li et al., 2019). It is thus essential to continue studying breast cancer and its treatments. Moreover, breast cancer is a very diverse disease whose outcome largely depends on molecular subtypes and stage at diagnosis.

Figure 1: Estimated number of deaths breast cancer from 2020 to 2040.

Cancer deaths will increase globally, but mainly in countries with low and medium human development index. This graph was generated on the global cancer observatory website of the IARC (International Agency for Research on Cancer) based on Globocan data. HDI : Human development Index.

B) Breast cancer subtypes

There are different types of breast cancer, which determine the course of treatment and risk profile (Waks and Winer, 2019). Classifications will depend on histological characteristics or molecular markers.

Histological subtypes depend on the invasive or non-invasive status identified :

- Non-Invasive: can be ductal carcinoma in situ (DCIS) or lobular carcinoma in situ (LCIS).
- Invasive: ductal carcinoma, also called no special type (NST), and lobular carcinoma.

The first molecular classification of intrinsic subtypes was published in the year 2000 by Perou & Sorlie (Perou et al., 2000) and is based on the expression of the Estrogen receptor (ER), the Progesterone receptor (PR), and the Human Epidermal Growth Factor 2 (HER2) (**Figure 2**). This classification is of great importance to define the most effective types of treatments.

- Luminal A and B tumors: these tumors arise from the transformation of the luminal epithelial cells of the breast ducts. Due to the function of the normal luminal epithelial cells, they usually have high expression of the estrogen receptor (ER) and the progesterone receptor (PR). Luminal B tumors will also express the Human Epidermal Growth Factor 2 (HER2) and have a higher proliferation rate compared to luminal A tumors. Luminal A tumors have the highest survival rate (
-
- **Figure 3**).

- HER2 enriched tumors: these tumors have an overamplification or overexpression of the Human Epidermal Growth Factor 2 (HER2). In contrast to luminal tumors, they do not express the estrogen receptor or the progesterone receptor.

- Claudin-low tumors: these tumors are triple-negative (HER2-/ER-/PR-) and have a markedly reduced expression of adhesion proteins, rendering them very invasive and with a mesenchymal phenotype.
- Basal-like tumors: These tumors are even more aggressive compared to Claudin-low tumors. They are also triple-negative with very high proliferation and high expression of basal-like genes.

Recently, another classification emerged called “Integrative Clusters” (IntClust) subtypes that can be identified and subgroups of copy number or gene expression profiles can be made (Curtis et al., 2012). This will allow for the increase of personalized therapy and better personalized assessment of the risk of relapse.

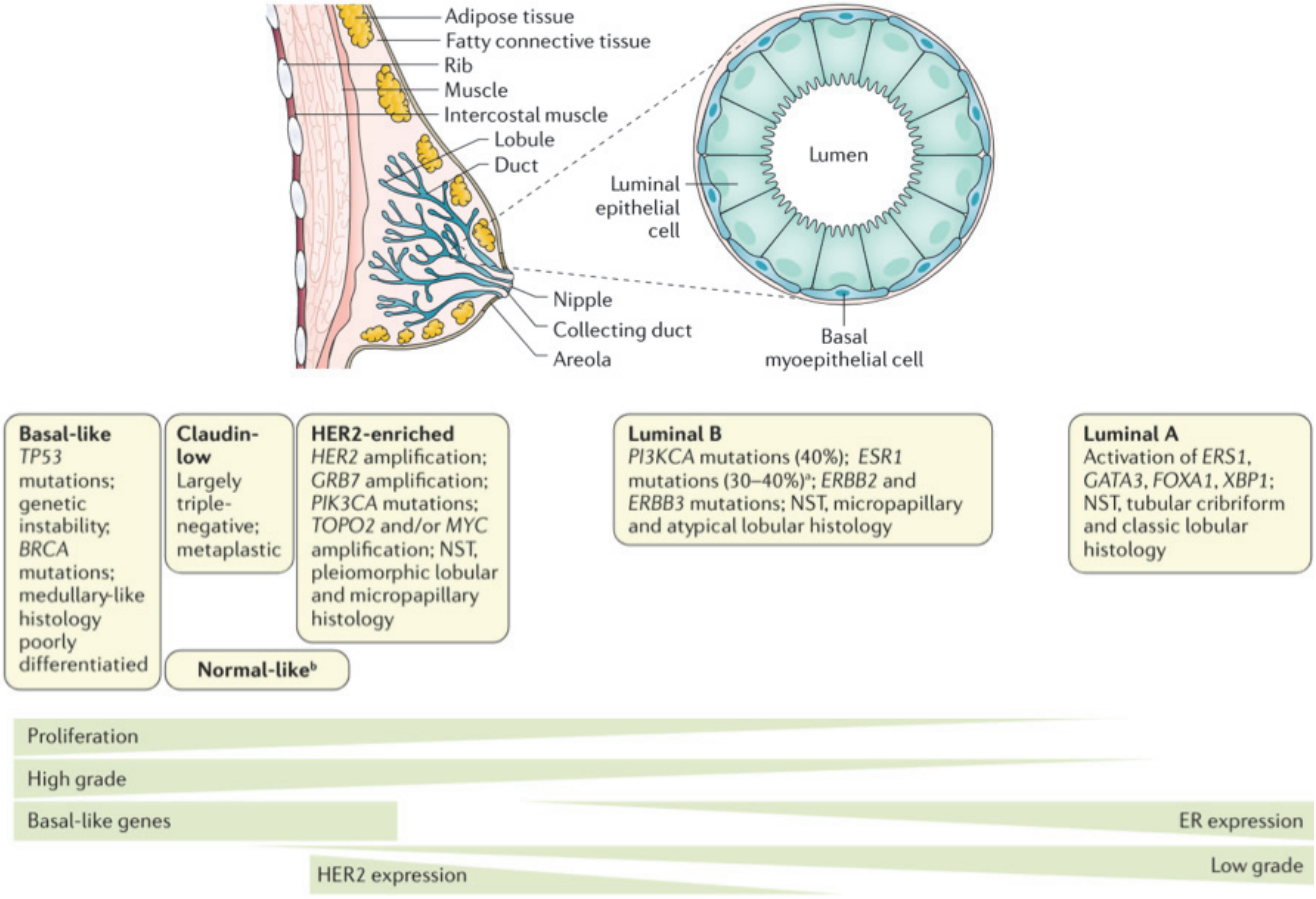

Figure 2 : Breast anatomy and breast cancer subtypes.

Breast cancer develops in the functional unit of the breast : the lobules of the ducts. Transformation of luminal epithelial cells will lead to luminal cancers types (luminal A or B), whereas if the transformation happens in the basal myoepithelial cell, the cancer will usually be hormone receptor negative and have a basal phenotype. Basal-like cancers

Survival rates depend on the cancer stage at diagnosis, but also the cancer type. Early diagnoses compared to late-stage diagnoses greatly improves the 5-year survival rate (**Figure 3**). Once cancer has spread, mortality increases dramatically. Thus, early detection of breast cancer is essential. Fortunately, only 6% of cancer are metastatic at diagnosis ([CSL STYLE ERROR: reference with no printed form.]), but long-term follow-up of patients is necessary as patients can relapse with distant metastasis several years after diagnosis. The intrinsic subtypes of the breast cancers will also determine the 5-year survival rate, with HER2+ and TNBC tumors being the most aggressive.

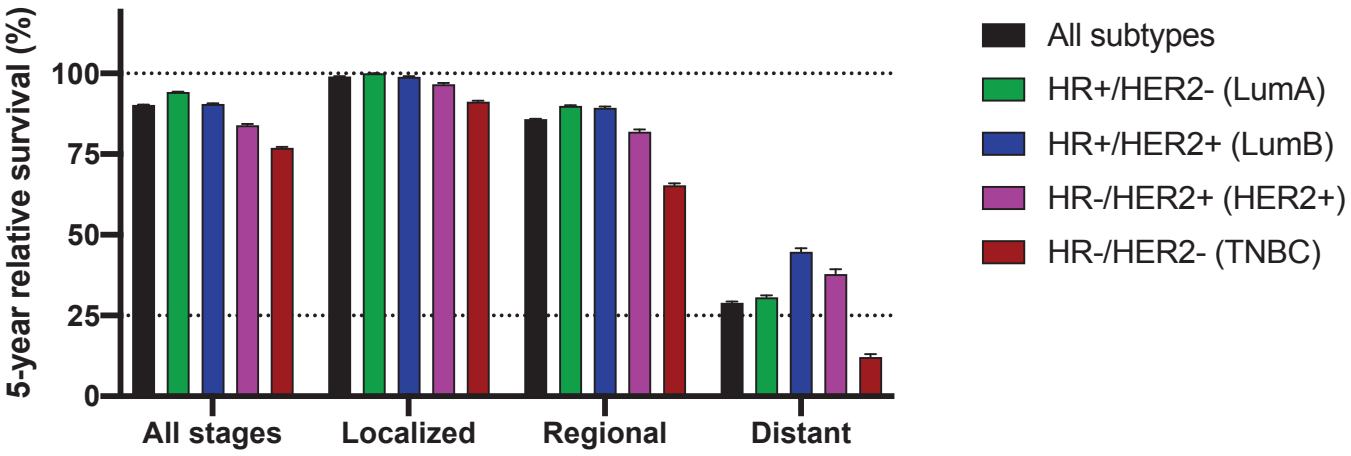

Figure 3: 5-year survival rate by stage at diagnosis and breast cancer subtype

The 5-year survival rate is plotted depending on the cancer stage at diagnosis and cancer subtype. When cancer is diagnosed at a localized stage, the 5-year survival rate is close to 100%. When cancer has invaded regionally or at distant sites, the 5-year survival rate drops. The molecular characteristics of cancer will also determine the mortality rate: patients with Luminal A (LumA) and Luminal B (LumB) will have a higher survival rate compared to patients with HER2+ or TNBC tumors. This figure was generated with data from the SEER (Surveillance, Epidemiology and End Results) database of the NCI (National Cancer Institute) with data from women in the USA from 2011 to 2018. Mean +/- SD. https://seer.cancer.gov/statfacts/html/breast-subtypes.html.

D) Treatments

Treatment recommendations are constantly evolving and improving. Individual indications will depend on tumor burden, molecular characteristics of the tumors, as well as clinical characteristics of patients. Here only the most common treatments will be discussed.

When a non-metastatic breast tumor is diagnosed in patients, most patients will undergo surgery. Systemic treatment will also usually be necessary before surgery (neoadjuvant) or after surgery (adjuvant). Since the biological origin of the different types of breast cancer varies, they will not have the same treatment methods. Patients with hormone receptors positive tumors will receive anti-estrogen therapy (Tamoxifen, Aromatase inhibitors) to block ER signaling, independently of their HER2 status. High-risk patients (high Ki67 staining, or lymph node involvement) can also receive chemotherapy. Patients with HER2+ tumors have greatly benefited from the development of HER2-targeted antibody therapy (Trastuzumab, Pertuzumab) or small molecule tyrosine kinase inhibitor therapy (lapatinib, neratinib) combined with chemotherapy, but tumors can still evade the treatment and form brain metastasis. Patients with TNBC tumors will mostly receive chemotherapy. Radiotherapy is also recommended post-surgery to target remaining cells (in lymph nodes for example), it improves substantially the disease-free and overall survival rate of patients by decreasing local regional relapse rates. Systemic adjuvant therapy will decrease distant relapse rates.

Breast cancer is a major public health problem as it has the highest incidence and mortality in women. Mortality and incidence are expected to increase, especially in low Human-Development Index countries. It is a very diverse disease where the outcome largely depends on molecular subtypes (luminal A, luminal B, HER2-enriched, basal-like, and claudin-low) and stage at diagnosis (localized, regional, distant spreading). The molecular subtype will also determine the type of treatment received by the patient (surgery, chemotherapy, HER2-targeted antibodies, anti-estrogen therapy).

II. Natural History of Breast Cancer

A) Risk factors & initiation

Apart from female sex and age, several other factors have been associated with enhanced risk of breast cancer: genetics, lifestyle, and environmental pollutants.

About 5-10% of cancers are linked to germline mutations acquired from hereditary transmission. The most common mutations are of BRCA1 or BRCA2 genes. BRCA proteins are tumor suppressors through their function in homology-directed DNA repair. Mutations in these genes will lead to decreased DNA repair efficiency and lead to an increased risk of breast and ovarian cancer.

Lifestyle factors have also been associated with a higher risk of breast cancer. For example, late pregnancy is a risk factor, probably because early pregnancy would reduce the number of stem or progenitor cells that could be targets of transformation (Siwko et al., 2008). Moreover, 20 % of breast cancers are attributed to modifiable risk factors such as smoking, alcohol use, obesity, and physical activity (Brody et al., 2007).

Exposure to environmental pollutants such as endocrine disruptors and air pollution (Rodgers et al., 2018), but also micro- and nano-plastics (Llorca and Farré, 2021) have also been linked to breast cancer. Indeed, the link between bisphenol A, which has estrogen-mimetic properties and is involved in breast cancer initiation by niche dysregulation is well-documented (Clément et al., 2017).

The exact mechanisms of breast cancer initiation are still an important area of research. By asymmetric division, bipotent mammary stem cells self-renew and allow for the breast epithelium adaptation during the normal life of female individuals: breast formation, pregnancy, and lactation (Lloyd-Lewis et al., 2017). Perturbation of signaling pathways involved in cellular proliferation or differentiation by mutation accumulation or niche disruption leads to the progressive transformation of the cells.

C) Dissemination

The most known and described mechanism of dissemination is late dissemination, but new clinical and pre-clinical evidence supports the fact that early dissemination, before the tumor is clinically detectable, also exists (Klein, 2020).

Cancer cells first proliferate in the epithelium of the lobule, and the tumor grows progressively *in situ*. Then it will continue to grow and invade its surroundings. After breaking the basal membrane of the epithelium, cancer cells invade the surrounding lymphatic and circulatory systems by intravasation (**Figure 4**). Eventually, cancer cells will extravasate and will reach the secondary organs.

However, emerging clinical and pre-clinical data now suggest that cancer cell dissemination can also occur at an early stage of cancer development. Pre-transformed epithelial cells can undergo epithelial to mesenchymal transition and disseminate in secondary organs. These early disseminated cells have been observed in patients with breast cancer (Schardt et al., 2005) (Hüsemann et al., 2008) (Garcia-Murillas et al., 2019), colorectal cancer (Hu et al., 2019) and melanoma (Werner-Klein et al., 2018). How this mechanism could be linked to cancer metastasis and relapse, and whether metastases arise from late, early dissemination, or both, is an expanding field of translational research (Harper et al., 2016) (Klein, 2020).

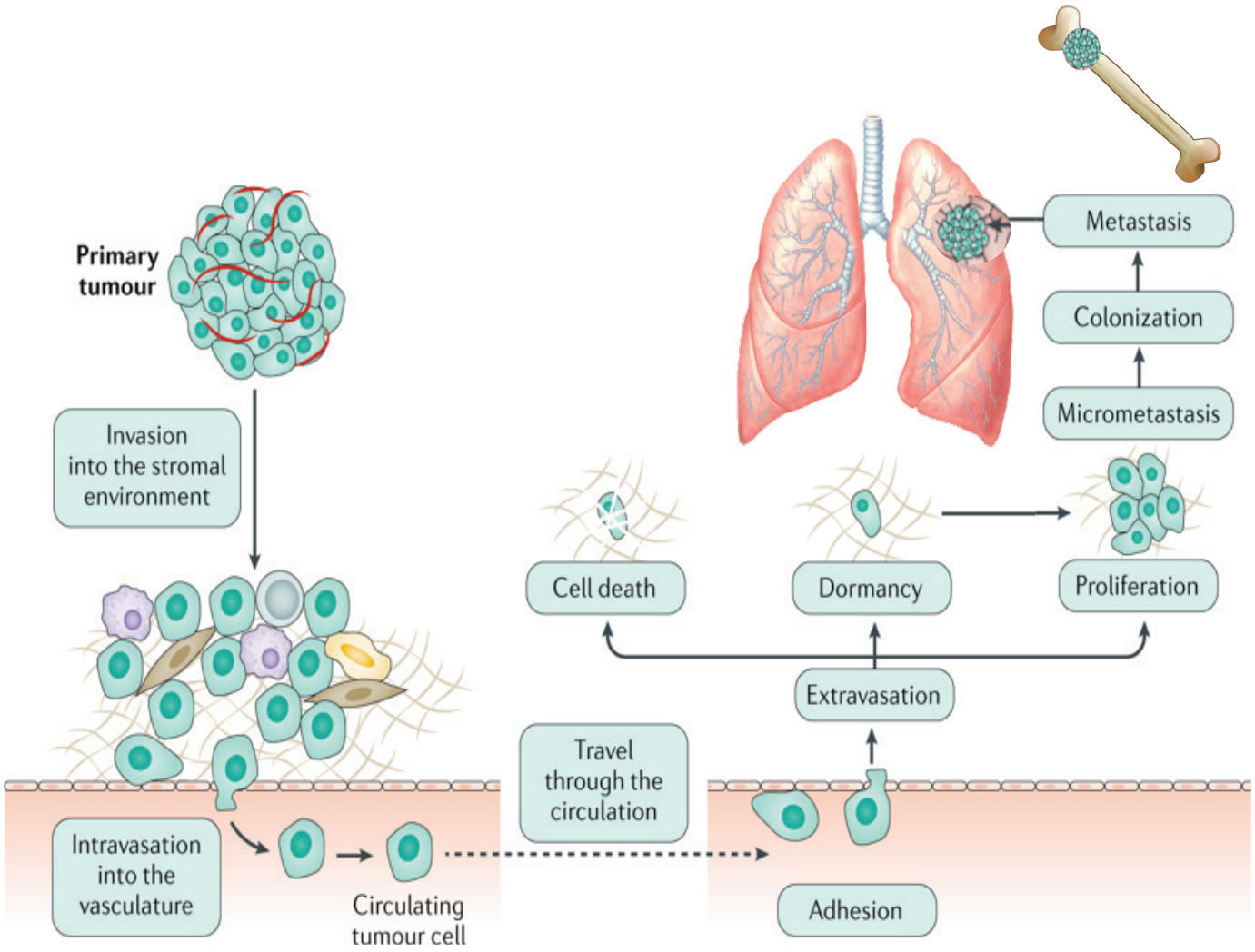

Figure 4: Steps leading to cancer metastasis

After breaking the basement membrane, cancer cells will intravasate into the vasculature and travel through the circulation. When reaching a secondary organ, the cancer cell can either die, start proliferating right away to lead to metastasis, or first enter a state of dormancy. These dormant cells can then awake and later lead to metastasis. Adapted from (Aguirre-Ghiso, 2007)

D) Metastasis & Tropism

After extravasation, cancer cells arrive in an unknown environment. They can either adapt, proliferate and develop metastasis, or die (**Figure 4**). Depending on their inner state or the microenvironment particularities, cells can also enter a state of dormancy, which will be later developed.

Breast cancer mainly metastases to lymph nodes, bones, livers, lungs, and brain (**Figure 5**). Brain metastasis occurs in 30% of patients with invasive HER2+ cancers whereas it occurs in less than 10% of patients with invasive luminal A subtype of breast cancer. The most overall common site of breast cancer metastasis is the bone, where almost 70% of patients with invasive breast cancer will develop metastasis.

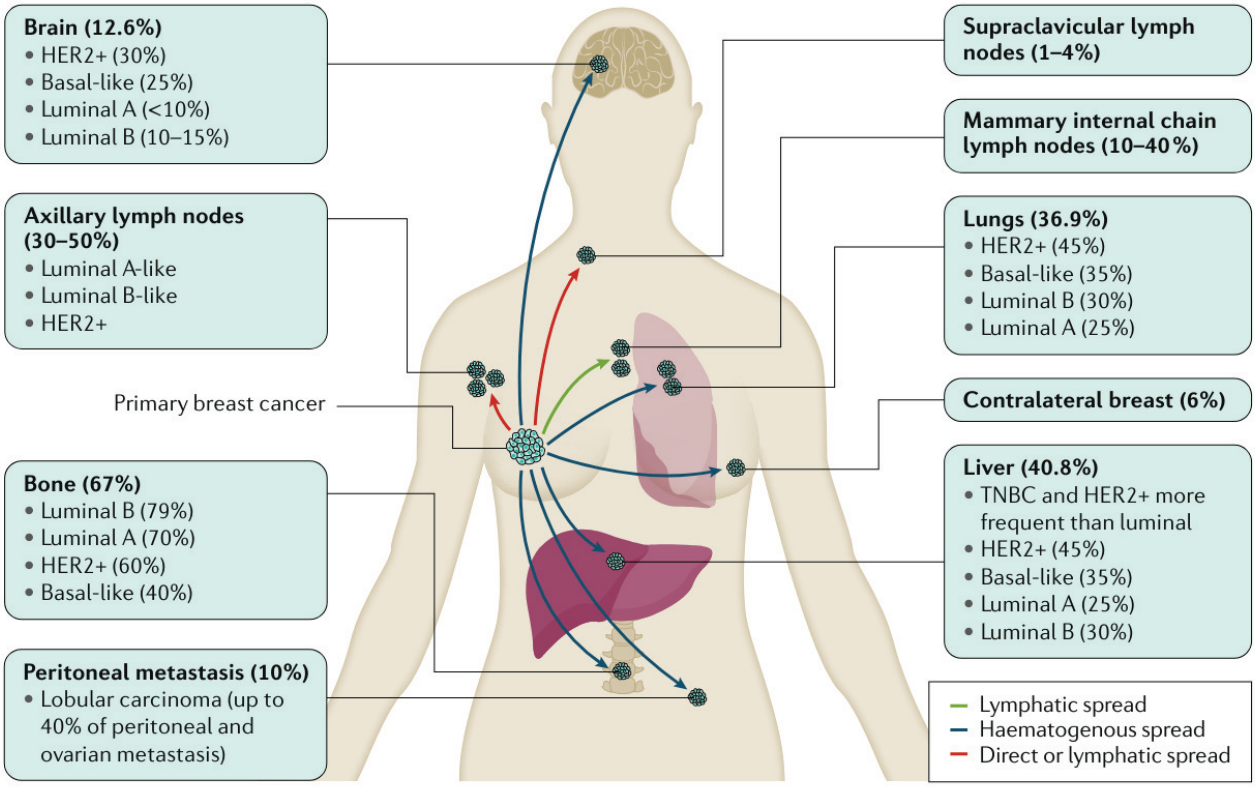

Figure 5: Metastatic tropism of invasive breast cancer depending on intrinsic subtypes.

The intrinsic subtype of cancer induces a different metastatic tropism among patients with invasive breast cancer. Brain metastasis occurs in 30% of patients with invasive HER2+ cancers whereas it occurs in less than 10% of patients with invasive luminal A subtype. Figure extracted from (Harbeck et al., 2019) with data from the SEER database of the NCI) from women in the USA from 2010 to 2014.

F) Late Relapse in Breast Cancer & Cancer Dormancy

The risk of relapse still exists up to 30 years after therapy, but this is largely dependent on the molecular subtype of breast cancer. TNBC tumors have a high risk of relapse in the first 5-years post primary tumor treatment. After this 5-year limit, the risk of relapse substantially decreases (Ignatov et al., 2018). An inverse phenomenon happens in ER+ tumors which have a lower risk of relapse at the beginning but show enhanced late relapse risk. A Danish study (Pedersen et al.) analyzed late relapse patterns of breast cancer patients that had not relapsed 10 years after primary tumor treatment. Patient outcome was evaluated for an additional 22 years (32-year follow-up in total). 20% of the patients that had not relapsed in the first 10 years post-surgery relapsed in the following 20 years. Patients with larger tumors, positive lymph nodes, or ER+ tumors were at a higher risk of relapse (**Figure 6**). A following study assessed the mortality of these late relapses (Pedersen et al., 2022a). Interestingly, patients who relapsed earlier had higher mortality compared to patients that relapsed late.

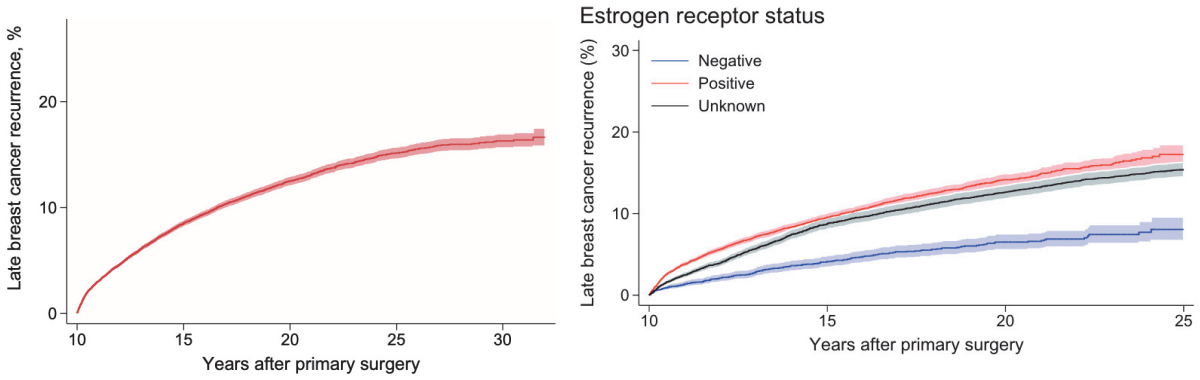

Figure 6: Cumulative incidence of late breast cancer recurrence.

Patients that had not relapsed 10 years after primary surgery were followed for an additional 20 years. Almost 20% of patients had relapsed 20 years later. Estrogen receptor status at diagnosis shows that From (Pedersen et al., n.d.)

A better understanding of the biology of early vs late relapse is essential as the identification of patients at higher risk of late relapse is essential will determine the course of therapy. Patients at risk of relapse can be kept under endocrine therapy while those at lower risk can stop treatment, thus reducing adverse effects. This field is in great expansion, and specific subgroups of late recurring ER+ tumors are being identified (Rueda et al., 2019). This will be further developed in the discussion of this dissertation.

After prolonged years of remission, late relapses are due to disseminated tumor cells (DTC) that can remain dormant in secondary organs for years (Aguirre-Ghiso, 2007). Indeed, most breast cancer-related deaths are triggered by metastases that can arise years or even decades after treatment and primary tumor removal. Dormant disseminated cancer cells are characterized by their growth arrest, expression of pluripotency markers, survival, and resistance to treatment (Risson et al., 2020). The next part of this introduction will focus on our current knowledge of cancer cell dormancy.

After cancer initiation, breast cancer cells can invade their surroundings and disseminate to secondary organs, leading to potential metastasis. Late relapse is also possible after long periods of minimal residual disease due to the dormancy of disseminated tumor cells. As the burden of breast cancer is predicted to increase, the number of breast cancer survivors that are at risk of relapse will also increase. Thus, a better understanding of dormancy mechanisms underlying late relapse is essential to continue improving patient care.

CANCER CELL DORMANCY

I. Generalities

Several cancer types also have late relapse and dormancy biology is being studied in different models (Phan and Croucher, 2020) (Aguirre-Ghiso and Sosa, 2018). In this part, the focus will be on breast cancer cell dormancy but dormancy mechanisms identified in other types of cancers will also be described.

A) Clinical Evidence of Cancer Dormancy in Patients

In a clinical setting, “dormancy” mainly refers to the long period between primary tumor resection and relapse. Relapse signifies that some cancer cells were not clinically detectable but were still surviving in the body: it is called minimal residual disease (MRD).

Evidence for a dormant invisible minimal disease is the case of “cancer transfer”. Transplanted organs from donors that were diseases free for many years led to the inadvertent transmission of cancer. Most of these cases happened in cutaneous malignant melanoma and renal cell carcinoma (Friberg and Nystrom, 2015). Evidence of MRD and dormancy has been identified in several cancers such as gastric cancer (Heiss et al., 2002), colon cancer (Cockrell et al., 2020), melanoma (Ossowski and Aguirre-Ghiso, 2010), prostate cancer (Morrissey et al., 2016), breast cancer (Braun et al., 2000a), and is associated with a high risk of metastatic relapse. (Janni et al., 2011). One of the most striking examples of solid cancer dormancy is in uveal melanoma (Ossowski and Aguirre-Ghiso, 2010): up to 50% of uveal melanoma patients have a metastatic relapse 10 years after the primary tumor removal when there was no sign of systemic dissemination. In this disease, the liver is the most common site of metastasis (Jager et al., 2020).

Minimal residual disease and dormancy are also observed in lymphoid malignancies (Brüggemann et al., 2004), and myeloid malignancies such as chronic myeloid leukemia (Bhatia et al., 2003) (Jeanpierre et al., 2020) or multiple myeloma (Serizawa et al., 2022).

B) Different Dormancy Types

Different models explain this prolonged time between primary tumor treatment and relapse: cancer cell dormancy, angiogenic dormancy, and immune equilibrium state. In angiogenic dormancy, impaired development of blood vessels leads to a balance between cell death and cell proliferation as described by Folkman (Almog et al., 2006) (Naumov et al., 2006). In the immune equilibrium model, proliferative tumor cells are continually recognized and targeted by cytotoxic immune cell responses (Uhr and Marches, 2001) and reach an equilibrium state (Koebel et al., 2007).

These two models describing “tumor mass dormancy” do not account for cell cycle arrest of cancer cells that have been identified in several models and shown to largely contribute to metastatic relapse (Phan and Croucher, 2020) (Risson et al., 2020). We will here focus on cancer cell dormancy where disseminated tumors single cells or small clusters enter a reversible growth arrest program governed by microenvironmental cues (Bragado et al., 2012) and specific intrinsic programs.

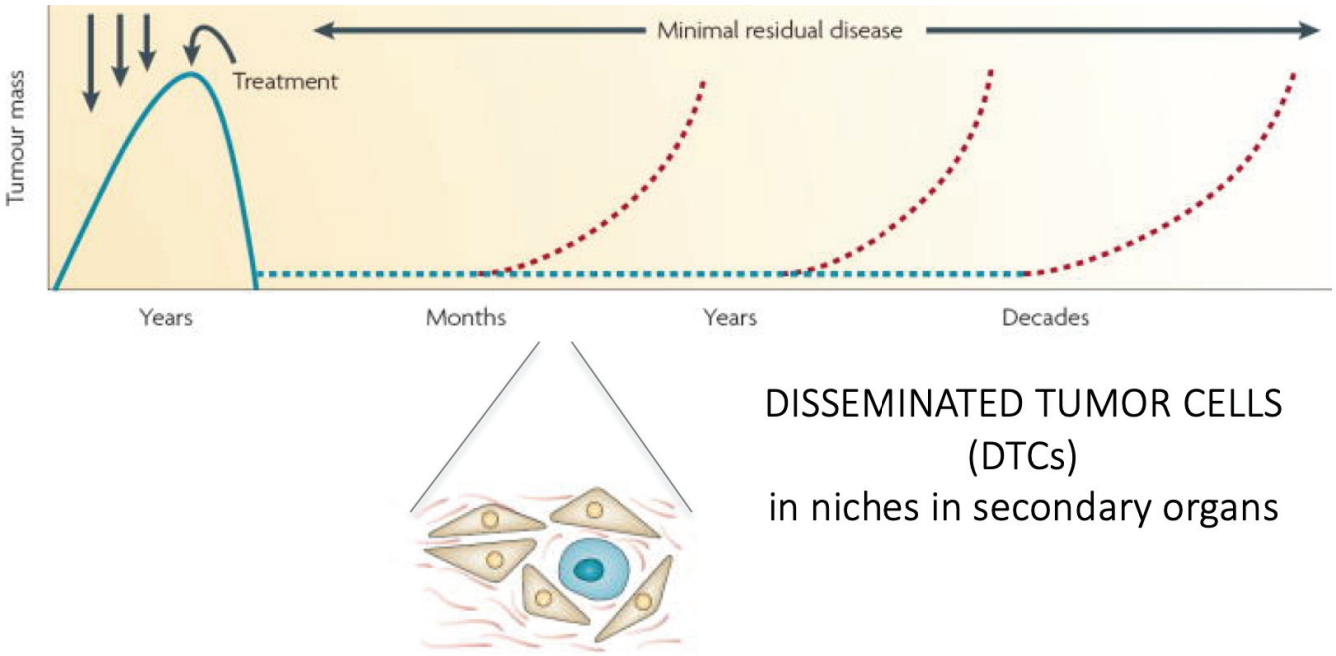

Figure 7. Dormant Disseminated Tumor Cells (DTCs) lead to Cancer Relapse

After primary tumor removal and treatment, patients can be considered in remission for several months, years, or decades before relapse. This period is called "minimal residual disease" (MRD). This relapse is due to disseminated tumor cells present in niches in secondary organs. Adapted from (Aguirre-Ghiso, 2007)

C) Dormancy & Senescence

Senescence or differentiation have also been proposed to underlie DTC dormancy. Growth arrest programs activated during senescence, dormancy, and differentiation indeed have similarities and there is an overlap in the regulation of the cell cycle (**Figure 8**). An important difference is that senescence is irreversible. Indeed, the dormancy of cancer cells must be reversible to lead to metastatic relapse. Senescent cells are also usually cleared by the immune system (Lujambio et al., 2013) (Xue et al., 2007). Moreover, DTCs activate programs of pluripotency (further described below) that are repressed in senescent cells (**Figure 8**). However, the possibility that a hybrid state of senescence is activated by microenvironmental signals or therapeutic stress, where senescent cancer cells would prepare a pre-metastatic niche for other proliferating cancer cells could also be hypothesized.

D) Cancer Dormancy & Stem Cell Quiescence

Whether the physiological quiescent state of stem cells and the dormancy of disseminated cancer cells are governed by similar, overlapping, or different pathways is an important question in the field of dormancy.

Stem cell quiescence is an actively preserved state in which cells are maintained in the G0 phase of the cell cycle. The underlying molecular mechanisms have been reviewed by (Rumman et al., 2015). Importantly, Retinoblastoma (Rb) proteins restrain cell cycle progression by inhibiting the G1-S phase transition. Cyclin-Dependent-Kinases (CDK) allow cell cycle progression and their inhibitors, p27, p21, and p57 maintain HSC quiescence (Sherr and Roberts, 1999). Correspondingly, these CDK inhibitors are upregulated in different types of dormant DTCs such as ovarian tumors (Lu et al., 2008) or head and neck squamous cell carcinoma (Bragado et al., 2013) and actively contribute to the maintenance of cancer dormancy. The quiescence of HSCs is reversible, which is also an important trait of dormant cancer cells: quiescent HSCs can re-enter the cell cycle to replenish the bone marrow niche during stress and then re-enter dormancy (Wilson et al., 2008).

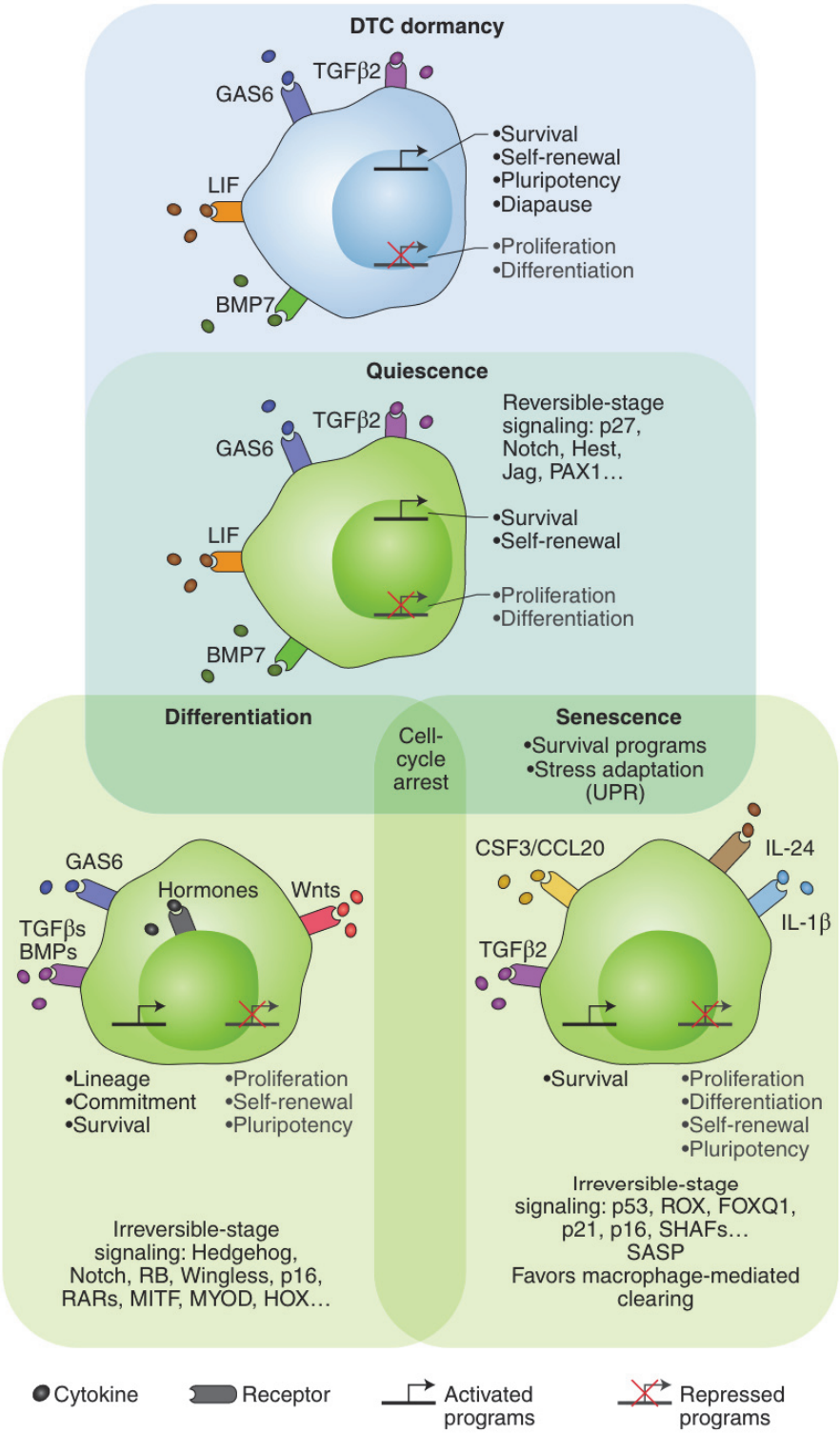

Figure 8: Difference and similarities between cancer dormancy, physiological stem cell quiescence, differentiation and senescence.

Survival programs and cell cycle arrest are shared among the programs. Quiescence and dormancy are reversible, whereas senescence is not. The factors involved in these phenotype induction will be described in the following part of this chapter. From (Risson et al. 2020)

In a study by (Balic et al., 2006), disseminated cells detected in the bone marrow of breast cancer patients had a stem cell phenotype with 72% of the cells being $CD44^+/CD24^-$ whereas this proportion was less than 10% in primary tumor cells. Moreover, in melanoma, niche signals that induce quiescence of hair follicle stem cells antagonize and are dominant over oncogene signaling. Strong stemness-inducing signals from the niche can thus override oncogene expression (White et al., 2014).

Some stemness markers such as SRY-box transcription factor 9 (SOX9) and NANOG, and the orphan nuclear receptor, nuclear receptor subfamily 2 group F member 1 (NR2F1) have been identified as markers of dormant cancer cells in some models such as head and neck cancers (Sosa et al., 2015). In addition, Notch2 is also a regulator of physiological stem cell quiescence (Bigas and Espinosa, 2012) and has also been identified as a mediator of breast cancer cell dormancy in the bone (Capulli et al., 2019). Some studies have not found these markers in dormant cells (Sun et al., 2021), suggesting that alternate pathways also exist.

Overall, there's a rewiring of cellular pathways in dormant cancer cells normally used in stem cell quiescence, leading to a dormancy state of DTCs while resisting apoptosis. Can dormant disseminated cells lead to metastasis when they awaken? Are they cancer stem cells?

E) Dormant Cancer Cells and Cancer Stem Cells

The cancer stem cells concept states that there is a limited number of cells that have self-renewal and differentiation capacity to give rise to cancer cells composing the bulk of the tumor, but with limited tumorigenicity. Cancer stem cells were first described in teratocarcinoma (Kleinsmith and Pierce, 1964). The existence of these cells was then demonstrated in acute myeloid leukemia (Lapidot et al., 1994) where only one immature CD34+/CD38- cell could lead to the development of leukemia in an irradiated mouse. Cancer stem cells were then also observed in breast cancer (Al-Hajj et al., 2003) by showing that only a subpopulation of CD44+/CD24- cancer cells were able to form tumors. Aggressive and metastatic breast cancers often have a reactivated embryonic stem cell transcriptional program (Wong et al., 2008). To

lead to late relapse when awakening, dormant cancer cells need to also be cancer stem cells. But we can wonder if all dormant cells are also cancer stem cells? Are cancer stem cells the only cells able to enter dormancy? Indeed, commonalities between cancer stem cells and dormant cancer cells exist, but also differences. It is unclear if all cancer cells that undergo dormancy are cancer stem cells, or if cancer stem cells can undergo long periods of cell cycle arrest. When C-MYC is inactivated in hepatocellular carcinoma cells, most cells will die but a subpopulation can enter dormancy. Reactivation of MYC led to the replenishment of the tumor, asserting the hypothesis that dormant cancer cells can also be cancer stem cells (Shachaf et al., 2004). In chronic myeloid leukemia, patients in remission have persisting immature leukemic cells that are also quiescent (Huettner et al., 2000) (Giustacchini et al., 2017) (Jeanpierre et al., 2020).

Hence, although similarities exist, it is unclear whether all cancer stem cells can enter dormancy or if all dormant cancer cells are also cancer stem cells. But a dormant cancer cell needs to be a cancer stem cell to lead to metastasis: the intersection of those two populations is probably what allows for late metastatic relapse.

Dormant cancer cells during minimal residual disease can lead to metastatic relapse in patients. Dormant cells are characterized by their growth arrest, expression of pluripotency markers, and activation of survival programs. They undergo prolonged cell cycle arrest by activating physiological quiescence programs. Unlike senescence, dormancy is reversible and cells can re-enter the cell cycle, and proliferate, leading to metastatic relapse. To lead to metastasis development, a dormant cancer cell should also be a cancer stem cell, but the intersection of these two populations is still unclear.

II. Hallmarks of dormancy

Dormant cancer cells are defined by several hallmarks (**Figure 9**) (Phan and Croucher, 2020). The dormant cancer cell is in a specific environment, it is in cell cycle arrest, resists treatments, evades immune system recognition, and can awaken to lead to metastasis.

A) Niche Dependence

Although dormancy can be a cell-intrinsic parameter of cancer cells, evidence is leading towards an important role of the microenvironment in inducing dormancy but also awakening. Understanding the crosstalk between disseminated tumor cells and their microenvironment is, therefore, essential to be able to treat or prevent relapse and metastatic disease.

Indeed, depending on which organ disseminated tumor cells seed, they will not have the same fate. In a model of head and neck cancer, disseminated cancer cells seeded in the lung grew and formed metastasis, while they did not grow in the bone marrow even if they were detected there (Bragado et al., 2013). Sensing of the microenvironmental signals can be through secreted factors and extracellular matrix proteins. Indeed, adherence to fibronectin (Aguirre-Ghiso et al., 2001) and integrins are essential in dormancy induction (Ghiso et al., 1999). Dormancy can be induced by several other signals in the microenvironment, which are interconnected, such as stromal cell bone morphogenetic protein signaling (Buijs et al. 2007; Kobayashi et al. 2011) (Jeanpierre et al., 2020), TGFβ related pathways (Prunier et al. 2019) (Bragado et al., 2013) (Nobre et al., 2021), GAS6 signaling (Taichman et al., 2013), nutrient deprivation (Jo et al. 2008) or hypoxia (Fluegen et al. 2017).

The bone marrow is a very common site of dissemination of breast cancer cells and is of particular interest for our project. How the bone marrow microenvironment regulates disseminated tumor cell dormancy will be further described below.

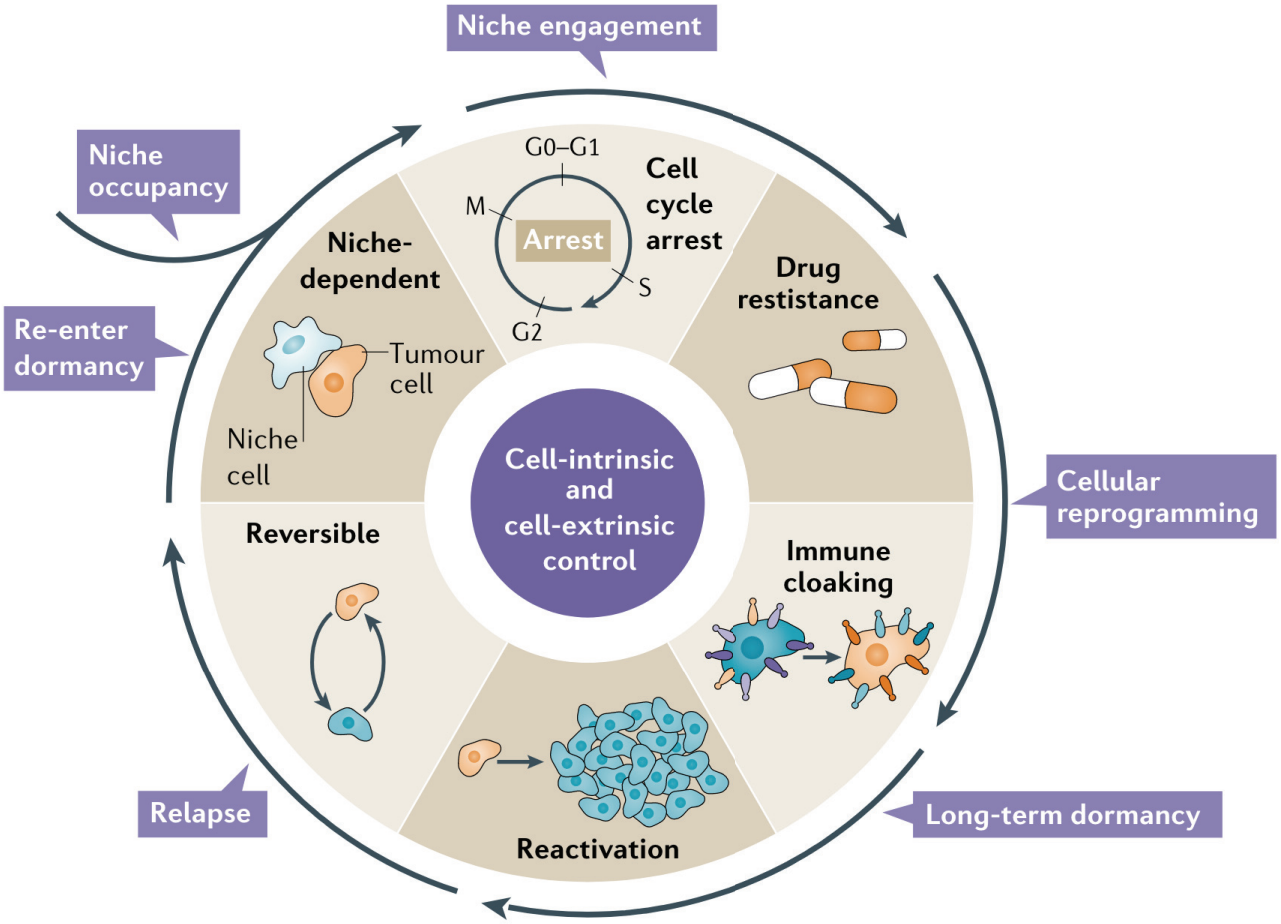

Figure 9: Hallmarks of cancer cell dormancy

Cancer cell dormancy is maintained through cell-intrinsic and cell extrinsic control. Niche dependence, cell cycle arrest leading to long term dormancy, immune system evasion, and awakening potential are the main and essential characteristic of dormant cells. From Phan and Crouchner, 2020.

B) Cell Cycle Arrest & Survival

As mentioned above, dormant disseminated tumor cells persist over long periods in cell cycle arrest by conserved growth arrest and survival mechanisms. Cell cycle arrest is induced by the induction of cyclin inhibitors such as p21 and p27. Moreover, studies have validated the quiescent phenotype by using membrane or cytoplasmic dyes. The dye being progressively lost with cell divisions, label-retaining cells are slow-cycling or quiescent cells. Upon cell cycle arrest, there is also downregulation of Ki67 and upregulation of histone-3 phosphorylation.

Cellular dormancy can also be induced by signaling through TAM receptor tyrosine kinases; in both solid tumors and hematological cancers TYRO3, MER, and AXL activation have been shown to induce cell cycle arrest. More specifically, a high AXL/Tyro ratio induces dormancy (Yumoto et al., 2016). The p38/ERK ratio has also been established as an important dormancy marker (Aguirre-Ghiso et al., 2001). Knockdown of MERK in prostate DTC cells induced a high p38/ERK ratio, increased expression of p27, NR2F1, SOX2, and NANOG, and induced a G1/G0 arrest (Cackowski et al., 2017).

On top of cell cycle arrest, dormant cells also activate specific metabolic pathways to survive. Indeed, reduced PI3K-AKT signaling is activated in dormant cells to induce autophagy and anti-oxidant response (Correa et al., 2012) which allows their survival and subsequent awakening (Vera-Ramirez et al., 2018). Endoplasmic reticulum unfolded protein response (UPR) is also activated in dormant cells. Major transducers of the UPR such as Activating Transcription alpha 6 (ATF6) or Pancreatic Endoplasmic Reticulum Kinase (PERK) are activated in dormant cells. PERK overexpression was also shown to induce cell cycle arrest of colon carcinoma cells but the molecular mechanism has not been identified (Ranganathan et al., 2008). Of interest, Glycerol-3-phosphate dehydrogenase 1 (GPD1), an enzyme involved in glycerol metabolism is specifically expressed and necessary to maintain the metabolic signatures of dormant glioma stem cells (Rusu et al., 2019). Although these dormant glioma stem cells were not isolated but were inside the glioma tumor, this suggests that dormant cells have a complete reorganization of their metabolic features.

C) Treatment Resistance

By not proliferating, thus being insensitive to chemotherapy, and by constitutively upregulating stress signaling pathways, dormant cancer cells are thought to be resistant to most treatments.

Resistance to chemotherapy was shown in breast cancer disseminated in the bone marrow: half of the patients with cytokeratin positive cells in the bone marrow before adjuvant therapy still had those cells after chemotherapy, leading to reduced survival of patients (Braun et al., 2000b). Treatment of gastrointestinal stromal tumors (GIST) with imatinib leads to good response, but a subpopulation of cancer cells survives and stays quiescent and activates autophagy pathways, leading to subsequent patient relapse. A study in mice showed that the combination of imatinib with autophagy inhibitors selectively killed dormant cells (Gupta et al., 2010). Another study targeted autophagy in dormant breast cells which led to their reactivation (La Belle Flynn et al., 2019). Although this study did not use another combinatory drug it raises the question of the role of autophagy in dormant cells: is it inducing dormancy or does it allow for the survival of the dormant cells?
Moreover, single-cell transcriptomic of patient tumors undergoing endocrine therapy showed the appearance of a quiescent subpopulation with specific activation of survival signals (Hong et al., 2019). Studying how administered treatments could induce the dormancy of cancer cells leading to late relapse is of utmost importance to be able to adapt our protocols.

How dormant cells could be therapeutically targeted or if they are indeed a good therapeutic target (Goss and Chambers, 2010) (Quesnel, 2008).

D) Immune Evasion

The link between cancer and the immune system is a crucial area of research. The cancer immunoediting hypothesis describes that cancer cells are first eliminated, then an equilibrium stage happens, where cancer cells proliferate and are killed by the immune system at the same rate (“tumor mass dormancy”). This is then followed by the escape phase where the immune system no longer controls cancer and tumor mass develops.

As described previously, tumor mass dormancy is not the same process as cellular dormancy. There is evidence showing that dormant cancer cells are not recognized and killed by the immune system. As it has been described in normal quiescent (but not proliferating) stem cells (Agudo et al., 2018), dormant cells downregulate the major histocompatibility class I (MHC-I) to reduce the exposure of non-self-antigens (Pantel et al., 1991). More recent evidence of this phenomenon was shown in a model of pancreatic ductal carcinoma, where endoplasmic stress response selected dormant cells in the liver that had a decreased MHC-I and tumor antigen cytokeratin-19 expression (Pommier et al., 2018), thus evading T-cell recognition. Other mechanisms that do not involve a decrease in major histocompatibility complex have also been described in persistent dormant leukemic cells in mouse acute myeloid leukemia through upregulation of the checkpoint inhibitor B7-H1 (PD-L1) and the immunomodulatory receptor CTLA-4 ligand B7.1 (Saudemont and Quesnel, 2004). Emerging evidence also shows that quiescent cancer cells form an immune-suppressive niche of tumor-protective fibroblast and exhausted T-cells by activating hypoxia-related programs (Baldominos et al., 2022). Moreover, the interaction between breast cancer cells and MSC induces TGFβ1 secretion by MSC (Patel et al., 2010), which activates Treg and inhibits Th17 response, which has been shown to lead to immune escape of DTCs (Patel et al., 2014). How immune cells can be dormancy regulators will be discussed below.

E) Awakening

For reasons that we ought to better understand, dormant cancer cells can sometimes reenter the cell cycle, which leads to their proliferation and ultimately causes patient relapse and possible death. Many different mechanisms of niche alteration over time (aging) or perturbations leading to dormancy awakening have been explored. Inflammation leads to niche remodeling, potentially awaking cancer cells. In a model of sustained lung inflammation (by tobacco smoke or nasal introduction of lipopolysaccharide), dormant cancer cells were awakened due to the production of nuclear extracellular traps (NETs) by neutrophils which modified laminin epitopes through the secretion of NE and MMP9 (**Figure 10**) (Albrengues et al., 2018). Similar evidence that matrix remodeling impacts dormancy awakening has been shown in a model of aging skin where collagen remodeling promoted metastasis (Kaur et al., 2019). Matrix remodeling is therefore essential to the awakening of cancer cells. Angiocrine signals also control this reactivation, as shown in a model of breast cancer where cancer cells could proliferate in aged BM but were kept dormant in young mice (Singh et al., 2019). Of interest, inflammatory cytokines such as IL1B and IL6 were upregulated in aged mice and the dormancy inducing cues were downregulated. Overall, dysregulation of balanced niche signals, aging, and inflammation can lead to the awakening of cancer cells. But somehow, even though all patients will age and many will undergo inflammatory processes throughout their lives, many will not relapse. Understanding what makes the robustness of dormancy-inducing cues will be essential to preventing relapse in patients.

Dormant cancer cells are highly regulated by microenvironment signals. Specific signals will induce cell cycle arrest and activation of survival programs. These programs lead to resistance to most treatments, mainly due to autophagy activation. Dormant cancer cells can also evade immune recognition by avoiding detection by immune cells or by forming immune-suppressive niches. Importantly, dormant cancer cells can awaken when their niche is perturbed.

III. How the Bone Marrow Niche Regulates DTC dormancy

One of the most robust environments controlling DTC dormancy is the bone marrow (BM). In this site cancer cells can persist for years without growing (Braun et al., 2000a) (Borgen et al., 2018) (Naume et al., 2014) but they are a commonly poor prognosis marker as dormant cells can eventually awaken. Hence, it is essential to understand what makes the robustness of the dormancy-inducing cues of the bone marrow as identifying key regulators of dormancy states could lead to treatments that can keep DTCs dormant and prevent them from proliferating.

Indeed, the BM niche is a complex microenvironment physiologically regulating HSC quiescence (Pinho and Frenette, 2019). Many cues regulating HSC quiescence also regulate cancer cell dormancy (Risson et al., 2020) (Cackowski and Taichman, 2018). Different cellular players are part of the BM microenvironment constituting the niche for HSCs maintenance and quiescence induction. Although identification of this niche has been an active area of research (Pinho and Frenette, 2019), a clear consensus has not been reached yet. Many cellular players such as osteoblast, osteoclasts, mesenchymal stem cells, HSCs progeny such as macrophages, megakaryocytes, NK cells, and lymphocytes, as well as sympathetic nerves, are part of the niche. Here, the different BM niche players with a focus on how they contribute to DTC dormancy regulation will be described.

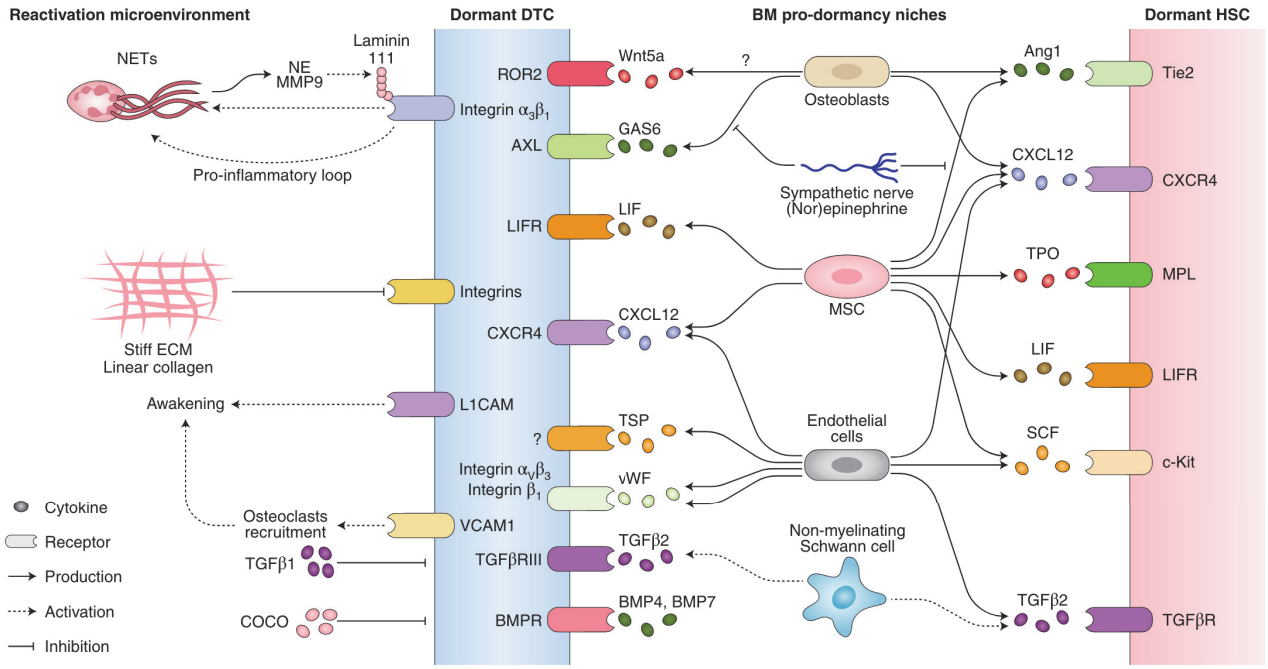

Figure 10 : Cues, receptors, and cell types involved in DTC reactivation and pro-dormancy niches.

In the bone marrow, a pro-dormancy niche involves the action of several factors that produce a pro-dormancy microenvironment that physiologically controls hematopoietic stem cell quiescence. Signals from this microenvironment can also lead to the induction of quiescence in DTCs. In contrast, reactivation niches that awaken dormant DTCs in a manner that involves formation of NETs, extracellular matrix stiffness, TGFβ1 and inhibitors of BMP molecules are also described.. From (Risson & Nobre et al., 2020)

B) Osteoblast & Osteoclasts

Osteoblasts are cells essential to bone formation and matrix mineralization. They have also been implicated in hematopoietic stem cell quiescence by the secretion of the extracellular matrix glycoprotein osteopontin (Nilsson et al., 2005).

Osteopontin has then been shown to also regulate lymphoblastic leukemia cell dormancy (Boyerinas et al., 2013) by anchoring them in specific niches. The secretion of GAS6 by osteoblasts has also been identified as an important factor in prostate cancer cell dormancy induction (Shiozawa et al., 2010). On the contrary, niche alteration by chemotherapy regularly given in breast cancer (paclitaxel and cisplatin) induced the secretion of Jagged1 by osteoblast cells in vivo, which led to the awakening of disseminated breast cancer cell (Zheng et al., 2017). Moreover, although the osteoblastic niche kept myeloma cells dormant, remodeling of the niche by osteoclasts also led to the awakening of quiescent myeloma cells (Lawson et al., 2015).

C) Immune Cells

Immune cells are the progeny of HSCs and some subtypes are important regulators of HSC quiescence in the BM (Mendelson and Frenette, 2014). Although the role of immune cells in solid cancer dormancy is being explored in other organs, evidence in the bone marrow microenvironment has not been fully assessed.

Macrophages of the primary tumor environment have been shown to induce cell dormancy (Borriello et al., 2022). In a spontaneous melanoma murine model, Depletion of CD8+ T cells resulted in the activation and outgrowth of early disseminated cells in visceral organs (Eyles et al., 2010). PD-1+CD8+ T cells were also shown to induce dormancy in the lung in a model of breast cancer (Tallón de Lara et al., 2021). The role of NK cells in mediating cancer dormancy has also been explored in the liver (Correia et al., 2021). However, immune system activation has also been shown to induce the reactivation of dormant cells and its role seems to be context-dependent: in a murine model of pancreatic cancer, T cells either induced dormancy or promoted proliferation depending on IFN-g signaling activation (Müller-Hermelink et al., 2008).

As described in part II.D) (p35), DTCs can also escape immune recognition. The role of immune cells in mediating cancer dormancy is an extensive field of ongoing research.

D) Neuro-Lineage cells

The bone marrow is innervated by autonomic nerve fibers, accompanied by non-myelinating Schwann cells. Sympathetic nerves in the bone marrow release adrenergic signals (Méndez-Ferrer et al., 2008) in a circadian cycle, inducing downregulation of CXCL12 expression by stromal cells (Méndez-Ferrer et al., 2008) which leads to a cyclical decrease of HSC retention. The extent to which this also applies to DTCs should be analyzed, to investigate if DTCs circulate or stay put in the BM for years. Moreover, norepinephrine has been shown to downregulate the expression of GAS6, by osteoblasts, which consequently led to the reentry in the cell cycle of prostate DTCs (Decker et al., 2017). Although the importance of this interaction remains to be tested *in vivo*, these findings suggest that stress might influence DTCs proliferation and cancer relapse. In contrast to these findings, non-myelinating Schwann cells have an important role in activating latent TGFβ (Yamazaki et al., 2011), which is important for HSC and DTC quiescence.

E) Vascular Niches

Endothelial cells make the surface of blood vessels inside the bone marrow and arterioles are an important niche component regulating HSCs and DTCs quiescence. Physiologically, endothelial cells are balancing self-renewal and differentiation of HSCs (Kobayashi et al., 2010). They secrete Thrombospondin (TSP), an angiocrine tumor suppressor, which induces dormancy of disseminated breast cancer cells localized near arterioles in the BM (Ghajar et al., 2013). Upon activation, endothelial cells can promote HSC expansion and proliferation (for hematopoietic recovery after ablation for example) (Kobayashi et al., 2010). In parallel, contrary to stable vasculature, sprouting vasculature secretes TGFβ1 and POSTN which promote DTC reactivation and metastatic growth (Ghajar et al., 2013). This shows the important role that the microvasculature of the BM niche has on HSC and DTCs quiescence, and that its role should be further investigated.

F) Mesenchymal Stem Cells

Mesenchymal stromal/stem cells (MSCs) are multipotent cells that can differentiate to generate bone, cartilage, and adipose tissue. Most of them are perivascular and it is now generally accepted that they are essential to HSC maintenance and regeneration. Among the wide MSC populations, there's a focus on NG2 (Neural Glial antigen 2) positive cells. NG2 is a proteoglycan found mostly in the central nervous system's glial cells and peripheral cells such as pericytes in the BM. Yet, they have been hard to characterize, as they can be labeled with different markers, resulting in different subpopulations that overlap. Nestin is an intermediate filament expressed by subpopulations of NG2+ cells. These NG2+/Nestin+ cells have been demonstrated to constitute a specific BM population of stromal cells essential to HSCs maintenance (Méndez-Ferrer et al., 2010) (Kunisaki et al., 2013) but also DTC dormancy through their secretion of TGFβ2 (Nobre et al., 2021). More evidence exists in prostate cancer cell dormancy (Cackowski and Taichman, 2018) where mesenchymal stem cells were shown to induce dormancy by their secretion of WNT5a (Ren et al., 2019). Leukemic stem cells from chronic myeloid leukemia were also kept dormant by CXCL12 secreted by the mesenchymal stem cell: specific deletion of CXCL12 in Prx1+ mesenchymal stem cells led to the increase of leukemic stem cell proliferation, but also rendered them more sensitive to tyrosine

kinase inhibitors. In (Nobre et al., 2021), the specific deletion of TGFβ2 in $NG2^+/Nestin^+$ MSCs led to the awakening of breast cancer disseminated tumor cells, but with a lower penetrance compared to the 50% deletion of $NG2^+/Nestin^+$ mesenchymal stem cells, raising the question of other contributing factors from the MSCs. Indeed, single-cell RNAseq from mouse bone marrow showed that MSCs are one of the most important sources of BMP4 in the BM (Tikhonova et al., 2019). In chronic myeloid leukemia, recent work from our lab showed that BMP-niche signals maintain persistent quiescent leukemic stem cells during undetectable minimal residual disease (Jeanpierre et al., 2020). BMP4 and TGFβ2 being important dormancy inducers in several models, this project emerged to assess if their effect would be interdependent.

Disseminated tumor cell dormancy relies on the activation of specific signaling pathways. Regulation of these pathways depends on the microenvironment of the cancer cell niche. The bone marrow is a complex multicellular and multifactorial restrictive environment physiologically regulating hematopoietic stem cell quiescence, that also regulates disseminated tumor cell dormancy. Mesenchymal stem cells, through their secretion of TGFβ-family cytokines, are important regulators of solid cancer and leukemic cell dormancy.

TGFB & BMP FAMILY

I. TGFβ & BMP signaling

A) Generalities

The term “bone morphogenic protein” was first used in the 1960s by Marshall Urist when he isolated proteins that induced bone formation from mesenchymal stem cells ([CSL STYLE ERROR: reference with no printed form.]). Transforming Growth Factor β1 (TGFβ1) was then isolated in the 1980s. The TGFβ-family has since become a significant interest in many fields, and our knowledge has greatly expanded. Biochemical purification, molecular cloning, and sequencing of the human genome showed that 33 other polypeptides are structurally similar to TGFβ1 (**Figure 11**) and make the TGFβ superfamily. These cytokines are characterized by a cystine knot by their symmetric conformations with a single disulfide bond between two monomers.

TGFβ superfamily of cytokines regulates multiple functions from developmental programs (Waite and Eng, 2003), reproductive system (Shimasaki et al., 2004), tissue homeostasis (Xu et al., 2018), metabolism, and immunity (Batlle and Massagué, 2019). The versatile effects of BMP ligands have even led to the suggestion to change their name to “**body** morphogenic proteins” (Wagner et al., 2010)! The effect of the TGFβ-family ligand largely depends on the cell type and the surrounding microenvironment: it is highly context-dependent (David and Massagué, 2018). It is an extensive field of research in many different areas, and our current knowledge of TGFB-family functions is being regularly reviewed (Morikawa et al., 2016).

Four main groups exist: TGFβs, BMPs, Activins and Inhibins, and Growth Differentiation Factors (GDF) (**Figure 11**). This introduction will focus on TGFβ and BMP cytokines, as their role has been the most described in cancer and cancer dormancy.

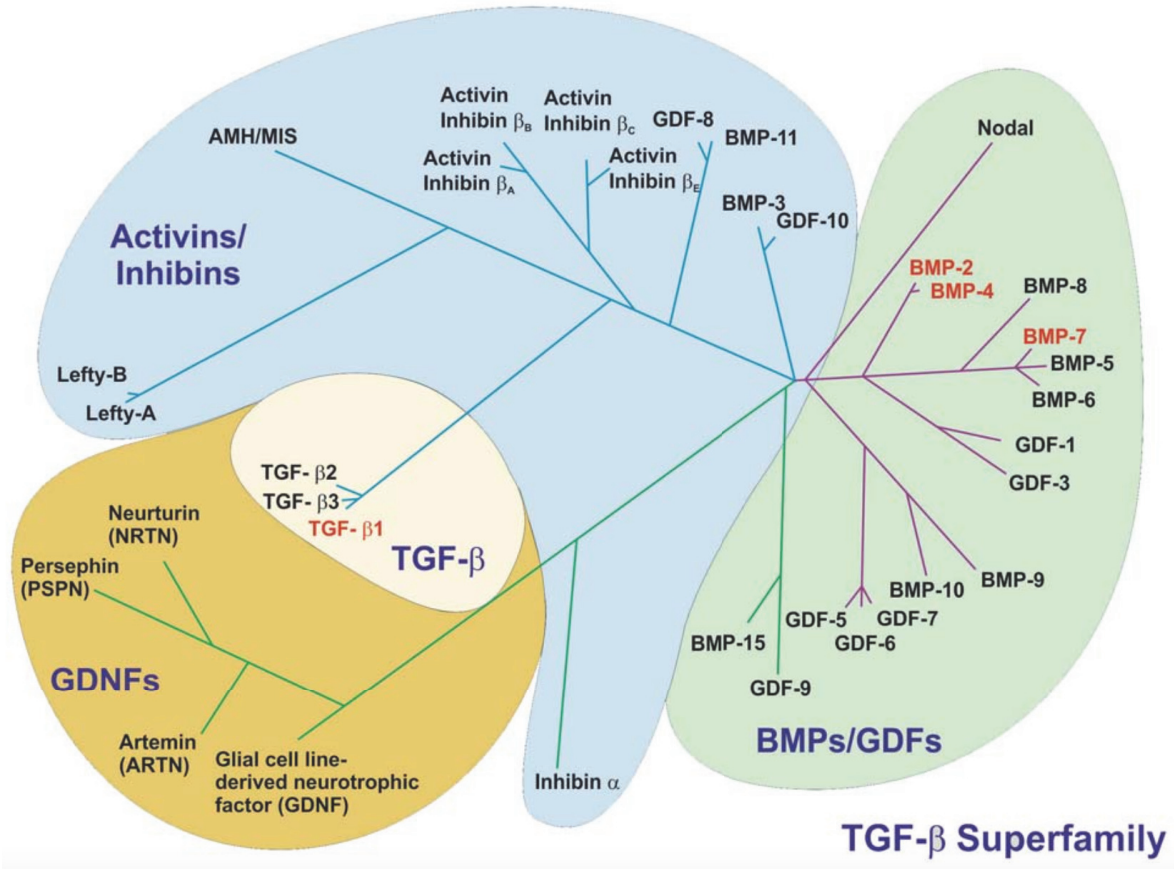

Figure 11: TGFB-family groups and members

Phylogenic tree based on sequence and structure similarity. Of note, BMP2/4 share 80% homology. Nodal is an inhibitor of BMP signaling.

Type-I Receptors	Type-II Receptors	Coreceptors
TGFβR1 (ALK5)	TGFβR2	Betaglycan Endoglin
BMPR1A (ALK3) BMPR1B (ALK6)	BMPR2	RGM BAMBI
ACVRL1 (ALK1) ACVR1 (ALK2) ACVR1B (ALK4) ACVR1C (ALK7)	ACVRIIA ACVRIIB AMHR2	

Table 1 : TGFβ-family receptors

A) Ligand & Receptors Interaction

Homology in the amino-acid sequence has led to the classification of BMPs in different subgroups: phylogenetic analysis groups BMP2/4, BMP5/6/7/8, BMP9/BMP10, or TGFβ1/2/3 (**Figure 11**). Although these cytokines can share up to 80% of homology, they can have very different effects (Wang et al., 2014). One example is the differential effect of BMP2 and BMP4 on mammary stem cell differentiation: BMP2, but not BMP4, induces luminal differentiation and expansion of the luminal progenitor compartment in the mammary gland (Forsman et al., 2013) (Chapellier et al., 2015). TGFβ2, but not TGFβ1, induces the dormancy of cancer cells (Bragado et al., 2013).

Cytokines of the TGFβ family are released in the microenvironment and will then form homodimers or heterodimers. A cell needs to express specific receptors to sense TGFβ and BMPs in their surrounding microenvironment. The mammalian genome encodes for seven type-I receptors and five type-II receptors (**Table 1**). Receptors do not have the same specificity or affinity for all the TGFβ family cytokines, and their differential expression can lead to different sensing of surrounding signals. The different possible combinations of receptors enhance the complexity and possibilities of TGFβ and BMP signaling. The structural basis of ligand and receptor interaction is an extensive field of research (Lin et al., 2006) (Khodr et al., 2021). TGFβs first bind to TGFβR2, and then a complex with TGFβR1 is formed. On the contrary, BMPs bind both to type-I and type-II receptors. After ligand binding, a heterotetrameric complex of 2 type-I receptors and two type-II receptors is formed. The serine/threonine kinase domain of the type 2 receptor will phosphorylate the Glycine/Serine rich domain of the type 1 receptor (**Figure 13**). The now activated type 1 receptor will then phosphorylate the intracellular effectors of the extracellular cytokines: receptor-regulated-SMADs (R-SMADs).

Of note, TGFβ2 has a lower affinity with TGFβR2 and needs TGFβR3 (Kim et al., 2019), also named betaglycan, which doesn't have any kinase activity, to be able to bind to TGFβR1 or TGFβR2. Moreover, the affinity of BMP2/4 is greater for BMPR1a or BMPR1b compared to BMPR2 (Koenig et al., 1994). On the contrary, BMP7 has a higher affinity to BMPR2.

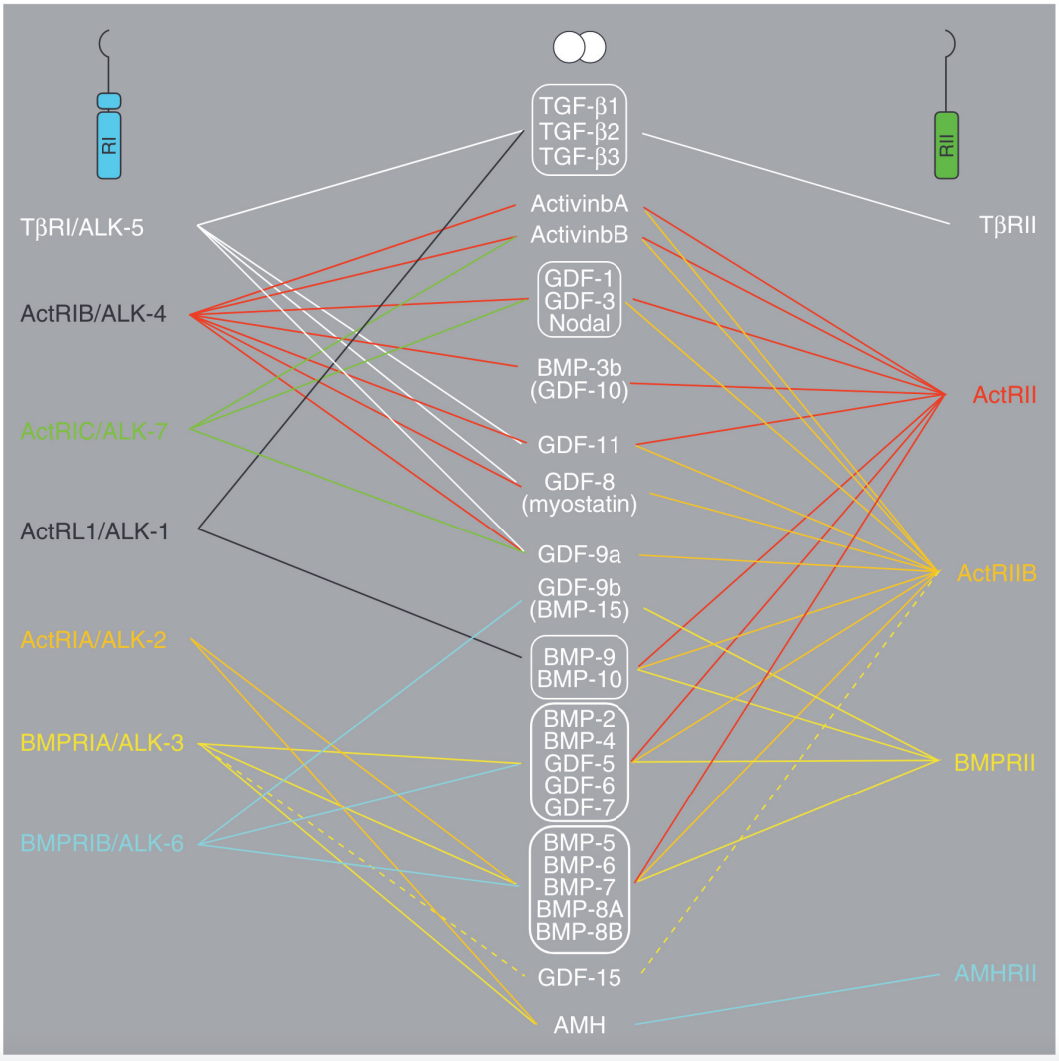

Figure 12: Selective interactions between cytokines and Type-I & Type-II Receptors

Schematic illustration of the selective interaction of TGFβ-family cytokines with type-I and type-II receptors. Many different combinations of cytokines/receptor complexes exist. From Heldin & Moustakas, 2016,

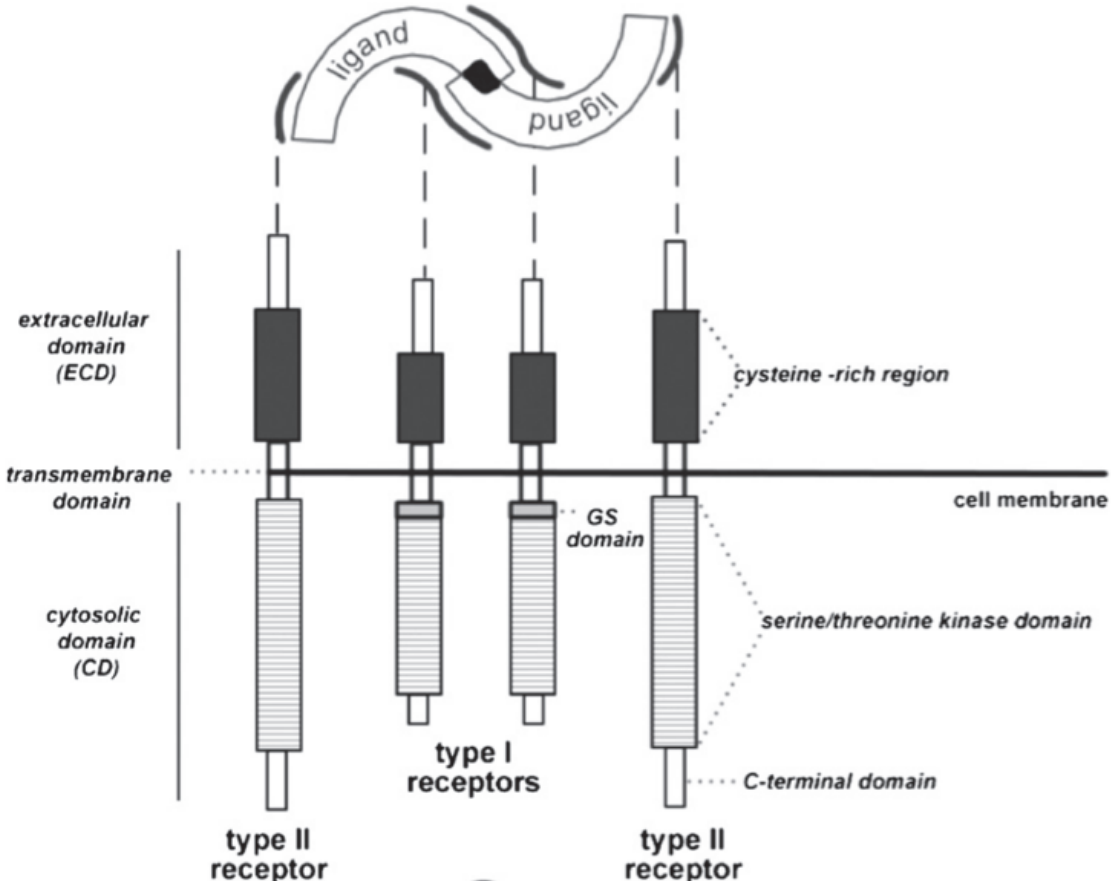

***Figure 13 : TGFB family general ligand-receptor complex**.*

The folded ligand dimer will bind to a heterotetrameric complex with type 2 and type 1 receptors. The Serine/Threonine kinase of the type 2 receptor will then phosphorylate the Type 1 receptor on its Glycine/Serine rich sequence (GS) domain. Adapted from Poorgholi Belverdi et al., 2012

B) Canonical SMAD signaling

The activated receptor complex will then phosphorylate the cytoplasmic effectors of the extracellular ligands: receptor-regulated-SMADs (R-SMADs). In most cases, BMPs will induce the phosphorylation of SMAD1/5/8 and TGFβs of SMAD2/3. Phosphorylated R-SMADs will then bind a common-SMAD, SMAD4, to form heterotrimers. The complex will translocate in the nucleus, regulating the expression of a set of genes by interacting with high-affinity DNA-binding transcription factors and binding to specific promoter regions.

C) Non-Canonical signaling

BMPs and TGFβs can also signal through several distinct SMAD independent pathways called non-canonical signaling. The main family is mitogen-activated protein kinase (MAPK) pathway activation. It is grouped into three subfamilies: extracellular signal-regulated kinases (ERK1 and ERK2), the c-Jun N-terminal kinase (JNK1, JNK2, JNK3), and the p38 MAPK. The PI3K-AKT-mTOR and Rho-like GTPase pathways also are activated by TGFβ-family ligands. These proteins also rely on phosphorylation to be activated. ERK was shown to be phosphorylated several hours after TGFβ treatment (Simeone et al., 2001), which could mean this effect is indirect and that another protein needs to be translated to then activate ERK signaling. But very rapid phosphorylation in 5-10 minutes (similar time course as with EGF) was also shown in other cell types (Olsson et al., 2001). Indeed, after ligand binding, activated TGFBR1 can then phosphorylate Src-homology-domain-2-containing (SHC), which will then lead to the activation of ERK (Lee et al., 2007).

These non-canonical pathways are also part of the wide diversity of effects that the TGFβ-superfamily can have and contribute to how the identical ligands can have multiple functions depending on context.

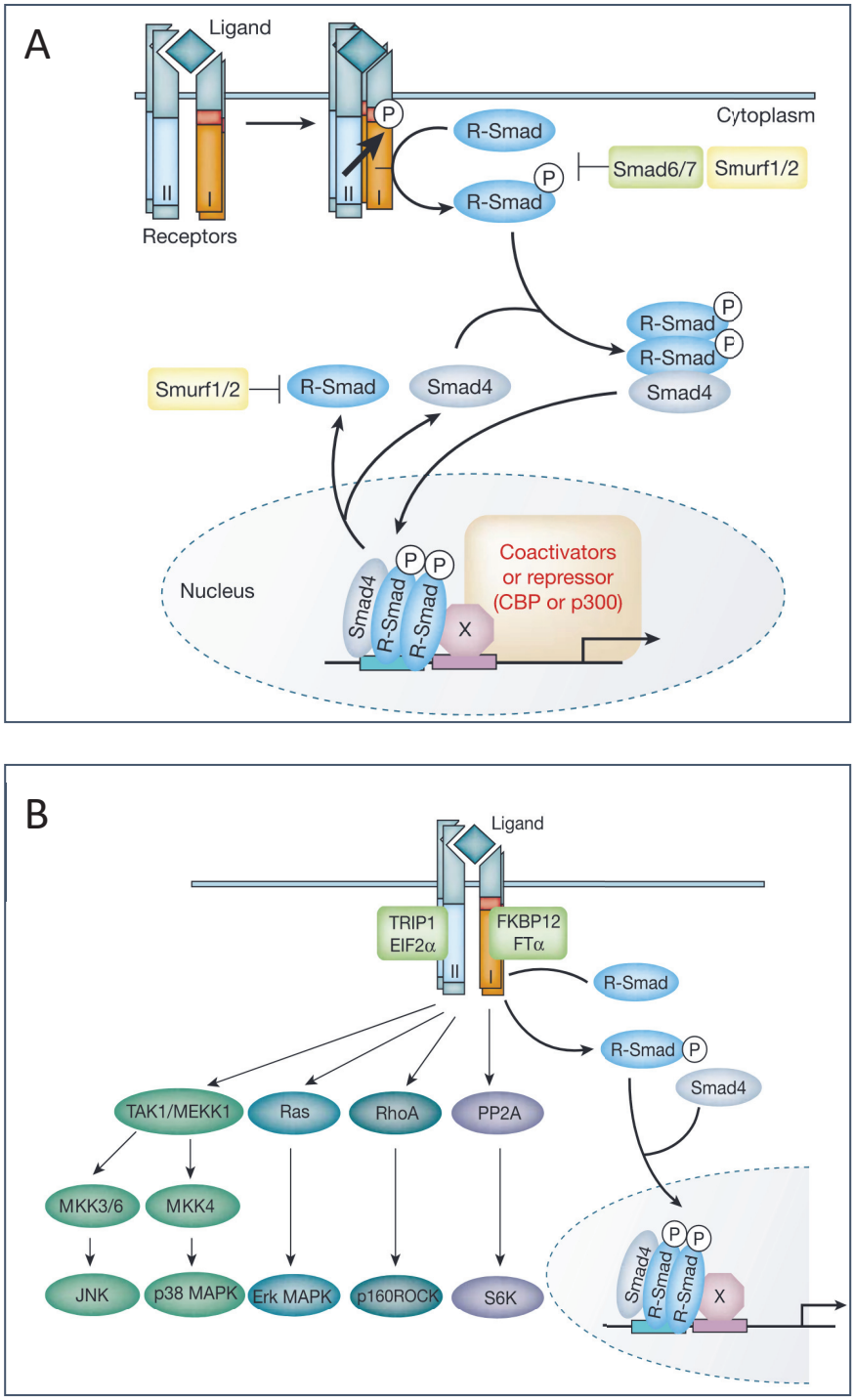

Figure 14: Canonical and non-canonical TGFB/BMP signaling

A. *Ligands binding leads to the formation of a heterotetrameric complex of type1 and type 2 receptors. Type 2 receptors will phosphorylate type 1 receptors, which will subsequently be activated and phosphorylates R-SMAD. R-SMAD will then form a complex with SMAD4 and enter the nucleus to regulate gene transcription by interacting with factors such as CBP or p300 or other DNA-binding proteins. This pathway can be inhibited by SMAD6/7 or Smurf1/2.* ***B****. Non-canonical signaling can also occur via MAPK pathways. Other pathways can include the activation of TRIP1 EIF2a FTa and FKBP12 by interaction with Type 1 or Type 2 receptors. R-SMAD: Receptor-SMAD. Figures adapted from (Derynck and Zhang, 2003)*

D) Regulation of BMP & TGFβ signaling

TGFβ signaling can be regulated at the extracellular level by inhibiting ligand/receptor interactions or at the intracellular level by inhibiting the downstream signaling cascade.

Soluble regulators

At the extracellular level, many other secreted proteins such as Follistatin, Noggin, Chordin, and Gremlin (Chang, 2016) can inhibit ligand interaction with the receptors by decreasing ligand availability or modifying its affinity with the receptor. This plays an essential role in ligand gradient generation, inducing the dorsal-ventral patterning during development (Yan and Wang, 2021). Soluble regulators may have a differential effect on the ligands of the TGFβ superfamily: Connective-tissue growth factor blocks (CTGF) BMP signaling but enhances TGFβ signaling (Abreu et al., 2002). The extracellular matrix is also an important regulator of BMP & TGFβ signaling. Indeed, BMPs have been shown to bind collagen IV to regulate gradient formation in Drosophila (Wang et al., 2008). Moreover, the activation of TGFβ from latent to active form requires interactions with integrins (Munger et al., 1999) and fibronectin (Zilberberg et al., 2012).

Coreceptors

Another way to regulate ligands availability in the extracellular space is by the expression of pseudo receptors. As mentioned above, TGFβR3 is essential to TGFβ2 binding to TGFβR1 and TGFβR2, but TGFβR3 can also be cleaved and secreted. Cleaved betaglycan (also called soluble-TGFβR3) can bind TGFβ2, BMP2, or BMP4 in the extracellular space, limiting their ability to bind to type 1 and type 2 receptors at the membrane (Kim et al., 2019) (Gatza et al., 2014).

Moreover, BAMBI is a truncated type 1 receptor (it does not have a kinase domain) that binds to TGFβs, activins, and BMPs. It dampens their effect by limiting the formation of receptor heterocomplexes (Onichtchouk et al., 1999)

RGM (repulsive guidance molecule) is a coreceptor that enhances BMP canonical signaling by increasing ligand/receptor interaction (Babitt et al., 2005). Endoglin, mainly expressed in endothelial cells and also called CD105, suppresses the TGFβ pathway but promotes BMP signaling (Scherner et al., 2007), and is an essential receptor to BMP9 and BMP10.

Cytoplasmic regulators

The regulation of TGFβ superfamily signaling also happens at the intracellular level with inhibitory SMADs: SMAD6 and SMAD7 (Miyazawa and Miyazono, 2017). They inhibit canonical SMAD signaling by inhibiting the interaction of R-SMADs and the type-I receptors (**Figure 14**) or by inhibiting the interaction of the R-SMADs with SMAD4 the co-SMAD. They also have been located in the nucleus, where they can be transcriptional corepressors of BMP-target genes. They represent an auto-inhibitory feedback mechanism as TGFβ and BMP signaling induce their expression. Smurf1/2 are ubiquitin ligase proteins that can cause the degradation of R-SMADs (**Figure 14**). Inhibitory SMADs can also enable signaling cross-talks. For example, the JAK-STAT pathway can induce SMAD7 expression (Jenkins et al., 2005), thus reducing TGFβ sensitivity.

Overall, TGFβs and BMPs ligands signal by binding to receptors and inducing the formation of heterotetrameric complexes of type 1 and type 2 receptors. The type 2 receptor will then phosphorylate R-SMADs (SMAD1/5/8 for BMPs and SMAD2/3 for TGFβs) that will bind SMAD4. The complex will then enter the nucleus to regulate gene expression. Non-canonical signaling can also occur. These signaling pathways are an integrative platform of extracellular signals that many proteins or other activated pathways can influence. The effect of the TGFβs and BMPs depends on the cellular context and regulates many aspects of cellular functions.

II. TGFβ and BMP in stem and cancer cells

TGFβ and BMP signaling are well-described regulators during development and in many different physiological cell types (Zhang et al., 2017). I am here choosing to focus on the role of BMP and TGFβ signaling in adult stem cells, as it is of strong interest to then compare it to their effect on cell cycle regulation of cancer cells.

A) Adult stem cells

Adult stem cells remain undifferentiated after development and are found in many different body parts to maintain tissue homeostasis. Adult stem cells can be quiescent (hematopoietic stem cells, mammary gland, hair follicles) or inconstant proliferation (intestinal stem cells). By asymmetric division, an adult stem cell can generate one cell that will differentiate and another identical to the cell of origin. These stem cells are localized in niches and respond to microenvironmental signals such as TGFβ and BMP signaling (Xu et al., 2018).

BMP4, but not BMP2 or BMP7, promotes **hematopoietic stem cell (HSC)** self-renewal (Bhatia et al., 1999) in humans. BMP4 has also been shown to promote megakaryocytic differentiation (Jeanpierre et al., 2008) whereas BMP2 commits progenitors towards erythroid differentiation (Maguer-Satta et al., 2003). The quiescence induction role of BMP4 on HSC has also been described in mice (Khurana et al., 2013). The role of TGFβ in HSC has mainly been studied in mice. Although TGFβR1 conditional knock-out in HSCs in mice did not impact their quiescence (Larsson et al., 2005). Instead, Endoglin, a type-III receptor (coreceptor) of the TGFβ family, was shown to promote TGFβ canonical and non-canonical signaling to ensure HSC quiescence in mice (Borges et al., 2019). On top of this, latent TGFβ activation by non-myelinating Schwann cells was shown to induce HSC quiescence (Yamazaki et al., 2011).

In **intestinal stem cells**, conditional knock-out of Bmpr1a in mice led to the expansion of the stem and progenitor cells, thus disturbing tissue homeostasis and leading to intestinal polyposis by suppressing Wnt signaling (He et al., 2004). A mechanistic understanding has been further described in Lgr5+ intestinal stem cells, where BMP signaling restricts their self-renewal. Indeed, Smad1/4 complexes in this model recruit histone deacetylase HDAC1 to negatively regulate stem cell signature programs (Qi et al., 2017). Of note, BMP signaling seems to be of great importance in the functional zonation of the crypt-villus axis (Beumer et al., 2022) on top of regulating intestinal stem cell renewal.

BMP signaling has an opposite effect in **neural stem cells**, where NOGGIN, a BMP inhibitor, induced stem cell differentiation and adult neurogenesis in the subventricular zone (Lim et al., 2000). Confirming this, BMP signaling through BMPR1A regulates the quiescence of neural stem cells in the hippocampus (Mira et al., 2010). TGFβ also induces quiescence of neural stem cells, but surprisingly TGFβR1 activation is also necessary for effective neurogenesis (He et al., 2014) (Kandasamy et al., 2014). Of interest, TGFβ1 has also been shown to participate in neuroprotection by activating survival pathways in neurons (Dhandapani and Brann, 2003).

Similarly, seminal work from Elaine Fuchs showed that BMP signaling mediates quiescence of the **hair follicle stem cell** of the bulge (Kobielak et al., 2007). The cyclic expression of BMP4 and BMP2 in the dermis regulates this process (Plikus et al., 2008). Of interest, TGFβ2 signaling, but not TGFβ1, seems to have an opposing role in this niche as an inducer of hair follicle morphogenesis (Foitzik et al., 1999) and follicle stem cell proliferation (Oshimori and Fuchs, 2012). This antagonistic aspect will be further developed in the TGFβ and BMP signaling interactions part.

In **skeletal muscle stem cells**, BMP & TGFβ signaling promotes differentiation and cell cycle arrest. Indeed, TGFβ effector SMAD3 interacts with the WNT target gene Lef1 during quiescence induction of skeletal muscle stem cells (Aloysius et al., 2018). Moreover, BMP4 inhibits the proliferation of myoblasts and promotes their differentiation by activating canonical SMAD1 signaling and JNK non-canonical signaling (Jeffery et al., 2005). Similar observations were made with BMP7 (Dorai et al., 2000). Additionally, BMPR2 mutations are reported in pulmonary arterial hypertension. In these patients, pulmonary artery smooth muscle stem cell hyperproliferation is observed (Dewachter et al., 2009). This seems to be mediated through reduced BMP4/BMP2 signaling but enhanced BMP6/BMP7 signaling, possibly through the interaction of ActR2a with BMP6/BMP7 instead. (Yu et al., 2005).

A) Dual Role of TGFβs and BMPs in cancer

BMPs and TGFβ have been described both as tumor suppressors and as oncogenes in several cancers (Bach et al., 2017) (David and Massagué, 2018), either in primary tumors or in metastasis. Moreover, the same ligand can have different effects depending on the cancer type and the stage of the cancer. Briefly, TGFβ signaling induces cell cycle arrests in the early phases of tumorigeneses. At later stages, TGFβ signaling in general promote growth and invasion by inducing epithelial to mesenchymal transition (EMT) (Miettinen et al., 1994) (Moustakas and Heldin, 2016). Of note, in studies involving TGFβ signaling, TGFβ1 but not TGFβ2 and TGFβ3 are usually studied. The comparison of the effect of TGFβ1 and TGFβ2 in head and neck cancer highlighted their differential functional consequences: TGFβ1 promoted proliferation, whereas it was inhibited by TGFβ2 (Bragado et al., 2013). BMPs have also been described as tumor promoters (Owens et al., 2012; Pickup et al., 2015) or suppressors (Gao et al., 2012) (Ye et al., 2009) in several models. Of note, BMP4 has also been described as an EMT inducer (Zeng et al., 2017).

Of importance, TGFβ and BMPs can also modulate the tumor microenvironment by activating or inhibiting the immune system. For example, BMP4 represses myeloid-derived suppressor cells that promote metastatic breast cancer tumors (Cao et al., 2014). TGFβ is a well-known inducer of Treg differentiation and attenuates the functions of cytotoxic T cells and NK cells (Sanjabi et al., 2017) (Li and Flavell, 2008). TGFβ and BMP9/10 are also angiogenesis promoters.

B) TGFβs and BMPs in cancer dormancy

As described above, TGFβs and BMPs have many roles in cancer progression and metastasis depending on the cell types and the surrounding cellular context. Evidence is accumulating on their specific role in dormancy induction (Prunier et al., 2019).

Although TGFβ1 was shown to induce quiescence of squamous cell carcinoma cells (Brown et al., 2017), most of the evidence in TGFβ signaling mediated dormancy has implicated TGFβ2. Several studies have identified the role of TGFβ2 in prostate cancer (Yu-Lee et al., 2018) (Yumoto et al., 2016) and breast cancer (Nobre et al., 2021) (Ghajar et al., 2013), and head and neck squamous cell carcinoma (Bragado et al., 2013). Moreover, dormant cells secrete an important amount of TGFβ2, suggesting the existence of a positive feedback loop (Sosa et al., 2015) (Fluegen et al., 2017)

BMP4 has been implicated in mediating the dormancy of breast cancer cells in the lung and leukemic stem cells in the bone marrow (Jeanpierre et al., 2020). It has also been shown to reduce the proliferation of the basal breast cancer cell line MDA-MB-231 (Ampuja et al., 2013). Moreover, BMP4 also reduced glioma stem cell proliferation and increased resistance to treatment through p21 upregulation (Sachdeva et al., 2019). BMP4 pathway activation has also been shown to induce cell cycle arrest in breast cancer cells but increased treatment sensitivity in this model (Shee et al., 2019). BMP7 mediates prostate cancer cell dormancy in mouse models of bone metastasis by promoting stem features of the cells (Kobayashi et al., 2011). A positive feedback loop was described in prostate cancer cells that produced Secreted protein acidic and rich in cysteine (SPARC), which stimulated the expression of BMP7 by mesenchymal stem cells in the bone marrow (Sharma et al., 2016). BMP9 acts as a quiescence factor in murine models of metastasis. Of interest, BMP10 was also tested in this model but did not alter tumor proliferation(Ouarné et al., 2018)

Overall, the TGFβ and BMP families are major regulators of adult stem cell quiescence regulation, but can have opposing roles depending on the context. In cancer, TGFβ and BMP ligand have been described as tumor promoters of inhibitors depending on the tissue type, the cell type, or the stage of the disease. However, increasing amount of literature supports their role as dormancy inducers in disseminated tumor cells.

III. TGFβ and BMP Signaling Interactions

Because of the variety of ligand/receptor complexes and the many different signaling pathways that can be activated, TGFβ and BMP pathways are highly intertwined. The result of the combination is difficult to predict and highly dependent on context. Depending on the cellular context and models, TGFβs and BMPs can have antagonistic or agonistic effects. This part will review TGFβ and BMP interactions in non-cancer settings before focusing on cancer-related interactions.

A) BMP & TGFβ interactions in non-cancer settings

Most description of the **opposite effect** between TGFβ and BMP signaling has been in the field of TGFβ-induced **fibrosis**. In liver fibrosis, BMP2 attenuated the pro-fibrotic effect of TGFβ1 by attenuating the induction of ECM matrices such as fibronectin and vimentin. Moreover, TGFβ1 suppressed BMP2 protein expression and vice versa. (Chung et al., 2018), possibly through the upregulation of SMAD6 and SMURF1, respectively (Wang et al., 2012). In a mouse model of asthma, BMP7 reduced the pro-fibrotic effect of TGFβ1 in the lung. In this model, there was a reduced p-SMAD2/3 and p-p38 when BMP7 was added. (Stumm et al., 2014). A similar molecular mechanism was identified when BMP7 reduced the epithelial to mesenchymal transition induced by TGFβ1 (Song et al., 2020). In the eye's trabecular meshwork, BMP4 inhibits actin-network formation (Mao et al., 2015) and the fibronectin secretion induced by TGFβ2 (Wordinger et al., 2007). The balance of TGFβ2 and BMP4 signaling is thus of importance in **glaucoma** pathophysiology.

In the **hair follicle** niche, TGFB2 signaling decreased BMP signaling to activate hair follicle stem cells by inducing the expression of a target gene, TMEFF1 (Oshimori and Fuchs, 2012). No modification of SMAD phosphorylation was observed. TGFβ and BMP antagonism thus exists in different models, and different molecular mechanisms such as target gene activation or signaling pathway modifications, although not wholly described, can lead to this opposed effect

On the contrary, BMPs and TGFβs can have an **additive or synergistic effect** in other contexts, such as **chondrogenic differentiation**. Several pairs of TGFβ and BMPs have been studied in the induction of chondrogenic differentiation of mesenchymal stem cells. BMP2 & TGFβ1 (Legendre et al., 2017), BMP7 & TGFβ1 (Iwakura et al., 2013), BMP7 & TGFβ3 (Crecente-Campo et al., 2017), and BMP2 & TGFβ3 (Shen et al., 2009, p. 1317) co-signaling all enhanced chondrogenesis. In (Shen et al., 2009, p. 1317), this effect was due to synergistic upregulation of SMAD6 and SMAD7 leading to SMAD3 downregulation, and surprisingly, inhibition of ERK signaling led to enhance synergy between BMP2 & TGFβ3.

In **osteogenic differentiation** induction of mesenchymal stem cells, a synergy between TGFβ1 & BMP2 (Asparuhova et al., 2018), BMP9 & TGFβ1 (Li et al., 2015) but also between BMP2 & TGFβ3 (Wang et al., 2016b) was observed. The prolonged BMP signaling activation with enhanced phosphorylation of SMAD1/5 led to increased osteoblast differentiation (Asparuhova et al., 2018).

In **immunity**, TGFβ is a well-known inducer of T cell differentiation towards the regulator T cell phenotype (immune-suppressive). TGFβ-induced Treg differentiation was stronger in combination with BMP2/BMP4, although BMP2/BMP4 alone would not induce this specific differentiation. The molecular mechanism suggested a higher induction of non-canonical signaling with higher ERK and JNK phosphorylation (Lu et al., 2010). The additive effect between TGFβ and BMP signaling can thus be dependent on non-canonical as well as canonical signaling activation depending on the context.

B) BMP & TGFβ interactions in cancer

BMP and TGFβ signaling interactions in cancer have not been extensively studied. In most studies, they have opposite effects (Ning et al., 2019).

BMP7 treatment on MDA-MB-231 breast cancer cells did not affect cell proliferation but was shown to counteract TGFβ2 mediated EMT and decrease bone metastasis in mice (Buijs et al., 2007). An in vitro invasion model of the fully transformed derivative of MCF10A MCF10A-CA1 (Kadota et al., 2010) showed that BMP7, but not BMP6, inhibited the invasion phenotype mediated bt TGFB1 by inhibiting the TGFβ-induced expression of integrin alpha-5 beta-3. (Naber et al., 2012). Moreover, BMP9 was shown to inhibit bone metastasis of breast cancer cells by downregulating connective tissue growth factor (CTGF), a downstream target of the TGFβ pathway (Ren et al., 2014)

In prostate cancer cells, BMP7 was shown to attenuate the growth inhibitory effect of TGFβ (Yang et al., 2005). Inactivation of TGFBR2 led to decreased TGFβ signaling but increased BMP signaling. This enhanced cellular plasticity and increased the expression of pluripotency markers (Zhao et al., 2018)

Interactions between TGFBs and BMP signaling can also occur at the membrane during ligand/receptor interaction. TGFBR3 can bind BMP2, BMP4, and BMP7 and present them to type 1 BMPR, enhancing BMP signaling activation. (Kirkbride et al., 2008). The balance of soluble TGFBR3 (TGFBR3 can be cleaved and secreted in the extracellular space) and membrane-bound TGFBR3 was indeed shown to regulate BMP signaling in normal and cancerous mammary epithelial cells (Gatza et al., 2014).

The BMP pathway inhibits the EMT and stem-like features mediated by TGFβ signaling in breast cancer. In prostate cancer, TGFβ signaling has been described to inhibit proliferation and stemness while BMP signaling promotes it. Overall, BMP and TGFβ interactions are highly context-dependent, and the receptors and molecular pathways involved are rarely fully explored.

RESULTS

PHD PROJECT – SCIENTIFIC CONTEXT

This project is the start of an exciting collaboration between Véronique Maguer-Satta and Julio Aguirre-Ghiso's lab which emerged from the common interest of Dr. Maguer-Satta, Pr. Aguirre-Ghiso and myself in understanding mechanisms that drive cancer relapse. Half of my PhD was spent in Dr. Maguer-Satta's lab, and the other half in Pr. Aguirre-Ghiso's lab.

Pr. Aguirre-Ghiso is an expert in cancer metastasis and has made seminal contributions to understand the biology of disseminated tumor cell dormancy. He has been working on disseminated tumor cell dormancy in the bone marrow (BM) for many years, which led to a better understanding of the role of mesenchymal stem cells and TGFβ2 in mediating cancer cell dormancy in the BM. I actively participated in this research during my Master 2 internship and during the first year of my PhD, which led to the publication (Nobre et al., 2021) where I am second author (pdf in Appendix 2). After my Master 2 internship, I decided to continue with a scientific PhD before continuing my medical studies. Véronique Maguer-Satta had the perfect common interest and complementary expertise to further expand the project. Indeed, Dr. Maguer-Satta has a long-standing expertise on BMP signaling in the stem cell niche and is now unraveling its implication in breast cancer initiation and in cancer stem cell persistence. Of importance, recent work from the lab showed that in patients with chronic myeloid leukemia in complete remission, BMP4 niche signals allow for the persistence and quiescence of leukemic stem cells.

Deep scientific discussions and exchanges on the recent results obtained from both labs led us with the strong will to better understand the coordination of BMP and TGFβ signaling in breast cancer cell dormancy in the bone marrow. Why is the bone marrow niche such a strong pro-dormancy microenvironment? Most studies assess the role of one cytokine or ligand. Does the combination of signals affect dormancy induction? We chose to focus on TGFβ2, BMP2 and BMP4 based on the expertise of Pr. Aguirre Ghiso on TGFβ2, of Dr. Maguer Satta on BMP2 and BMP4. Moreover, as described in the introduction of this manuscript, there is an important scientific literature on the interaction of TGFβ and BMP signaling, but this interaction in cancer cell dormancy had not been previously studied.

For this PhD project, we developed 3 aims:

- Aim 1 : **Functional evidence of the co-signaling effect of BMP4 and TGFβ2 on the regulation of breast cancer cell dormancy**

This aim was fully reached as I have demonstrated the synergistic effect of BMP4 and TGFβ2 in breast cancer cell dormancy in both human and murine *in vitro* 2D and 3D models with several assays. As you will assess in this results part, we focused only on TGFβ2 and BMP4: BMP2 had no effect on cell cycle regulation in our models (this will be further discussed in the discussion part).

- Aim 2 : **Mechanistic understanding of the signaling pathways involved in TGFβ2 and BMP4 dormancy induction**

To assess this, bulk and single-cell RNAseq were performed and shed light to the co-signaling effect of BMP4 and TGFβ2 on gene transcription. I did the single-cell RNAseq analysis by myself and I am still continuing to further analyze this data. I am now mentoring a master student to decipher the differential signaling pathways activated and preliminary data will be shown in the second results part.

- Aim 3 **: *in vivo* validation using murine models and a 3D-microphysiological system of the human bone marrow niche**

To study breast cancer cell metastasis under in more physiological conditions, I have optimized a 3D-microphysiological system of the BM niche previously developed in Dr. Maguer-Satta's lab to study leukemic cells *in situ* (Voeltzel et al., 2022) and performed preliminary *in vivo* experiments in Pr. Aguirre-Ghiso's lab.

Results from Aim 1 and Aim 2 are presented in the results section in a scientific paper format soon to be submitted. Optimization and preliminary experiments of additional experiments of Aim 2 and Aim 3 have been performed and are presented in a second part of the results section.

Thus, the overall objective of my PhD was to understand the co-signaling effect of TGFβ2 and BMP4 on dormancy induction of breast cancer cells disseminated in the bone marrow. This will hopefully lead to a better understanding of cancer dormancy and the identification of potential therapeutic target to prevent relapse in patients.

SCIENTIFIC PAPER

Heterogeneity of breast cancer cell dormancy in the bone marrow is co-regulated by TGFB2 and BMP4

Emma Risson[1,2,3], Boris Guyot[2], Laurine Moindrot[2], Sandrine Jeanpierre[2], Sylvain Lefort[2], Ana Rita Nobre[3], Julio A. Aguirre-Ghiso[3,*], Véronique Maguer-Satta[2,*]

[1]Université de Lyon, Lyon, France,

[2] Centre de Recherche en Cancérologie de Lyon, Lyon, France,

[3]CDTMI, Albert Einstein College of Medecine, NYC, NY, USA

*Corresponding authors

Dormancy of disseminated tumor cells in secondary organs leads to late breast cancer-related deaths after relapse. The bone marrow is one of the primary breast cancer metastatic sites and is associated with poor prognosis. Here, we investigated the role of major factors of the bone marrow, BMP4 and TGFβ2, in regulating cancer cell dormancy. Unexpectedly, we observed that TGFβ2 and BMP4 have a synergistic effect that induces dormancy in both normal and transformed mammary stem cells. Several assays (3D matrigel, FUCCI Cell Cycle Indicator) showed that co-exposure to TGFβ2 and BMP4 had a stronger anti-proliferative effect than each ligand alone. In addition, transformed cells fully retained this synergistic effect while they became less sensitive to individual cytokines. Surprisingly, single-cell RNAseq analysis revealed the heterogeneity of the G0 compartment at the transcriptomic level. We identified a unique deep dormant cluster under TGFβ2 and BMP4 co-exposure characterized by a blended signature from treatments by TGFβ2 or BMP4 alone. These findings reveal that disseminated breast cancer cells in the bone marrow are placed in a deep dormant stage by the synergistic effect of TGFβ2 and BMP4 that neither factor can achieve alone. Lastly, our data suggest that the local BMP4 levels decrease with tissue aging and can therefore contribute to dormant cell awakening. By providing a better understanding of BMP4/TGFβ2 signaling, our results open opportunities to prevent cancer relapse.

Introduction

Among all cancers, breast cancer has the highest incidence and mortality[1]. Most breast cancer-related deaths are triggered by metastasis that can arise years or even decades after treatment and primary tumor removal. Indeed, twenty percent of the patients who have not relapsed in the first ten years post-surgery will do so in the following 20 years[2]. These late relapses are due to disseminated tumor cells (DTC) that can remain dormant in secondary organs for years[3]. Growth arrest, expression of pluripotency markers, survival, and resistance to treatment characterize dormant DTCs[4]. For reasons we ought to better understand, dormant cancer cells can sometimes awaken and re-enter the cell cycle, leading to their proliferation and secondary tumor formation, ultimately causing patient relapse and possible death. Observations have documented that the fate of the DTC is niche-dependent[5]: depending on which organ and niche the DTC seeds, it will not have the same phenotype and outcome. Understanding the crosstalk between DTCs and their microenvironment is therefore essential to treat or prevent relapse. Dysregulation of balanced niche signals[6], aging[7,6], and inflammation[8] can awaken dormant cancer cells. But somehow, even though all patients will age, and many will undergo inflammatory processes throughout their lives, many will not relapse. Understanding what makes the robustness of dormancy-inducing cues will be essential to preventing relapse in patients.

One of the most robust environments controlling DTC dormancy is the bone marrow (BM). In this site, while cancer cells can persist for years without growing[9,10,11], they are commonly considered a poor prognosis marker since BM-dormant cells can eventually awake. Hence, it is essential to understand which cues of the BM support cancer cell dormancy. Indeed, the BM niche is a complex microenvironment physiologically where many signals that regulate hematopoietic stem cell quiescence[12] also control cancer cell dormancy[4,13]. In murine models, Mesenchymal Stem Cells (MSCs) cells constitute a BM population of stromal cells essential to hematopoietic stem cell maintenance[14,15]. Indeed, the specific deletion of TGFβ2 in $NG2^{+}$/$Nestin^{+}$ MSCs led to the awakening of breast cancer disseminated tumor cells[16], but with a lower penetrance than the 50% depletion $NG2^{+}$/$Nestin^{+}$ MSCs. This data suggest that other contributing factors secreted from the MSCs could be involved in cancer cell dormancy. In this context, single-cell RNAseq from mouse BM showed that MSCs are

one of the most important sources of BMP4[17]. Inhibition of BMP signaling awakens dormant breast cancer cells in the lung[18]. In chronic myeloid leukemia, BMP4-niche signals maintain persistent quiescent leukemic stem cells during undetectable minimal residual disease in patients[19]. Although BMP4 and TGFβ2 are dormancy inducers in several models[20], their crosstalk and interdependency have never been assessed, even though they often drive opposite functional effects. Here, we investigated whether crosstalk or antagonism between these two cytokines would contribute to the robust dormancy induction observed in the BM. We reveal an unknown synergistic effect between TGFβ2 and BMP4 in inducing breast cancer cell dormancy. TGFβ2 and BMP4 co-exposure caused a deep dormancy phenotype in human and murine breast cancer models, independently of the transformation mechanism. Bulk and single-cell RNAseq revealed the heterogeneity of the G0 compartment and led to the identification of a unique deep dormancy signature.

Results

BMP4 and TGFB2 treatment induce an elevated and specific dormant stage in murine breast cancer models. In the bone marrow, TGFβ2 has been identified as a regulator of breast cancer dormancy[16] while BMP4 regulates leukemic stem cell quiescence[19]. To determine the relative function of these two members of the TGFβ family on breast cancer cell dormancy, we analyzed the ability of BMP4 alone or in combination with TGFβ2 to induce breast cancer cell dormancy. For that purpose, we used the murine PYMT breast cancer cell line that responds to TGFβ2 dormancy induction in the BM niche *in vivo*[16]. We first used a 3D matrigel model to evaluate cell dormancy[21]. Murine PYMT cells were seeded on top of matrigel at a very low density to mimic their arrival in a secondary organ. Cells were treated with TGFβ2 and/or BMP4 (5 ng/mL) for three days, then the medium was changed, and the percentage of single cells and clusters was quantified seven days later (Fig.1a). PYMT cells responded to TGFβ2 or BMP4 by growth arrest, as shown in Fig. 1b,c. Interestingly, when combined, TGFβ2 and BMP4 displayed a higher anti-proliferative effect compared to individual ligands, as indicated by the increase in the proportion of single cells (3-fold, 2-fold or 5-fold increase under TGFβ2, BMP4, or combined treatment) and a marked reduction in the proportion of clusters (2-fold, 1.5-fold or 7-fold decrease under TGFβ2, BMP4 or combined treatment, Fig. 1b). This additive effect was confirmed by a marked reduction in the proportion of Ki67-positive cells when both

cytokines were combined (Fig. 1D, Supplementary Fig. 1A). Interestingly, treatment with both TGFβ2 and BMP4 also reduces stem capacities of PYMT cells, as indicated by their decrease in mammospheres formation (Supplementary Fig. 1b). To verify that other mechanisms did not arrest cells, we evaluated cell apoptosis (Fig. 1e, Supplementary Fig 1c) and senescence (Fig. 1f) by classical caspase-3 cleavage or B-galactosidase assays in the 3D matrigel experiments. We did not observe any significant differences in TGFβ2 or BMP4 treatment alone or in combination. This indicates that apoptosis and senescence are not involved in the measured cell cycle arrest. To verify whether the observed effect is related to the PYMT model, we used the E0771[22] model, another murine cell line of luminal breast cancer subtype. We used a label retention assay where doxycycline induces H2B-GFP expression. After cytokine treatment in 3D matrigel, the fraction of GFP^{high} cells that have not diluted the H2B-GFP by division was quantified by flow cytometry. The highest proportion of GFP^{high} cells had almost a 2-fold increase (34% to 64%) under BMP4 and TGFβ2 co-exposure as compared to nontreated (NT), while only 1.1- and 1.4-folds were observed under TGFβ2 or BMP4 alone (Supplementary Fig. 1d).

To further characterized the dormancy status induced by the co-exposure to BMP4 and TGFβ2, we performed RNAseq analysis on PYMT-treated cells. This revealed that 21.6% of upregulated and 15.9% of downregulated genes were specific to the BMP4/TGFB2 combined treatment. This indicates that a distinct transcriptional program was induced in the combinatory condition: additional genes were regulated on top of the ones regulated by TGFβ2 or BMP4 alone (Fig. 1g,h, and Supplementary Fig. 1e,f). Moreover, genes uniquely downregulated in the BMP4/TGFβ2 condition showed enrichment for cell cycle signatures (“Cell Cycle”, “S Phase”, “DNA Replication”), proving the induction of a more robust growth arrest program in the combinatory condition compared to TGFβ2 of BMP4 solo effect (Fig. 1i,j). Notably, the dormancy status is confirmed by the fact that genes upregulated in all treatments are enriched in the urokinase plasminogen activator pathway, already associated with dormancy[23]. Interestingly, a downregulation of the interferon signaling was also identified (Supplementary Fig. 1g,h). Analysis of transcription factor signatures identified RXR, NRF2, MYOD1, FOXA1, and E2F4 as transcription factors uniquely activated in the combinatory condition (Supplementary Fig. 1i). Overall, BMP4 and TGFβ2 co-signaling appeared to control a specific dormancy compared to single cytokine signaling.

Dormancy induction by BMP4 and TGFβ2 is conserved in human mammary cell lines regardless of their transformation and ER status. To evaluate whether the TGFβ2 and BMP4-induced cell arrest is also observed in human cells, a range of non-transformed and transformed mammary cell models were treated by cytokines alone or in combination. First, we analyzed the effect of TGFβ2 and BMP4 treatments on classical estrogen receptor-positive (ER+) human breast cancer models, the MCF7 and T47D cell lines. Similar to murine cells, substantial growth restriction was observed in both cell lines under simultaneous TGFβ2 and BMP4 treatment (Fig. 2a). Interestingly, the T47D human cell line appeared more sensitive to BMP4 than to TGFβ2. Next, we evaluated whether TGFβ2 and BMP4 effects apply in different transformation contexts using estrogen receptor-negative (ER-) models: RAS-induced transformed DCIS.com[24] and MCF10A-derived cell lines[25,26]. The majority of DCIS cells entered dormancy when treated with TGFβ2 or BMP4 alone (almost 75%) and reached 95% of arrested cells in the presence of combined cytokines (Fig. 2a). We also used another MCF10A-derived model of oncogene-independent progression previously generated by long-term exposure to IL6 & BMP2[25] (Guyot et al., 2022, submitted). The CT, MC26, and more advanced M1B26 cell lines are the progressively transformed cell lines (Supplementary Fig. 2a). In the MCF10A-CT control and MC26 or M1B26 transformed cell lines, the combinatory effect of BMP4 and TGFβ2 was again the same as in murine and other tested models (Fig. 2b,c). Although a similar functional effect of BMP4 and TGFβ2 was observed across cell lines, flow cytometry staining of CD44/CD24 and EpCAM/CD10 expression and TDLU assays confirmed their differential stem cells phenotypical features[25,26] (Fig. 2d,e and Supplementary Fig. 2b). Thus, the BMP4 and TGFβ2 effect seemed to be a general mechanism in the mammary epithelium that also exists in normal stem cells (MCF10A cell line) and that is conserved upon transformation, independently of the transformation mechanism and ER status.

Effect of TGFβ2 and BMP4 on the proportion of cells in G0 state in normal and transformed breast cancer cells. To better quantify the cytokine effect and cell cycle state of the cells, the Fluorescent and Ubiquination-based Cell Cycle Indicator (FUCCI)[27] was incorporated into our models to generate the MCF10A-FUCCI and M1B26-FUCCI cell lines (Fig. 3a). Cell cycle phase are identified based on the intensity of mCherry and mVenus fluorescence (G0 phase: $mCherry^{high}/mVenus^{-}$, G1 phase: $mCherry^{low}/mVenus^{-}$, S phase: $mCherry^{-}/mVenus^{+}$, G2/M phase: $mCherry^{+}/mVenus^{+}$, Fig. 3b and Supplementary Fig. 3a). $mCherry^{high}/mVenus^{neg}$ cells (G0) have a lower Ki67 expression compared to $mCherry^{low}mVenus^{neg}$ (G1) cells (Fig. 3c and Supplemental Fig. 3b). Indeed, G0 and G1 separation based on mCherry intensity was already demonstrated in other models[28,29]. Moreover, functional evidence of G0 and G1 difference was observed in our model after sorting different cell cycle phases in a mammosphere assay: G0 cells formed more mammosphere but were smaller in size compared to G1 cells or cells from all the cell cycle phases combined (Fig. 3d,e).

Performing cell cycle analysis in FUCCI cell lines treated with TGFβ2 and BMP4 confirmed the pro-dormancy effect of TGFβ2 accumulation of cells in the G0 phase upon treatment, particularly in the TGFβ2+BMP4 (Supplemental Fig. 3c). As previously observed using the 3D matrigel assay, an impressive combined effect of TGFβ2 and TGFβ2 on cell cycle arrest was detected. This effect was specific to BMP4, as BMP2 treatment did not increase the proportion of G0 cells (Supplemental Fig. 3d). Moreover, BMP2 treatment did not affect the BMP4 or TGFβ2 effect. A factorial design experiment was performed to further characterize the relative importance of TGFβ2 and BMP4 cytokines to test multiple concentrations ranging from 0.5 to 20ng/mL. When MCF10A-CT cells were treated with TGFβ2 only, a 3-fold increase in the percentage of G0 cells was induced. A plateau was reached at 5ng/mL. This increase reached 4-fold in cells treated with BMP4 only. When cells were treated with the combination of both cytokines, the effect was then maximum, reaching an 8-fold increase in the proportion of G0 cells (Fig. 3f, Supplemental Fig 3e-g). In the transformed cell line M1B26, a tendency to a reduced effect of single cytokine effect but a conserved effect of the combination of the cytokines was observed (Supplemental Fig. 3h).

To determine if the combinatory effect of the cytokine was additive or synergistic, the zero-interaction potency (ZIP) synergy score[30] was computed with the SynergyFinderPlus software[31], showing that the BMP4 and TGFβ2 effect was indeed synergistic (Fig. 3g). In human bone marrow supernatant samples from healthy donors, there is a tendency for a decrease in BMP4 levels with age (Fig. 3h), which could explain the awakening of cancer cells after prolonged periods of dormancy. Overall, the FUCCI cell cycle indicator confirmed the strong dormancy induction by TGFβ2 and BMP4 co-signaling in MCF10A-CT cells. This synergistic effect is fully retained in transformed M1B26 cells while they are less sensitive to individual cytokines.

Cells treated with BMP4+TGFB2 are in a deeper dormancy state. To better assess the combinatory effect of TGFβ2 and BMP4 on inducing cell cycle arrest, we took advantage of the FUCCI system that allows for the sorting of cells in specific cell cycle phases. To define the particular effect of the BMP4 and TGFβ2, we focused on the G0 cell compartment. Cells from nontreated, TGFβ2-treated, BMP4-treated, or TGFβ2+BMP4 treated cells were sorted for G0 fraction and seeded at equal numbers in different assays without any treatment (Fig. 4a). Functional evidence showed that G0 cells from the co-exposure to BMP4 and TGFB2 conditions were in a deeper arrest than in the other conditions (Fig. 4b-e). Indeed, 2D growth kinetics (Fig. 4b,c), 3D matrigel low-density assay (Fig. 4d), and mammosphere assay (Fig. 4e) showed that G0 cells from the BMP4+ TGFβ2-treated condition required longer time to re-enter cell cycle as compared to nontreated cells or cells treated by TGFβ2 or BMP4 alone. Importantly, the fact that quiescent G0 cells proliferate again after seeding shows that these cells are not senescent, confirming what was observed with murine cells (Fig. 1f). It also indicates that BMP4+TGFβ2-treated cells can awake and re-enter the cell cycle. The differences observed in cell awakening suggest that although all sorted cells were in the G0 phase, they were not in the same dormancy state. Dormant cells from BMP4+TGFβ2 treated condition seemed in deeper dormancy as compared to other conditions.

To assess this heterogeneity of the G0 compartment at the molecular level, single-cell RNAseq was performed on sorted G0 fractions of controlled (CT) or transformed (M1B26) MCF10A-cells treated by cytokines alone or in combination. UMAP representation of cells based on their sample of origin showed a clear separation of

NT, TGFβ2, BMP4, and BMP4+TGFB2 treated cells in both models. Clustering based on similarity identified 8 clusters in the MCF10A non-transformed cell line and 6 clusters in the M1B26 transformed cell line (Fig. 4f). Cluster 0 in MCF10A-CT and cluster 3 in M1B26 were specific to the TGFβ2 +BMP4 conditions. Both of these clusters had a higher dormancy signature score[32] compared to the mean score across all cells (Fig. 4g). Cluster 3 in MCF10A and cluster 2 in M1B26 mainly represent G0 cells from the NT conditions and significantly lower dormancy scores (Fig. 4g). Of note, C4, C5, C6, C7 in MCF10A and C4 and C5 in M1B26 are shared across several samples of origin and have a lower dormancy score and a higher Ki67 expression (Fig. 4g, Supplementary Fig. 4e). We hypothesize that they are contamination by cycling (non-G0) cells, as they have high Ki67 expression compared to other clusters. Overall, functional and molecular evidence reveals the heterogeneity of the G0 compartment, with some clusters being in deeper dormancy compared to others.

TGFB2 and BMP4 signaling rewiring and identification of a deep dormant signature in breast cancer cells. Pathway enrichment analysis of the overlap of downregulated markers in MCF10A and M1B26 confirmed these cells' strong cell cycle arrest with FOXM1, MYC, and E2F4 signatures (Fig. 5a). This signature is also enriched in extracellular matrix (ECM) genes and epithelial-to-mesenchymal transition (EMT) signatures (Fig. 5b). Heatmap representation of upregulated markers in the CT (Fig. 5c) and M1B26 (Fig. 5e) cell lines shows that there is a complete rewiring of the TGFβ2 and BMP4 signature when cytokines are combined (Fig. 5c): new genes are upregulated specifically in the BMP4+TGFB2 conditions (A group). In contrast, other genes from TGFB2 or BMP4 condition are maintained at similar levels in the BMP4+TGFB2 condition (B group). Indeed, specific genes are not markers in the single-cytokine treatment but only in the combinatory condition are in tables (Fig. 5c,d, and Supplementary Fig. 4b-d). Genes specific to the combinatory conditions are listed in Supplemental Table 1 and Supplemental Table 2. Future potential targets of interest are highlighted depending on their cellular functions (Fig. 5e,f). Of interest, extra-cellular matrix proteins (collagens and integrins), TGFβ/BMP inhibitors, and immune regulatory proteins are upregulated in the combinatory conditions. On the contrary, anti-apoptotic (BAX, TNFRSF6B) and proliferation-associated genes (MYC, RAN,

RHOD) are down-regulated specifically in the combinatory condition. Interestingly, some genes specific to the combinatory condition in the M1B26 cell line are not specific to the combinatory condition in the transformed MCF10A cell line. Overall, there is a qualitative and quantitative rewiring of the TGFB2 and BMP4 signatures when both cytokines are combined, leading to a deeper cell cycle arrest with a specific deep dormant signature.

Discussion

Overall, this work led to the first description of a synergistic co-signaling of TGFB2 and BMP4 signaling on breast cancer dormancy induction. This effect exists in normal human mammary cells and is conserved in human and murine cancer cells, independently of the transformation mechanism or the estrogen receptor status of the cells. Functional assays revealed the heterogeneity of the G0 compartment, and single-cell RNAseq identified a specific deep dormant signature.

Although Ki67 levels are different across cell cycle phases, functional characterization of the difference between $mCherry^{high}/mVenus^{neg}$ (G0) and $mCherry^{low}/mVenus^{neg}$ cells (G1) in the FUCCI system. However, G0 and G1 cells were already separated using the FUCCI system in other models of embryonic development[28] and immune system[29]. Live imaging showed that $mCherry^{high}/mVenus^{neg}$ (G0) took longer to enter the cell cycle than $mCherry^{low}/mVenus^{neg}$ cells (G1)[29]. The fact that quiescent G0 cells proliferate again after seeding shows that these cells are not senescent and can re-enter the cell cycle, potentially leading to relapse in patients. Diversity is also found inside a specific condition, meaning that all cells did not respond to the signal in the same manner. Cells from the BMP4+TGFB2 conditions are divided into two main clusters: cluster 3 and cluster 5 (and a few cells in cluster 4). Cluster 3 and Cluster 5 both have a high dormancy score. On the other hand, although MKi67 was not detected in most of the cells in cluster 3, the cells from cluster 5 had a higher MKi67 expression. A similar observation can be made in the TGFB2 condition divided into clusters 1 and 4: they have similar dormancy signatures scores, but cluster 4 has a higher KI67 expression. We hypothesize that these clusters could be contaminated from cells in the G1 or G2/M phase. This could be due to a technical issue with the sorter or a non-perfect FUCCI system. The analysis of the deep dormant signatures was thus focused

on the signature of cluster 3. Incorporating actively cycling cells (G1 or S/G2/M phases) signatures in this single-cell RNAseq would assess if the cells from clusters 4 and 5 are indeed cycling as these Ki67 levels might be very low compared to cells in the G2/M phase. Incorporating other cell cycle phases in this analysis would have also allowed us to assess if this heterogeneity was specific to the G0 cell cycle phase or if a similar pattern exists in other cell cycle phases.

A specific signature of the BMP4+TGFβ2 condition in both the bulk PYMT data and the MCF10A scRNAseq is the E2F4 signature. Of interest, SMAD3 and E2F4 were shown to form a complex pre-assembled in the cytoplasm[33] that is associated with SMAD4 to repress MYC expression upon TGFβ treatment. Assessing if a specific SMAD heterocomplex is formed with E2F4 could lead to a potential therapeutic target? Indeed, the E2F4 signature has been associated with treatment resistance in ER+ breast cancer[34]. Could the dormancy phenotype induced by TGFB2 and BMP4 also lead to treatment resistance?

Moreover, aging remodels the bone marrow microenvironement[6, 7]. The decrease of BMP4 levels with age can explain late relapses in ER+ breast cancer patients. According to our study, one factor decreasing would be enough to awake cancer cells and lead to metastatic relapse. Moreover, BMP4 could serve as a biomarker to predict if the patient is at risk of relapse and if treatment uptake is needed.

Altogether, we have shown that BMP4 and TGFβ2 co-signaling strongly reinforce a pro-dormancy phenotype induced by both cytokines alone. The balance of niche signals is thus essential to keeping cancer cells dormant. A better understanding of cancer cell dormancy will lead to a therapeutic breakthrough to prevent or predict metastatic relapse in patients.

Methods

Cell culture. MCF10A-CT, MC26, M1B26, MCF10A-DCIS, MCF10A-CA.1a and MCF10-AT1 cell lines were cultured in Dulbecco's Modified Eagles Medium Ham's F12 (DMEM-F12, Gibco), without phenol red, supplemented with 2% horse serum (Gibco), 10 000U/ml - penicillin and 10 000µg/ml - streptomycin (Gibco) (P/S), 10µg/ml insulin (NovoRapid CLB pharmacy), 0,5µg/ml hydrocortisone (Sigma), 100ng/ml cholera toxin (Sigma), 20ng/ml epithelial growth factor (Sigma). Media of MC26 and M1B26 was supplemented with 5ng/ml BMP2 (R&D) and 10ng/ml IL6 (Peprotech). PYMT cell line was cultured in Dulbecco's Modified Eagles Medium Ham's F12 (DMEM-F12, Gibco), without phenol red, supplemented with 10% fetal bovine serum (Dutcher), 1% P/S, 10µg/ml insulin (NovoRapid CLB pharmacy), 1µg/ml hydrocortisone (Sigma), 50ng/ml epithelial growth factor (Sigma). HS27A, MCF7, T47D, MDA MB231, E0771-tetON-H2B-GFP, and 22RV1 were cultured in RPMI 1640 with Glutamax (Gibco) supplemented with 10% fetal bovine serum. HMEC1 cell line were cultured in MCDB131 (Gibco) supplemented with 1°% fetal bovine serum, 1% glutamax (Giboc), 1 µg/ml hydrocortisone, and 10ng/ml epithelial growth factor. For functional assays, cells were treated with concentrations ranging from 0.5ng/mL to 20ng/mL of TGFB2, BMP4, or both in serum-free media. For all experiments, M1B26 were not cultured with BMP2 and IL6.

Functional assays. For the 3D on-top of matrigel in a low-density assay, the protocol was adapted from[21]. Briefly, a total of 500–1,000 cells were seeded in 400 µl assay medium (each cell line medium with reduced fetal bovine serum, or horse serum, content (2–5%) in eight-well chamber slides (Falcon) on top of 50 µl of growth factor-reduced Matrigel (Corning). Cultures were treated every 24 h for 3 days, starting at day 0 with TGF-β2 (R&D), BMP4 (R&D), or both. The media were changed on day 3. The size and numbers of SCs, doublets, and clusters were quantified after 10 days with ImageJ software.

To assess cell cycle phases in culture with the FUCCI system, 25,000 cells were seeded in a 24-well-plate well in serum-free MCF10A-CT media and treated with TGFB2, BMP4, or both (concentrations specified in the figures). 72h later, cells were trypsinized and were analyzed for their mCherry and mVenus intensity by flow cytometry.

For mammosphere assays, sorted MCF10A-FUCCI or M1B26-FUCCI cells were seeded at limiting dilutions (50 cells/ml) on 96-well ultra-low-attachment plates (BD Corning) in serum-free basal mammary epithelial growth medium (Promocell) supplemented with B27, 4 mg/ml heparin, 20 ng/ml basic fibroblast growth factor (both Life Technologies) and epithelial growth factor (EGF) (Sigma). The number and sizes of spheres were quantified on day 4 and day 7.
Terminal duct lobular unit (TDLU) assays were performed using matrigel protocols. Briefly, Lab-Tek chamber slides (Nunc) were coated with 300uL growth factor-reduced Matrigel Matrix (BD Biosciences). Cells were then plated inside the matrigel (500 cells per well), and their own medium was added. Cells were cultured for 15 days at 5% CO2,37.

Western blot. Samples were collected in RIPA buffer, and protein concentrations were calculated using Pierce™ Coomassie Protein Assay Kit (Thermo Fisher Scientific) and a standard BSA curve. Samples were boiled for 5 min at 100°C in sample buffer (0.05M Tris (pH 6.8), 2% SDS, 2,5% β-mercaptoethanol and 5% glycerol). The 10% SDS–PAGE gradient gels were run in running buffer (25 mM Tris, 192 mM glycine, 0,1% SDS) and transferred to PVDF membranes in transfer buffer (Transfer buffer (Biorad), 20% ethanol). Membranes were blocked in 5% BSA in TBS-T buffer (Tris-buffered saline 10X (Euromedex) containing 1% Tween-20 (Euromedex). Primary antibodies described in the Nature Research Reporting Summary linked to this article were incubated overnight at 4 °C and washed with TBS-T buffer. HRP-conjugated secondary antibodies were left at room temperature for 1 h and washed with TBS-T buffer. Western blot development was performed using Clarity™ Western ECL Substrate (Biorad) and Chemidoc™ Imaging System (Biorad).

qPCR. For RT-PCR analysis, the cells pellet was resuspended in 300µl of Trizol Reagent (Life technologies™) and performed using standard protocols. Total RNA was purified using Direct-zol RNA MicroPrep w/ Zymo-Spin IC Columns (Ozyme). For RT-qPCR, cDNA was produced using PrimeScript™ RT Reagent Kit (Takara)and quantified using TB Green® Premix Ex Taq™ (Takara) and Real-Time PCR system (Roche, LC480). Your results are normalized with fibroblast RNA. TATA-binding protein (TBP) and hypoxanthineguanine phosphoribosyl transferase (HPRT) genes

were also used for normalization. Arbitrary Unit (AU) corresponds to the expression ratio between samples and a single normal sample used as a reference in each PCR.

Flow cytometry. Cytometric analysis of cells was performed on an LSRFortessa cytometer. The software Diva was used for acquisition and Flow-Jo for analysis. For intracellular staining, cells were fixed 10min with 4% paraformaldehyde at 37°C and washed and permeabilized 30min with 80% ethanol or 0,1% triton before adding APC-conjugated anti-Ki67 for 30min (BD Biosciences).

Generation of cell lines. To generate MCF10A-FUCCI, MC26-FUCCI, and M1B26-FUCCI cell lines, fucci constructs (mVenus-hGeminin/pcDNA3 and mCherry-hCdt1/pcDNA3) obtained from Riken Institute were transfected into cell lines and selected with 1ug/ml puromycin. For HS27a-shTGFB2 and HS27a-shBMP4, parental HS27a cells were transfected with the pCT3-GEPIR-shBMP4 and pCT3-GEPIR shTGFB2 plasmids. Short-hairpin sequences are in supplementary table X.

Quantification of Soluble BMP4 and TGFB2. To determine the concentration of secreted BMPs in the microenvironment of primary tissue samples, standardized normal and tumor tissue supernatants were prepared (Faget et al., 2011). Undigested tissue was mechanically dissociated in DMEM/F-12 nutrient mix, 2% bovine serum albumin (BSA) at a concentration of 1 ml/0.5 g tissue using scalpels. Supernatants were filtered using a 40mM cell strainer and used to quantify soluble BMP2 and BMP4. ELISA quantifications of BMP2 and BMP4 were performed following the manufacturer's instructions. Bone marrow plasma or HS5/HS27A supernatants were precleared of cellular debris by rapid centrifugation and processed for BMP4 & TGFB2 ELISA quantification (R&D Systems) following the manufacturer's instructions.

Immunofluorescence. 3D cultures were fixed with PFA 2% and 0.005% glutaraldehyde for 5min. They were then permeabilized using 0.5% Triton X-100 in PBS for 20 min. Blocking with 3% bovine serum albumin (BSA; Fisher Bioreagents) and 5% normal goat serum (Gibco PCN5000) in PBS for 1 h at room temperature. Primary antibodies listed in Supplementary Table X were incubated overnight at 4 °C, followed by washing and secondary antibodies (Invitrogen, 1:1,000 dilution) incubation at room temperature for 1 h in the dark. Slides were mounted with ProLong Gold Antifade reagent with DAPI (Invitrogen, P36931), and images were obtained using

Leica Software on a Leica SPE confocal microscope. For B-gal positive control 100uM as previously described (31092810)

Cell treatment and RNA collection for bulk RNAseq. PYMT cells were treated with 5ng/mL of TGFB2, BMP4, or both for 3 days, then media was changed, and cells were collected 2 days later (day3+2) after matrigel depolymerization (Corning, CLS354253) following the manufacturer's instructions. RNA extraction, sample QC, library preparations, and sequencing reactions were conducted at GENEWIZ, as follows:
Total RNA was extracted using the Qiagen RNeasy Plus Universal kit following the manufacturer's instructions (Qiagen). Extracted RNA samples were quantified using Qubit 2.0 Fluorometer (Life Technologies), and RNA integrity was checked using Agilent TapeStation 4200 (Agilent Technologies). RNA sequencing libraries were prepared using the NEBNext Ultra II RNA Library Prep Kit for Illumina following the manufacturer's instructions (NEB). Briefly, mRNAs were first enriched with
Oligo(dT) beads. Enriched mRNAs were fragmented for 15 minutes at 94 °C. First-strand and second-strand cDNAs were subsequently synthesized. cDNA fragments were end-repaired and adenylated at 3'ends, and universal adapters were ligated to cDNA fragments, followed by index addition and library enrichment by limited-cycle PCR. The sequencing libraries were validated on the Agilent TapeStation (Agilent Technologies), and quantified by using Qubit 2.0 Fluorometer (Invitrogen) as well as by quantitative PCR (KAPA Biosystems). The sequencing libraries were clustered on a flowcell. After clustering, the flowcell was loaded on the Illumina HiSeq instrument (4000 or equivalent) according to the manufacturer's instructions. The samples were sequenced using a 2x150bp Paired-End (PE) configuration. Image analysis and base calling were conducted by Illumina Control Software. Raw sequence data (.bcl files) generated from the Illumina instrument was converted into fastq files and de-multiplexed using Illumina's bcl2fastq 2.17 software. One mismatch was allowed for index sequence identification.

Bulk RNA-Seq alignment and quality control. Analysis was performed by the BiNGS shared resource facility at Mount Sinai Hospital. Briefly, a total of 12 paired-end RNA-Seq libraries from 4 conditions (triplicates for nontreated, BMP4, TGFβ2, and BMP4+TGFB2) are processed using the same pipeline for compatibility. Quality control has been performed using FastQC (v0.11.8)[39]. Trim Galore! (version 0.6.5) has been

used to trim the adapter sequences with a quality threshold of 20[40]. The mouse genome reference used was GRCm38.p6 and GENCODE release M25 was used as the transcriptome reference. The alignment is performed by using STAR aligner (v2.7.5b)[41]. Gene level read counts are obtained by using Salmon (v1.2.1) for all libraries[42]. All samples have passed the quality control requirements with > 85% of reads uniquely mapping (>25M uniquely mapped reads for each library) using STAR aligner.

Differential expression and functional analysis. Differential expression analysis was performed using the gene-level read counts and the DESeq2 (v1.28.1) R package[43]. Genes with less than 5 reads in total across all samples are filtered as inactive genes. A gene is considered differentially expressed if the adjusted p-value is less than 0.05 and the absolute log2 fold change is greater than 0.5. Gene lists of genes uniquely differentially expressed in specific conditions were identified with Venn diagrams[44,45]. The over-representation analysis for functional enrichment is performed using the Enrichr webserver[46].

Single-cell isolation and RNA sequencing of mCherry^{high}/mVenus^{neg} MCF10A-CT-FUCCI and M1B26-FUCCI cells. mCherry^{high}/mVenus^{neg} MCF10A-CT-FUCCI and M1B26-FUCCI cells treated with 10ng/mL of TGFB2, 10ng/mL of BMP4, or 5+5ng/mL of TGFB2+BMP4 during 72h in serum-free media were sorted with Biorad S3e sorter. Sorted cells were resuspended in PBS with 0.04% BSA and the number of live cells was determined with a CellDrop FL (DeNovix) cell counter. 100 000 cells of each eight samples were individually tagged with CellPlex reagent according to manufacturer instructions (10X Genomics). Samples were counted and pooled together at the same frequency. The pooled cell suspension was loaded on a 10X chip and run on the Chromium Controller system (10X Genomics) to obtain an expected cell recovery population of 10,000 cells. Gene expression and cellplex libraries were generated with the Chromium Single Cell 3′ v3.1 assay with feature barcoding (10X Genomics) and sequenced on the NovaSeq 6000 platform (Illumina, SP flow cell) to obtain around 100,000 reads per cell for gene expression and 5,000 reads per cell for cellplex. Data were demultiplexed and aligned to the human genome, 10X and cellplex barcodes were assigned for each cell, and genes were counted by unique molecular.identifier (UMI) counts, using cellranger multi pipeline (v6.0).

Data processing and cell clustering. Pre-processed data was further analyzed using the R package Seurat on Rstudio. Cells with more than 7.5% of mitochondrial genes were removed from the analysis. The number of features and number of counts per cell was homogeneous across samples, so additional. We then normalized data using the NormalizeData function (LogNormalize function, scale factor = 10000) and extracted highly variable features using the FindVariableFeatures (vst method, n = 500 features) function. Normalized data underwent a linear transformation (scaling) and principal component analysis (PCA) based on variable features using the RunPCA function. Graph-based clustering was then performed according to gene expression profiles using the FindNeighbors (with 1:20 dimensions) and FindClusters (resolution = 0.5) functions. Results were visualized using a nonlinear dimensional reduction UMAP technique running RunUMAP and DimPlot functions. Batch effect correction and data integration were unnecessary as all samples were obtained and processed together.

Differential Expression of Genes analysis. DEG analysis was performed using the FindMarkers or FindAllMarkers functions with a minimum of 25% of the gene-expressing cells and a minimum log fold-change of 0.25 in gene expression between each cluster and other clusters. Gene ontology enrichment analysis of DEGs in particular clusters was performed using Enrichr[46] (https://maayanlab.cloud/Enrichr/). For signature scoring, the Ucell signature scoring[47] R package was used using the signature of genes upregulated in dormant cells described in[32].

Statistical analysis. Unless otherwise specified, statistical analysis was performed using a one-way ANOVA test followed by Holm-Sidak's multiple comparisons test. The statistical analyses and graphs were performed with Graphpad Prism (version 8). Significant P values are given in the text or symbolized by asterisks (*p<0,05 ; **p<0,01 ; ***p<0,001). The zero-interaction potency (ZIP) synergy score[30] was computed with the SynergyFinderPlus software[31].

References

1. Sung, H. *et al.* Global Cancer Statistics 2020: GLOBOCAN Estimates of Incidence and Mortality Worldwide for 36 Cancers in 185 Countries. *CA: A Cancer Journal for Clinicians* **71**, 209–249 (2021).

2. Pedersen, R. N. *et al.* The Incidence of Breast Cancer Recurrence 10-32 Years After Primary Diagnosis. *J Natl Cancer Inst* **114**, 391–399 (2022).

3. Aguirre-Ghiso, J. A. Models, mechanisms and clinical evidence for cancer dormancy. *Nature Reviews Cancer* **7**, 834–846 (2007).

4. Risson, E., Nobre, A. R., Maguer-Satta, V. & Aguirre-Ghiso, J. A. The current paradigm and challenges ahead for the dormancy of disseminated tumor cells. *Nature Cancer* **1**, 672–680 (2020).

5. Phan, T. G. & Croucher, P. I. The dormant cancer cell life cycle. *Nature Reviews Cancer* **20**, 398–411 (2020).

6. Singh, A. *et al.* Angiocrine signals regulate quiescence and therapy resistance in bone metastasis. *JCI Insight* **4**, 125679 (2019).

7. Kaur, A. *et al.* Remodeling of the Collagen Matrix in Aging Skin Promotes Melanoma Metastasis and Affects Immune Cell Motility. *Cancer Discov* **9**, 64–81 (2019).

8. Albrengues, J. *et al.* Neutrophil extra-cellular traps produced during inflammation awaken dormant cancer cells in mice. *Science* **361**, eaao4227 (2018).

9. Braun, S. *et al.* Cytokeratin-positive cells in the bone marrow and survival of patients with stage I, II, or III breast cancer. *N. Engl. J. Med.* **342**, 525–533 (2000).

10. Borgen, E. *et al.* NR2F1 stratifies dormant disseminated tumor cells in breast cancer patients. *Breast Cancer Research* **20**, (2018).

11. Naume, B. *et al.* Clinical outcome with correlation to disseminated tumor cell (DTC) status after DTC-guided secondary adjuvant treatment with docetaxel in early breast cancer. *J. Clin. Oncol.* **32**, 3848–3857 (2014).

12. Pinho, S. & Frenette, P. S. Haematopoietic stem cell activity and interactions with the niche. *Nature Reviews Molecular Cell Biology* (2019) doi:10.1038/s41580-019-0103-9.

13. Cackowski, F. C. & Taichman, R. S. Parallels between hematopoietic stem cell and prostate cancer disseminated tumor cell regulation. *Bone* (2018) doi:10.1016/j.bone.2018.02.025.

14. Méndez-Ferrer, S. *et al.* Mesenchymal and haematopoietic stem cells form a

unique bone marrow niche. *Nature* **466**, 829–834 (2010).

15. Kunisaki, Y. *et al.* Arteriolar niches maintain haematopoietic stem cell quiescence. *Nature* **502**, 637–643 (2013).

16. Nobre, A. R. *et al.* Bone marrow NG2 + /Nestin + mesenchymal stem cells drive DTC dormancy via TGF-β2. *Nature Cancer* 1–13 (2021) doi:10.1038/s43018-021-00179-8.

17. Tikhonova, A. N. *et al.* The bone marrow microenvironment at single-cell resolution. *Nature* **569**, 222–228 (2019).

18. Gao, H. *et al.* The BMP Inhibitor Coco Reactivates Breast Cancer Cells at Lung Metastatic Sites. *Cell* **150**, 764–779 (2012).

19. Jeanpierre, S. *et al.* The quiescent fraction of chronic myeloid leukemic stem cells depends on BMPR1B, Stat3 and BMP4-niche signals to persist in patients in remission. *Haematologica* (2020) doi:10.3324/haematol.2019.232793.

20. Prunier, C., Baker, D., Ten Dijke, P. & Ritsma, L. TGF-β Family Signaling Pathways in Cellular Dormancy. *Trends Cancer* **5**, 66–78 (2019).

21. Lee, G. Y., Kenny, P. A., Lee, E. H. & Bissell, M. J. Three-dimensional culture models of normal and malignant breast epithelial cells. *Nature Methods* **4**, 359–365 (2007).

22. Le Naour, A. *et al.* EO771, the first luminal B mammary cancer cell line from C57BL/6 mice. *Cancer Cell Int* **20**, 328 (2020).

23. Aguirre-Ghiso, J. A., Liu, D., Mignatti, A., Kovalski, K. & Ossowski, L. Urokinase Receptor and Fibronectin Regulate the ERK ^{MAPK} to p38 ^{MAPK} Activity Ratios That Determine Carcinoma Cell Proliferation or Dormancy In Vivo. *Molecular Biology of the Cell* **12**, 863–879 (2001).

24. Miller, F. R., Santner, S. J., Tait, L. & Dawson, P. J. MCF10DCIS.com Xenograft Model of Human Comedo Ductal Carcinoma In Situ. *JNCI: Journal of the National Cancer Institute* **92**, 1185a–11186 (2000).

25. Chapellier, M. *et al.* Disequilibrium of BMP2 Levels in the Breast Stem Cell Niche Launches Epithelial Transformation by Overamplifying BMPR1B Cell Response. *Stem Cell Reports* **4**, 239–254 (2015).

26. Clement, J. H. *et al.* Bone morphogenetic protein 2 (BMP-2) induces in vitro invasion and in vivo hormone independent growth of breast carcinoma cells. *Int. J. Oncol.* **27**, 401–407 (2005).

27. Sakaue-Sawano, A. *et al.* Genetically Encoded Tools for Optical Dissection of

the Mammalian Cell Cycle. *Molecular Cell* **68**, 626-640.e5 (2017).

28. Cuitiño, M. C. *et al.* Two Distinct E2F Transcriptional Modules Drive Cell Cycles and Differentiation. *Cell Reports* **27**, 3547-3560.e5 (2019).

29. Tomura, M. *et al.* Contrasting Quiescent G0 Phase with Mitotic Cell Cycling in the Mouse Immune System. *PLOS ONE* **8**, e73801 (2013).

30. Yadav, B., Wennerberg, K., Aittokallio, T. & Tang, J. Searching for Drug Synergy in Complex Dose–Response Landscapes Using an Interaction Potency Model. *Computational and Structural Biotechnology Journal* **13**, 504–513 (2015).

31. Zheng, S. *et al.* SynergyFinder Plus: Toward Better Interpretation and Annotation of Drug Combination Screening Datasets. *Genomics, Proteomics & Bioinformatics* S1672022922000080 (2022) doi:10.1016/j.gpb.2022.01.004.

32. Kim, R. S. *et al.* Dormancy Signatures and Metastasis in Estrogen Receptor Positive and Negative Breast Cancer. *PLoS ONE* **7**, e35569 (2012).

33. Chen, C.-R., Kang, Y., Siegel, P. M. & Massague, J. E2F4/5 and p107 as Smad Cofactors Linking the TGFβ Receptor to c-myc Repression. 14.

34. Guerrero-Zotano, A. L. *et al.* ER + Breast Cancers Resistant to Prolonged Neoadjuvant Letrozole Exhibit an E2F4 Transcriptional Program Sensitive to CDK4/6 Inhibitors. *Clin Cancer Res* **24**, 2517–2529 (2018).

35. Carlson, P. *et al.* Targeting the perivascular niche sensitizes disseminated tumour cells to chemotherapy. *Nature Cell Biology* 1 (2019) doi:10.1038/s41556-018-0267-0.

36. Bragado, P. *et al.* TGF-β2 dictates disseminated tumour cell fate in target organs through TGF-β-RIII and p38α/β signalling. *Nature Cell Biology* **15**, 1351–1361 (2013).

37. Yumoto, K. *et al.* Axl is required for TGF-β2-induced dormancy of prostate cancer cells in the bone marrow. *Scientific Reports* **6**, (2016).

38. Ning, J., Zhao, Y., Ye, Y. & Yu, J. Opposing roles and potential antagonistic mechanism between TGF-β and BMP pathways: Implications for cancer progression. *EBioMedicine* **41**, 702–710 (2019).

39. FastQC: a quality control tool for high throughput sequence data – ScienceOpen. https://www.scienceopen.com/document?vid=de674375-ab83-4595-afa9-4c8aa9e4e736.

40. Babraham Bioinformatics - Trim Galore! https://www.bioinformatics.babraham.ac.uk/projects/trim_galore/.

41. Dobin, A. *et al.* STAR: ultrafast universal RNA-seq aligner. *Bioinformatics* **29**, 15–21 (2013).

42. Patro, R., Duggal, G., Love, M. I., Irizarry, R. A. & Kingsford, C. Salmon provides fast and bias-aware quantification of transcript expression. *Nat Methods* **14**, 417–419 (2017).

43. Love, M. I., Huber, W. & Anders, S. Moderated estimation of fold change and dispersion for RNA-seq data with DESeq2. *Genome Biology* **15**, 550 (2014).

44. Hulsen, T., de Vlieg, J. & Alkema, W. BioVenn – a web application for the comparison and visualization of biological lists using area-proportional Venn diagrams. *BMC Genomics* **9**, 1–6 (2008).

45. jvenn: an interactive Venn diagram viewer | BMC Bioinformatics | Full Text. https://bmcbioinformatics.biomedcentral.com/articles/10.1186/1471-2105-15-293.

46. Xie, Z. *et al.* Gene Set Knowledge Discovery with Enrichr. *Current Protocols* **1**, e90 (2021).

47. Andreatta, M. & Carmona, S. J. UCell: Robust and scalable single-cell gene signature scoring. *Computational and Structural Biotechnology Journal* **19**, 3796–3798 (2021).

48. Cabezas-Wallscheid, N. *et al.* Vitamin A-Retinoic Acid Signaling Regulates Hematopoietic Stem Cell Dormancy. *Cell* **169**, 807-823.e19 (2017).

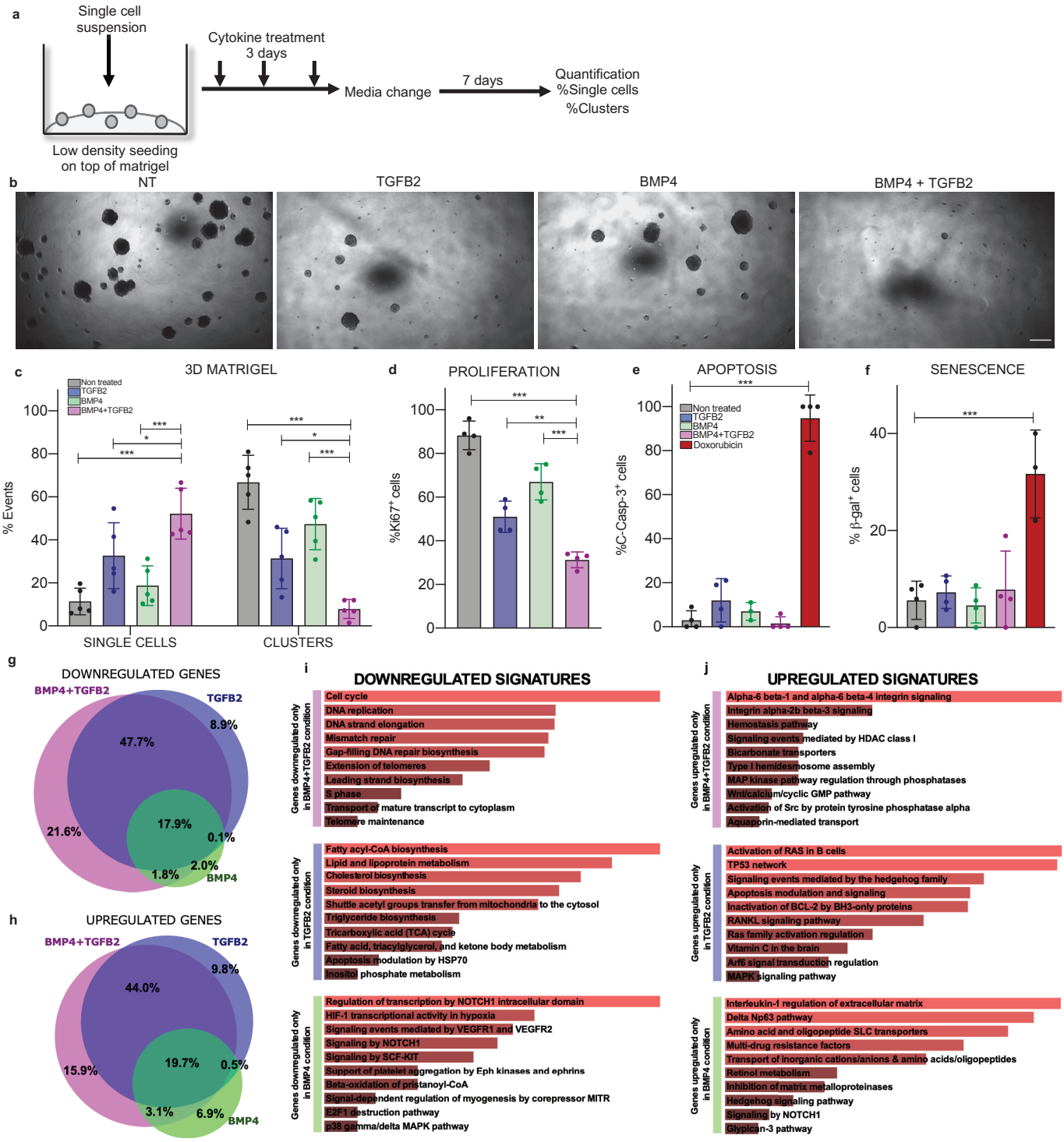

Fig. 1 | BMP4 and TGFB2 co-signaling controls a more profound dormancy. a, Representative scheme of 3D matrigel assay in low density: PYMT cells were treated with 5ng/mL of TGFB2, BMP4 or both for 3 days, then media was changed, pictures were taken 7 days later (d10). **b**, Representative images at d10 of the 3D matrigel assay. **c**, Quantification on the percentage of single cells+doublets and clusters at d10 (n=5, one-way ANOVA). **d-f**, Quantification of Ki67 (d), cleaved-caspase-3 (e) and B-galactosidase (f) staining of PYMT cells on matrigel two days after the end of the 3-day treatment (d3+2). To have a positive control for cell death cells were treated with 1uM of doxorubicin. To have a positive control for senescence, cells were treated with sub-lethal levels of doxorubicin (100nM) for 1 day and then were in fresh media for 3 days (n=4, one-way ANOVA). **g, h**, overlap in percentage of the differentially expressed genes in TGFB2, BMP4 or BMP4+TGFB2 conditions compared to non-treated conditions identified by bulk RNAseq. Genes were selected if log2FC > 0.5 (upregulated, g) or if log2FC < -0.5 (downregulated, h), with the adjusted p-value < 0.05. **i, j**, Pathway Enrichment analysis of the BioPlanet 2019 library of genes uniquely differentially regulated in BMP4+TGFB2, TGFB2 or BMP4 conditions.

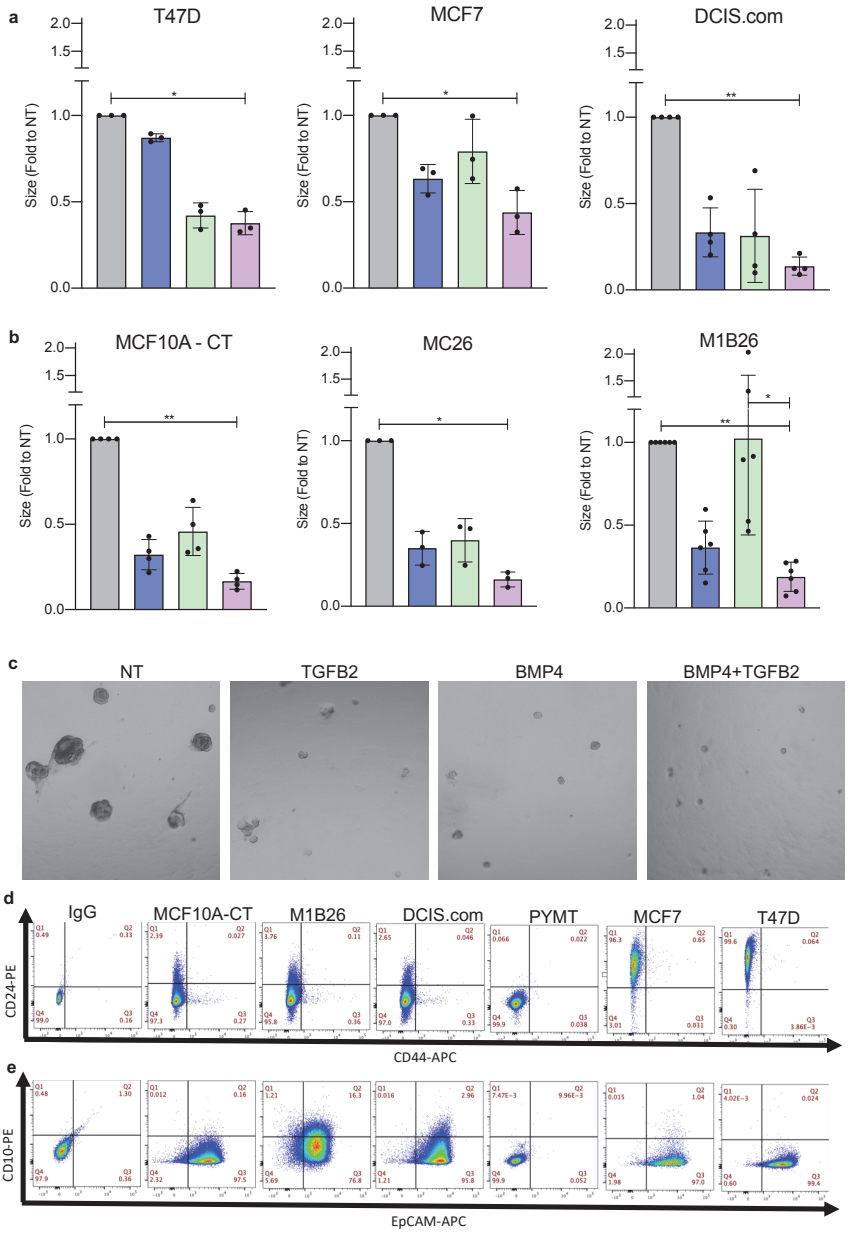

Fig. 2 | BMP4 and TGFB2 effect is conserved across human normal and breast cancer cell lines independently on the transformation mechanism and ER status. a, b, Cell lines cells were treated with 10ng/mL of TGFB2, BMP4 or both (5+5 ng/mL) during 3 days, then media was changed, pictures were taken 7 days later (d10) and the cluster size was quantified (n=3 to 6, mean+/-sd Kruskal-wallis non parametric test, followed by Dunn's multiple comparisons test). **C,** Representative images of MCF10A-CT cells at d10 in 3D matrigel culture. **d,** CD44/CD24 and **e,** EpCAM/CD10 staining by flow cytometry across cell lines. *p<0,05; **p<0,01; ***p<0,001

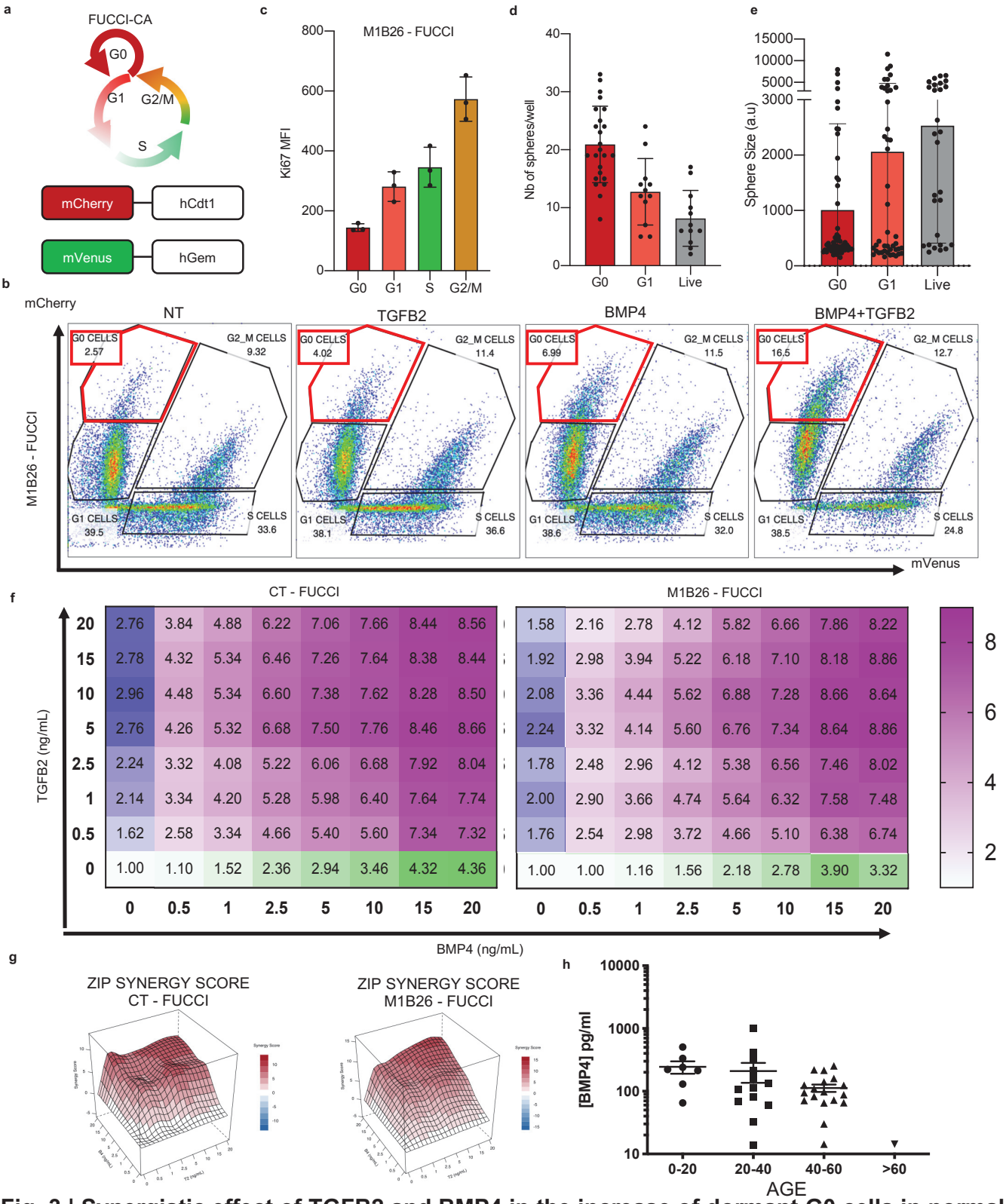

Fig. 3 | Synergistic effect of TGFB2 and BMP4 in the increase of dormant G0 cells in normal and transformed breast cancer cells. **a**, Scheme explanation of the FUCCI-CA model. **b**, Representative FACS plot of the M1B26-FUCCI system and the increase of proportion of G0 cells with TGFB2 (10ng/mL), BMP4 (10ng/mL) or BMP4+TGFB2 (5+5ng/mL) treatments. **c**, Ki67 staining intensity by flow cytometry across cell cycle phases (G0, G1, S, G2/M) identified by the FUCCI system with the gates shown in (b). **d, e**, Number (d) and size (e) of mammospheres (day 7) obtained after sorting G0, G1 or live (all cell cycle phases) M1B26-FUCCI cells. **f**, Factorial design and quantification of the G0 proportion fold increase across cell lines after 72h treatments in culture in serum free media with concentrations ranging from 0.5 to 20ng/mL (n=5, mean is shown). **g**, ZIP synergy score effect of TGFB2 and BMP4 computed by SynergyFinderPlus. **h**, BMP4 levels in normal bone marrow supernatant from healthy human donors according to age.

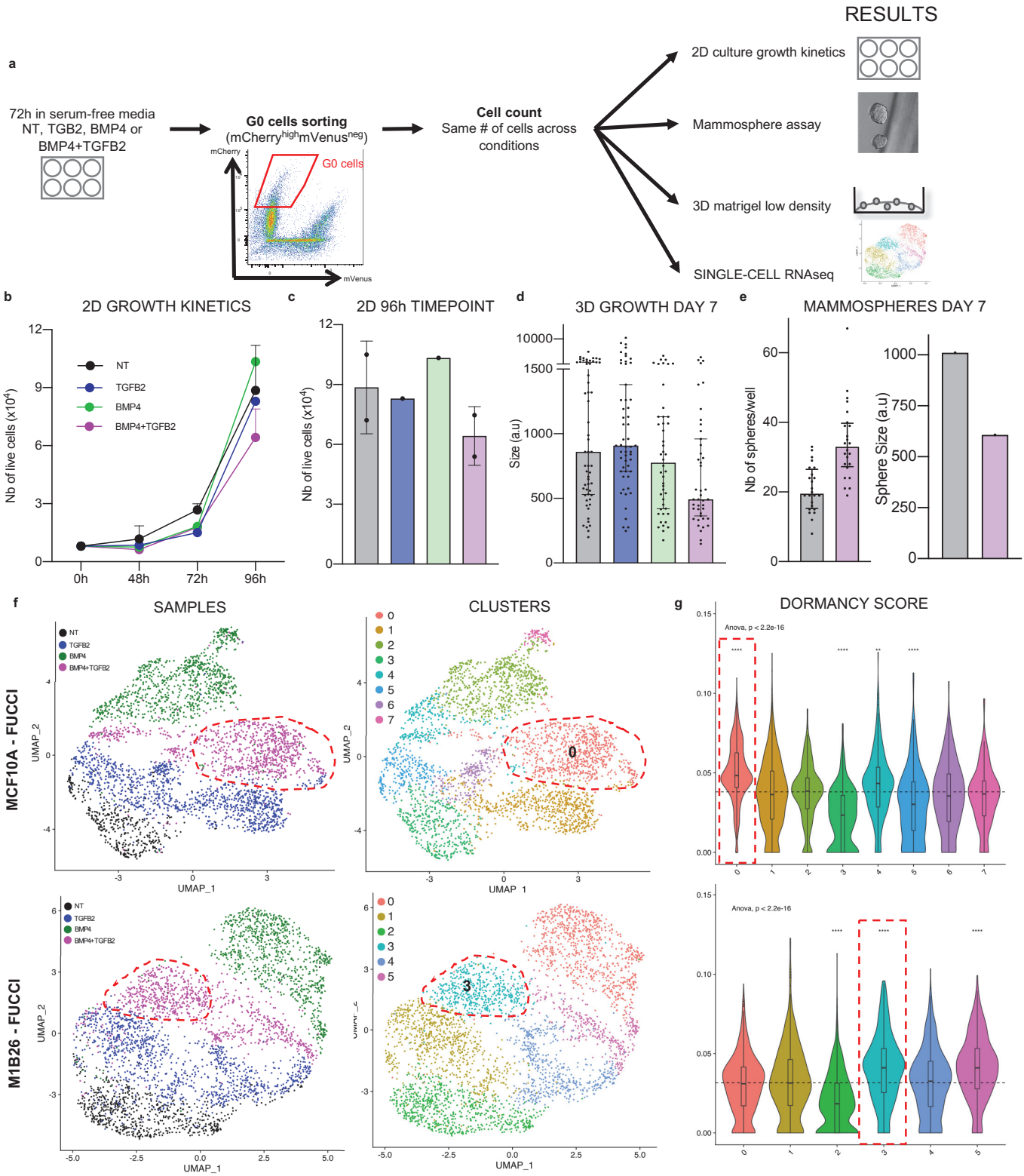

Fig. 4 | G0 cells treated with BMP4+TGFB2 are in a deeper dormancy state. **a**, Scheme of the experimental design: after 72h treatment with TGFB2 (10ng/mL), BMP4 (10ng/mL), or BMP4+TGFB2 (5+5ng/mL), G0 cells were sorted by flow cytometry and equal number of cells were seeded in functional assays, or were used for single-cell RNAseq. **b,** Growth kinetics of sorted G0 cells put back in culture in regular media without cytokine treatment (n=2). **c**, Barplot of the 96h timepoint of b. **d**, Quantification of the size of clusters 7 days after sorting and seeding of G0 cells in the 3D matrigel assay in regular media without cytokine treatment (n=1). **e**, Quantification of the number and size of mammospheres at 7 days (n=1). **f**, Cellular maps of MCF10A (top panels) or M1B26 (bottom panels) at single-cell resolution displayed on UMAP dimension-based on sample of origin (left panels) or identified clusters (right panels). **g**, Dormancy signature score across clusters in MCF10A (top panel) and M1B26 (bottom panel), dotted line represents the mean dormancy score across all clusters (one-way ANOVA, followed multiple pairwise comparison against all, based on mean expression).

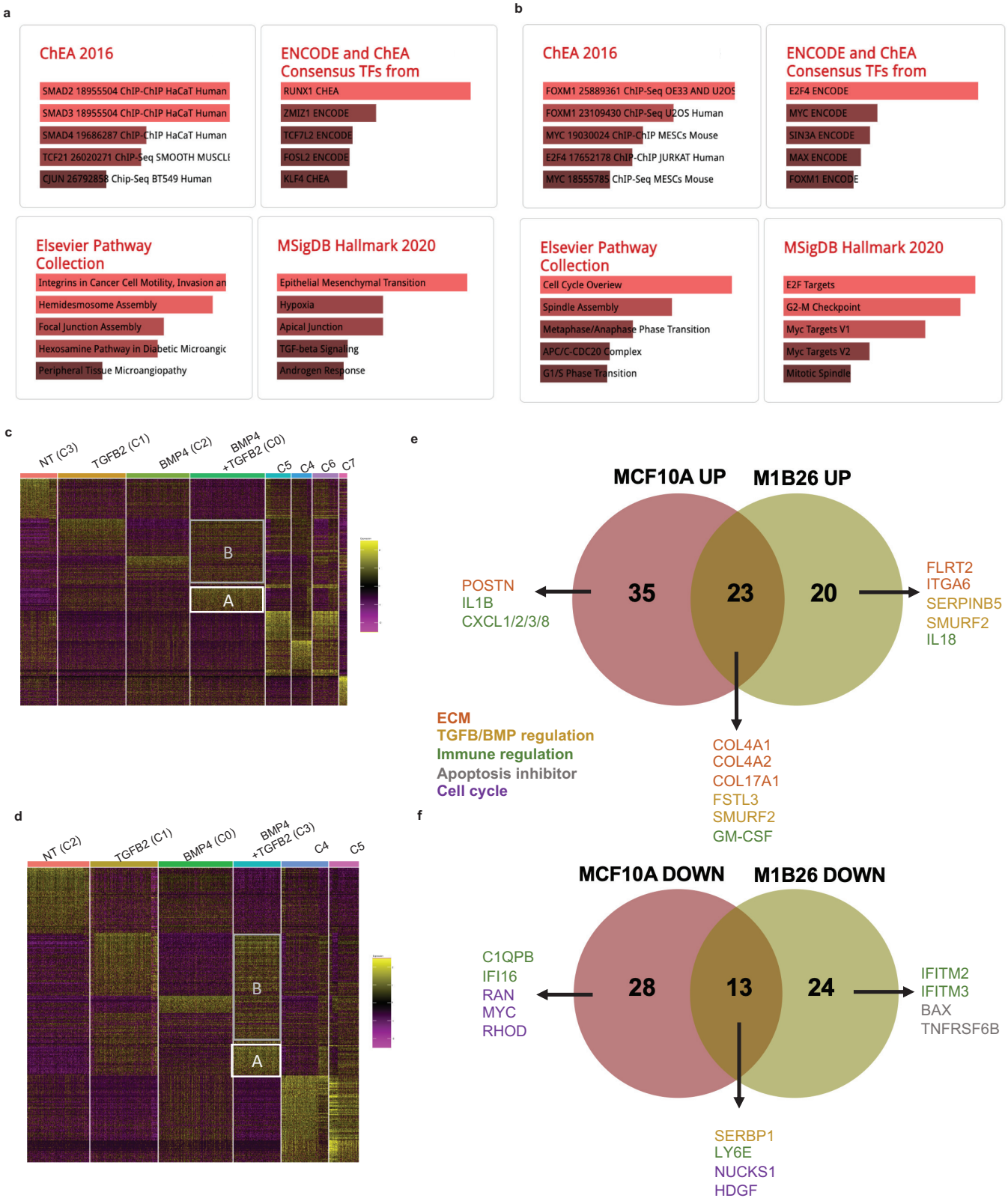

Fig. 5 | Identification of a deep dormant signature in breast cancer cells. **a,b** Pathway enrichment analysis of upregulated (a) and downregulated (b) overlapping markers of cluster 3 from M1B26 and cluster 0 from MCF10A. **c**, Heatmap of the main markers of each cluster in MCF10A cells. **d**, Heatmap of the main markers of each cluster in M1B26 cells (the cluster number is in parenthesis). **e**, Overlap of the upregulated markers of cluster 3 from M1B26 and cluster 0 from MCF10A, genes of functional interest are highlighted. **f,** Overlap of the downregulated markers of cluster 3 from M1B26 and cluster 0 from MCF10A, genes of functional interest are highlighted.

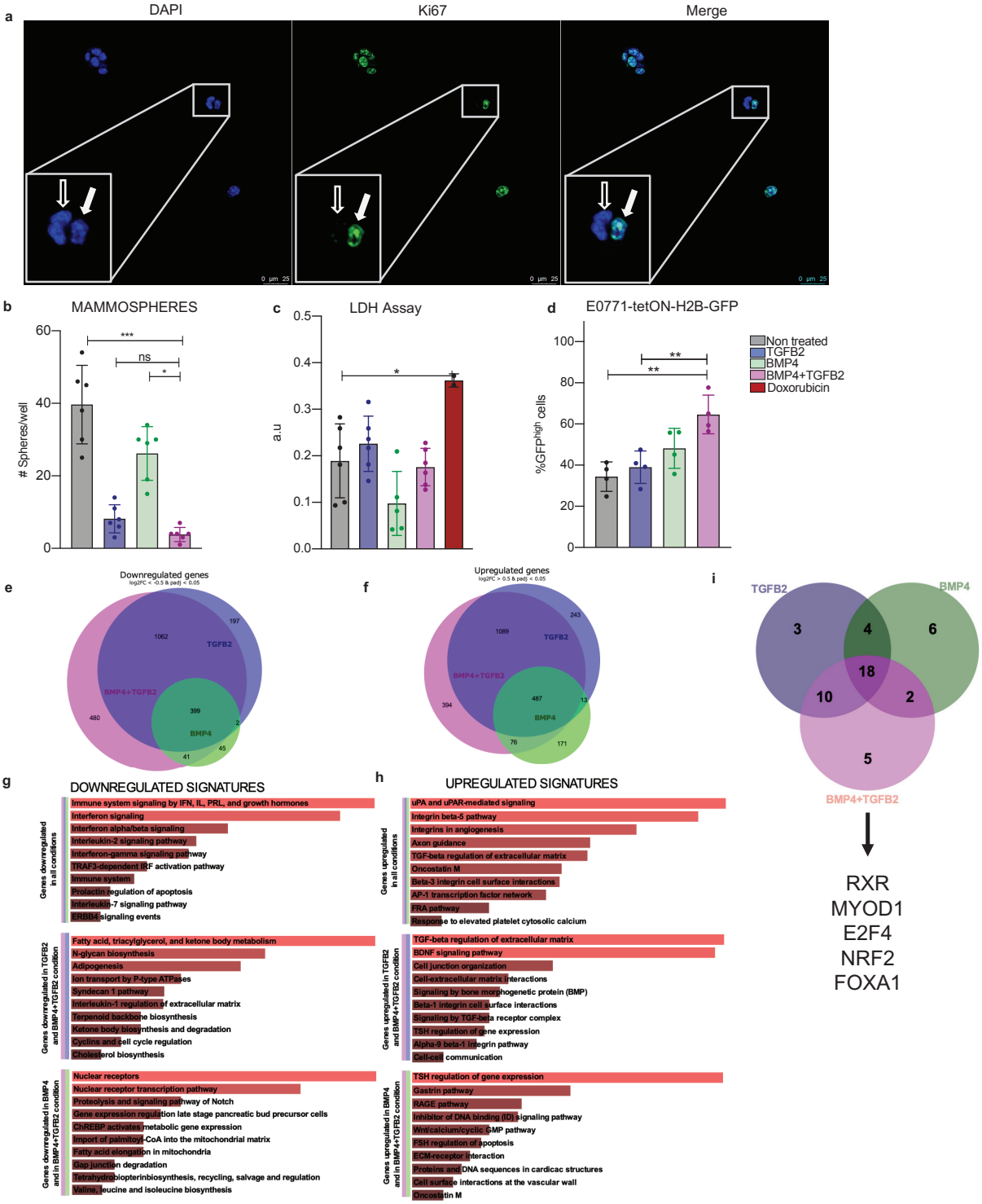

Supplemental Fig. 1 | BMP4 and TGFB2 signaling controls a more profound dormancy. (**a**) Ki67 staining representative images of PYMT cells cultured in 3D matrigel. Empty arrow represents a Ki67 negative cell, while full arrow represents Ki67 positive cell. (**b**) Mammosphere assay quantified at day 7 (n=6, mean+/-sd, one-way ANOVA). (**c**) LDH assay performed on the media of PYMT cells cultured 3 days in 3D matrigel. Triton permeabilizes cells and is used as a positive control (n=6, mean+/-sd, one-way ANOVA). (**d**) E0771-tetON-H2B-GFP cells were induced with doxycycline during 24h and were then seeded in 3Dmatrigel. Cells were treated with doxycycline for an additional 24h and treated with cytokines during 4 days before collection and flow cytometry quantification of GFP^{high} cells (n=4, mean+/-sd, one-way ANOVA). **(e, f)** Overlap in absolute numbers of the differentially expressed genes in TGFB2, BMP4 or BMP4+TGFB2 conditions compared to non-treated conditions identified by bulk RNAseq. Genes were selected if log2FC > 0.5 (upregulated, **g**) or if log2FC < -0.5 (downregulated, **h**), with the adjusted p-value < 0.05. (**i,j**) Pathway Enrichment analysis of the BioPlanet 2019 library of genes differentially regulated in all conditions, BMP4+TGFB2 and TGFB2 conditions, or in BMP4+TGFB2 and BMP4 conditions. i, overlap of the enrich signatures of transcription factors, with a highlight on the 5 transcription factors specific to the BMP4+TGFβ2 condition.

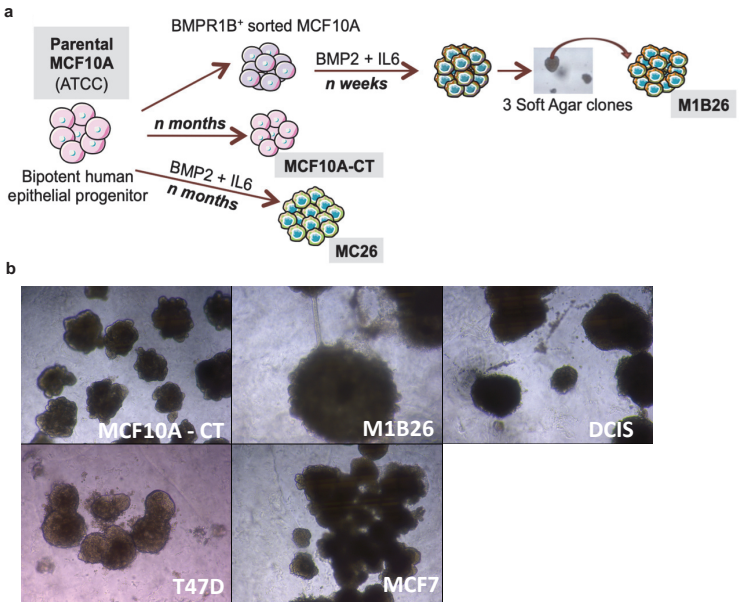

Supplemental Fig 2 | BMP4 and TGFB2 effect is conserved across human normal and breast cancer cell lines independently on the transformation mechanism and ER status. (**a**) Scheme illustrating the oncogene independent transformation model by exposure to IL6 & BMP2 (**b**) Representative images of Terminal Duct Lobular Unit (TDLU) assay across cell lines after 21 days.

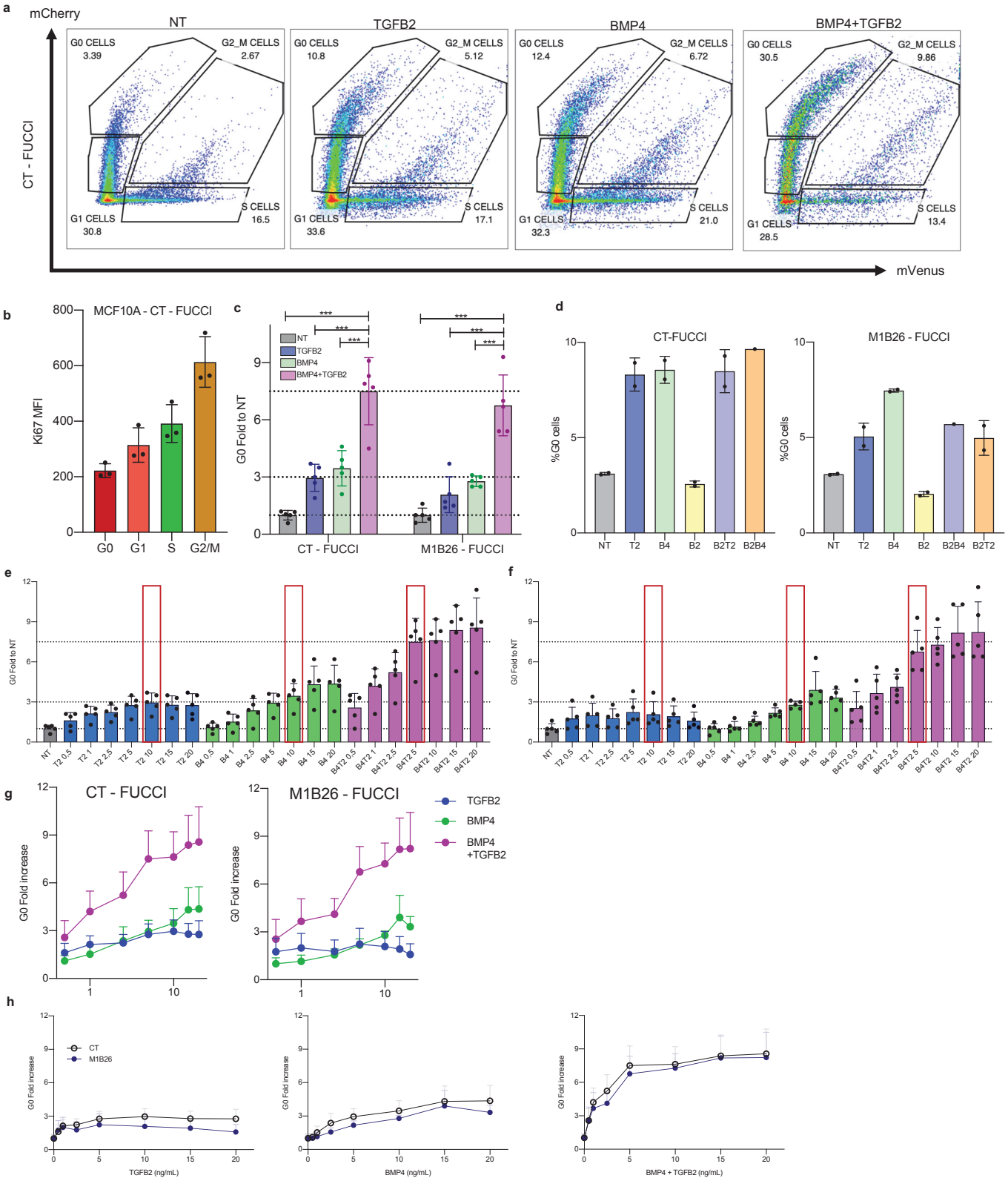

Supplemental Fig 3 | Synergistic effect of TGFB2 and BMP4 in the increase of dormant G0 cells in normal and transformed breast cancer cells

(**a**) Representative FACS plot of the CT-FUCCI system and the increase of proportion of G0 cells with TGFB2 (10ng/mL), BMP4 (10ng/mL) or BMP4+TGFB2 (5+5ng/mL) treatments. (**b**) Ki67 staining intensity by flow cytometry across cell cycle phases (G0, G1, S, G2/M) identified by the FUCCI system. (**c**) Quantification of the G0 fold increase across cell lines after 72h treatments in culture in serum free media with TGFB2 (10ng/mL), BMP4 (10ng/mL) or BMP4+TGFB2 (5+5ng/mL) treatments (n=5, mean+/-sd one-way ANOVA). (**d**) Representation of the diagonal from the factorial design. (**f**) Dose-response curve of MCF10A-CT-FUCCI and M1B26-FUCCI cell lines. (**g**) Comparison of the response of MC10A-CT and M1B26 (n=5, mean+/-sd).

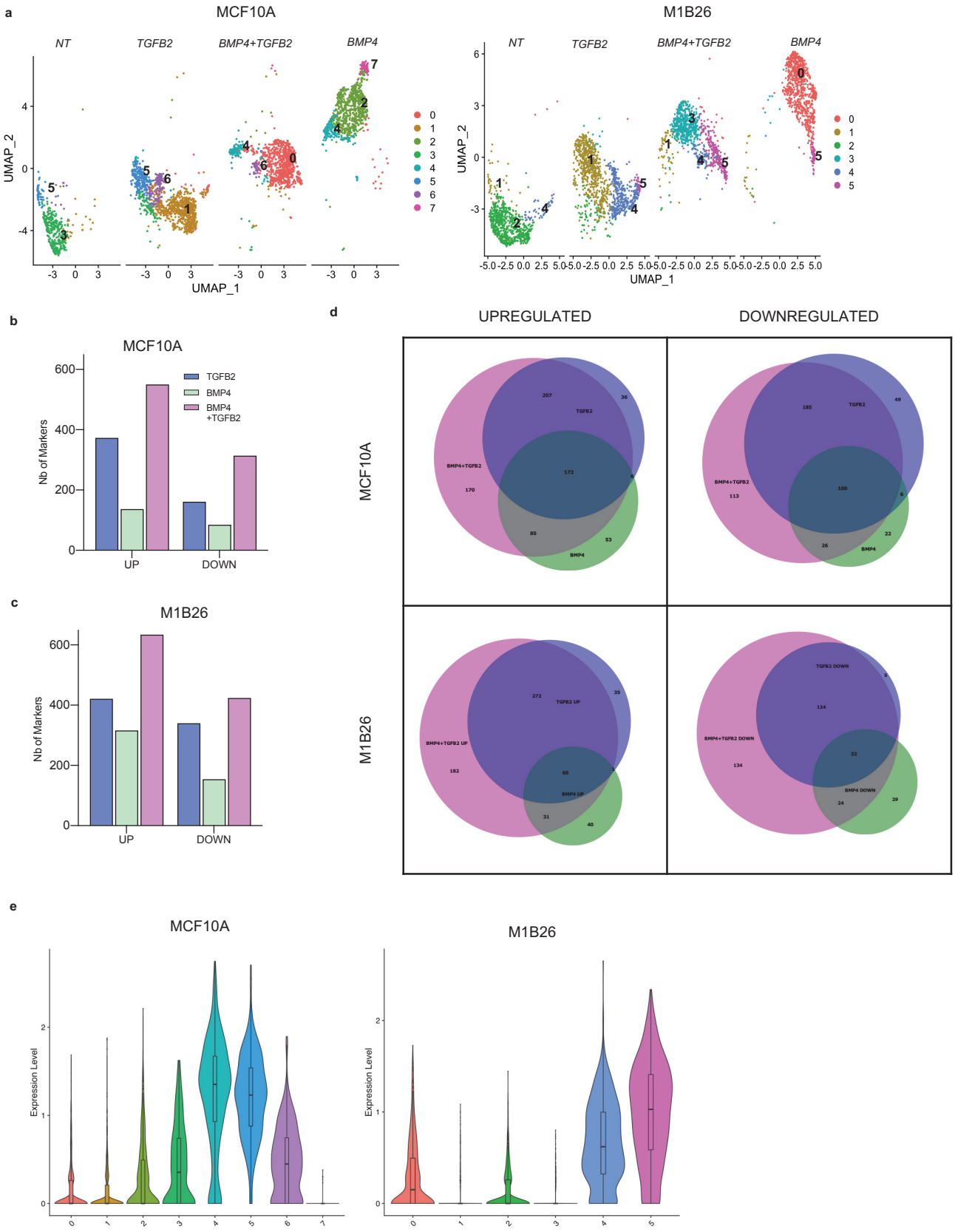

Supplemental Fig. 4 | Signatures overlap of the TGFB2, BMP4 or BMP4+TGFB2 conditions (**a**) Cellular maps of MCF10A (left panel) or M1B26 (right panel) at single-cell resolution displayed on UMAP dimension-based on sample of origin and identified clusters. **(b,c)** Number of upregulated (log2FC > 0.25 & adjusted p-value < 0.05) or downregulated genes across clusters (log2FC < -0.25 & adjusted p-value < 0.05) compared to the non-treated cluster in MCF10A (**b**) or M1B26 cells (**c**). (**d**) Venn Diagram showing the overlap of upregulated or downregulated genes across clusters compared to the non-treated cluster. (**e**) Violin of MKI67 expression across clusters.

Unique Upregulated Markers of BMP4+TGFB29				Unique Downregulated Markers of BMP4+TGFB2		
TPM1	ZBED2	GDPD3	FGF2	MED24	SNRPF	RHOD
CCDC80	IGFBP7	TMEM265	SKIL	TKT	CACYBP	NUCKS1
UGP2	NAV1	LIMA1	CCN1	LDHB	TMEM97	HNRNPD
LCE3D	TPM4	TLN1	KRT8	C1QBP	KRT5	HNRNPA2 B1
TAGLN	GNPNAT1	FSTL3	BIRC2	KRT18	PRMT1	S100A14
COL4A1	CRYAB	FERMT1	IDI1	LY6E	IFI16	FTL
CXCL1	COL17A1	FLNA	HERPUD1	ANP32B	DANCR	S100A8
CXCL3	TUBB3	CLIC3	CXCL2	PTMA	GCSH	TSC22D1
POSTN	IL1B	HSPA5	C12orf75	RAN	SRSF7	FTH1
CD24	SELENOM	ACTN1	AMTN	SERBP1	MRPS26	MT-ND6
COL4A2	F3	CD59	CAP1	CEBPD	MYC	NEAT1
P4HA2	CXCL8	KANK4	PLXNA2	TFAM	NOP16	
ALCAM	MYL6	CALD1	NRDC	HDGF	SET	
CSF3	ATP1B1	FADS1		FABP5	SYT8	
KRT7	SLC26A2	B3GNT2		SLC25A5	PSIP1	

Supplemental Table 1 : Markers genes of the BMP4+TGFB2 Cluster 0 in MCF10A-FUCCI identified by scRNAseq

Unique Upregulated Markers of BMP4+TGFB2			Unique Downregulated Markers of BMP4+TGFB2		
KRT7	COL4A1	SKIL	LDHB	HDGF	TFRC
CCDC80	COL17A1	SERPINB5	MED24	TFAM	IFITM2
KANK4	IGFBP7	TMEM154	DDIT4	PRMT1	HNRNPA3
PDPN	FLRT2	LIMA1	CAV1	NUCKS1	AREG
MYL6	MLLT11	CSF3	SNRPG	SYT8	SLC3A2
FSTL3	FAM114A1	SMURF2	TYMS	KRT5	HNRNPU
ANXA2	ZBED2	SAT1	SERBP1	BAX	PEG10
CLIC3	GNPNAT1	TPM4	SLC25A5	IFITM3	
COL4A2	PDXK	TUBB3	LSM7	CITED4	
SCD	IDI1	NRDC	TNFRSF6B	SNHG25	
YIPF5	TPM1	FADS1	STMN1	DANCR	
TAGLN2	ITGA6	LCE3D	HSP90AB1	TOP1	
GNAS	GPAM	MALAT1	LY6E	CCDC85B	
IL18	MAGED1		SET	NNMT	
P4HB	B3GNT2		NPM3	ANP32E	

Supplemental Table 2 : Markers genes of the BMP4+TGFB2 Cluster 3 in M1B26-FUCCI identified by scRNAseq

ADDITIONAL DATA

Additional experiments have been performed to better characterize the molecular mechanism explaining the BMP4 and TGFβ2 phenotype (Aim 2) and validate these findings *in situ* and *in vivo* (Aim 3), but were too preliminary to incorporate in the manuscript of the paper.

I. Inhibitory SMADs

SMAD6 and SMAD7 were upregulated in our PYMT model by bulk RNAseq (**Figure 15**a), but also in our MCF10A model by qPCR (**Figure 15**b) and scRNAseq (**Figure 15**c). Although differences are not clear between the conditions in the bulk data, the single cell RNAseq data really shows that a higher proportion of cells express SMAD7 in the BMP4+TGFB2 condition compared to the single cytokine treated conditions. Of note, SMAD6 was not detectable in the scRNAseq data (data not shown). We questioned if this upregulation would lead to an inhibition of canonical SMAD signaling, potentially leading to non-canonical signaling pathways activation instead. To test if canonical SMAD signaling was necessary to mediate BMP4 and TGFβ2 pro-dormancy effect, we optimized siRNA targeting the different SMADs. To our surprise, downregulating SMAD1/2/3/4/5 led to an important decrease in cell proliferation (**Figure 15**d). Because of the strong effect of downregulated canonical SMAD signaling on proliferation, we were unable to assess whether it would have affected BMP4 and TGFB2 synergy. Indeed, as this effect was so strong, it would have refrained us from observing the loss of increased effect of TGFB2 and BMP4 when canonical SMAD signaling was inhibited.

Downregulation of SMAD6/7, the inhibitory SMADs, led to the opposite effect: we observed an increase in proliferation(**Figure 15**d). A partial reversion of the BMP4+TFB2 induced phenotype when SMAD6 and SMAD7 were downregulated (**Figure 15**e). Of interest, SMURF2, a ubiquitin ligase regulation SMAD signaling by inducing the degradation of canonical SMADs, is upregulated specifically in the TGF2+BMP4 condition in our scRNAseq (**Figure 15**f). Of note, SMURF1 was not detectable in the scRNAseq data (data not shown).

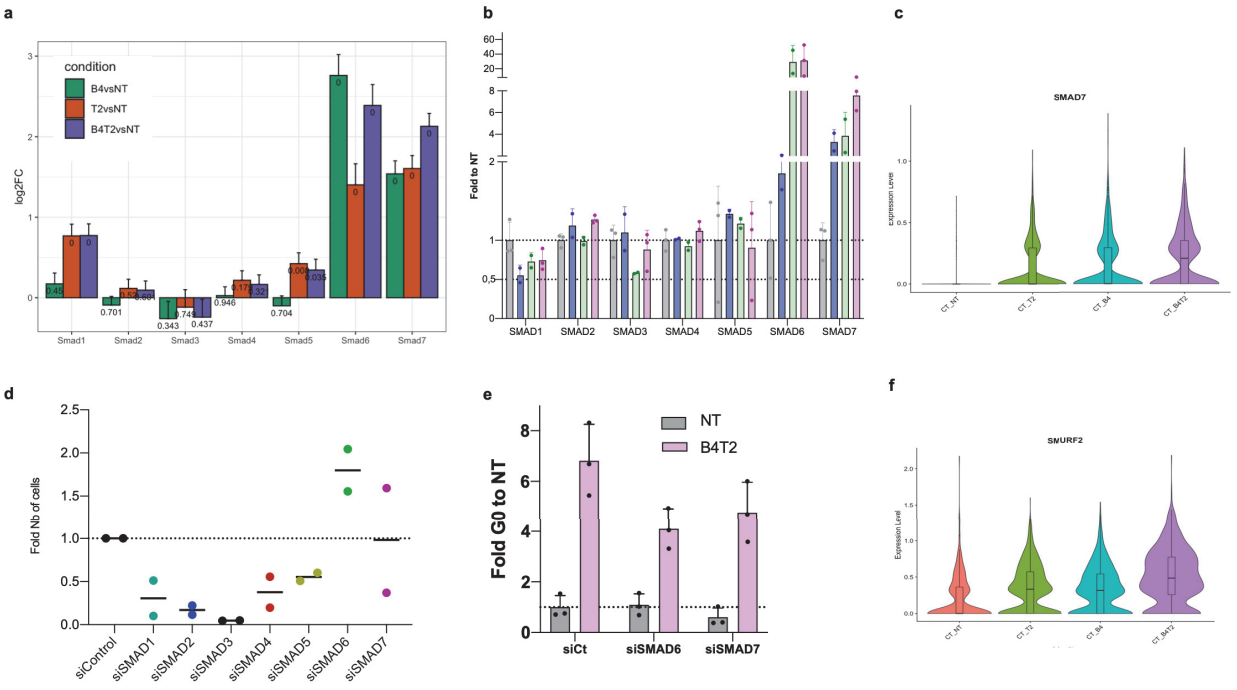

Figure 15: Role of inhibitory SMADs on BMP4 and TGFB2 co-signaling

***a**, bulk RNAseq data from PYMT cells. **b**, qPCR from MCF10A cells treated with TGFβ2 (blue), BMP4 (green) or both (purple) during 72h. **c**, SMAD7 expression in M1B26 cells in the single-cell RNAseq data. **d**, fold number of cells after 72h siRNA transfection. **e**, fold percentage of G0 cells quantified by flow cytometry in M1B26-FUCCI cells. **f**, SMURF2 expression in MCF10A cells in the single-cell RNAseq data.*

II. Signaling pathways

To assess which signaling pathways were involved in TGFβ2 and BMP4 co-signaling, preliminary western blot of canonical and non-canonical signaling were performed. Of interest, in murine PYMT cells 24h after treatment, increase of SMAD1/5 and SMAD2 phosphorylation was observed in the combinatory condition (**Figure 16**a), suggesting an increase in the activation of the activation of SMAD canonical signaling when both cytokine signal at the same time. This was nonetheless this not confirmed in MCF10A cells (**Figure 16**b), but this could come from the fact that not the same timepoints and concentration of cytokines were used. Nevertheless, an increase in the phosphorylation of STAT3 in the TGFβ2 condition is observed, whereas a decrease is observed in the BMP4 condition. The BMP4+TGFB2 condition seems to balance both response and have no change in the phosphorylation of STAT3 compared to the non-treated condition.

Of note, although the p38/ERK ratio has been described as an important dormancy inducer (Aguirre-Ghiso et al., 2004), no major modification in the phosphorylation of both p38 and ERK was observed compared to the GAPDH (**Figure 16**c).

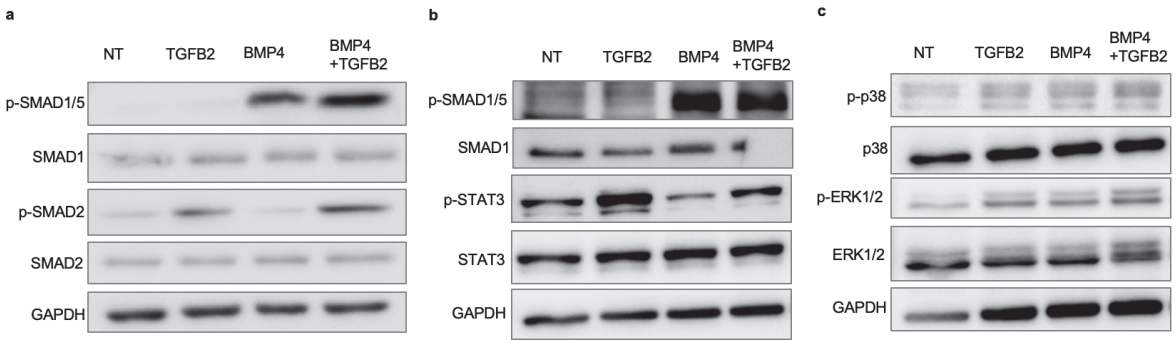

Figure 16: Signaling pathways involved in TGFB2 and BMP4 co-signaling

***a**, western blots of murine PYMT cells treated in serum free media during 24h with 5ng/mL of TGFβ2, 5ng/mL of BMP4 and 5+5ng/mL of TGFβ2+BMP4. **b**,**c**, western blots of human MCF10A cells treated in serum free media during 72h with 10ng/mL of TGFβ2, 10ng/mL of BMP4 and 5+5ng/mL of TGFβ2+BMP4*

III. *In vivo* characterization of the role BMPR2

During my stay in Julio Aguirre-Ghiso's lab, one of my objectives was to functionalize the role of TGFBR3 and BMPR2 in murine models. The aim was to develop murine cancer cell lines (E0771 and PYMT) lacking TGFBR3 or BMPR2 expression or lacking both TGFBR3 and BMPR2 expression to investigate the synergistic effect of BMP4 and TGFB2 signaling in inducing DTC dormancy in the mouse bone marrow. I was able to develop E0771-shBMPR2 and become proficient in intra-cardiac injection of mice. Nonetheless, my 18 months stay (Jan 2020 - July 2021) was impacted by the pandemic, the supply chain shortages and important mycoplasma contamination. BMPR2 knock-down was evidenced by RTqPCR quantification of BMPR2, shBMPR2 #C being the most efficient (**Figure 17**a). Western-blot of SMAD1/5 phosphorylation showed the diminished activation of SMAD1/5 afterBMP4 or BMP7 treatment in the E0771-GFP-shBMPR2 cell line (**Figure 17**b,c). E0771-GFP-shControl and shBMPR2 cells were injected intra-cardiac in mice and the number of cancer cells in the bone marrow was quantified two weeks later(**Figure 17**d). Surprisingly, there were less cancer cells in the bone marrow of animals injected with E0771-shBMPR2 (**Figure 17**e). To verify if the survival of the cells was affected, anoikis assay where cells are in suspension was performed. A reduce number of live cells was observed in the shBMPR2 cell line, indicative of reduced survival (**Figure 17**f). Thus, the reduced number of cancer cells in the bone marrow of animals injected with E0771-GFP-shControl could be due to a decrease in survival instead of a reduced proliferation. I could not repeat these experiments as the E0771-GFP-shControl and E0771-GFP-shBMPR2 were contaminated with mycoplasma. I instead used siRNA in E0771-GFP and PYMT-CFP cell lines. Cancer cells were transfected two days before intra-cardiac injections, and the number of cancer cells in the bone marrow assessed one week later (**Figure 17**g). A shorter timepoint (one week instead of two weeks) was chosen as siRNA have short-term effects only. No difference in cell growth in the bone marrow (**Figure 17**h,i) nor in cell survival in anoikis assay (**Figure 17**j) was observed. In the pilot *in vivo* experiments I was able to perform, we were thus not able to determine if we had a real functional result, or a technical problem in our system. I was not able to repeat these experiments. I also did not have enough time to generate the double knockdown cell line (E0771-shBMPR2-shTGFBR3).

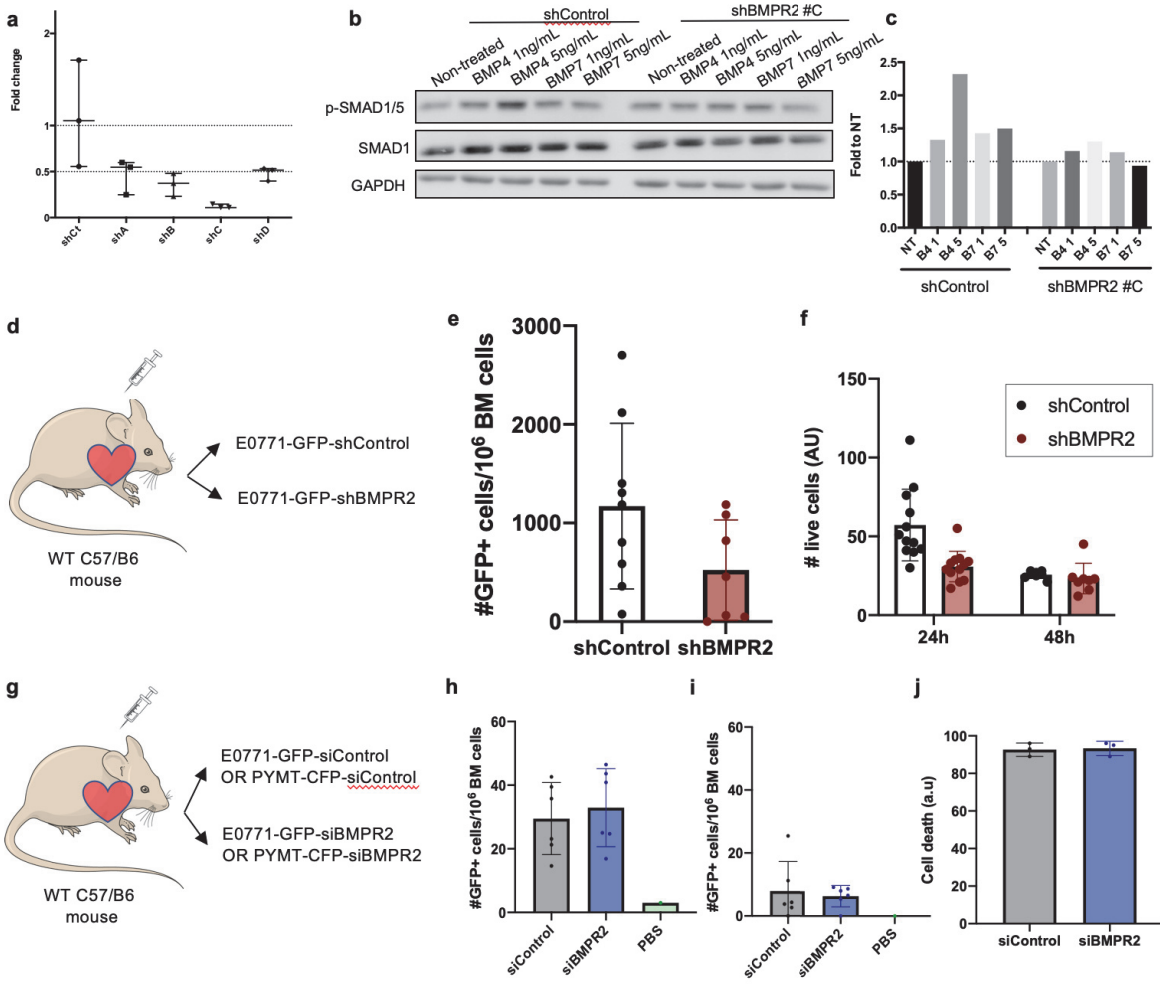

Figure 17: **in vivo *characterization of the impact of cancer cell BMPR2 expression in the bone marrow***

a, *RTqPCR of BMPR2 in E0771-GFP cell lines transduced with shControl of different shBMPR2* ***b****, Western blot of SMAD1/5 phosphorylation in E0771-shControl and E0771-shBMPR2 cell lines treated with BMP4 or BMP7.* ***c****, Fold increase of the SMAD1/5 phosphorylation normalized to SMAD1 expression.* ***d****, experimental design scheme where 3.10^5 E0771-GFP-shControl or shBMPR2 cells were intra-cardiac injected in mice.* ***e****, Quantification of the number of GFP+ cells in the bone marrow (BM flush) two weeks after injection in mice.* ***f****, quantification of the number of live cells in after 24h or 48h in suspension (anoikis assay).* ***g****, experimental design scheme where 3.10^5 E0771-GFP-siControl or siBMPR2 (or PYMT-CFP-siControl or siBMPR2) cells were intra-cardiac injected in mice. siControl and siBMPR2 were transfected in the cells 48h before intra cardiac injections.* ***h****, Quantification of the number of GFP+ cells in the bone marrow (BM flush) one week after injection in mice.* ***i****, Quantification of the number of CFP+ cells in the bone marrow (BM flush) one week after injection in mice.* ***j****, quantification of the number of live E0771-GFP cells in after 24h or 48h in suspension (anoikis assay), siControl and siBMPR2 were transfected in the cells 48h before the assay.*

IV. *In situ* characterization of the role of MSC in mediating cancer cell dormancy in the BM

M1B26-FUCCI were incorporated in the 3D model of the bone marrow niche recently developed in Dr. Maguer-Satta's lab (Voeltzel et al., 2022) to complexify our model and asses the role of mesenchymal stem cells (MSCs) in mediating breast cancer cell dormancy.

Briefly, This model is based on the coculture of a MSC line, HS27, and endothelial cell line, HMEC, with biphasic calcium phosphate (BCP) particles. After 3 weeks of differentiation and calcification, a disk resembling a mini-bone is formed (**Figure 18**a,b), supporting normal hematopoiesis for example, and then allowing for histological and functional analysis of cells. This model was ideal for us to complexify the effect of TGFβ2 and BMP4 as HS27 secrete those cytokine more than other MSC such as HS5 (**Figure 18**c). HS27 cell lines with inducible downregulation of the secretion of TGFβ2 and BMP4 were generated (**Figure 18**Xd,e). 3D-microenvironment with reduced TGFβ2 or BMP4 levels led to a decrease of the fraction of cells in the G0 state ($mCherry^{high}/mVenus^{neg}$). Although this experiment was only done once for the moment, this is a good preliminary indication that secretion of BMP4 or TGFβ2 by MSCs is mediating dormancy induction in the bone marrow.

Figure 18 (legend)

a, *BMP4 and TGFβ2 ELISA of HS5 and HS27 supernatant in culture.* ***b****, Representative scheme of the 3D bone marrow model.* ***c****, Experimental plan for the incorporation of M1B26-FUCCI cells in the 3D bone marrow model.* ***d****, TGFβ2 ELISA of HS27 and HS27-shTGFB2 supernatant in culture, with or without doxycycline treatment.* ***e****, BMP4 ELISA of HS27 and HS27-shBMP4 supernatant in culture, with or without doxycycline induction.* ***f****, Flow cytometry plot of the FUCCI pattern of M1B26-FUCCI incorporated in the 3D system during 7 days (doxycycline treatment was started 3 days before adding the M1B26-FUCCI cells.* ***g****, Representative flow cytometry plots of the M1B26-FUCCI incorporated in the 3D system during 7 days .*

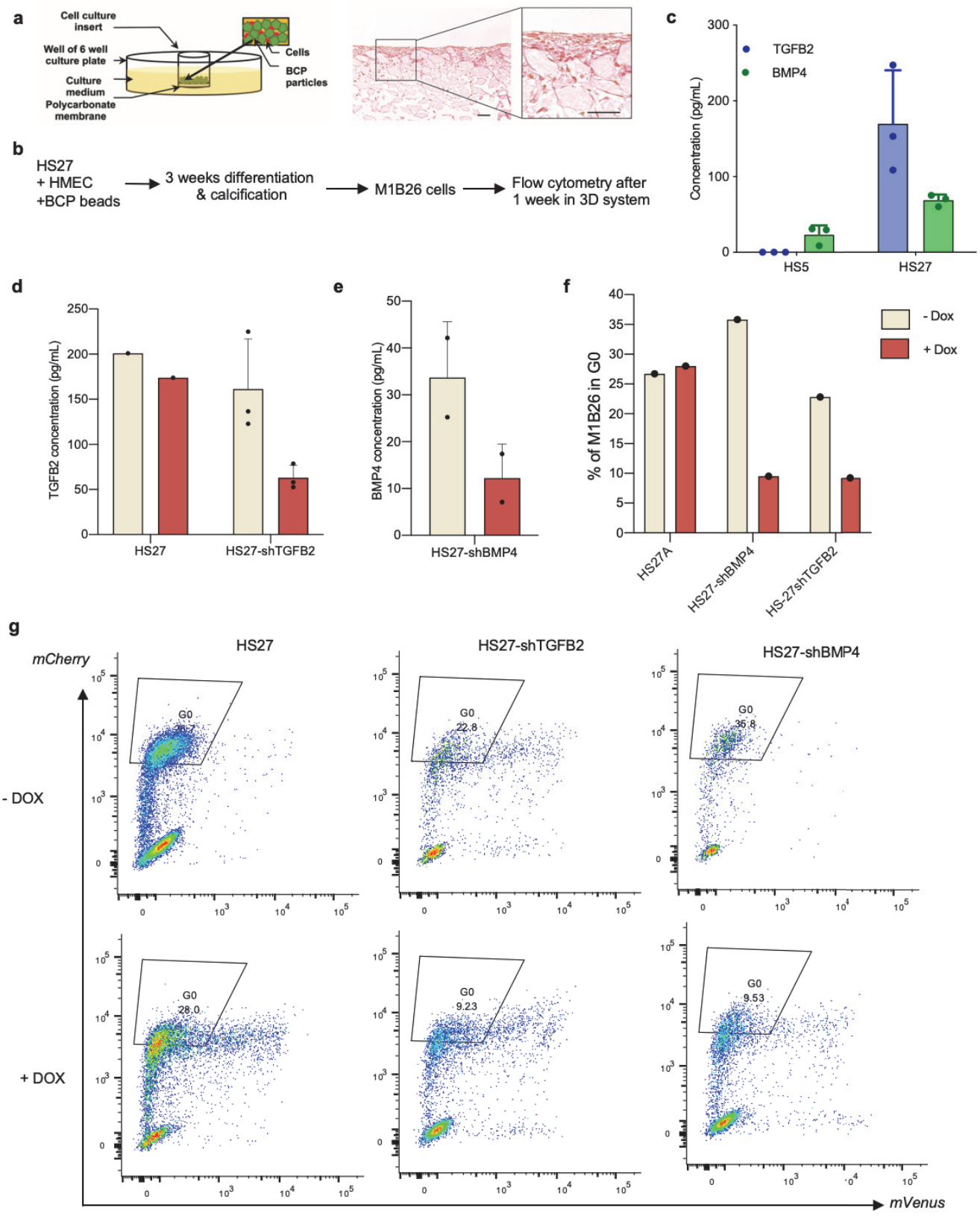

Figure 18: In situ characterization of the role of TGFB2 and BMP4 secretion by mesenchymal stem cell in breast cancer cell dormancy induction

DISCUSSION

Overall, this work led to the first description of a synergistic co-signaling of TGFB2 and BMP4 signaling on cancer dormancy induction. This effect exists in normal human mammary cells, and is conserved in human and murine cancer cells, independently of the transformation mechanism or the ER status. We also revealed the heterogeneity of the G0 compartment in dormant cancer cells with several functional assays. Single-cell RNAseq identified a specific deep dormant signature. We will here now discuss the results obtained in this project.

I. Functional evidence of BMP4 and TGFβ2 synergy

We have shown that BMP4 and TGFβ2 co-signaling strongly reinforces a pro-dormancy phenotype induced by both cytokine alone. Ample evidence had already shown the role of TGFβ2 dormancy induction in breast cancer (Nobre et al., 2021), head and neck cancer (Bragado et al., 2013) and prostate cancer (Yumoto et al., 2016). BMP4 production from the lung microenvironment enforces dormancy of disseminated cancer cells (Gao et al., 2012), and mediates quiescence of persistent leukemic stem cells in the bone marrow (Jeanpierre et al., 2020). TGFβ and BMP signaling are usually antagonistic in cancer cells, and the specific role of the interaction of these pathways in cancer dormancy has never been studied. We revealed that BMP4 and TGFβ2 co-signaling instead has a synergistic effect on dormancy induction.

On top of functional assays (3D matrigel and FUCCI cell cycle indicator), downregulation of Ki67 expression and upregulation of dormancy signature in bulk and scRNAseq are observed in cells treated with both TGFβ2 and BMP4 compared to cells treated with only one cytokine. Protein validation of dormancy markers (p21, p27, NR2F1, DEC2..) is ongoing and will reinforce our data.

Most of the studies on BMP and TGFβ signaling interaction in vitro involve high concentration of BMPs (100-300ng/mL) compared to lower levels of TGFβ (2-10ng/mL). The factorial design of BMP4 and TGFβ2 functional effects with increasing concentrations was performed to establish the dose correlation of the functional effect. A treatment with a 5ng/mL concentration of each cytokine (10ng/mL total concentration) leads to an increased effect compared to a final concentration of 10ng/mL of a single cytokine.

A part from cell cycle arrest induction, transcription of several extra-cellular matrix protein transcription is also observed, although protein validation is still needed. As described in the introduction of this manuscript (part III.A), in fibrosis studies, BMP signaling tends to inhibit the matrix formation induced by TGFβ. Of interest, in trabecular meshwork human cells, BMP4 blocked the TGFβ2-induced fibronectin induction (Wordinger et al., 2007), but BMP4 enhances this induction in our model. What would be needed now is to test this in human samples of normal and breast tumors if the TGFβ2, BMP4 or combinatory treatment leads to dormancy induction and if similar target genes identified in the scRNAseq are also upregulated in dormant cells.

This functional synergistic effect between TGFβ and BMP in cancer dormancy had not been described before and brings important understanding on the regulation of cancer dormancy. What is now needed and how we are continuing this project is by better understanding the molecular mechanisms explaining this synergy : which receptors and signaling pathways mediate this effect ?

II. Which receptors mediate TGFB2 and BMP4 pro-dormancy effect?

The TGFB super-family being very complex and multifunctional, the identification of the receptors mediating this effect is of main interest to understand how to target TGFB and BMP signaling and their diverse effects in cancer cells.

In (Chapellier et al., 2015), higher BMP2 levels were measured in luminal breast tumors compared to normal samples whereas BMP4 levels were unchanged. Moreover, long term exposure led to the transformation of MCF10A cells, whereas BMP4 long-term exposure did not. We have shown in our model that BMP2 does not affect cell cycle regulation (Supplementary Fig. 3 of the paper). Thus, BMP2 drives transformation without regulating the cell cycle, and BMP4 induces dormancy in normal and transformed mammary cells. Treated MCF10A or M1B26 with both BMP2 and BMP4 did not affect the pro-dormancy effect of BMP4. This could mean that the signal is not saturated, that many receptors are still available to mediate the BMP4 effect, or that BMP2 and BMP4 do not signal through the same receptors. Indeed, BMP4 has a lower association constant but higher dissociation constant to BMPR1a and BMPR1b compared to BMP2: BMP4 binds less rapidly to these receptors but stays longer bound to them (Khodr et al., 2020). Moreover, BMP4 has higher affinity to BMPR1a compared to BMPR1b, whereas BMP2 has a higher affinity to BMPR1b.
Identifying which type 1 receptor mediates BMP4 signaling in our model is of strong interest to better assess how this signal could be targeted. BMPR1a is reported to be essential in mediating quiescence of neural stem cells (Mira et al., 2010) and hair follicle stem cells (Kobielak et al., 2007). BMPR1b has been involved in transforming mammary epithelial cells (Chapellier et al., 2015), but its expression is reduced upon breast cancer cell proliferation (Bokobza et al., 2009). Moreover, in the hematopoietic system, the quiescent fraction of leukemic stem cells depends on BMPR1b signal to persist in patients in remission (Jeanpierre et al., 2020).

One objective of my stay in Pr. Aguirre-Ghiso's lab, was to functionalize the role of BMPR2 in vivo in mice. We chose to focus on BMPR2 instead of a type 1 BMP

receptor as BMPR2 was identified as essential to mediate BMP7's effect as a pro-dormancy induced of prostate cancer cells *in vivo* (Kobayashi et al., 2011) and the expression of a dominant negative BMPR2 in mammary tumors in mice led to increased lung metastasis (Owens et al., 2012). On the other hand, BMPR2 seems to have an opposite effect in human cancer cells, in which the expression of a dominant negative BMPR2 inhibited cancer cell growth (Pouliot et al., 2003). Results obtained (**Figure 17**) could not confirm the role of BMPR2 in murine breast cancer cells. Due to the discrepancy of the effect of the BMP family between human and mice cell lines, molecular studies will now focus on human models would be more efficient.

Necessary to mediate TGFβ2 signaling, TGFβR3, also called betaglycan, is a transmembrane proteoglycan with no kinase activity that functions as a coreceptor in the TGFβ super-family. As described in the introduction of this dissertation, TGFβ2 has a lower affinity for TGFβR2 compared to TGFβ1 and needs TGFβR3 to signal. This receptor has been shown to suppress breast cancer progression (Dong et al., 2007) and is a mediator of TGFβ2-driven dormancy of cancer cells (Bragado et al., 2013). Of strong interest for our study, BMP4 has also been shown to bind to TGFβR3, which led to enhanced BMP signaling activation (Kirkbride et al. 2008). Moreover, TGFβR3 can be cleaved and secreted in the extra-cellular space. It becomes a trap and binds extra-cellular TGFβ2 and BMP4, decreasing the amount of cytokine available to bind membrane-bound receptors and activate signaling pathways (Gatza et al., 2014). Thus, the ratio of membrane-bound TGFβR3 and soluble TGFβR3 that could determine the effect of BMP4 and TGFβ2. TGFβR3 has also been involved in mediating FGF signaling (Andres et al., 1992). This receptor could thus be involved in coordinating multiple signaling pathways by limiting ligand availability or forming specific receptor heterocomplexes. The specific role of betaglycan will now be assessed in our models to evaluate if TGFβR3 is necessary to BMP4's pro-dormancy effect.

To elucidate which receptor is involved in the synergic effect of TGFβ2 and BMP4, we plan to target the expression of receptors with siRNA and verify if the pro-dormancy effect is still observed with our FUCCI model.

III. Which signaling pathway is mediating the synergistic effect of TGFB2 & BMP4?

A redundant observation made in several of our models is the upregulation of inhibitory SMADs upon TGFB2 and BMP4 treatments (**Figure 15**). As decreased expression of canonical SMAD1/2/3/4/5 led to a strong reduction in proliferation (**Figure 15**), are we mimicking the effect of TGFβ2+BMP4 treatment through reduction of canonical SMAD signaling? Moreover, downregulation of SMAD6 and SMAD7, inhibitory SMADs, led to a partial reduction of the BMP4+TGFβ2 pro-dormancy induction. SMAD (and SMURFs) in cancer are described as both pro and anti-proliferation depending on the cancer types and models (Stolfi et al., 2013). Of note, the BMP4/SMAD7 axis was shown to suppress metastasis by inducing anoikis while cancer cells are circulating in vessels. It also predicts improved survival in patients (Eckhardt et al., 2020). Although the mechanism proposed in this study does not involve quiescence induction, influence of inhibitory SMADs on TGFβ/BMP signaling in breast cancer dormancy needs further elucidation, perhaps by using cell lines with a full knock-out of SMAD6 and SMAD7 instead of transient downregulation.

As presented in the introduction, TGFβ and BMP signaling interactions are often mediated by non-canonical signaling. Moreover, the upregulation of inhibitory SMADs could decrease SMAD canonical signaling, thus directing the signal towards non-canonical signaling. Indeed, p38 and ERK activation balance (Aguirre-Ghiso et al., 2001) is a well described regulator of dormancy in head and neck cancer models (Bragado et al., 2013) and prostate cancer models (Kobayashi et al., 2011). In our MCF10A model, p38 and ERK activation does not seem to play a role in dormancy induction. Nonetheless, we observed alteration of STAT signaling in single-cytokine treatment that seem to be normalized in the combinatory conditions. Indeed, interactions of STAT and SMAD signaling pathways have been described in various models. BMP2 and LIF were shown to act synergistically to induce the differentiation of astrocytes through SMAD1/STAT3 interaction (Nakashima et al., 1999). Also, TGFB/IL6 co-signaling led to the interaction of SMAD2/STAT3 in hepatic cells (Yamamoto et al., 2001). On the other hand, antagonism between STAT and SMAD

signaling has been described in mammary epithelial cells where SMAD signaling antagonized the effect of STAT5 by preventing its binding to CEBP, leading to the inhibition of mammary gland differentiation (Cocolakis et al., 2008). Could enhanced STAT signaling lead to a molecular interaction between STAT and SMAD to reduce TGFB signaling as previously described (Wang et al., 2016a)? Indeed, SMAD and STAT co-activation was also described in persistent chronic myeloid leukemia stem cells to mediate their quiescence (Jeanpierre et al., 2020). If an interaction between SMAD and STAT signaling pathway occurs to enhance or decrease the activation of canonical target genes, it would be of great interest to decipher at the molecular level the integration and signaling pathways rewiring happening in the BMP4+TGFB2 condition. The increase or decrease in STAT3 phosphorylation could also be an indirect effect of the treatment inducing or inhibiting the expression of cytokines that activate the JAK/STAT pathway.

It is the resulting activation or repression of certain genes that will mediate cytokine effects. Activated cytoplasmic signal transducers enter the nucleus to regulate gene expression. We searched for a transcription factor whose signature was enriched uniquely in the BMP4+TGFβ2 condition in the bulk PYMT data set (**Supplementary Fig.1i of the paper**) and the MCF10A scRNAseq (**Fig.5a of the paper**) and identified E2F4. This transcriptional repressor is involved in inhibiting cell cycle progression. Interestingly, SMAD3 and E2F4 were shown to form a complex pre-assembled in the cytoplasm (Chen et al.). When cells are treated with TGFB, SMAD4 joins the complex, inducing nuclear localization of the complex and MYC repression. Co-immunoprecipitation experiments will evaluate if TGFB2 and BMP4 co-signaling allows for a specific SMAD protein to interact with E2F4 in our models, by limiting the availability of SMAD4 perhaps. If so, CHIP-seq assay would then allow to identify genes specifically regulated in TGFB2 and BMP4 co-exposure. Integrating this data with the scRNAseq will then be essential.

IV. Heterogeneity of the G0 compartment

Using three different functional assays, we showed that G0 sorted cells from non-treated condition re-entered the cell cycle faster than G0-sorted cells from the BMP4+TGFB2 condition. After 72h treatment in culture, the same number of G0 cells were seeded without the cytokines treatment to assess the speed of re-entry in to the cell cycle. In 2D, this led to fewer cells in the B4T2 condition compared to others. In 3D, the BMP4+TGFB2 G0-sorted cells formed smaller clusters. In a mammosphere assay, G0-sorted cells generated more spheres, but smaller.
These results need more biological replicates, but suggest that not all G0 cells are in the same state of quiescence. **Two hypothesis can be made on the heterogeneity of quiescence: is there only one type of quiescence and does BMP4 and TGFβ2 signaling increase the duration of quiescence? Or does it induce a qualitatively different quiescence program with different molecular mechanisms? Could both mechanisms co-exist?** These questions relate to understanding cellular quiescence ranging from unicellular to multicellular organisms (Daignan-Fornier et al., 2021), and a clear consensus constitutes a breakthrough in the field.

Regarding the duration of quiescence, in prostate cancer cells cultured *in vitro*, the length of time spend in G0 has been shown to be highly heterogenous (ranging from 5 to 27 hours) compared to the length of time cells spend in G1/S/G2/M (raging from 10 to 15 hours) (Pulianmackal et al., 2021). In these PC2 cells, TGFβ2 treatment led to a higher increase in the proportion of G0 cells and a lower number of cells that underwent division compared to GAS6, a ligand previously shown to induce prostate cancer dormancy (Taichman et al., 2013). However, GAS6 treatment increased the time spent in G0, whereas TGFβ2 treatment did not (Pulianmackal et al., 2021). Could TGFβ2 and BMP4 co-signaling affect the duration of dormancy on top of increasing the proportion of cells in dormancy ? To assess this, we now plan to do live imaging of single G0 cells to quantify the time that $mCherry^{high}/mVenus^{neg}$ (G0) cells take to re-enter cell cycle, and compare it across conditions. In addition, in our models $mCherry^{high}/mVenus^{neg}$ (G0) have lower Ki67 expression compared to $mCherry^{low}/mVenus^{neg}$ cells (G1) (**Figure 3c of the paper**). Being a molecular evidence of how the FUCCI model can allow for the separation

of those two cell cycle phases, this marker could also inform on the duration of quiescence. Indeed, cells under long-term quiescence have less Ki67 expression than cells that are also in quiescence for a shorter time : Ki67 levels steadily decrease with the time the cells spend in quiescence (Miller et al., 2018). KI67 expression can thus be a graded marker instead of a binary marker (positive or negative) and could inform the length and depth of dormancy.

Moreover, recent evidence sustained the potential existence of heterogeneity of quiescence stages as quiescent cells have been reported to be arrested with 2N or 4N DNA copy. Yeast biology has indeed shown that yeast cells can enter a quiescent state through all the phases of the cell cycle (Wei et al., 1993). This was also shown in drosophila, where quiescent neural stem cells (qNSCs) can be arrested in the G2 phase (and have 4N DNA) or in the G0 phase (and have 2N DNA) (Otsuki and Brand, 2018). Of interest, G2 qNSCs could re-enter the cell cycle faster compared to G0 qNSCs. Similar observations were made in a cell line used to model breast cancer dormancy, D2.OR, in which 20% of arrested cells are in a 4N state (Prunier et al., 2021). Could BMP4 and TGFβ2 co-signaling lead to a cell cycle arrest in any cell cycle phases? At the beginning of this PhD project, DNA staining was used as a cell cycle marker (G0/G1 have 2N DNA content, whereas G2/M cells have a 4N DNA content). We observed smaller differences across conditions (data not shown) compared to our 3D matrigel assays or our later implemented FUCCI reporter system. Could an arrest in 4N state explain this reduced effect observed when staining DNA content? A simple Hoechst staining in our FUCCI cells could answer this question.

To assess the qualitative difference between quiescence programs, and based on the functional evidence of the heterogeneity of the G0 compartment, we decided to perform single-cell RNAseq on this population across our conditions. Indeed, functional synergy in cell cycle arrest induction does not necessarily mean that a molecular synergy exist, as the results could simply come from and addition of two signals.

$mCherry^{high}/mVenus^{neg}$ cells (G0) were sorted from cells that had been treated with vehicle, TGFB2 (10ng/mL), BMP4 (10ng/mL) or TGFB2+BMP4 (5+5ng/mL) during 72h. Before performing this single-cell RNAseq, we were not certain that we would obtain differences among our conditions : we were using a cell line (not tumors with different stromal and immune cell types as in most of the single-cell RNAseq uses), and cells were even more homogenized because we sorted G0 cells by flow cytometry, taking advantage of the FUCCI system. G0 cells are also characterized by their reduced mRNA expression and cell cycle analysis with single cell RNAseq data is challenging. Most studies even remove cell cycle genes for their analysis! But overall, this bioinformatic of G0 single-cell RNAseq analysis has shown us that even G0 cells can have different molecular signatures, confirming the heterogeneity we have observed in functional assays. Indeed, the identification of genes uniquely differentially regulated in the BMP4+TGFβ2 conditions shows that we have new signal being transmitted in these treated cells (qualitative) instead of an addition of two different signals (quantitative addition).

These differential programs identified show that different quiescence programs can exist depending on the initiating signal. This is consistent with previous studies where different cell-cycle arrest signals (mitogen withdrawal, contact inhibition and loss of adhesion) led to different cell-cycle arrest transcriptional programs in fibroblasts (Coller et al., 2006). Furthermore, the intensity of quiescence programs can also be regulated: muscle stem cells (Rodgers et al., 2014) and neural stem cells (Llorens-Bobadilla et al., 2015) can be primed for fast cell cycle-reentry while remaining quiescent, indicating different deepness of dormancy with differential molecular programs. Of strong interest for our model, the transition between dormant-quiescent and primed-quiescent state relies on BMP4 signaling regulation. BMP4 signaling induces the dormant-quiescent state, whereas BMP4/FGF2 co-signaling induces the primed-quiescent state. Transposing this to our model, we

could interpret our data as BMP4 and TGFβ2 co-signaling induce a deep dormant state whereas BMP4 alone or TGFβ2 alone induce a shallower state of quiescence. Additional analysis of this single-cell RNAseq is still ongoing. I am currently trying to perform pathway enrichment and network analysis to identify super-regulators of the deep dormancy program.

Overall, we have shown that a distinct molecular mechanisms maintain cells in the G0 state and that G0 cells from BMP4+TGFβ2 conditions are in a deeper cell cycle arrest. G0 cells from the BMP4+TGFβ2 conditions also take longer to re-enter the cell cycle. Assessing if these differences have a functional consequence in more complex models and is patients is now necessary.

V. Microenvironmental control of DTC dormancy by MSCs in the BM

In the main part of my PhD work, I mainly studied the role of the combination of TGFB2 and BMP4 cytokines on cancer dormancy induction, but it is now essential to introduce more complexity to identify the role of mesenchymal stem cells in this co-signaling phenotype of BMP4 and TGFB2.

Part of my PhD work included working on the role of $NG2^{+}$/$Nestin^{+}$ Mesenchymal Stem Cells (MSC) on the regulation of breast cancer dormancy in *in vivo* murine models. The specific depletion of $NG2^{+/}Nestin^{+}$ MSCs in the bone marrow led disseminated breast cancer cells awakening (Nobre et al., 2021). When the TGFβ2 gene was knocked-out of $NG2^{+/}Nestin^{+}$ MSCs specifically, a similar phenotype was observed but with less penetrance. Indeed, scRNAseq from mouse bone marrow showed that MSCs secrete other factors such as an important amount of BMP4 (Tikhonova et al., 2019), suggesting that secretion of both cytokines by MSCs enforces a strong pro-dormancy signal in disseminated breast cancer cells in the bone marrow.

To test this, we have optimized the 3D micro-physiological model of the bone marrow niche developed in Dr. Maguer-Satta's lab (Voeltzel et al., 2022). This allows us to mimic the first events upon arrival of cancer cells in the bone marrow microenvironment. The first preliminary experiment showed that reduction of the secretion of TGFβ2 and BMP4 by HS27 in the microenvironment led to increased proliferation of the M1B26-FUCCI cells (**Figure 18**). Reproduction of this experiment is necessary, and we plan on optimizing the *in situ* visualization of the cell cycle state (with mCherry and mVenus fluorescence) of the cells after incorporation in paraffin sections.

VI. Extra-Cellular Matrix in Dormancy Regulation

Cells interact with their microenvironment through the extra-cellular matrix (ECM) network. In the scRNAseq signatures of TGFβ2, BMP4 or TGFβ2+BMP4 deep dormant cluster, many ECM genes are upregulated, consistent with the known effect of TGFβ and BMP on fibrosis and EMT (Moustakas and Heldin, 2016).

ECM proteins have been implicated in mediating dormancy signals such as fibronectin (Aguirre-Ghiso et al., 2001) or laminin-211 in breast cancer cell disseminated to the brain (Dai et al., 2022). In fibrosis studies, BMP signaling usually opposes the ECM secretion induced by TGFβ (Wordinger et al., 2007). However, in our scRNAseq data, fibronectin (FN1) and laminin (LAMA3, LAMB3, LAMC1) are upregulated by TGFβ2 and BMP4 condition, but are even more upregulated in the TGFβ2+BMP4 condition (data not shown).

Moreover, Integrin alpha-6 (ITGA6), Collagen-4 and Collagen-17 (COL4A1, COL4A2, COL17A1) are specific markers of the combinatory condition (Figure 5 of the paper): this is of particular interest as integrin alpha-6 is involved in latent TGFβ activation (Annes et al., 2004) and collagen-4 binds BMP ligands and modifies their diffusion (Zakin and De Robertis, 2010). A recent study revealed that Collagen-3 secretion by dormant tumor cells was necessary to maintain their dormancy (Di Martino et al., 2022). When Collagen-3 secretion was inhibited, proliferation was restored through STAT1 phosphorylation. As we have found that STAT3 is differentially phosphorylated across our conditions, the potential link with the collagen-4 identified in this scRNAseq is of particular interest. On top of inducing BMP/TGFβ pathway inhibitors described above in this discussion, deep dormant cluster seem to have an important ECM production, leading to a potential different sensing of BMP/TGFβ signals.

PERSPECTIVES

As the synergistic effect of BMP and TGFβ signaling in cancer dormancy had not been previously described, this work raises important questions and perspectives.

A continuation of this work would be to include other ligands of the BMP and TGFβ family to better assess signal specificity and combination. BMP2 did not affect cell cycle regulation in our model, but we could have also tested BMP7 as it was involved in prostate cancer cell dormancy in the bone marrow (Kobayashi et al., 2011). Moreover, assessing the role of ligands from different pathways with a multi-dimensional factorial design could be of great interest as the TGFβ/BMP family crosstalk with many other pathways (Luo, 2017). For example, Wnt5a has been shown to induce breast cancer cell dormancy (Ren et al., 2019) and there is significant scientific literature on the combinatory effect of TGFβ, BMP, and Wnt signaling (Guo and Wang, 2009). High-throughput microculture system identified out of 500 other possibilities that the specific combination of TGFβ, BMP-4, Wnt-3a and Ephrin-B2 coordinated neuronal differentiation and maturation (Muckom et al., 2019). Using high-throughput screens to identify combinatory signals could lead us to better understand the microenvironmental regulation of cancer dormancy.

We have focused our analysis on the effect of two cytokines on cancer cell lines in culture. However, do all disseminated cells from tumors respond similarly to the same cues? Do pro-dormancy cues induce the dormancy of all cancer cells, or do only a subpopulation of cells that have been “primed” can enter dormancy? Gene expression signatures from the primary tumor can inform on the potential for metastatic relapse (Kim et al., 2012) and post hypoxic disseminated tumor cells in the primary tumor were more prone to enter dormancy in the lung (Fluegen et al., 2017). Moreover, a recent study specifically assessed the difference in extravasation capacity and dormancy of cancer cells in mice that were injected in the tail vein (experimental metastasis assay) or injected in the mammary fat pad (spontaneous metastasis assay) (Borriello et al., 2022). Systemic depletion of macrophages and co-culture experiments before tail vein injection showed that the priming of cancer cells by macrophages mediated enhanced survival and dormancy of breast cancer cells in the lung (Borriello et al., 2022). Moreover, elevated BMP levels were shown to induce a pro-dormancy microenvironment in the lung (Gao et al., 2012). However, a subpopulation of cells expressing the BMP inhibitor Coco

could start proliferating, suggesting that an intrinsic characteristic of the cells allowed them to proliferate. Furthermore, late and distant relapse in ER+ breast cancer patients was associated with an accumulation of cancer-associated fibroblast subset S1 (Bonneau et al., 2020) in the primary tumor. Hence, signals received by cells in the primary tumor can influence how they respond to secondary organ microenvironment cues. Identifying if only a subset of cells respond to BMP4 and TGFβ2 pro-dormancy signals and if this is linked to primary tumor priming would be of particular interest to better understand how to predict the risk of metastasis.

As discussed previously, our work here focuses on the regulation of breast cancer cell dormancy in the bone marrow microenvironment by the secretion of TGFβ2 and BMP4 by MSCs. However, MSCs are not the only source of TGFβ2 and BMP4 in the BM: osteoblasts, endothelial cells, and chondrocytes also secrete them (Tikhonova et al., 2019) among others. Cells of particular interest in mediating TGFβ signaling in the BM are non-myelinating Schwann cells: they modulate latent TGFβ activation to regulate HSC quiescence(Yamazaki et al., 2011). In pancreatic tumors, they have also been shown to regulate the effect of TGFβ on the tumor microenvironment (Roger et al., 2019). The role of this cell type would thus be of strong interest in our model to understand its interplay with TGFβ ligand availability and activation.

Moreover, this work could have implications beyond breast cancer and bone marrow induced dormancy: as abundantly discussed in this manuscript, TGFβ and BMP signaling have been shown to regulate cellular quiescence or cancer cell dormancy in lungs and brain microenvironment for example (Prunier et al., 2019). Moreover, cancers of several origins respond to TGFβ and BMP signaling. Most of the evidence is in prostate cancer cell dormancy (Prunier et al., 2019). Indeed, in our hands, the 22RV1 prostate cancer cell line responded to BMP4+TGFβ2 and entered dormancy, whereas cells exposed to a single cytokine did not (data not shown). This BMP4 and TGFβ2 co-signaling effect could thus also be of great importance in other cancers and other niches.

As mentioned in the introduction of this manuscript, a very intriguing phenomenon for physicians is the relapse pattern depending on the breast cancer molecular subtypes. Why do patients with TNBC relapse often and early but are considered cured if they have not relapsed within five years? Why do patients with ER+ cancer relapse late? Indeed, patients with ER+ tumors are still at risk of relapse 20-30 years later, and the risk of relapse is stable beyond the first five years after diagnosis. (Pan et al., 2017) (Pedersen et al., 2022b). A better evaluation of the risk of relapse is essential. A recent study studied the dynamics of breast cancer relapse among integrative clusters subtypes (Rueda et al., 2019). Two groups of patients with TNBC were identified: one who rarely relapses after five years and one who remains at risk. They also identify late recurring ER+ subgroups. These subgroups represent about 25% of patients with ER+ tumors and are characterized by specific genomic-copy-number alterations. These integrative subtypes improve the prediction of late recurrences compared to clinical covariates (TN stage, age, tumor size,..). This allows for a better risk of relapse assessment for patients to decide if they would benefit from continued endocrine therapy beyond 5-years. However, extending endocrine therapy from 5 to 10 years only leads to a slight reduction in cancer relapse but has considerable side effects by increasing the risk of endometrial cancer and osteoporosis (Richman and Dowsett, 2019). It is, therefore, essential to find better therapeutic options to target dormant cancer cells during the remission phase to avoid relapse.

On top of this, the (Tikhonova et al., 2019) study assessed the effect of chemotherapy (5-FU) on the bone marrow. A very strong increase in the proportion of adipo-poised MSC after 5-FU treatment was observed in the mesenchymal compartment. The osteoblastic lineage also went through subsequent reprogramming. Thus, the cytokine profile of the different cells was altered: overall expression of Bmp4 was increased in the MSCs as well as Notch ligands (Dll1 and Dll4) and Wnt ligands (Wnt5a and Wnt4) in the vascular compartment. It is interesting to note that this considerable reprogramming of the niche after chemotherapy led to the increase of signals that have been shown to induce prostate cancer dormancy (Wnt5a, Ren et al. 2019) and breast cancer dormancy (Notch2, Capulli et al. 2019), as well as BMP4 that we show here induces breast

cancer cell dormancy. It would be of great interest to know the altered levels of TGFβ2 in this model. Could this reprogramming lead to the induction of quiescence of a subpopulation of cancer cells instead of killing them?

We have identified decreased BMP4 levels in aging normal bone marrow samples (**Fig. 3e of the paper**). Decreased BMP4 signaling would be a removal of a dormancy-inducing cue, and the co-signaling effect of TGFβ2 and BMP4 would not be mediated anymore even if TGFβ2 was still in high amounts in the bone marrow. We have also performed TGFβ2 ELISA on the same samples, but no signal higher than the background noise was detected. As TGFβ2 is often trapped in the extracellular matrix, this does not necessarily mean it is not present in the human bone marrow. Indeed, in (Nobre et al., 2021) patients with ER+ breast cancer with no systemic recurrence had a 2.28 higher frequency of detectable TGFβ2 compared to patients with systemic recurrence. Hence, monitoring BMP4 or TGFβ2 levels in patients in remission could be a biomarker to assess the risk of dormant breast cancer cell awakening to know when treatment uptake should re-start.

To prevent late metastatic relapse, developing targeted therapies against dormant cells is essential. Disseminated cancer cell identification in the BM after neo-adjuvant treatment identifies breast cancer patients at high risk of relapse (Naume et al., 2014). Thus, we ought to find ways to target dormant cells with the continual increase in cancer cell dormancy understanding (Recasens and Munoz, 2019). We should not wait for minimal residual disease to awake before starting treatment and take advantage of the minimal residual disease window to target dormant cancer: DTCs should be specifically targeted even though they are not actively proliferating yet. This can be done in different ways: 1) awakening dormant cells rendering them sensitive to anti-proliferation therapy, 2) maintaining cancer cells in a dormant state, or 3) killing dormant cancer cells. For each of these options, we can target extrinsic and microenvironmental cues regulating dormancy or intrinsic characteristics of the dormant cancer cells.

CXLC12 secretion by MSCs was shown to induce dormancy of chronic myeloid leukemia stem cells in mice. Specific deletion of this factor in MSC led to increased leukemic stem cell proliferation and subsequent elimination by tyrosine kinase inhibitors (Agarwal et al., 2019). Although targeting microenvironment signals was

possible in this murine genetic model, this is not easily translatable to humans. Moreover, alteration of the microenvironment can have many unknown effects. In our case, increasing BMP4 and TGFβ2 levels in the bone marrow might not be a solution to keep cells dormant as it will have significant effects on bone marrow homeostasis. Targeting intrinsic characteristics of dormancy could lead to less adverse effects and be more efficient. Dual targeting of STAT3 and BMPR1b inhibited leukemic stem cell quiescence induced by mesenchymal stem cells (Jeanpierre et al., 2020). However, chronic myeloid leukemia cells have a unique oncogene addiction with effective treatment, but solid cancers can be more heterogeneous, and response to chemotherapy is less predictable. In solid cancer, Fbxw7 was identified as essential for maintaining breast cancer dormancy (Shimizu et al., 2019): genetic ablation of Fbxw7 induced the proliferation of dormant cells and their subsequent killing by chemotherapy in a mice model. Despite that, this awakening option is very high-risk for patients whose cancer cells could have perhaps stayed dormant for many more months or years.

A pilot study tested dormancy maintenance in pre-clinical models by using an agonist of NR2F1, an orphan nuclear involved in inducing cancer dormancy (Sosa et al., 2015), which stratifies the risk of relapse in breast cancer patients (Borgen et al., 2018). The NR2F1 agonist suppressed metastasis in murine models of Head and Neck Squamous Cell Carcinoma (HNSCC) by inducing dormancy (Khalil et al., 2022). This hypothesis would require life-long therapy requiring patient compliance and would thus make cancer a chronic disease. The possibility of awakening and relapse might also still exist if cells evade therapy.

The fact that we have data on the effect of BMP4 and TGFβ2 co-signaling on non-transformed and transformed cells allows the identification of targets specific to the transformed cell lines. Of interest, integrin alpha-6 is uniquely upregulated in the combinatory condition only in transformed M1B26. Disrupting DTC interaction with its niche by downregulating integrin beta-1 has been shown to sensitize cells to chemotherapy without inducing DTC proliferation (Carlson et al., 2019). As integrin is also expressed by normal stem cells (Krebsbach and Villa-Diaz, 2017), deciphering the specific signaling pathways and targets activated in transformed cells is needed. Hence, if we functionalize the importance of ITGA6 signaling in mediating the deep dormant phenotype, it could become an attractive clinical target.

Studying cancer dormancy and late relapses in pre-clinical models, especially the 15-20 year period of late relapse occurring in ER+ breast cancers. Technical advances are now allowing the detection of these rare cells to study them better. The development of combined spatial information and single-cell studies will enhance knowledge of dormancy regulation by the niche. Another major issue in studying cancer dormancy is obtaining patient samples when patients are in remission, as the design of clinical trials to study dormancy is challenging. Collaborations between physicians and scientists are needed to incorporate the measurement of endpoints related to dormancy in clinical trials.

CONCLUSION

Dormant cancer cells underlie metastatic relapse in patients upon awakening. Most treatments only target components identified in proliferating primary tumors, but dormant disseminated cancer cells in secondary organs have very distinct biology. A more profound comprehension of these mechanisms is needed to target dormant cells. For this purpose, this work led to the first description of a synergistic co-signaling of TGFβ2 and BMP4 signaling on cancer dormancy induction. This effect exists in normal human mammary cells and is conserved in human and murine cancer cells, independently of the transformation mechanism. We also revealed the heterogeneity of the G0 compartment in dormant cancer cells with functional assays. Single-cell RNAseq identified a specific deep dormant signature. Moreover, our work identified decreasing BMP4 levels in the aging human bone marrow. This work brings a new understanding of how multiple signals can cooperate to regulate the length of breast cancer dormancy. It opens novel therapeutic opportunities for patients to prevent late relapses by identifying specific cues regulating cancer cell dormancy. Moreover, it identifies potential biomarkers to monitor the risk of awakening in patients in remission. These findings could also apply to other types of cancer or metastatic sites in which dormancy and late metastatic relapse have been described.

BIBLIOGRAPHIE

Abreu, J.G., Ketpura, N.I., Reversade, B., and De Robertis, E.M. (2002). Connective-tissue growth factor (CTGF) modulates cell signalling by BMP and TGF-β. Nat Cell Biol *4*, 599–604. https://doi.org/10.1038/ncb826.

Agarwal, P., Isringhausen, S., Li, H., Paterson, A.J., He, J., Gomariz, Á., Nagasawa, T., Nombela-Arrieta, C., and Bhatia, R. (2019). Mesenchymal Niche-Specific Expression of Cxcl12 Controls Quiescence of Treatment-Resistant Leukemia Stem Cells. Cell Stem Cell *24*, 769-784.e6. https://doi.org/10.1016/j.stem.2019.02.018.

Agudo, J., Park, E.S., Rose, S.A., Alibo, E., Sweeney, R., Dhainaut, M., Kobayashi, K.S., Sachidanandam, R., Baccarini, A., Merad, M., et al. (2018). Quiescent Tissue Stem Cells Evade Immune Surveillance. Immunity *48*, 271-285.e5. https://doi.org/10.1016/j.immuni.2018.02.001.

Aguirre-Ghiso, J.A. (2007). Models, mechanisms and clinical evidence for cancer dormancy. Nature Reviews Cancer *7*, 834–846. https://doi.org/10.1038/nrc2256.

Aguirre-Ghiso, J.A., and Sosa, M.S. (2018). Emerging Topics on Disseminated Cancer Cell Dormancy and the Paradigm of Metastasis. Annual Review of Cancer Biology *2*, 377–393. https://doi.org/10.1146/annurev-cancerbio-030617-050446.

Aguirre-Ghiso, J.A., Liu, D., Mignatti, A., Kovalski, K., and Ossowski, L. (2001). Urokinase Receptor and Fibronectin Regulate the ERK ^{MAPK} to p38 ^{MAPK} Activity Ratios That Determine Carcinoma Cell Proliferation or Dormancy In Vivo. Molecular Biology of the Cell *12*, 863–879. https://doi.org/10.1091/mbc.12.4.863.

Aguirre-Ghiso, J.A., Estrada, Y., Liu, D., and Ossowski, L. (2004). ERK(MAPK) activity as a determinant of tumor growth and dormancy; regulation by p38(SAPK). Urologic Oncology: Seminars and Original Investigations *22*, 82. https://doi.org/10.1016/j.urolonc.2003.12.012.

Albrengues, J., Shields, M.A., Ng, D., Park, C.G., Ambrico, A., Poindexter, M.E., Upadhyay, P., Uyeminami, D.L., Pommier, A., Küttner, V., et al. (2018). Neutrophil extracellular traps produced during inflammation awaken dormant cancer cells in mice. Science *361*, eaao4227. https://doi.org/10.1126/science.aao4227.

Al-Hajj, M., Wicha, M.S., Benito-Hernandez, A., Morrison, S.J., and Clarke, M.F. (2003). Prospective identification of tumorigenic breast cancer cells. Proc Natl Acad Sci U S A *100*, 3983–3988. https://doi.org/10.1073/pnas.0530291100.

Almog, N., Henke, V., Flores, L., Hlatky, L., Kung, A.L., Wright, R.D., Berger, R., Hutchinson, L., Naumov, G.N., Bender, E., et al. (2006). Prolonged dormancy of human liposarcoma is associated with impaired tumor angiogenesis. FASEB J *20*, 947–949. https://doi.org/10.1096/fj.05-3946fje.

Aloysius, A., DasGupta, R., and Dhawan, J. (2018). The transcription factor Lef1 switches partners from β-catenin to Smad3 during muscle stem cell quiescence. Sci Signal *11*, eaan3000. https://doi.org/10.1126/scisignal.aan3000.

Ampuja, M., Jokimäki, R., Juuti-Uusitalo, K., Rodriguez-Martinez, A., Alarmo, E.-L., and Kallioniemi, A. (2013). BMP4 inhibits the proliferation of breast cancer cells and

induces an MMP-dependent migratory phenotype in MDA-MB-231 cells in 3D environment. BMC Cancer *13*, 1–13. https://doi.org/10.1186/1471-2407-13-429.

Andres, J.L., DeFalcis, D., Noda, M., and Massagué, J. (1992). Binding of two growth factor families to separate domains of the proteoglycan betaglycan. J Biol Chem *267*, 5927–5930. .

Annes, J.P., Chen, Y., Munger, J.S., and Rifkin, D.B. (2004). Integrin αVβ6-mediated activation of latent TGF-β requires the latent TGF-β binding protein-1. J Cell Biol *165*, 723–734. https://doi.org/10.1083/jcb.200312172.

Asparuhova, M.B., Caballé-Serrano, J., Buser, D., and Chappuis, V. (2018). Bone-conditioned medium contributes to initiation and progression of osteogenesis by exhibiting synergistic TGF-β1/BMP-2 activity. Int J Oral Sci *10*, 1–9. https://doi.org/10.1038/s41368-018-0021-2.

Babitt, J.L., Zhang, Y., Samad, T.A., Xia, Y., Tang, J., Campagna, J.A., Schneyer, A.L., Woolf, C.J., and Lin, H.Y. (2005). Repulsive guidance molecule (RGMa), a DRAGON homologue, is a bone morphogenetic protein co-receptor. J Biol Chem *280*, 29820–29827. https://doi.org/10.1074/jbc.M503511200.

Bach, D.-H., Park, H.J., and Lee, S.K. (2017). The Dual Role of Bone Morphogenetic Proteins in Cancer. Mol Ther Oncolytics *8*, 1–13. https://doi.org/10.1016/j.omto.2017.10.002.

Baldominos, P., Barbera-Mourelle, A., Barreiro, O., Huang, Y., Wight, A., Cho, J.-W., Zhao, X., Estivill, G., Adam, I., Sanchez, X., et al. (2022). Quiescent cancer cells resist T cell attack by forming an immunosuppressive niche. Cell S0092867422003439. https://doi.org/10.1016/j.cell.2022.03.033.

Balic, M., Lin, H., Young, L., Hawes, D., Giuliano, A., McNamara, G., Datar, R.H., and Cote, R.J. (2006). Most early disseminated cancer cells detected in bone marrow of breast cancer patients have a putative breast cancer stem cell phenotype. Clin Cancer Res *12*, 5615–5621. https://doi.org/10.1158/1078-0432.CCR-06-0169.

Batlle, E., and Massagué, J. (2019). Transforming Growth Factor-β Signaling in Immunity and Cancer. Immunity *50*, 924–940. https://doi.org/10.1016/j.immuni.2019.03.024.

Beumer, J., Puschhof, J., Yengej, F.Y., Zhao, L., Martinez-Silgado, A., Blotenburg, M., Begthel, H., Boot, C., van Oudenaarden, A., Chen, Y.-G., et al. (2022). BMP gradient along the intestinal villus axis controls zonated enterocyte and goblet cell states. Cell Reports *38*, 110438. https://doi.org/10.1016/j.celrep.2022.110438.

Bhatia, M., Bonnet, D., Wu, D., Murdoch, B., Wrana, J., Gallacher, L., and Dick, J.E. (1999). Bone morphogenetic proteins regulate the developmental program of human hematopoietic stem cells. J Exp Med *189*, 1139–1148. https://doi.org/10.1084/jem.189.7.1139.

Bhatia, R., Holtz, M., Niu, N., Gray, R., Snyder, D.S., Sawyers, C.L., Arber, D.A., Slovak, M.L., and Forman, S.J. (2003). Persistence of malignant hematopoietic progenitors in chronic myelogenous leukemia patients in complete cytogenetic

remission following imatinib mesylate treatment. Blood *101*, 4701–4707. https://doi.org/10.1182/blood-2002-09-2780.

Bigas, A., and Espinosa, L. (2012). Hematopoietic stem cells: to be or Notch to be. Blood *119*, 3226–3235. https://doi.org/10.1182/blood-2011-10-355826.

Bokobza, S.M., Ye, L., Kynaston, H.E., Mansel, R.E., and Jiang, W.G. (2009). Reduced expression of BMPR-IB correlates with poor prognosis and increased proliferation of breast cancer cells. Cancer Genomics Proteomics *6*, 101–108. .

Bonneau, C., Eliès, A., Kieffer, Y., Bourachot, B., Ladoire, S., Pelon, F., Hequet, D., Guinebretière, J.-M., Blanchet, C., Vincent-Salomon, A., et al. (2020). A subset of activated fibroblasts is associated with distant relapse in early luminal breast cancer. Breast Cancer Res *22*, 1–22. https://doi.org/10.1186/s13058-020-01311-9.

Borgen, E., Rypdal, M.C., Sosa, M.S., Renolen, A., Schlichting, E., Lønning, P.E., Synnestvedt, M., Aguirre-Ghiso, J.A., and Naume, B. (2018). NR2F1 stratifies dormant disseminated tumor cells in breast cancer patients. Breast Cancer Research *20*. https://doi.org/10.1186/s13058-018-1049-0.

Borges, L., Oliveira, V.K.P., Baik, J., Bendall, S.C., and Perlingeiro, R.C.R. (2019). Serial transplantation reveals a critical role for endoglin in hematopoietic stem cell quiescence. Blood *133*, 688–696. https://doi.org/10.1182/blood-2018-09-874677.

Borriello, L., Coste, A., Traub, B., Sharma, V.P., Karagiannis, G.S., Lin, Y., Wang, Y., Ye, X., Duran, C.L., Chen, X., et al. (2022). Primary tumor associated macrophages activate programs of invasion and dormancy in disseminating tumor cells. Nat Commun *13*, 626. https://doi.org/10.1038/s41467-022-28076-3.

Boyerinas, B., Zafrir, M., Yesilkanal, A.E., Price, T.T., Hyjek, E.M., and Sipkins, D.A. (2013). Adhesion to osteopontin in the bone marrow niche regulates lymphoblastic leukemia cell dormancy. Blood *121*, 4821–4831. https://doi.org/10.1182/blood-2012-12-475483.

Bragado, P., Sosa, M.S., Keely, P., Condeelis, J., and Aguirre-Ghiso, J.A. (2012). Microenvironments Dictating Tumor Cell Dormancy. Recent Results Cancer Res *195*, 25–39. https://doi.org/10.1007/978-3-642-28160-0_3.

Bragado, P., Estrada, Y., Parikh, F., Krause, S., Capobianco, C., Farina, H.G., Schewe, D.M., and Aguirre-Ghiso, J.A. (2013). TGF-β2 dictates disseminated tumour cell fate in target organs through TGF-β-RIII and p38α/β signalling. Nature Cell Biology *15*, 1351–1361. https://doi.org/10.1038/ncb2861.

Braun, S., Pantel, K., Müller, P., Janni, W., Hepp, F., Kentenich, C.R., Gastroph, S., Wischnik, A., Dimpfl, T., Kindermann, G., et al. (2000a). Cytokeratin-positive cells in the bone marrow and survival of patients with stage I, II, or III breast cancer. N. Engl. J. Med. *342*, 525–533. https://doi.org/10.1056/NEJM200002243420801.

Braun, S., Kentenich, C., Janni, W., Hepp, F., de Waal, J., Willgeroth, F., Sommer, H., and Pantel, K. (2000b). Lack of effect of adjuvant chemotherapy on the elimination of single dormant tumor cells in bone marrow of high-risk breast cancer patients. J Clin Oncol *18*, 80–86. https://doi.org/10.1200/JCO.2000.18.1.80.

Brody, J.G., Rudel, R.A., Michels, K.B., Moysich, K.B., Bernstein, L., Attfield, K.R., and Gray, S. (2007). Environmental pollutants, diet, physical activity, body size, and breast cancer. Cancer *109*, 2627–2634. https://doi.org/10.1002/cncr.22656.

Brown, J.A., Yonekubo, Y., Hanson, N., Sastre-Perona, A., Basin, A., Rytlewski, J.A., Dolgalev, I., Meehan, S., Tsirigos, A., Beronja, S., et al. (2017). TGF-β-Induced Quiescence Mediates Chemoresistance of Tumor-Propagating Cells in Squamous Cell Carcinoma. Cell Stem Cell *21*, 650-664.e8. https://doi.org/10.1016/j.stem.2017.10.001.

Brüggemann, M., Pott, C., Ritgen, M., and Kneba, M. (2004). Significance of Minimal Residual Disease in Lymphoid Malignancies. AHA *112*, 111–119. https://doi.org/10.1159/000077566.

Buijs, J.T., Henriquez, N.V., van Overveld, P.G.M., van der Horst, G., Que, I., Schwaninger, R., Rentsch, C., Ten Dijke, P., Cleton-Jansen, A.-M., Driouch, K., et al. (2007). Bone morphogenetic protein 7 in the development and treatment of bone metastases from breast cancer. Cancer Res. *67*, 8742–8751. https://doi.org/10.1158/0008-5472.CAN-06-2490.

Cackowski, F.C., and Taichman, R.S. (2018). Parallels between hematopoietic stem cell and prostate cancer disseminated tumor cell regulation. Bone https://doi.org/10.1016/j.bone.2018.02.025.

Cackowski, F.C., Eber, M.R., Rhee, J., Decker, A.M., Yumoto, K., Berry, J.E., Lee, E., Shiozawa, Y., Jung, Y., Aguirre-Ghiso, J.A., et al. (2017). Mer Tyrosine Kinase Regulates Disseminated Prostate Cancer Cellular Dormancy. Journal of Cellular Biochemistry *118*, 891–902. https://doi.org/10.1002/jcb.25768.

Cao, Y., Slaney, C.Y., Bidwell, B.N., Parker, B.S., Johnstone, C.N., Rautela, J., Eckhardt, B.L., and Anderson, R.L. (2014). BMP4 inhibits breast cancer metastasis by blocking myeloid-derived suppressor cell activity. Cancer Res *74*, 5091–5102. https://doi.org/10.1158/0008-5472.CAN-13-3171.

Capulli, M., Hristova, D., Valbret, Z., Carys, K., Arjan, R., Maurizi, A., Masedu, F., Cappariello, A., Rucci, N., and Teti, A. (2019). Notch2 pathway mediates breast cancer cellular dormancy and mobilisation in bone and contributes to haematopoietic stem cell mimicry. British Journal of Cancer 1. https://doi.org/10.1038/s41416-019-0501-y.

Carlson, P., Dasgupta, A., Grzelak, C.A., Kim, J., Barrett, A., Coleman, I.M., Shor, R.E., Goddard, E.T., Dai, J., Schweitzer, E.M., et al. (2019). Targeting the perivascular niche sensitizes disseminated tumour cells to chemotherapy. Nature Cell Biology 1. https://doi.org/10.1038/s41556-018-0267-0.

Chang, C. (2016). Agonists and Antagonists of TGF-β Family Ligands. Cold Spring Harb Perspect Biol *8*, a021923. https://doi.org/10.1101/cshperspect.a021923.

Chapellier, M., Bachelard-Cascales, E., Schmidt, X., Clément, F., Treilleux, I., Delay, E., Jammot, A., Ménétrier-Caux, C., Pochon, G., Besançon, R., et al. (2015). Disequilibrium of BMP2 Levels in the Breast Stem Cell Niche Launches Epithelial

Transformation by Overamplifying BMPR1B Cell Response. Stem Cell Reports *4*, 239–254. https://doi.org/10.1016/j.stemcr.2014.12.007.

Chen, C.-R., Kang, Y., Siegel, P.M., and Massague, J. E2F4/5 and p107 as Smad Cofactors Linking the TGFβ Receptor to c-myc Repression. 14. .

Chung, Y.-H., Huang, Y.-H., Chu, T.-H., Chen, C.-L., Lin, P.-R., Huang, S.-C., Wu, D.-C., Huang, C.-C., Hu, T.-H., Kao, Y.-H., et al. (2018). BMP-2 restoration aids in recovery from liver fibrosis by attenuating TGF-β1 signaling. Lab Invest *98*, 999–1013. https://doi.org/10.1038/s41374-018-0069-9.

Clément, F., Xu, X., Donini, C.F., Clément, A., Omarjee, S., Delay, E., Treilleux, I., Fervers, B., Le Romancer, M., Cohen, P.A., et al. (2017). Long-term exposure to bisphenol A or benzo(a)pyrene alters the fate of human mammary epithelial stem cells in response to BMP2 and BMP4, by pre-activating BMP signaling. Cell Death Differ *24*, 155–166. https://doi.org/10.1038/cdd.2016.107.

Cockrell, C., Teague, J., and Axelrod, D.E. (2020). Prevention of Colon Cancer Recurrence From Minimal Residual Disease: Computer Optimized Dose Schedules of Intermittent Apoptotic Adjuvant Therapy. JCO Clinical Cancer Informatics 514–520. https://doi.org/10.1200/CCI.20.00016.

Cocolakis, E., Dai, M., Drevet, L., Ho, J., Haines, E., Ali, S., and Lebrun, J.-J. (2008). Smad Signaling Antagonizes STAT5-mediated Gene Transcription and Mammary Epithelial Cell Differentiation*. Journal of Biological Chemistry *283*, 1293–1307. https://doi.org/10.1074/jbc.M707492200.

Coller, H.A., Sang, L., and Roberts, J.M. (2006). A New Description of Cellular Quiescence. PLOS Biology *4*, e83. https://doi.org/10.1371/journal.pbio.0040083.

Correa, R.J.M., Peart, T., Valdes, Y.R., DiMattia, G.E., and Shepherd, T.G. (2012). Modulation of AKT activity is associated with reversible dormancy in ascites-derived epithelial ovarian cancer spheroids. Carcinogenesis *33*, 49–58. https://doi.org/10.1093/carcin/bgr241.

Correia, A.L., Guimaraes, J.C., Auf der Maur, P., De Silva, D., Trefny, M.P., Okamoto, R., Bruno, S., Schmidt, A., Mertz, K., Volkmann, K., et al. (2021). Hepatic stellate cells suppress NK cell-sustained breast cancer dormancy. Nature *594*, 566–571. https://doi.org/10.1038/s41586-021-03614-z.

Crecente-Campo, J., Borrajo, E., Vidal, A., and Garcia-Fuentes, M. (2017). New scaffolds encapsulating TGF-β3/BMP-7 combinations driving strong chondrogenic differentiation. European Journal of Pharmaceutics and Biopharmaceutics *114*, 69–78. https://doi.org/10.1016/j.ejpb.2016.12.021.

Curtis, C., Shah, S.P., Chin, S.-F., Turashvili, G., Rueda, O.M., Dunning, M.J., Speed, D., Lynch, A.G., Samarajiwa, S., Yuan, Y., et al. (2012). The genomic and transcriptomic architecture of 2,000 breast tumours reveals novel subgroups. Nature *486*, 346–352. https://doi.org/10.1038/nature10983.

Dai, J., Cimino, P.J., Gouin, K.H., Grzelak, C.A., Barrett, A., Lim, A.R., Long, A., Weaver, S., Saldin, L.T., Uzamere, A., et al. (2022). Astrocytic laminin-211 drives

disseminated breast tumor cell dormancy in brain. Nat Cancer *3*, 25–42. https://doi.org/10.1038/s43018-021-00297-3.

Daignan-Fornier, B., Laporte, D., and Sagot, I. (2021). Quiescence Through the Prism of Evolution. Front Cell Dev Biol *9*, 745069. https://doi.org/10.3389/fcell.2021.745069.

David, C.J., and Massagué, J. (2018). Contextual determinants of TGFβ action in development, immunity and cancer. Nature Reviews Molecular Cell Biology *19*, 419–435. https://doi.org/10.1038/s41580-018-0007-0.

Decker, A.M., Jung, Y., Cackowski, F.C., Yumoto, K., Wang, J., and Taichman, R.S. (2017). Sympathetic Signaling Reactivates Quiescent Disseminated Prostate Cancer Cells in the Bone Marrow. Mol. Cancer Res. *15*, 1644–1655. https://doi.org/10.1158/1541-7786.MCR-17-0132.

Derynck, R., and Zhang, Y.E. (2003). Smad-dependent and Smad-independent pathways in TGF-β family signalling. Nature *425*, 577–584. https://doi.org/10.1038/nature02006.

Dewachter, L., Adnot, S., Guignabert, C., Tu, L., Marcos, E., Fadel, E., Humbert, M., Dartevelle, P., Simonneau, G., Naeije, R., et al. (2009). Bone morphogenetic protein signalling in heritable versus idiopathic pulmonary hypertension. Eur Respir J *34*, 1100–1110. https://doi.org/10.1183/09031936.00183008.

Dhandapani, K.M., and Brann, D.W. (2003). Transforming growth factor-beta: a neuroprotective factor in cerebral ischemia. Cell Biochem Biophys *39*, 13–22. https://doi.org/10.1385/CBB:39:1:13.

Di Martino, J.S., Nobre, A.R., Mondal, C., Taha, I., Farias, E.F., Fertig, E.J., Naba, A., Aguirre-Ghiso, J.A., and Bravo-Cordero, J.J. (2022). A tumor-derived type III collagen-rich ECM niche regulates tumor cell dormancy. Nat Cancer *3*, 90–107. https://doi.org/10.1038/s43018-021-00291-9.

Dong, M., How, T., Kirkbride, K.C., Gordon, K.J., Lee, J.D., Hempel, N., Kelly, P., Moeller, B.J., Marks, J.R., and Blobe, G.C. (2007). The type III TGF-β receptor suppresses breast cancer progression (American Society for Clinical Investigation).

Dorai, H., Vukicevic, S., and Sampath, T.K. (2000). Bone morphogenetic protein-7 (osteogenic protein-1) inhibits smooth muscle cell proliferation and stimulates the expression of markers that are characteristic of SMC phenotype in vitro. J Cell Physiol *184*, 37–45. https://doi.org/10.1002/(SICI)1097-4652(200007)184:1<37::AID-JCP4>3.0.CO;2-M.

Eckhardt, B.L., Cao, Y., Redfern, A.D., Chi, L.H., Burrows, A.D., Roslan, S., Sloan, E.K., Parker, B.S., Loi, S., Ueno, N.T., et al. (2020). Activation of Canonical BMP4-SMAD7 Signaling Suppresses Breast Cancer Metastasis. Cancer Res *80*, 1304–1315. https://doi.org/10.1158/0008-5472.CAN-19-0743.

Eyles, J., Puaux, A.-L., Wang, X., Toh, B., Prakash, C., Hong, M., Tan, T.G., Zheng, L., Ong, L.C., Jin, Y., et al. (2010). Tumor cells disseminate early, but

immunosurveillance limits metastatic outgrowth, in a mouse model of melanoma. J Clin Invest *120*, 2030–2039. https://doi.org/10.1172/JCI42002.

Fluegen, G., Avivar-Valderas, A., Wang, Y., Padgen, M.R., Williams, J.K., Nobre, A.R., Calvo, V., Cheung, J.F., Bravo-Cordero, J.J., Entenberg, D., et al. (2017). Phenotypic heterogeneity of disseminated tumour cells is preset by primary tumour hypoxic microenvironments. Nature Cell Biology *19*, 120–132. https://doi.org/10.1038/ncb3465.

Foitzik, K., Paus, R., Doetschman, T., and Dotto, G.P. (1999). The TGF-beta2 isoform is both a required and sufficient inducer of murine hair follicle morphogenesis. Dev Biol *212*, 278–289. https://doi.org/10.1006/dbio.1999.9325.

Friberg, S., and Nystrom, A. (2015). Cancer Metastases: Early Dissemination and Late Recurrences. Cancer□Growth□Metastasis *8*, CGM.S31244. https://doi.org/10.4137/CGM.S31244.

Gao, H., Chakraborty, G., Lee-Lim, A.P., Mo, Q., Decker, M., Vonica, A., Shen, R., Brogi, E., Brivanlou, A.H., and Giancotti, F.G. (2012). The BMP Inhibitor Coco Reactivates Breast Cancer Cells at Lung Metastatic Sites. Cell *150*, 764–779. https://doi.org/10.1016/j.cell.2012.06.035.

Garcia-Murillas, I., Chopra, N., Comino-Méndez, I., Beaney, M., Tovey, H., Cutts, R.J., Swift, C., Kriplani, D., Afentakis, M., Hrebien, S., et al. (2019). Assessment of Molecular Relapse Detection in Early-Stage Breast Cancer. JAMA Oncology *5*, 1473–1478. https://doi.org/10.1001/jamaoncol.2019.1838.

Gatza, C.E., Elderbroom, J.L., Oh, S.Y., Starr, M.D., Nixon, A.B., and Blobe, G.C. (2014). The Balance of Cell Surface and Soluble Type III TGF-β Receptor Regulates BMP Signaling in Normal and Cancerous Mammary Epithelial Cells. Neoplasia *16*, 489–500. https://doi.org/10.1016/j.neo.2014.05.008.

Ghajar, C.M., Peinado, H., Mori, H., Matei, I.R., Evason, K.J., Brazier, H., Almeida, D., Koller, A., Hajjar, K.A., Stainier, D.Y.R., et al. (2013). The perivascular niche regulates breast tumor dormancy. Nat Cell Biol *15*, 807–817. https://doi.org/10.1038/ncb2767.

Ghiso, J.A.A., Kovalski, K., and Ossowski, L. (1999). Tumor Dormancy Induced by Downregulation of Urokinase Receptor in Human Carcinoma Involves Integrin and MAPK Signaling. The Journal of Cell Biology *147*, 89–104. https://doi.org/10.1083/jcb.147.1.89.

Giustacchini, A., Thongjuea, S., Barkas, N., Woll, P.S., Povinelli, B.J., Booth, C.A.G., Sopp, P., Norfo, R., Rodriguez-Meira, A., Ashley, N., et al. (2017). Single-cell transcriptomics uncovers distinct molecular signatures of stem cells in chronic myeloid leukemia. Nature Medicine *23*, 692–702. https://doi.org/10.1038/nm.4336.

Goss, P.E., and Chambers, A.F. (2010). Does tumour dormancy offer a therapeutic target? Nature Reviews Cancer *10*, 871–877. https://doi.org/10.1038/nrc2933.

Guo, X., and Wang, X.-F. (2009). Signaling cross-talk between TGF-β/BMP and other pathways. Cell Res *19*, 71–88. https://doi.org/10.1038/cr.2008.302.

Gupta, A., Roy, S., Lazar, A.J.F., Wang, W.-L., McAuliffe, J.C., Reynoso, D., McMahon, J., Taguchi, T., Floris, G., Debiec-Rychter, M., et al. (2010). Autophagy inhibition and antimalarials promote cell death in gastrointestinal stromal tumor (GIST). Proc Natl Acad Sci U S A *107*, 14333–14338. https://doi.org/10.1073/pnas.1000248107.

Harbeck, N., Penault-Llorca, F., Cortes, J., Gnant, M., Houssami, N., Poortmans, P., Ruddy, K., Tsang, J., and Cardoso, F. (2019). Breast cancer. Nat Rev Dis Primers *5*, 66. https://doi.org/10.1038/s41572-019-0111-2.

Harper, K.L., Sosa, M.S., Entenberg, D., Hosseini, H., Cheung, J.F., Nobre, R., Avivar-Valderas, A., Nagi, C., Girnius, N., Davis, R.J., et al. (2016). Mechanism of early dissemination and metastasis in Her2+ mammary cancer. Nature *540*, 588–592. https://doi.org/10.1038/nature20609.

He, X.C., Zhang, J., Tong, W.-G., Tawfik, O., Ross, J., Scoville, D.H., Tian, Q., Zeng, X., He, X., Wiedemann, L.M., et al. (2004). BMP signaling inhibits intestinal stem cell self-renewal through suppression of Wnt–β-catenin signaling. Nat Genet *36*, 1117–1121. https://doi.org/10.1038/ng1430.

He, Y., Zhang, H., Yung, A., Villeda, S.A., Jaeger, P.A., Olayiwola, O., Fainberg, N., and Wyss-Coray, T. (2014). ALK5-dependent TGF-β signaling is a major determinant of late-stage adult neurogenesis. Nat Neurosci *17*, 943–952. https://doi.org/10.1038/nn.3732.

Heiss, M.M., Simon, E.H., Beyer, B.C.M., Gruetzner, K.U., Tarabichi, A., Babic, R., Schildberg, F.W., and Allgayer, H. (2002). Minimal residual disease in gastric cancer: evidence of an independent prognostic relevance of urokinase receptor expression by disseminated tumor cells in the bone marrow. J Clin Oncol *20*, 2005–2016. https://doi.org/10.1200/jco.2002.08.003.

Hong, S.P., Chan, T.E., Lombardo, Y., Corleone, G., Rotmensz, N., Bravaccini, S., Rocca, A., Pruneri, G., McEwen, K.R., Coombes, R.C., et al. (2019). Single-cell transcriptomics reveals multi-step adaptations to endocrine therapy. Nat Commun *10*, 3840. https://doi.org/10.1038/s41467-019-11721-9.

Hu, Z., Ding, J., Ma, Z., Sun, R., Seoane, J.A., Scott Shaffer, J., Suarez, C.J., Berghoff, A.S., Cremolini, C., Falcone, A., et al. (2019). Quantitative evidence for early metastatic seeding in colorectal cancer. Nature Genetics *51*, 1113–1122. https://doi.org/10.1038/s41588-019-0423-x.

Huettner, C.S., Zhang, P., Van Etten, R.A., and Tenen, D.G. (2000). Reversibility of acute B-cell leukaemia induced by BCR-ABL1. Nat Genet *24*, 57–60. https://doi.org/10.1038/71691.

Hüsemann, Y., Geigl, J.B., Schubert, F., Musiani, P., Meyer, M., Burghart, E., Forni, G., Eils, R., Fehm, T., Riethmüller, G., et al. (2008). Systemic Spread Is an Early Step in Breast Cancer. Cancer Cell *13*, 58–68. https://doi.org/10.1016/j.ccr.2007.12.003.

Ignatov, A., Eggemann, H., Burger, E., and Ignatov, T. (2018). Patterns of breast cancer relapse in accordance to biological subtype. J Cancer Res Clin Oncol *144*, 1347–1355. https://doi.org/10.1007/s00432-018-2644-2.

Iwakura, T., Sakata, R., and Reddi, A.H. (2013). Induction of Chondrogenesis and Expression of Superficial Zone Protein in Synovial Explants with TGF-β1 and BMP-7. Tissue Engineering Part A *19*, 2638–2644. https://doi.org/10.1089/ten.tea.2013.0047.

Jager, M.J., Shields, C.L., Cebulla, C.M., Abdel-Rahman, M.H., Grossniklaus, H.E., Stern, M.-H., Carvajal, R.D., Belfort, R.N., Jia, R., Shields, J.A., et al. (2020). Uveal melanoma. Nat Rev Dis Primers *6*, 24. https://doi.org/10.1038/s41572-020-0158-0.

Janni, W., Vogl, F.D., Wiedswang, G., Synnestvedt, M., Fehm, T., Jückstock, J., Borgen, E., Rack, B., Braun, S., Sommer, H., et al. (2011). Persistence of disseminated tumor cells in the bone marrow of breast cancer patients predicts increased risk for relapse--a European pooled analysis. Clin. Cancer Res. *17*, 2967–2976. https://doi.org/10.1158/1078-0432.CCR-10-2515.

Jeanpierre, S., Nicolini, F.E., Kaniewski, B., Dumontet, C., Rimokh, R., Puisieux, A., and Maguer-Satta, V. (2008). BMP4 regulation of human megakaryocytic differentiation is involved in thrombopoietin signaling. Blood *112*, 3154–3163. https://doi.org/10.1182/blood-2008-03-145326.

Jeanpierre, S., Arizkane, K., Thongjuea, S., Grockowiak, E., Geistlich, K., Barral, L., Voeltzel, T., Guillemin, A., Gonin-Giraud, S., Gandrillon, O., et al. (2020). The quiescent fraction of chronic myeloid leukemic stem cells depends on BMPR1B, Stat3 and BMP4-niche signals to persist in patients in remission. Haematologica https://doi.org/10.3324/haematol.2019.232793.

Jeffery, T.K., Upton, P.D., Trembath, R.C., and Morrell, N.W. (2005). BMP4 inhibits proliferation and promotes myocyte differentiation of lung fibroblasts via Smad1 and JNK pathways. American Journal of Physiology-Lung Cellular and Molecular Physiology *288*, L370–L378. https://doi.org/10.1152/ajplung.00242.2004.

Jenkins, B.J., Grail, D., Nheu, T., Najdovska, M., Wang, B., Waring, P., Inglese, M., McLoughlin, R.M., Jones, S.A., Topley, N., et al. (2005). Hyperactivation of Stat3 in gp130 mutant mice promotes gastric hyperproliferation and desensitizes TGF-beta signaling. Nat Med *11*, 845–852. https://doi.org/10.1038/nm1282.

Kadota, M., Yang, H.H., Gomez, B.P., Sato, M., Clifford, R.J., Meerzaman, D., Dunn, B.K., Wakefield, L.M., and Lee, M.P. (2010). Delineating Genetic Alterations for Tumor Progression in the MCF10A Series of Breast Cancer Cell Lines. In PloS One, p.

Kandasamy, M., Lehner, B., Kraus, S., Sander, P.R., Marschallinger, J., Rivera, F.J., Trümbach, D., Ueberham, U., Reitsamer, H.A., Strauss, O., et al. (2014). TGF-beta signalling in the adult neurogenic niche promotes stem cell quiescence as well as generation of new neurons. J Cell Mol Med *18*, 1444–1459. https://doi.org/10.1111/jcmm.12298.

Kaur, A., Ecker, B.L., Douglass, S.M., Kugel, C.H., Webster, M.R., Almeida, F.V., Somasundaram, R., Hayden, J., Ban, E., Ahmadzadeh, H., et al. (2019). Remodeling of the Collagen Matrix in Aging Skin Promotes Melanoma Metastasis and Affects Immune Cell Motility. Cancer Discov *9*, 64–81. https://doi.org/10.1158/2159-8290.CD-18-0193.

Khalil, B.D., Sanchez, R., Rahman, T., Rodriguez-Tirado, C., Moritsch, S., Martinez, A.R., Miles, B., Farias, E., Mezei, M., Nobre, A.R., et al. (2022). An NR2F1-specific agonist suppresses metastasis by inducing cancer cell dormancy. Journal of Experimental Medicine *219*, e20210836. https://doi.org/10.1084/jem.20210836.

Khodr, V., Machillot, P., Migliorini, E., Reiser, J.-B., and Picart, C. (2020). High throughput measurements of BMP/BMP receptors interactions using bio-layer interferometry (Biophysics).

Khodr, V., Machillot, P., Migliorini, E., Reiser, J.-B., and Picart, C. (2021). High-throughput measurements of bone morphogenetic protein/bone morphogenetic protein receptor interactions using biolayer interferometry. Biointerphases *16*, 031001. https://doi.org/10.1116/6.0000926.

Khurana, S., Buckley, S., Schouteden, S., Ekker, S., Petryk, A., Delforge, M., Zwijsen, A., and Verfaillie, C.M. (2013). A novel role of BMP4 in adult hematopoietic stem and progenitor cell homing via Smad independent regulation of integrin-α4 expression. Blood *121*, 781–790. https://doi.org/10.1182/blood-2012-07-446443.

Kim, R.S., Avivar-Valderas, A., Estrada, Y., Bragado, P., Sosa, M.S., Aguirre-Ghiso, J.A., and Segall, J.E. (2012). Dormancy Signatures and Metastasis in Estrogen Receptor Positive and Negative Breast Cancer. PLoS ONE *7*, e35569. https://doi.org/10.1371/journal.pone.0035569.

Kim, S.K., Henen, M.A., and Hinck, A.P. (2019). Structural biology of betaglycan and endoglin, membrane-bound co-receptors of the TGF-beta family. Exp Biol Med (Maywood) *244*, 1547–1558. https://doi.org/10.1177/1535370219881160.

Kirkbride, K.C., Townsend, T.A., Bruinsma, M.W., Barnett, J.V., and Blobe, G.C. (2008). Bone morphogenetic proteins signal through the transforming growth factor-beta type III receptor. J. Biol. Chem. *283*, 7628–7637. https://doi.org/10.1074/jbc.M704883200.

Klein, C.A. (2020). Cancer progression and the invisible phase of metastatic colonization. Nat Rev Cancer *20*, 681–694. https://doi.org/10.1038/s41568-020-00300-6.

Kleinsmith, L.J., and Pierce, G.B., Jr. (1964). Multipotentiality of Single Embryonal Carcinoma Cells*. Cancer Research *24*, 1544–1551. .

Kobayashi, A., Okuda, H., Xing, F., Pandey, P.R., Watabe, M., Hirota, S., Pai, S.K., Liu, W., Fukuda, K., Chambers, C., et al. (2011). Bone morphogenetic protein 7 in dormancy and metastasis of prostate cancer stem-like cells in bone. The Journal of Experimental Medicine *208*, 2641–2655. https://doi.org/10.1084/jem.20110840.

Kobayashi, H., Butler, J.M., O'Donnell, R., Kobayashi, M., Ding, B.-S., Bonner, B., Chiu, V.K., Nolan, D.J., Shido, K., Benjamin, L., et al. (2010). Angiocrine factors from Akt-activated endothelial cells balance self-renewal and differentiation of haematopoietic stem cells. Nat. Cell Biol. *12*, 1046–1056. https://doi.org/10.1038/ncb2108.

Kobielak, K., Stokes, N., de la Cruz, J., Polak, L., and Fuchs, E. (2007). Loss of a quiescent niche but not follicle stem cells in the absence of bone morphogenetic protein signaling. Proceedings of the National Academy of Sciences *104*, 10063–10068. https://doi.org/10.1073/pnas.0703004104.

Koebel, C.M., Vermi, W., Swann, J.B., Zerafa, N., Rodig, S.J., Old, L.J., Smyth, M.J., and Schreiber, R.D. (2007). Adaptive immunity maintains occult cancer in an equilibrium state. Nature *450*, 903–907. https://doi.org/10.1038/nature06309.

Koenig, B.B., Cook, J.S., Wolsing, D.H., Ting, J., Tiesman, J.P., Correa, P.E., Olson, C.A., Pecquet, A.L., Ventura, F., and Grant, R.A. (1994). Characterization and cloning of a receptor for BMP-2 and BMP-4 from NIH 3T3 cells. Mol Cell Biol *14*, 5961–5974. .

Krebsbach, P.H., and Villa-Diaz, L.G. (2017). The Role of Integrin α6 (CD49f) in Stem Cells: More than a Conserved Biomarker. Stem Cells Dev *26*, 1090–1099. https://doi.org/10.1089/scd.2016.0319.

Kunisaki, Y., Bruns, I., Scheiermann, C., Ahmed, J., Pinho, S., Zhang, D., Mizoguchi, T., Wei, Q., Lucas, D., Ito, K., et al. (2013). Arteriolar niches maintain haematopoietic stem cell quiescence. Nature *502*, 637–643. https://doi.org/10.1038/nature12612.

La Belle Flynn, A., Calhoun, B.C., Sharma, A., Chang, J.C., Almasan, A., and Schiemann, W.P. (2019). Autophagy inhibition elicits emergence from metastatic dormancy by inducing and stabilizing Pfkfb3 expression. Nat Commun *10*, 3668. https://doi.org/10.1038/s41467-019-11640-9.

Lapidot, T., Sirard, C., Vormoor, J., Murdoch, B., Hoang, T., Caceres-Cortes, J., Minden, M., Paterson, B., Caligiuri, M.A., and Dick, J.E. (1994). A cell initiating human acute myeloid leukaemia after transplantation into SCID mice. Nature *367*, 645–648. https://doi.org/10.1038/367645a0.

Larsson, J., Blank, U., Klintman, J., Magnusson, M., and Karlsson, S. (2005). Quiescence of hematopoietic stem cells and maintenance of the stem cell pool is not dependent on TGF-beta signaling in vivo. Exp Hematol *33*, 592–596. https://doi.org/10.1016/j.exphem.2005.02.003.

Lawson, M.A., McDonald, M.M., Kovacic, N., Hua Khoo, W., Terry, R.L., Down, J., Kaplan, W., Paton-Hough, J., Fellows, C., Pettitt, J.A., et al. (2015). Osteoclasts control reactivation of dormant myeloma cells by remodelling the endosteal niche. Nat Commun *6*, 8983. https://doi.org/10.1038/ncomms9983.

Legendre, F., Ollitrault, D., Gomez-Leduc, T., Bouyoucef, M., Hervieu, M., Gruchy, N., Mallein-Gerin, F., Leclercq, S., Demoor, M., and Galéra, P. (2017). Enhanced chondrogenesis of bone marrow-derived stem cells by using a combinatory cell

therapy strategy with BMP-2/TGF-β1, hypoxia, and COL1A1/HtrA1 siRNAs. Sci Rep *7*, 3406. https://doi.org/10.1038/s41598-017-03579-y.

Li, M.O., and Flavell, R.A. (2008). TGF-β: A Master of All T Cell Trades. Cell *134*, 392–404. https://doi.org/10.1016/j.cell.2008.07.025.

Li, N., Deng, Y., Zhou, L., Tian, T., Yang, S., Wu, Y., Zheng, Y., Zhai, Z., Hao, Q., Song, D., et al. (2019). Global burden of breast cancer and attributable risk factors in 195 countries and territories, from 1990 to 2017: results from the Global Burden of Disease Study 2017. J Hematol Oncol *12*, 140. https://doi.org/10.1186/s13045-019-0828-0.

Li, X.L., Liu, Y.B., Ma, E.G., Shen, W.X., Li, H., and Zhang, Y.N. (2015). Synergistic effect of BMP9 and TGF-β in the proliferation and differentiation of osteoblasts. Genet. Mol. Res. *14*, 7605–7615. https://doi.org/10.4238/2015.July.13.4.

Lim, D.A., Tramontin, A.D., Trevejo, J.M., Herrera, D.G., García-Verdugo, J.M., and Alvarez-Buylla, A. (2000). Noggin antagonizes BMP signaling to create a niche for adult neurogenesis. Neuron *28*, 713–726. https://doi.org/10.1016/s0896-6273(00)00148-3.

Lin, S.J., Lerch, T.F., Cook, R.W., Jardetzky, T.S., and Woodruff, T.K. (2006). The structural basis of TGF-β, bone morphogenetic protein, and activin ligand binding. Reproduction *132*, 179–190. https://doi.org/10.1530/rep.1.01072.

Llorca, M., and Farré, M. (2021). Current Insights into Potential Effects of Micro-Nanoplastics on Human Health by in-vitro Tests. Frontiers in Toxicology *3*. .

Llorens-Bobadilla, E., Zhao, S., Baser, A., Saiz-Castro, G., Zwadlo, K., and Martin-Villalba, A. (2015). Single-Cell Transcriptomics Reveals a Population of Dormant Neural Stem Cells that Become Activated upon Brain Injury. Cell Stem Cell *17*, 329–340. https://doi.org/10.1016/j.stem.2015.07.002.

Lloyd-Lewis, B., Harris, O.B., Watson, C.J., and Davis, F.M. (2017). Mammary Stem Cells: Premise, Properties, and Perspectives. Trends in Cell Biology *27*, 556–567. https://doi.org/10.1016/j.tcb.2017.04.001.

Lu, L., Ma, J., Wang, X., Wang, J., Zhang, F., Yu, J., He, G., Xu, B., Brand, D.D., Horwitz, D.A., et al. (2010). Synergistic effect of TGF-β superfamily members on the induction of Foxp3+ Treg. European Journal of Immunology *40*, 142–152. https://doi.org/10.1002/eji.200939618.

Lu, Z., Luo, R.Z., Lu, Y., Zhang, X., Yu, Q., Khare, S., Kondo, S., Kondo, Y., Yu, Y., Mills, G.B., et al. (2008). The tumor suppressor gene ARHI regulates autophagy and tumor dormancy in human ovarian cancer cells. J. Clin. Invest. *118*, 3917–3929. https://doi.org/10.1172/JCI35512.

Lujambio, A., Akkari, L., Simon, J., Grace, D., Tschaharganeh, D.F., Bolden, J.E., Zhao, Z., Thapar, V., Joyce, J.A., Krizhanovsky, V., et al. (2013). Non-cell-autonomous tumor suppression by p53. Cell *153*, 449–460. https://doi.org/10.1016/j.cell.2013.03.020.

Luo, K. (2017). Signaling Cross Talk between TGF-β/Smad and Other Signaling Pathways. Cold Spring Harb Perspect Biol *9*, a022137. https://doi.org/10.1101/cshperspect.a022137.

Maguer-Satta, V., Bartholin, L., Jeanpierre, S., Ffrench, M., Martel, S., Magaud, J.-P., and Rimokh, R. (2003). Regulation of human erythropoiesis by activin A, BMP2, and BMP4, members of the TGFbeta family. Exp Cell Res *282*, 110–120. https://doi.org/10.1016/s0014-4827(02)00013-7.

Mao, W., Montecchi-Palmer, M., Clark, A.F., and Glaucoma (2015). TGFβ2 induces cross-linked actin network formation in the trabecular meshwork via Smad and non-Smad pathways. Investigative Ophthalmology & Visual Science *56*, 3296. .

Mendelson, A., and Frenette, P.S. (2014). Hematopoietic stem cell niche maintenance during homeostasis and regeneration. Nature Medicine *20*, 833–846. https://doi.org/10.1038/nm.3647.

Méndez-Ferrer, S., Lucas, D., Battista, M., and Frenette, P.S. (2008). Haematopoietic stem cell release is regulated by circadian oscillations. Nature *452*, 442–447. https://doi.org/10.1038/nature06685.

Méndez-Ferrer, S., Michurina, T.V., Ferraro, F., Mazloom, A.R., MacArthur, B.D., Lira, S.A., Scadden, D.T., Ma'ayan, A., Enikolopov, G.N., and Frenette, P.S. (2010). Mesenchymal and haematopoietic stem cells form a unique bone marrow niche. Nature *466*, 829–834. https://doi.org/10.1038/nature09262.

Miettinen, P.J., Ebner, R., Lopez, A.R., and Derynck, R. (1994). TGF-beta induced transdifferentiation of mammary epithelial cells to mesenchymal cells: involvement of type I receptors. J Cell Biol *127*, 2021–2036. https://doi.org/10.1083/jcb.127.6.2021.

Miller, I., Min, M., Yang, C., Tian, C., Gookin, S., Carter, D., and Spencer, S.L. (2018). Ki67 is a Graded Rather than a Binary Marker of Proliferation versus Quiescence. Cell Rep *24*, 1105-1112.e5. https://doi.org/10.1016/j.celrep.2018.06.110.

Mira, H., Andreu, Z., Suh, H., Lie, D.C., Jessberger, S., Consiglio, A., San Emeterio, J., Hortigüela, R., Marqués-Torrejón, M.Á., Nakashima, K., et al. (2010). Signaling through BMPR-IA Regulates Quiescence and Long-Term Activity of Neural Stem Cells in the Adult Hippocampus. Cell Stem Cell *7*, 78–89. https://doi.org/10.1016/j.stem.2010.04.016.

Miyazawa, K., and Miyazono, K. (2017). Regulation of TGF-β Family Signaling by Inhibitory Smads. Cold Spring Harb Perspect Biol *9*, a022095. https://doi.org/10.1101/cshperspect.a022095.

Morikawa, M., Derynck, R., and Miyazono, K. (2016). TGF-β and the TGF-β Family: Context-Dependent Roles in Cell and Tissue Physiology. Cold Spring Harb Perspect Biol *8*, a021873. https://doi.org/10.1101/cshperspect.a021873.

Morrissey, C., Vessella, R.L., Lange, P.H., and Lam, H.-M. (2016). The Biology and Clinical Implications of Prostate Cancer Dormancy and Metastasis. J Mol Med (Berl) *94*, 259–265. https://doi.org/10.1007/s00109-015-1353-4.

Moustakas, A., and Heldin, C.-H. (2016). Mechanisms of TGFβ-Induced Epithelial-Mesenchymal Transition. J Clin Med *5*, E63. https://doi.org/10.3390/jcm5070063.

Muckom, R., McFarland, S., Yang, C., Perea, B., Gentes, M., Murugappan, A., Tran, E., Dordick, J.S., Clark, D.S., and Schaffer, D.V. (2019). High-throughput combinatorial screening reveals interactions between signaling molecules that regulate adult neural stem cell fate. Biotechnology and Bioengineering *116*, 193–205. https://doi.org/10.1002/bit.26815.

Müller-Hermelink, N., Braumüller, H., Pichler, B., Wieder, T., Mailhammer, R., Schaak, K., Ghoreschi, K., Yazdi, A., Haubner, R., Sander, C.A., et al. (2008). TNFR1 Signaling and IFN-γ Signaling Determine whether T Cells Induce Tumor Dormancy or Promote Multistage Carcinogenesis. Cancer Cell *13*, 507–518. https://doi.org/10.1016/j.ccr.2008.04.001.

Munger, J.S., Huang, X., Kawakatsu, H., Griffiths, M.J., Dalton, S.L., Wu, J., Pittet, J.F., Kaminski, N., Garat, C., Matthay, M.A., et al. (1999). The integrin alpha v beta 6 binds and activates latent TGF beta 1: a mechanism for regulating pulmonary inflammation and fibrosis. Cell *96*, 319–328. https://doi.org/10.1016/s0092-8674(00)80545-0.

Naber, H.P.H., Wiercinska, E., Pardali, E., van Laar, T., Nirmala, E., Sundqvist, A., van Dam, H., van der Horst, G., van der Pluijm, G., Heckmann, B., et al. (2012). BMP-7 inhibits TGF-β-induced invasion of breast cancer cells through inhibition of integrin β3 expression. Cell Oncol. *35*, 19–28. https://doi.org/10.1007/s13402-011-0058-0.

Nakashima, K., Yanagisawa, M., Arakawa, H., Kimura, N., Hisatsune, T., Kawabata, M., Miyazono, K., and Taga, T. (1999). Synergistic signaling in fetal brain by STAT3-Smad1 complex bridged by p300. Science *284*, 479–482. https://doi.org/10.1126/science.284.5413.479.

Naume, B., Synnestvedt, M., Falk, R.S., Wiedswang, G., Weyde, K., Risberg, T., Kersten, C., Mjaaland, I., Vindi, L., Sommer, H.H., et al. (2014). Clinical outcome with correlation to disseminated tumor cell (DTC) status after DTC-guided secondary adjuvant treatment with docetaxel in early breast cancer. J. Clin. Oncol. *32*, 3848–3857. https://doi.org/10.1200/JCO.2014.56.9327.

Naumov, G.N., Akslen, L.A., and Folkman, J. (2006). Role of Angiogenesis in Human Tumor Dormancy: Animal Models of the Angiogenic Switch. Cell Cycle *5*, 1779–1787. https://doi.org/10.4161/cc.5.16.3018.

Nilsson, S.K., Johnston, H.M., Whitty, G.A., Williams, B., Webb, R.J., Denhardt, D.T., Bertoncello, I., Bendall, L.J., Simmons, P.J., and Haylock, D.N. (2005). Osteopontin, a key component of the hematopoietic stem cell niche and regulator of primitive hematopoietic progenitor cells. Blood *106*, 1232–1239. https://doi.org/10.1182/blood-2004-11-4422.

Ning, J., Zhao, Y., Ye, Y., and Yu, J. (2019). Opposing roles and potential antagonistic mechanism between TGF-β and BMP pathways: Implications for cancer progression. EBioMedicine *41*, 702–710. https://doi.org/10.1016/j.ebiom.2019.02.033.

Nobre, A.R., Risson, E., Singh, D.K., Di Martino, J.S., Cheung, J.F., Wang, J., Johnson, J., Russnes, H.G., Bravo-Cordero, J.J., Birbrair, A., et al. (2021). Bone marrow NG2 + /Nestin + mesenchymal stem cells drive DTC dormancy via TGF-β2. Nature Cancer 1–13. https://doi.org/10.1038/s43018-021-00179-8.

Olsson, N., Piek, E., Sundström, M., ten Dijke, P., and Nilsson, G. (2001). Transforming growth factor-beta-mediated mast cell migration depends on mitogen-activated protein kinase activity. Cell Signal *13*, 483–490. https://doi.org/10.1016/s0898-6568(01)00176-0.

Onichtchouk, D., Chen, Y.G., Dosch, R., Gawantka, V., Delius, H., Massagué, J., and Niehrs, C. (1999). Silencing of TGF-beta signalling by the pseudoreceptor BAMBI. Nature *401*, 480–485. https://doi.org/10.1038/46794.

Oshimori, N., and Fuchs, E. (2012). Paracrine TGF-β Signaling Counterbalances BMP-Mediated Repression in Hair Follicle Stem Cell Activation. Cell Stem Cell *10*, 63–75. https://doi.org/10.1016/j.stem.2011.11.005.

Ossowski, L., and Aguirre-Ghiso, J.A. (2010). Dormancy of metastatic melanoma. Pigment Cell & Melanoma Research *23*, 41–56. https://doi.org/10.1111/j.1755-148X.2009.00647.x.

Otsuki, L., and Brand, A.H. (2018). Cell cycle heterogeneity directs the timing of neural stem cell activation from quiescence. Science *360*, 99–102. https://doi.org/10.1126/science.aan8795.

Ouarné, M., Bouvard, C., Boneva, G., Mallet, C., Ribeiro, J., Desroches-Castan, A., Soleilhac, E., Tillet, E., Peyruchaud, O., and Bailly, S. (2018). BMP9, but not BMP10, acts as a quiescence factor on tumor growth, vessel normalization and metastasis in a mouse model of breast cancer. J Exp Clin Cancer Res *37*, 1–12. https://doi.org/10.1186/s13046-018-0885-1.

Owens, P., Pickup, M.W., Novitskiy, S.V., Chytil, A., Gorska, A.E., Aakre, M.E., West, J., and Moses, H.L. (2012). Disruption of bone morphogenetic protein receptor 2 (BMPR2) in mammary tumors promotes metastases through cell autonomous and paracrine mediators. PNAS *109*, 2814–2819. https://doi.org/10.1073/pnas.1101139108.

Pan, H., Gray, R., Braybrooke, J., Davies, C., Taylor, C., McGale, P., Peto, R., Pritchard, K.I., Bergh, J., Dowsett, M., et al. (2017). 20-Year Risks of Breast-Cancer Recurrence after Stopping Endocrine Therapy at 5 Years. New England Journal of Medicine *377*, 1836–1846. https://doi.org/10.1056/NEJMoa1701830.

Pantel, K., Schlimok, G., Kutter, D., Schaller, G., Genz, T., Wiebecke, B., Backmann, R., Funke, I., and Riethmüller, G. (1991). Frequent down-regulation of major histocompatibility class I antigen expression on individual micrometastatic carcinoma cells. Cancer Res *51*, 4712–4715. .

Patel, S.A., Meyer, J.R., Greco, S.J., Corcoran, K.E., Bryan, M., and Rameshwar, P. (2010). Mesenchymal Stem Cells Protect Breast Cancer Cells through Regulatory T Cells: Role of Mesenchymal Stem Cell-Derived TGF-. The Journal of Immunology *184*, 5885–5894. https://doi.org/10.4049/jimmunol.0903143.

Patel, S.A., Dave, M.A., Bliss, S.A., Giec-Ujda, A.B., Bryan, M., Pliner, L.F., and Rameshwar, P. (2014). Treg/Th17 polarization by distinct subsets of breast cancer cells is dictated by the interaction with mesenchymal stem cells. J Cancer Stem Cell Res *2014*. https://doi.org/10.14343/JCSCR.2014.2e1003.

Pedersen, R.N., Mellemkjær, L., Ejlertsen, B., Nørgaard, M., and Cronin-Fenton, D.P. (2022a). Mortality After Late Breast Cancer Recurrence in Denmark. JCO JCO.21.02062. https://doi.org/10.1200/JCO.21.02062.

Pedersen, R.N., Esen, B.Ö., Mellemkjær, L., Christiansen, P., Ejlertsen, B., Lash, T.L., Nørgaard, M., and Cronin-Fenton, D. (2022b). The Incidence of Breast Cancer Recurrence 10-32 Years After Primary Diagnosis. J Natl Cancer Inst *114*, 391–399. https://doi.org/10.1093/jnci/djab202.

Pedersen, R.N., Christiansen, P., Ejlertsen, B., Lash, T.L., Nørgaard, M., and Cronin-Fenton, D. The Incidence of Breast Cancer Recurrence 10-32 Years After Primary Diagnosis. 9. .

Perou, C.M., Sørlie, T., Eisen, M.B., van de Rijn, M., Jeffrey, S.S., Rees, C.A., Pollack, J.R., Ross, D.T., Johnsen, H., Akslen, L.A., et al. (2000). Molecular portraits of human breast tumours. Nature *406*, 747–752. https://doi.org/10.1038/35021093.

Phan, T.G., and Croucher, P.I. (2020). The dormant cancer cell life cycle. Nature Reviews Cancer *20*, 398–411. https://doi.org/10.1038/s41568-020-0263-0.

Pickup, M.W., Hover, L.D., Guo, Y., Gorska, A.E., Chytil, A., Novitskiy, S.V., Moses, H.L., and Owens, P. (2015). Deletion of the BMP receptor BMPR1a impairs mammary tumor formation and metastasis. Oncotarget *6*, 22890–22904. https://doi.org/10.18632/oncotarget.4413.

Pinho, S., and Frenette, P.S. (2019). Haematopoietic stem cell activity and interactions with the niche. Nature Reviews Molecular Cell Biology https://doi.org/10.1038/s41580-019-0103-9.

Plikus, M.V., Mayer, J.A., de la Cruz, D., Baker, R.E., Maini, P.K., Maxson, R., and Chuong, C.-M. (2008). Cyclic dermal BMP signalling regulates stem cell activation during hair regeneration. Nature *451*, 340–344. https://doi.org/10.1038/nature06457.

Pommier, A., Anaparthy, N., Memos, N., Kelley, Z.L., Gouronnec, A., Yan, R., Auffray, C., Albrengues, J., Egeblad, M., Iacobuzio-Donahue, C.A., et al. (2018). Unresolved endoplasmic reticulum stress engenders immune-resistant, latent pancreatic cancer metastases. Science *360*, eaao4908. https://doi.org/10.1126/science.aao4908.

Pouliot, F., Blais, A., and Labrie, C. (2003). Overexpression of a Dominant Negative Type II Bone Morphogenetic Protein Receptor Inhibits the Growth of Human Breast Cancer Cells1. Cancer Research *63*, 277–281. .

Prunier, C., Baker, D., Ten Dijke, P., and Ritsma, L. (2019). TGF-β Family Signaling Pathways in Cellular Dormancy. Trends Cancer *5*, 66–78. https://doi.org/10.1016/j.trecan.2018.10.010.

Prunier, C., Alay, A., van Dijk, M., Ammerlaan, K.L., van Gelderen, S., Marvin, D.L., Teunisse, A., Slieker, R.C., Szuhai, K., Jochemsen, A.G., et al. (2021). Breast cancer dormancy is associated with a 4NG1 state and not senescence. NPJ Breast Cancer *7*, 140. https://doi.org/10.1038/s41523-021-00347-0.

Pulianmackal, A.J., Sun, D., Yumoto, K., Li, Z., Chen, Y.-C., Patel, M.V., Wang, Y., Yoon, E., Pearson, A., Yang, Q., et al. (2021). Monitoring Spontaneous Quiescence and Asynchronous Proliferation-Quiescence Decisions in Prostate Cancer Cells. Frontiers in Cell and Developmental Biology *9*. .

Qi, Z., Li, Y., Zhao, B., Xu, C., Liu, Y., Li, H., Zhang, B., Wang, X., Yang, X., Xie, W., et al. (2017). BMP restricts stemness of intestinal Lgr5+ stem cells by directly suppressing their signature genes. Nat Commun *8*, 13824. https://doi.org/10.1038/ncomms13824.

Quesnel, B. (2008). Dormant tumor cells as a therapeutic target? Cancer Letters *267*, 10–17. https://doi.org/10.1016/j.canlet.2008.02.055.

Ranganathan, A.C., Ojha, S., Kourtidis, A., Conklin, D.S., and Aguirre-Ghiso, J.A. (2008). Dual function of pancreatic endoplasmic reticulum kinase in tumor cell growth arrest and survival. Cancer Res *68*, 3260–3268. https://doi.org/10.1158/0008-5472.CAN-07-6215.

Recasens, A., and Munoz, L. (2019). Targeting Cancer Cell Dormancy. Trends Pharmacol. Sci. *40*, 128–141. https://doi.org/10.1016/j.tips.2018.12.004.

Ren, D., Dai, Y., Yang, Q., Zhang, X., Guo, W., Ye, L., Huang, S., Chen, X., Lai, Y., Du, H., et al. (2019). Wnt5a induces and maintains prostate cancer cells dormancy in bone. J. Exp. Med. *216*, 428–449. https://doi.org/10.1084/jem.20180661.

Ren, W., Sun, X., Wang, K., Feng, H., Liu, Y., Fei, C., Wan, S., Wang, W., Luo, J., Shi, Q., et al. (2014). BMP9 inhibits the bone metastasis of breast cancer cells by downregulating CCN2 (connective tissue growth factor, CTGF) expression. Mol Biol Rep *41*, 1373–1383. https://doi.org/10.1007/s11033-013-2982-8.

Richman, J., and Dowsett, M. (2019). Beyond 5 years: enduring risk of recurrence in oestrogen receptor-positive breast cancer. Nature Reviews Clinical Oncology *16*, 296. https://doi.org/10.1038/s41571-018-0145-5.

Risson, E., Nobre, A.R., Maguer-Satta, V., and Aguirre-Ghiso, J.A. (2020). The current paradigm and challenges ahead for the dormancy of disseminated tumor cells. Nature Cancer *1*, 672–680. https://doi.org/10.1038/s43018-020-0088-5.

Rodgers, J.T., King, K.Y., Brett, J.O., Cromie, M.J., Charville, G.W., Maguire, K.K., Brunson, C., Mastey, N., Liu, L., Tsai, C.-R., et al. (2014). mTORC1 controls the adaptive transition of quiescent stem cells from G0 to GAlert. Nature *510*, 393–396. https://doi.org/10.1038/nature13255.

Rodgers, K.M., Udesky, J.O., Rudel, R.A., and Brody, J.G. (2018). Environmental chemicals and breast cancer: An updated review of epidemiological literature informed by biological mechanisms. Environ Res *160*, 152–182. https://doi.org/10.1016/j.envres.2017.08.045.

Roger, E., Martel, S., Bertrand-Chapel, A., Depollier, A., Chuvin, N., Pommier, R.M., Yacoub, K., Caligaris, C., Cardot-Ruffino, V., Chauvet, V., et al. (2019). Schwann cells support oncogenic potential of pancreatic cancer cells through TGFβ signaling. Cell Death Dis *10*, 1–19. https://doi.org/10.1038/s41419-019-2116-x.

Rueda, O.M., Sammut, S.-J., Seoane, J.A., Chin, S.-F., Caswell-Jin, J.L., Callari, M., Batra, R., Pereira, B., Bruna, A., Ali, H.R., et al. (2019). Dynamics of breast-cancer relapse reveal late-recurring ER-positive genomic subgroups. Nature *567*, 399–404. https://doi.org/10.1038/s41586-019-1007-8.

Rumman, M., Dhawan, J., and Kassem, M. (2015). Concise Review: Quiescence in Adult Stem Cells: Biological Significance and Relevance to Tissue Regeneration: ASC Quiescence: Role and Relevance to Tissue Regeneration. STEM CELLS *33*, 2903–2912. https://doi.org/10.1002/stem.2056.

Rusu, P., Shao, C., Neuerburg, A., Acikgöz, A.A., Wu, Y., Zou, P., Phapale, P., Shankar, T.S., Döring, K., Dettling, S., et al. (2019). GPD1 Specifically Marks Dormant Glioma Stem Cells with a Distinct Metabolic Profile. Cell Stem Cell *25*, 241-257.e8. https://doi.org/10.1016/j.stem.2019.06.004.

Sachdeva, R., Wu, M., Johnson, K., Kim, H., Celebre, A., Shahzad, U., Graham, M.S., Kessler, J.A., Chuang, J.H., Karamchandani, J., et al. (2019). BMP signaling mediates glioma stem cell quiescence and confers treatment resistance in glioblastoma. Scientific Reports *9*, 14569. https://doi.org/10.1038/s41598-019-51270-1.

Sanjabi, S., Oh, S.A., and Li, M.O. (2017). Regulation of the Immune Response by TGF-β: From Conception to Autoimmunity and Infection. Cold Spring Harb Perspect Biol *9*, a022236. https://doi.org/10.1101/cshperspect.a022236.

Saudemont, A., and Quesnel, B. (2004). In a model of tumor dormancy, long-term persistent leukemic cells have increased B7-H1 and B7.1 expression and resist CTL-mediated lysis. Blood *104*, 2124–2133. https://doi.org/10.1182/blood-2004-01-0064.

Schardt, J.A., Meyer, M., Hartmann, C.H., Schubert, F., Schmidt-Kittler, O., Fuhrmann, C., Polzer, B., Petronio, M., Eils, R., and Klein, C.A. (2005). Genomic analysis of single cytokeratin-positive cells from bone marrow reveals early mutational events in breast cancer. Cancer Cell *8*, 227–239. https://doi.org/10.1016/j.ccr.2005.08.003.

Scherner, O., Meurer, S.K., Tihaa, L., Gressner, A.M., and Weiskirchen, R. (2007). Endoglin Differentially Modulates Antagonistic Transforming Growth Factor-β1 and BMP-7 Signaling *. Journal of Biological Chemistry *282*, 13934–13943. https://doi.org/10.1074/jbc.M611062200.

Serizawa, K., Tanaka, H., Ueda, T., Fukui, A., Kakutani, H., Taniguchi, T., Inoue, H., Kumode, T., Taniguchi, Y., Rai, S., et al. (2022). CD34+ myeloma cells with self-renewal activities are therapy-resistant and persist as MRD in cell cycle quiescence. Int J Hematol *115*, 336–349. https://doi.org/10.1007/s12185-021-03261-0.

Shachaf, C.M., Kopelman, A.M., Arvanitis, C., Karlsson, A., Beer, S., Mandl, S., Bachmann, M.H., Borowsky, A.D., Ruebner, B., Cardiff, R.D., et al. (2004). MYC inactivation uncovers pluripotent differentiation and tumour dormancy in hepatocellular cancer. Nature *431*, 1112–1117. https://doi.org/10.1038/nature03043.

Sharma, S., Xing, F., Liu, Y., Wu, K., Said, N., Pochampally, R., Shiozawa, Y., Lin, H.-K., Balaji, K.C., and Watabe, K. (2016). Secreted Protein Acidic and Rich in Cysteine (SPARC) Mediates Metastatic Dormancy of Prostate Cancer in Bone*. Journal of Biological Chemistry *291*, 19351–19363. https://doi.org/10.1074/jbc.M116.737379.

Shee, K., Jiang, A., Varn, F.S., Liu, S., Traphagen, N.A., Owens, P., Ma, C.X., Hoog, J., Cheng, C., Golub, T.R., et al. (2019). Cytokine sensitivity screening highlights BMP4 pathway signaling as a therapeutic opportunity in ER+ breast cancer. FASEB J *33*, 1644–1657. https://doi.org/10.1096/fj.201801241R.

Sherr, C.J., and Roberts, J.M. (1999). CDK inhibitors: positive and negative regulators of G1-phase progression. Genes Dev. *13*, 1501–1512. .

Shimasaki, S., Moore, R.K., Otsuka, F., and Erickson, G.F. (2004). The Bone Morphogenetic Protein System In Mammalian Reproduction. Endocrine Reviews *25*, 72–101. https://doi.org/10.1210/er.2003-0007.

Shimizu, H., Takeishi, S., Nakatsumi, H., and Nakayama, K.I. (2019). Prevention of cancer dormancy by Fbxw7 ablation eradicates disseminated tumor cells. JCI Insight *4*. https://doi.org/10.1172/jci.insight.125138.

Shiozawa, Y., Pedersen, E.A., Patel, L.R., Ziegler, A.M., Havens, A.M., Jung, Y., Wang, J., Zalucha, S., Loberg, R.D., Pienta, K.J., et al. (2010). GAS6/AXL Axis Regulates Prostate Cancer Invasion, Proliferation, and Survival in the Bone Marrow Niche. Neoplasia *12*, 116–127. .

Simeone, D.M., Zhang, L., Graziano, K., Nicke, B., Pham, T., Schaefer, C., and Logsdon, C.D. (2001). Smad4 mediates activation of mitogen-activated protein kinases by TGF-β in pancreatic acinar cells. American Journal of Physiology-Cell Physiology *281*, C311–C319. https://doi.org/10.1152/ajpcell.2001.281.1.C311.

Singh, A., Veeriah, V., Xi, P., Labella, R., Chen, J., Romeo, S.G., Ramasamy, S.K., and Kusumbe, A.P. (2019). Angiocrine signals regulate quiescence and therapy resistance in bone metastasis. JCI Insight *4*, 125679. https://doi.org/10.1172/jci.insight.125679.

Siwko, S.K., Dong, J., Lewis, M.T., Liu, H., Hilsenbeck, S.G., and Li, Y. (2008). Evidence that an early pregnancy causes a persistent decrease in the number of functional mammary epithelial stem cells--implications for pregnancy-induced protection against breast cancer. Stem Cells *26*, 3205–3209. https://doi.org/10.1634/stemcells.2008-0103.

Song, Y., Lv, S., Wang, F., Liu, X., Cheng, J., Liu, S., Wang, X., Chen, W., Guan, G., Liu, G., et al. (2020). Overexpression of BMP-7 reverses TGF-β1-induced epithelial-mesenchymal transition by attenuating the Wnt3/β-catenin and TGF-β1/Smad2/3 signaling pathways in HK-2 cells. Molecular Medicine Reports *21*, 833–841. https://doi.org/10.3892/mmr.2019.10875.

Sosa, M.S., Parikh, F., Maia, A.G., Estrada, Y., Bosch, A., Bragado, P., Ekpin, E., George, A., Zheng, Y., Lam, H.-M., et al. (2015). NR2F1 controls tumour cell dormancy via SOX9- and RARβ-driven quiescence programmes. Nature Communications *6*. https://doi.org/10.1038/ncomms7170.

Stolfi, C., Marafini, I., De Simone, V., Pallone, F., and Monteleone, G. (2013). The Dual Role of Smad7 in the Control of Cancer Growth and Metastasis. International Journal of Molecular Sciences *14*, 23774–23790. https://doi.org/10.3390/ijms141223774.

Stumm, C.L., Halcsik, E., Landgraf, R.G., Camara, N.O.S., Sogayar, M.C., and Jancar, S. (2014). Lung Remodeling in a Mouse Model of Asthma Involves a Balance between TGF-β1 and BMP-7. PLOS ONE *9*, e95959. https://doi.org/10.1371/journal.pone.0095959.

Sun, D., Filipescu, D., Hasson, D., Singh, D.K., Carcamo, S., Khalil, B., Miles, B.A., Westra, W., Sproll, K.C., Bernstein, E., et al. (2021). MacroH2A impedes metastatic growth by enforcing a discrete dormancy program in disseminated cancer cells. 2021.12.07.471619. https://doi.org/10.1101/2021.12.07.471619.

Sun, H., Yang, Y., Zhang, J., Liu, T., Wang, H., Garg, S., and Zhang, B. (2019). Fear of cancer recurrence, anxiety and depressive symptoms in adolescent and young adult cancer patients. Neuropsychiatr Dis Treat *15*, 857–865. https://doi.org/10.2147/NDT.S202432.

Sung, H., Ferlay, J., Siegel, R.L., Laversanne, M., Soerjomataram, I., Jemal, A., and Bray, F. (2021). Global Cancer Statistics 2020: GLOBOCAN Estimates of Incidence and Mortality Worldwide for 36 Cancers in 185 Countries. CA: A Cancer Journal for Clinicians *71*, 209–249. https://doi.org/10.3322/caac.21660.

Taichman, R.S., Patel, L.R., Bedenis, R., Wang, J., Weidner, S., Schumann, T., Yumoto, K., Berry, J.E., Shiozawa, Y., and Pienta, K.J. (2013). GAS6 receptor status is associated with dormancy and bone metastatic tumor formation. PLoS ONE *8*, e61873. https://doi.org/10.1371/journal.pone.0061873.

Tallón de Lara, P., Castañón, H., Vermeer, M., Núñez, N., Silina, K., Sobottka, B., Urdinez, J., Cecconi, V., Yagita, H., Movahedian Attar, F., et al. (2021). CD39+PD-1+CD8+ T cells mediate metastatic dormancy in breast cancer. Nat Commun *12*, 769. https://doi.org/10.1038/s41467-021-21045-2.

Tikhonova, A.N., Dolgalev, I., Hu, H., Sivaraj, K.K., Hoxha, E., Cuesta-Domínguez, Á., Pinho, S., Akhmetzyanova, I., Gao, J., Witkowski, M., et al. (2019). The bone marrow microenvironment at single-cell resolution. Nature *569*, 222–228. https://doi.org/10.1038/s41586-019-1104-8.

Uhr, J.W., and Marches, R. (2001). Dormancy in a model of murine B cell lymphoma. Seminars in Cancer Biology *11*, 277–283. https://doi.org/10.1006/scbi.2001.0383.

Vera-Ramirez, L., Vodnala, S.K., Nini, R., Hunter, K.W., and Green, J.E. (2018). Autophagy promotes the survival of dormant breast cancer cells and metastatic tumour recurrence. Nature Communications *9*, 1944. https://doi.org/10.1038/s41467-018-04070-6.

Voeltzel, T., Fossard, G., Degaud, M., Geistlich, K., Gadot, N., Jeanpierre, S., Mikaelian, I., Brevet, M., Anginot, A., Bousse-Kerdilès, M.-C.L., et al. (2022). A minimal standardized human bone marrow microphysiological system to assess resident cell behavior during normal and pathological processes. Biomater. Sci. *10*, 485–498. https://doi.org/10.1039/D1BM01098K.

Wagner, D.O., Sieber, C., Bhushan, R., Börgermann, J.H., Graf, D., and Knaus, P. (2010). BMPs: from bone to body morphogenetic proteins. Sci Signal *3*, mr1. https://doi.org/10.1126/scisignal.3107mr1.

Waite, K.A., and Eng, C. (2003). From developmental disorder to heritable cancer: it's all in the BMP/TGF-β family. Nat Rev Genet *4*, 763–773. https://doi.org/10.1038/nrg1178.

Waks, A.G., and Winer, E.P. (2019). Breast Cancer Treatment: A Review. JAMA *321*, 288–300. https://doi.org/10.1001/jama.2018.19323.

Wang, G., Yu, Y., Sun, C., Liu, T., Liang, T., Zhan, L., Lin, X., and Feng, X.-H. (2016a). STAT3 selectively interacts with Smad3 to antagonize TGF-β. Oncogene *35*, 4388–4398. https://doi.org/10.1038/onc.2015.446.

Wang, R.N., Green, J., Wang, Z., Deng, Y., Qiao, M., Peabody, M., Zhang, Q., Ye, J., Yan, Z., Denduluri, S., et al. (2014). Bone Morphogenetic Protein (BMP) signaling in development and human diseases. Genes & Diseases *1*, 87–105. https://doi.org/10.1016/j.gendis.2014.07.005.

Wang, S., Sun, A., Li, L., Zhao, G., Jia, J., Wang, K., Ge, J., and Zou, Y. (2012). Up-regulation of BMP-2 antagonizes TGF-β1/ROCK-enhanced cardiac fibrotic signalling through activation of Smurf1/Smad6 complex. Journal of Cellular and Molecular Medicine *16*, 2301–2310. https://doi.org/10.1111/j.1582-4934.2012.01538.x.

Wang, X., Harris, R.E., Bayston, L.J., and Ashe, H.L. (2008). Type IV collagens regulate BMP signalling in Drosophila. Nature *455*, 72–77. https://doi.org/10.1038/nature07214.

Wang, Y., He, T., Liu, J., Liu, H., Zhou, L., Hao, W., Sun, Y., and Wang, X. (2016b). Synergistic effects of overexpression of BMP-2 and TGF-β3 on osteogenic

differentiation of bone marrow mesenchymal stem cells. Molecular Medicine Reports *14*, 5514–5520. https://doi.org/10.3892/mmr.2016.5961.

Wei, W., Nurse, P., and Broek, D. (1993). Yeast Cells Can Enter a Quiescent State through G1, S, G2, or M Phase of the Cell Cycle1. Cancer Research *53*, 1867–1870. .

Werner-Klein, M., Scheitler, S., Hoffmann, M., Hodak, I., Dietz, K., Lehnert, P., Naimer, V., Polzer, B., Treitschke, S., Werno, C., et al. (2018). Genetic alterations driving metastatic colony formation are acquired outside of the primary tumour in melanoma. Nat Commun *9*, 595. https://doi.org/10.1038/s41467-017-02674-y.

White, A.C., Khuu, J.K., Dang, C.Y., Hu, J., Tran, K.V., Liu, A., Gomez, S., Zhang, Z., Yi, R., Scumpia, P., et al. (2014). Stem cell quiescence acts as a tumour suppressor in squamous tumours. Nature Cell Biology *16*, 99–107. https://doi.org/10.1038/ncb2889.

Wilson, A., Laurenti, E., Oser, G., van der Wath, R.C., Blanco-Bose, W., Jaworski, M., Offner, S., Dunant, C.F., Eshkind, L., Bockamp, E., et al. (2008). Hematopoietic stem cells reversibly switch from dormancy to self-renewal during homeostasis and repair. Cell *135*, 1118–1129. https://doi.org/10.1016/j.cell.2008.10.048.

Wong, D.J., Liu, H., Ridky, T.W., Cassarino, D., Segal, E., and Chang, H.Y. (2008). Module map of stem cell genes guides creation of epithelial cancer stem cells. Cell Stem Cell *2*, 333–344. https://doi.org/10.1016/j.stem.2008.02.009.

Wordinger, R.J., Fleenor, D.L., Hellberg, P.E., Pang, I.-H., Tovar, T.O., Zode, G.S., Fuller, J.A., and Clark, A.F. (2007). Effects of TGF-beta2, BMP-4, and gremlin in the trabecular meshwork: implications for glaucoma. Invest Ophthalmol Vis Sci *48*, 1191–1200. https://doi.org/10.1167/iovs.06-0296.

Xu, X., Zheng, L., Yuan, Q., Zhen, G., Crane, J.L., Zhou, X., and Cao, X. (2018). Transforming growth factor-β in stem cells and tissue homeostasis. Bone Res *6*, 1–31. https://doi.org/10.1038/s41413-017-0005-4.

Xue, W., Zender, L., Miething, C., Dickins, R.A., Hernando, E., Krizhanovsky, V., Cordon-Cardo, C., and Lowe, S.W. (2007). Senescence and tumour clearance is triggered by p53 restoration in murine liver carcinomas. Nature *445*, 656–660. https://doi.org/10.1038/nature05529.

Yamamoto, T., Matsuda, T., Muraguchi, A., Miyazono, K., and Kawabata, M. (2001). Cross-talk between IL-6 and TGF-β signaling in hepatoma cells. FEBS Letters *492*, 247–253. https://doi.org/10.1016/S0014-5793(01)02258-X.

Yamazaki, S., Ema, H., Karlsson, G., Yamaguchi, T., Miyoshi, H., Shioda, S., Taketo, M.M., Karlsson, S., Iwama, A., and Nakauchi, H. (2011). Nonmyelinating Schwann cells maintain hematopoietic stem cell hibernation in the bone marrow niche. Cell *147*, 1146–1158. https://doi.org/10.1016/j.cell.2011.09.053.

Yan, Y., and Wang, Q. (2021). BMP Signaling: Lighting up the Way for Embryonic Dorsoventral Patterning. Front Cell Dev Biol *9*, 799772. https://doi.org/10.3389/fcell.2021.799772.

Yang, S., Zhong, C., Frenkel, B., Reddi, A.H., and Roy-Burman, P. (2005). Diverse biological effect and Smad signaling of bone morphogenetic protein 7 in prostate tumor cells. Cancer Res *65*, 5769–5777. https://doi.org/10.1158/0008-5472.CAN-05-0289.

Yang, Y., Cameron, J., Bedi, C., and Humphris, G. (2018). Fear of cancer recurrence trajectory during radiation treatment and follow-up into survivorship of patients with breast cancer. BMC Cancer *18*, 1002. https://doi.org/10.1186/s12885-018-4908-2.

Ye, L., Kynaston, H., and Jiang, W.G. (2009). Bone morphogenetic protein-10 suppresses the growth and aggressiveness of prostate cancer cells through a Smad independent pathway. J Urol *181*, 2749–2759. https://doi.org/10.1016/j.juro.2009.01.098.

Yu-Lee, L.-Y., Yu, G., Lee, Y.-C., Lin, S.-C., Pan, J., Pan, T., Yu, K.-J., Liu, B., Creighton, C.J., Rodriguez-Canales, J., et al. (2018). Osteoblast-Secreted Factors Mediate Dormancy of Metastatic Prostate Cancer in the Bone via Activation of the TGFβRIII-p38MAPK-pS249/T252RB Pathway. Cancer Res. *78*, 2911–2924. https://doi.org/10.1158/0008-5472.CAN-17-1051.

Yumoto, K., Eber, M.R., Wang, J., Cackowski, F.C., Decker, A.M., Lee, E., Nobre, A.R., Aguirre-Ghiso, J.A., Jung, Y., and Taichman, R.S. (2016). Axl is required for TGF-β2-induced dormancy of prostate cancer cells in the bone marrow. Scientific Reports *6*. https://doi.org/10.1038/srep36520.

Zakin, L., and De Robertis, E.M. (2010). Extracellular regulation of BMP signaling. Current Biology *20*, R89–R92. https://doi.org/10.1016/j.cub.2009.11.021.

Zeng, S., Zhang, Y., Ma, J., Deng, G., Qu, Y., Guo, C., Han, Y., Yin, L., Cai, C., Li, Y., et al. (2017). BMP4 promotes metastasis of hepatocellular carcinoma by an induction of epithelial-mesenchymal transition via upregulating ID2. Cancer Lett. *390*, 67–76. https://doi.org/10.1016/j.canlet.2016.12.042.

Zhang, Y., Alexander, P.B., and Wang, X.-F. (2017). TGF-β Family Signaling in the Control of Cell Proliferation and Survival. Cold Spring Harb Perspect Biol *9*. https://doi.org/10.1101/cshperspect.a022145.

Zhao, W., Zhu, Q., Tan, P., Ajibade, A., Long, T., Long, W., Li, Q., Liu, P., Ning, B., Wang, H.Y., et al. (2018). Tgfbr2 inactivation facilitates cellular plasticity and development of Pten-null prostate cancer. Journal of Molecular Cell Biology *10*, 316–330. https://doi.org/10.1093/jmcb/mjx052.

Zheng, H., Bae, Y., Kasimir-Bauer, S., Tang, R., Chen, J., Ren, G., Yuan, M., Esposito, M., Li, W., Wei, Y., et al. (2017). Therapeutic Antibody Targeting Tumor- and Osteoblastic Niche-Derived Jagged1 Sensitizes Bone Metastasis to Chemotherapy. Cancer Cell *32*, 731-747.e6. https://doi.org/10.1016/j.ccell.2017.11.002.

Zilberberg, L., Todorovic, V., Dabovic, B., Horiguchi, M., Couroussé, T., Sakai, L.Y., and Rifkin, D.B. (2012). Specificity of latent TGF-β binding protein (LTBP)

incorporation into matrix: role of fibrillins and fibronectin. J Cell Physiol *227*, 3828–3836. https://doi.org/10.1002/jcp.24094.

Cancer of the Breast (Female) - Cancer Stat Facts.

Bone: Formation by Autoinduction.

APPENDICES

APPENDIX 1

Intense scientific discussion of the development of the project led to the publication of a review of the recent scientific literature on cancer dormancy.

Risson E*, Nobre AR*, Maguer-Satta V, Aguirre-Ghiso JA: **The current paradigm and challenges ahead for the dormancy of disseminated tumor cells**.
Nature Cancer 2020, doi: 10.1038/s43018-020-0088-5.

nature cancer

PERSPECTIVE

https://doi.org/10.1038/s43018-020-0088-5

The current paradigm and challenges ahead for the dormancy of disseminated tumor cells

Emma Risson[1,2,3,4,6], Ana Rita Nobre[4,5,6], Veronique Maguer-Satta[1,2,3] and Julio A. Aguirre-Ghiso[4] ✉

Disseminated tumor cells (DTCs) are known to enter a state of dormancy that is achieved via growth arrest of DTCs and/or a form of population equilibrium state, strongly influenced by the organ microenvironment. During this time, expansion of residual disseminated cancer is paused and DTCs survive to fuel relapse, sometimes decades later. This notion has opened a new window of opportunity for intervening and preventing relapse. Here we review recent data that have further augmented the understanding of cancer dormancy and discuss how this is leading to new strategies for monitoring and targeting dormant cancer.

In recent years, the understanding of metastasis biology and cancer cell dormancy has advanced considerably. The current knowledge of how cancer dormancy proceeds stemmed from pioneering work on angiogenesis[1–3], on the immunoregulation of equilibrium states and antibody signaling[4–13] and on how microenvironmental and signaling mechanisms control cellular dormancy through growth-arrest programs[14,15]. Key findings based on this body of work proposed that dormant cells might evade anti-proliferative therapies in a passive manner[16]. Since then, the field has expanded considerably to reveal the importance of the tissue microenvironment in driving dormancy and the reactivation of dormant cells. Developmental cues that contribute to tissue homeostasis by controlling the quiescence of normal adult stem cells, as well as various niche cells of different organs, have also been shown to drive dormancy[17–19]. Dormant cancer cells were also found to regulate active signaling mechanisms of adaptation and survival after therapies[20–24], which demonstrated that dormant tumor cells do not merely survive chemotherapeutic drug insults in a passive manner. These findings have strengthened the notion that dormant DTCs persist over long periods of time by co-opting conserved growth-arrest and survival mechanisms that are active during development and in adult tissues.

In this Perspective, we focus on recent, mainly in vivo and human data and discuss how they inform evolving concepts about tumor dormancy, including the active role of the microenvironment.

Discussing definitions

The cancer dormancy field has worked on the basis of three definitions that are not necessarily mutually exclusive and may be complementary. These have led to the working hypothesis that asymptomatic minimal residual disease (MRD) can be defined and explained by the following three potential scenarios: (1) angiogenic dormancy, an impaired angiogenic response that maintains tumor mass constant in size by balancing proliferation and cell death;[1–3] (2) immune-mediated dormancy, in which proliferative tumor-cell populations are constantly trimmed by cytotoxic immune-cell responses that also maintain an equilibrium between cell death and proliferation;[4–13] and (3) cellular dormancy, in which solitary DTCs or small cell clusters enter a prolonged growth arrest with no increase in cell death[19,24–27].

Equilibrium states, as described in the angiogenic dormancy program[3], have long been proposed as a defining feature of dormant tumor-cell-mass dynamics, with evidence accumulating since the 1990s. This concept and the relevant literature have been reviewed extensively elsewhere[18,26,28]. The immune equilibrium hypothesis suggests that immunosurveillance keeps proliferating cell populations in check during MRD through T cell–mediated killing or anti-idiotypic antibody networks that cause growth suppression in mouse lymphoma; this hypothesis has also been reviewed previously[26,29]. Recent studies focused more on cellular dormancy and its relationship with immune cells indicate that quiescent DTCs are in fact evading $CD8^+$ T cell– and natural killer cell (NK cell)–mediated detection and clearance[27,30]. Thus, as proposed in an integrated scenario[26], quiescent DTCs may evade detection by the immune system, but as they switch into proliferation, they may be maintained in equilibrium by immune cytotoxic responses, which shows how these two processes can be complementary. To our knowledge there are no available studies showing that dormant solitary DTCs that become reactivated are then kept under tumor-mass dormancy by an angiogenic switch failure, but this possibility has also been proposed[26]. The large body of literature discussed in this Perspective has independently discovered that dormant cancer-cell populations consist of single solitary DTCs or small DTC clusters of 10–20 cells[18,23,27,31–36]. These DTCs are able to enter a reversible growth-arrest or quiescence state, in support of the proposal that this may be a common feature of solitary dormant cancer cells.

Whether all the scenarios discussed above can co-exist in patients remains an open question. The tissues that are sampled for further study may also bias the identification of the mechanisms involved. For example, several dormancy studies that complement the study of human DTCs from bone marrow (BM) with mouse models seem to point to quiescence as a feature of solitary DTCs[17,19,26,37–39]. This process seems to be governed by microenvironmental cues, resembling the lifelong quiescence program active in dormant adult stem

[1]Université de Lyon, Lyon, France. [2]CNRS UMR5286, Centre de Recherche en Cancérologie de Lyon, Lyon, France. [3]Inserm U1052, Centre de Recherche en Cancérologie de Lyon, Lyon, France. [4]Division of Hematology and Oncology, Department of Medicine, Department of Otolaryngology, Department of Oncological Sciences, Black Family Stem Cell Institute, Tisch Cancer Institute, Icahn School of Medicine at Mount Sinai, New York, NY, USA. [5]Abel Salazar Biomedical Sciences Institute, University of Porto, Porto, Portugal. [6]These authors contributed equally: Emma Risson, Ana Rita Nobre. ✉e-mail: julio.aguirre-ghiso@mssm.edu

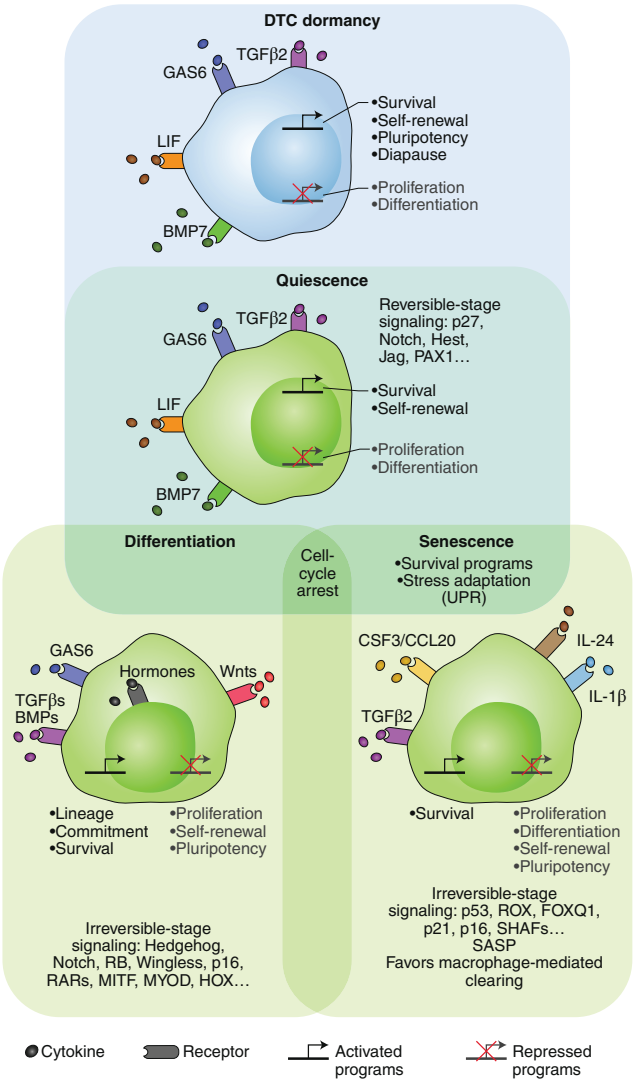

Fig. 1 | Differences and commonalities among normal quiescent, senescent, differentiated cells and dormant cancer cells. Cell-cycle arrest and survival programs are shared across all programs. Although differentiation and senescence are typically irreversible or highly stable stages, quiescence and dormancy are reversible. It would appear that normal quiescent cells and dormant cancer cells interpret the same microenvironmental factors in a similar manner, and this leads to the activation of survival and self-renewal programs. However, dormant DTCs also turn on diapause and pluripotency programs and an unfolded protein response (UPR) also observed in senescent cells. Normal quiescent, senescent and differentiated cells are green;[44] the dormant cancer cell is blue[26]. SASP, senescence-associated secretory phenotype.

cells, including hematopoietic, muscle, neural and hair-follicle stem cells[17,26,37,38,40,41] (Fig. 1). However, mechanisms of senescence or differentiation have also been proposed to underlie DTC dormancy[18,42,43]. A confounding factor is that growth-arrest programs during quiescence, senescence and differentiation exhibit substantial overlap in their regulation of the cell-cycle machinery (Fig. 1). Nevertheless, senescence is by definition irreversible, and regulators of this program, such as p16 and p53, are commonly mutated or silenced early in tumorigenesis[44]. Additionally, senescence leads to the clearing of senescent cells by innate immune cells[45], which has so far not been documented for potentially 'senescent' DTCs. Notably, several studies have documented that DTCs activate variations of pluripotency programs and a certain degree of chromatin remodeling linked to enhanced epigenetic plasticity[46–51] (discussed below). On the contrary, senescent cells commonly show highly repressive heterochromatin, which limits plasticity[52] (Fig. 1). However, the possibility that a hybrid state of senescence programs is activated by microenvironmental cues[43] or therapeutic stress[53] cannot be ruled out.

Indeed, a key attribute of dormant DTCs is their ability to retain a high degree of epigenetic and transcriptional plasticity and to reactivate different developmental programs to arrest growth and survive[17,54] (discussed below). This high level of plasticity that enables cancer cells to employ various regulatory programs to induce a reversible growth arrest, which ensures persistence and confers an adaptive advantage, may be the true defining feature of dormancy. Thus, two key elements emerge as being necessary for better understanding of DTC dormancy. One is better definition of the identified programs functionally and molecularly, to understand how they resemble quiescence, senescence or differentiation and how they intersect with angiogenic dormancy and immune-mediated equilibrium. The second is definition of which of the programs identified in models are functionally relevant in patients.

Target-organ microenvironments

The tumor microenvironment consists of cellular and extracellular components that surround cancer cells. In the primary tumor site it can represent half or more of the tumor mass. However, in target organs in which solitary DTCs or small clusters of DTCs reside following dissemination, DTCs are initially a minor constituent of the tissue. Thus, how they interpret this new microenvironment and how the signals 'encoded' in these initially normal tissue niches affect the induction of, maintenance of and escape from dormancy in cancer are important questions.

BM niches. Animal and human biopsy studies support the notion that DTCs probably reach multiple organs but survive and eventually grow only in specific tissues and in a cancer-specific manner. Many studies have focused on the BM, as cancer cells can persist in this site for years without growing, and the detection of BM DTCs is commonly a marker of poor prognosis[55–58]. In the BM, osteoblasts have been suggested to induce solid-tumor DTC dormancy[59], with osteoclasts being involved in the escape from dormancy during the process of osteolytic bone metastases[60] (Fig. 2). The role of osteoblasts in dormancy and bone metastasis, however, is more complex. Whereas the endosteal niche and osteoblasts can promote cancer-cell dormancy[59], remodeling of this niche could cause the reactivation of or promote the survival of cancer cells[61]. For example, cancer cells depend on physical interactions with osteogenic cells through gap junctions to increase their intracellular calcium levels, and therefore the osteogenic niche, which includes osteoblasts, serves as a calcium reservoir for cancer cells to form micro-metastases[62]. Additionally, changes in osteoblast phenotype, such as the acquisition of an aged or senescent phenotype, could fuel metastasis[63]. Recently, considerable work has focused on vascular niches that induce sustained DTC dormancy in the BM[23,31], brain[35] and lungs[34] (Fig. 2). BM vascular niches were shown to protect DTCs from chemotherapy through an integrin-mediated interaction between DTCs and molecules, including von Willebrand factor and the integrin ligand VCAM1, within the perivascular niches[23]. Disrupting these interactions with integrin-blocking antibodies results in a reduction in the DTC burden and the prevention of bone metastasis. Notably, although chemoprotection by the vascular niche seems to be cell cycle independent, inhibiting integrin β_1 and/or integrin $\alpha_V\beta_3$ enhanced the chemotherapeutic response. How chemotherapy kills non-dividing DTCs with ablated integrin signaling is still unknown. Perhaps cancer cells become sensitized during the first divisions after their

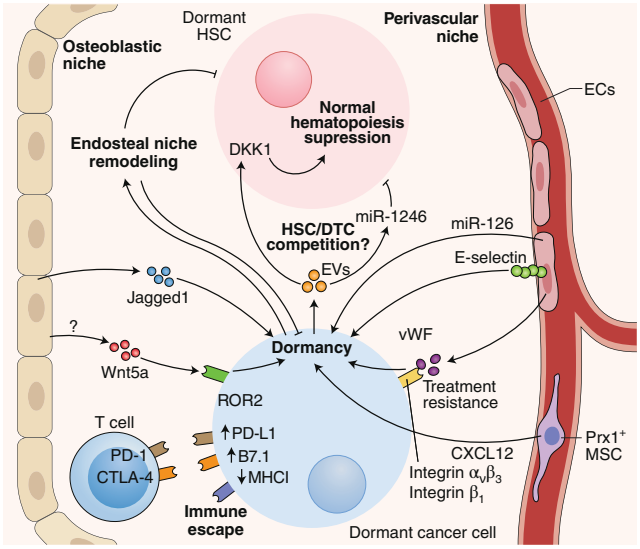

Fig. 2 | The various BM niches, cell types and cues that regulate the dormancy of DTCs and HSCs. Both the osteoblastic niche and the perivascular niche in the BM are involved in DTC dormancy by producing a wide range of cues (cytokines, microRNA, extracellular vesicles, cell–cell contact signaling, etc.) that drive dormancy. Additionally, dormant cancer cells downregulate antigen presentation and upregulate immunosuppressive ligands in order to evade recognition by the immune system. Over time and reciprocally, cancer cells also remodel their surrounding microenvironment and hypothetically feed a proliferative positive loop. EVs, extracellular vesicles; ECs, endothelial cells; PD-1, receptor for PD-L1; MHCI, MHC class I; vWF, von Willebrand factor; MSC, mesenchymal stem cell.

exit from the single-cell state. In the mouse brain, DTCs breach the blood–brain barrier and adhere to brain capillaries[35]. The position and morphology of DTCs is reminiscent of that of pericytes, as these cells spread on brain capillaries between pericytes and capillary surfaces, migrated along the vessels and remained dormant for long periods[34]. Although the mechanism of dormancy was not explored in that study[34], the adhesion molecule L1CAM on DTCs was found to mediate access to the perivascular niche and drive transcriptional programs that awakened dormant DTCs, which led to the initiation of metastasis. Whether the reactivation of DTCs was caused by their pericyte-like behavior or changes in the niche itself is unclear. However, changes in the niche, as elicited by tip endothelial cells, are known to cause reactivation, whereas stalk endothelial cells promote dormancy[64]. Similarly, endothelial-cell expression of L1CAM ligands allows L1CAM$^+$ DTCs to engage in proliferative programs, but it is possible that if the endothelium or other perivascular cells do not express such ligands, L1CAM$^+$ DTCs may not be able to overcome dormancy signals. Therefore, the perivascular niche could induce or maintain DTC dormancy in a context-dependent manner.

Elegant conditional, tissue-specific knockout mouse models and bone-transplantation approaches revealed that perivascular Prx1$^+$ mesenchymal stem cells expressing the chemokine CXCL12 maintained leukemic stem cells (LSCs) in a quiescent and treatment-resistant state in the BM[65]. Targeted deletion of CXCL12 in mesenchymal stem cells reduced the number of normal hematopoietic stem cell (HSCs) but promoted LSC expansion by increasing self-renewing cell divisions, with LSCs being eliminated by treatment with a tyrosine kinase inhibitor. Moreover, chronic myeloid leukemia (CML) cells induced a reduction in CXCL12-expressing mesenchymal stem cells and an increase in CXCL12-expressing endothelial cells, alterations that may provide a competitive advantage to LSCs over HSCs (Fig. 3). This work highlights how the perivascular niche may allow targeting of DTC–niche interactions in solid and hematopoietic cancer-cell dormancy to interfere with dormant DTCs that cause recurrence.

Open questions are whether DTCs move stochastically or are actively recruited into a perivascular niche, where they enter dormancy, or whether these are simply the niches that promote survival and quiescence. A recent study[66] showed that similar to benign and malignant hematopoietic cells[67], breast cancer DTCs enter the BM through sinusoidal vasculature that expresses the inflammatory molecules E-selectin and SDF-1, both in mice and in human samples[66] (Fig. 3). Mice treated with an E-selectin inhibitor had fewer DTCs in the BM, indicative of decreased homing. In another model, E-selectin was identified as a pro-metastatic receptor of the bone vascular niche, with its pharmacological inhibition increasing survival and decreasing bone metastasis–associated bone degradation[68]. Thus, rather than suggesting homing, this study suggested a growth-promoting effect for E-selectin that was dependent on the Wnt signaling pathway and was bone specific. The differences between the specific findings of these two studies[66,68] are unclear but may depend on differences in the models of BM colonization used and in the timing and type of endpoints assessed.

BM colonization and metastasis are common late relapse occurrences in ER$^+$ breast cancer regulated by hormones (and thus the microenvironment). A recent study identified the kinase MSK1 as a potential regulator of dormancy in ER$^+$ breast cancer[69]. Depletion of MSK1 was shown to lead to the epigenetic downregulation of genes encoding molecules that control luminal cell fate, such as FOXA1 and GATA3, and contribute to an increased metastasis-initiating potential. This effect was also observed when signaling via the kinase p38 was chemically inhibited, as MSK1 is a target of p38;[69] this reproduced the role of this pathway in dormancy[14]. Anti-estrogen therapy is an effective therapy in human breast cancer[70,71] but does not eradicate the disease in many patients[71]. Whether tamoxifen activates an MSK1–p38α (or other) signaling mechanism for dormancy is not clear, but understanding whether anti-estrogen therapies work through the induction of dormancy may be illuminating. Interestingly, dormant cell populations were recently shown to be prevalent during targeting of the estrogen receptor ERα[71]. A similar question was explored in humans[72] through the sequential analysis of samples from patients undergoing extended neoadjuvant hormonal treatment. 'Dormant' tumors (i.e., tumors from patients with tumor-size reduction and no progression after long post-treatment periods of time) displayed enhanced DNA methylation and a more repressive chromatin state, whereas resistant tumors displayed the opposite profile. Although these data were not directly derived from DTCs, they may provide insights into the biomarkers to look for in DTCs or stroma in the adjuvant setting and to determine if anti-estrogens induce dormancy of residual DTCs. The BM is also a common site for dormancy for prostate cancer cells[73]. Wnt5a delivered systemically in in a prostate cancer model of metastasis induced a dormancy-like phenotype in cancer cells and a reduction in bone metastasis, potentially via ROR2 signaling[72]. This treatment also revealed that Wnt5a favored chemoresistance to docetaxel. Additional analyses may be needed to reveal whether these mechanisms are active in prostate cancer DTCs in the BM. Interestingly, Wnt5a has also been linked to a senescence- or dormancy-like phenotype in melanoma[74].

Inflammation and extracellular matrix remodeling. Given that dormancy is a reversible state regulated by the microenvironment, it is necessary to determine the microenvironmental changes that could trigger awakening from dormancy (Fig. 2). Bacterial lipopolysaccharide– or tobacco smoke–induced lung inflammation was recently shown to activate neutrophils to form neutrophil extracellular

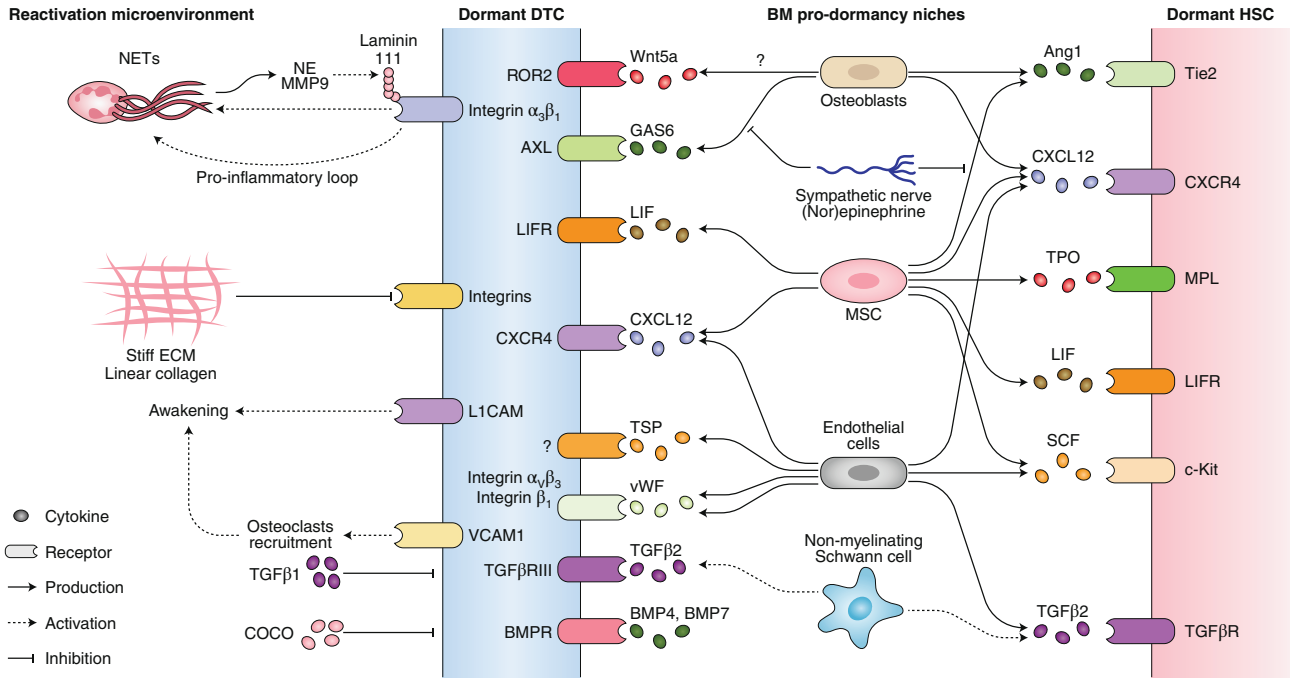

Fig. 3 | Cues, receptors and cell types involved in DTC reactivation and pro-dormancy niches. In the BM, a pro-dormancy niche involves the action of several factors (such as LIF, TGFβ2, GAS6, BMPs; additional details, Table 1) that leads to the induction of quiescence in both DTCs and HSCs. In contrast, reactivation niches in the lung and liver awaken dormant DTCs in a manner that involves formation of NETs, extracellular matrix stiffness, TGFβ1 and inhibitors of BMP molecules. NE, neutrophil elastase.

DNA traps (NETs)[32]. NETs were found to trigger the awakening of dormant DTCs through the release of neutrophil elastase and MMP9, enzymes that promote the laminin 111– and $\alpha_3\beta_1$ integrin–dependent activation of a signaling axis involving the kinases FAK, ERK and MLCK and, ultimately, activation of the transcriptional regulator YAP. Interestingly, for full awakening of DTCs, loss of perivascular thrombospondin TSP1 was also required. Metastatic breast cancer cells can themselves induce NETs[32,75], which raises the possibility that they may create a positive pro-inflammatory proliferative loop. Surgical stress was also shown to trigger DTC awakening through an increase in NET formation, in a mouse model of liver ischemia–reperfusion[76]. Consistent with that, in a cohort of patients undergoing attempted curative liver resection for metastatic colorectal cancer, a correlation was observed between increased post-operative NET formation and a reduction in disease-free survival[76]. In a model of pancreatic ductual adenocarcinoma (PDAC), the TRAIL-R2 pathway was also suggested to lead to liver inflammation and the awakening of dormant DTCs during tumor resection[77]. Thus, it is possible that tissues that remain homeostatic may maintain DTC dormancy, whereas changes (such as inflammation) that alter the homeostatic balance (for example, through NETs and remodeling of the extracellular matrix) may trigger the awakening of DTCs from dormancy.

An important question is the link between aging and metastatic relapse and the age- and microenvironment-related signals that may regulate DTC dormancy and reactivation. Recently, in a mouse model of aging, metastatic cell lines were shown to be highly proliferative in aged BM, with the frequency of dormant DTCs decreasing in aged mice but not in young mice[78]. Mechanistic analysis revealed that several inflammatory cytokines known to promote cell proliferation (including the interleukins IL-1β, IL-6, IL-27 and IL-1F9 and factors such as CCL4, CCL5 and Tnfsf14) were upregulated in bones of aged mice, whereas proposed quiescence-inducing factors (including BMP4, BMP6, BMP7, Kitl, TGFβ2, Thbs2, Dkk1 and Dkk3) were downregulated[78] (Table 1). Remodeling of the extracellular matrix may also stimulate metastasis and perhaps awakening from dormancy, as revealed by changes in age-related remodeling of the collagen matrix that stimulated metastasis in melanoma[79–81].

The concept of reverting a malignant phenotype by normalizing the microenvironment is not new[82–85] and supports the proposal that — in the appropriate context — cancer cells could remodel their epigenetic programs to silence mutated genomes. Axolotl embryos have been shown to fully reprogram malignant breast cancer cells into quiescence by inhibiting induction of the cell-cycle inhibitor p27 mediated by the kinases ERK1 and ERK2 and reducing signaling dependent on the transcription factor JUN and the tumor suppressor Rb[86]. These reprogrammed breast cancer cells also displayed a repressive chromatin state that was previously reported in retinoic acid–induced dormancy[46]. Although the mechanisms activated by the axolotl extract were not identified, this reveals how microenvironmental signals can epigenetically silence malignancy traits.

Such studies have expanded understanding of how the homeostasis of target-organ microenvironments may maintain dormancy, probably governed by adult stem-cell quiescence niches. They also support the proposal that alterations over time (in this case the organism's age) or perturbations that alter target-organ microenvironments, such as inflammation and remodeling of the extracellular matrix, can control dormancy. A key question is how robust the dormancy-inducing microenvironments are. Given that, for example, in breast cancer, relapse that occurs more than 5 years after surgery is mostly stochastic and can be delayed for long periods, it is possible that multiple homeostatic barriers need to be eliminated for DTCs to awaken. Although patients will encounter situations that may activate inflammatory processes many times during their lives, many do not show immediate relapse.

Table 1 | Summary of dormancy- and reactivation-inducing factors

	Factor	In vitro data	In vivo data	Human data	Refs.
Dormancy inducers	CXCL12	Y	Y	Y	65
	vWF	Y	Y	N	23
	TGFβ2	Y	Y	N	36
	BMP4, BMP7	Y	Y	N	43,48
	Hypoxia	Y	Y	Y	33
	GAS6	Y	Y	N	115,116
	RA	Y	Y	N	46
	LIF	Y	Y	N	97
	TSP1	Y	Y	N	31
	WNTs	Y	Y	N	27,117
	DNA methylation repressive chromatin state	Y	Y	Y	46,72
	Wnt5a	Y	Y	N	72
	Axolotl embryo	Y	N	N	86
	miR-126	Y	Y	Y	104
	Jagged 1	Y	Y	N	118
Reactivation inducers	COCO	Y	Y	Y	48
	Inflammation and NETs	Y	Y	Y	32,75,76
	Stiff collagen	Y	Y	N	79
	Aging	Y	Y	Y	78,79,119
	VCAM1	Y	Y	N	60
	Periostin	Y	Y	N	31
	TGFβ1	Y	Y	N	36

Known cancer cell– and microenvironment-derived regulators that promote the dormancy or reactivation of dormant cancer cells in solid and liquid cancers. The type of data available for each factor is also indicated. These findings are compiled from different cancer types and thus these signaling pathways might not all be associated with the dormancy of every type of cancer or microenvironment. Y, yes; N, no.

Autophagy and metabolism. Another important but poorly explored mechanism in dormancy biology is metabolic plasticity. For example, unfolded-protein-response pathways and signaling via the transcription factor HIF1α, which are intimately linked to metabolic changes, can enable residual cancer cells to persist and evade chemotherapy[87]. Recently, the glycerol biosynthesis enzyme GPD1 (glycerol-3-phosphate dehydrogenase 1) was shown to mark slow-cycling brain tumor stem cells with the ability to repopulate the tumor after temozolomide therapy in glioblastoma mouse models[88]. These GPD1$^+$ cells were present in tumor margins, which suggested that they might escape resection and therapy. However, whereas GPD1$^+$ cells were mostly negative for proliferation markers, they were the cells able to repopulate the lesions after therapy. This suggests that GPD1 is involved in the metabolic plasticity of slowly cycling cells that mediates reactivation but does not regulate long-term dormancy.

Autophagy is intimately linked to stress signaling and metabolic changes, as it is not only a source of metabolites for energy production but also a way to protect from proteotoxicity. Dormant cancer cells were shown to be more autophagic than their proliferating counterparts, which allowed them to survive in a quiescent state[89]. Notably, inhibiting autophagy specifically blocked the survival of dormant cells in the lungs in a manner dependent on the autophagy-related molecule ATG7[89]. A separate study recently showed that the enzyme Pfkfb3 (6-phosphofructo-2-kinase/fructose-2,6-biphosphatase 3) is linked to metastatic relapse of breast cancer[90]. Interestingly, Pfkfb3 was downregulated by the onset of autophagy, which coincided with dormancy induction. Unlike an earlier study[89], but consistent with other work reporting that autophagy may induce dormancy[18,91], this paper[90] showed that inhibition of autophagy restored PFKFB3 expression, which led to reactivation from dormancy. When autophagy functions only as a survival pathway and when it coordinates induction and maintenance of dormancy remains unclear. Elucidating this point is important because the second possibility supports the proposal that targeting autophagy could have deleterious effects for patients by causing reactivation from dormancy.

The immune system and DTC dormancy. Major advances in immuno-oncology have fundamentally altered the understanding of the relationship between the adaptive immune system and cancer cells, which has led to the current breakthroughs in immunotherapies. A key question is whether dormant DTCs are restrained from expanding by an immune equilibrium mechanism and/or whether dormant DTCs evade recognition by the immune system (Fig. 2). Pioneering studies of carcinogenesis and disseminated cancer have provided support for the possibility of a role for immune equilibrium as a mechanism of dormancy[13,92]. Similarly, studies of a B cell lymphoma that establishes dormancy through a vaccination protocol revealed important components of how dormancy could be induced and maintained by CD8$^+$ T cells and interferon-γ signaling[6]. Additionally, immunoevasion was shown to allow the persistence of dormant leukemic cells in mouse acute myeloid leukemia (AML) through upregulation of the checkpoint inhibitor B7-H1 (PD-L1) and the immunomodulatory receptor CTLA-4 ligand B7.1, but without involving a decrease in major histocompatibility complex (MHC) class I (ref. [93]). More recently, it was shown that mice vaccinated against PDAC cells were protected against rechallenge with the same PDAC cells injected to colonize the mouse livers, as expected[30]. However, although the immune system eradicated most cancer cells, persistent single DTCs were detected. The immunoevasive DTCs were quiescent, did not express E-cadherin and upregulated the unfolded protein response, a pathway previously linked also to the drug resistance of dormant cancer cells[22]. The unfolded protein response was found to downregulate MHC class I, which reduced antigen presentation and rendered dormant DTCs invisible to CD8$^+$ T cells. Although the molecular mechanisms differ, both leukemic cells and epithelial cancer cells that enter dormancy seem to find ways to escape detection by the immune system. As proposed earlier, immunoevasion by dormant DTCs may simply be reflective of the hijacking of developmental or tissue homeostasis mechanisms. For example, quiescent hair-follicle stem cells were shown to evade immune recognition by CD8$^+$ T cells[94]. It would be interesting to test whether the signals that induce dormancy discussed in this Perspective (Table 1) modulate the expression of key immunoregulatory molecules such as MHC class I, PD-L1 and/or CTLA-4 and thereby influence immunodetection. Dormant lung cancer DTCs and HER2$^+$ breast cancer DTCs were also shown to evade detection by NK cells and to be susceptible to eradication by NK cells only after escape from dormancy[27]. Although these studies support the proposal that DTCs are NK cell evasive during quiescence, they provide only partial insight into their immunoregulation, as they were performed in nude mice. Unlike the results reported in those papers, the immune system of mice carrying the EMT6 syngeneic triple-negative breast cancer model was shown to be able to fully eradicate dormant and proliferative DTCs, suggestive of their vulnerability to immunorecognition[95]. In contrast, a separate study in immunocompetent mice showed that D2A1 breast cancer cells were kept from forming metastases by immune-mediated killing, which led to an equilibrium that produced population dormancy[96]. However, when mice underwent sham surgery, the injury-associated

inflammation and myeloid-cell mobilization led to immunosuppression, with the cancer-cell population progressing to metastasis. Studies in which no exogenous antigens were used[95] may be relevant to understanding how patients with triple-negative breast cancer who survive beyond 5–8 years after surgery never relapse with metastasis. It would also be interesting to determine whether primary tumor removal, as is done routinely in patients, would yield the same results as sham surgery in mice[96]. Studies such as these, which formally investigated DTC biology and recognition by the immune system, raise new questions related to DTC dormancy and immunotherapies.

Commonalities of leukemia and DTC dormancy

The HSC and leukemia fields have made considerable advances in delineating how specific niches control the dormancy of HSCs and LSCs. At steady state, the BM niche is a tightly controlled microenvironment that regulates the proliferation, self-renewal, differentiation and migration of HSCs[37]. HSCs and DTCs in the BM seem to be cell-cycle arrested. Moreover, these two types of cells have been proposed to occupy the same BM niches and to respond to the microenvironmental cues similarly[17,73] (Fig. 3). Both dormant HSCs and DTCs seem to adopt quiescence and survival mechanisms that enable them to avoid apoptosis and/or resist therapies. However, dormant solid-cancer cells share characteristics with embryonic and adult stem cells, such as upregulation of the pluripotency-related genes *NR2F1*, *SOX9*, *SOX2*, *POU5F1* (which encodes OCT4) and *NANOG*[17,27,46,48,97]. This may be a distinction between the quiescence programs in HSCs and those in DTCs, whereby the latter cells may adopt developmental programs that provide additional cell plasticity and less ability to commit to differentiation states. However, other similarities are clear. For example, adult stem-cell niches have also been shown to be immune-protected sites[94], which may be advantageous for DTCs. Adult stem cells and quiescent DTCs may also show downregulation of antigen presentation[30,94], in support of the proposal that escaping immunosurveillance may also be a common attribute. Another example involves the ubiquitin ligase FBXW7, inhibition of which was shown to prevent the quiescence of LSCs[98] and to be involved in the quiescence of lung adenocarcinoma cells[99] and the awakening and subsequent chemotherapy-mediated killing of breast cancer DTCs[100]. These data suggest that some quiescence and/or dormancy mechanisms may be shared by LSCs and DTCs and thus provide novel potential anti-cancer targets for experimental exploration. Notably, the notion of awakening LSCs might work in some cases, given the unique oncogene addiction pathways of these cells[65], but in solid cancers, awakening dormant cells may be too risky, given that chemotherapy is not uniformly effective and responses may vary depending on the organ in which metastases grow.

Hematopoietic malignancies may also inform cancer-cell heterogeneity during dormancy. Longitudinal BM sampling from patients to delineate clonal evolution from pre-leukemia to established AML has revealed that some rare, probably dormant, leukemic cell sub-clones were already present at diagnosis and were resistant to therapy, which led to relapse; this highlights the importance of understanding the dynamics of LSC heterogeneity[101]. Similar studies of solid-cancer DTCs, such as DTCs of melanoma, breast cancer and prostate cancer in patients at the M0 stage (no evidence of metastasis at diagnosis or surgery), were able to identify dormant DTCs that could be studied and targeted early on. A single-cell transcriptomic analysis of BM leukemic cells revealed that a specific sub-fraction among the heterogeneous population of LSCs, characterized by stem-cell and quiescence signatures, survived in the BM environment of patients with asymptomatic CML under treatment with a tyrosine kinase inhibitor and served as a reservoir for the emergence of resistant cells[102]. Treatment-induced quiescence of residual LSCs in this setting was demonstrated to rely on the activation of Jak2–Stat3 signaling dependent on non-canonical BMP4 signaling, with the ligand delivered by surrounding mesenchymal cells[103]. Dual targeting of BMP4 and Jak2 was efficient in reversing this tyrosine kinase inhibitor–dependent induced quiescence of the $BMPR1B^{+}$ LSC sub-fraction adherent to stroma and allowed these cells to re-enter a differentiation process[103]. Such a strategy might contribute to elimination of the reservoir of dormant LSCs.

Another study of treatment-induced quiescence in CML showed that the microRNA miR-126 from endothelial or leukemic cells induced the quiescence of CML LSCs[104]. Interestingly, the tyrosine kinase BCR–ABL is known to inhibit the biogenesis of miR-126, and inhibition of BCR-ABL restored miR-126 expression in the cancer cells, which led to a quiescent LSC pool with enhanced survival. Moreover, combining inhibition of BCR-ABL and downregulation of miR-126 resulted in the elimination of LSCs, in support of the proposal that this microRNA may also coordinate survival during quiescence. Assessing if dormant DTCs from solid cancers are regulated by similar mechanisms when targeted therapies are used (for example, anti-estrogens, anti-androgen receptor, anti-HER2 or other kinases) could reveal novel cancer cell–intrinsic and/or microenvironmentally induced mechanisms of DTC quiescence and survival triggered by therapeutic interventions.

There is growing evidence not only that the niche influences cancer cells but also that leukemic cells can modulate their host BM microenvironment to survive and expand. For example, AML cells can remodel the vascular organization of the endosteal niche and thereby alter the number of stromal cells[105] and render the niche less supportive of normal HSCs and their quiescence. Additionally, vascular permeability can be altered through the enhanced production of nitric oxide by endothelial cells[106]. Additional studies have highlighted the role of AML-derived extracellular vesicles in suppressing normal hematopoiesis by inhibiting protein synthesis[107] through the internalization of miR-1246 in normal HSCs or by inducing the expression of DKK1, a suppressor of normal hematopoiesis[108]. In both studies, inhibiting this niche remodeling led to enhanced efficiency of chemotherapy[107,108]. These models may provide insight into how solid-cancer DTCs may change the niches in which they reside over time until they switch from a homeostatic pro-dormancy function to a reactivation state. Given that the molecules derived from these niches may be more abundant than the DTCs that lodged there, these soluble factors could serve as biomarkers that provide information on niches supportive of reactivation.

Future prospects

The treatment of metastasis has been limited to very few adjuvant therapies that rely on primary tumor data and aggressive targeting of metastatic lesions in patients at stage IV. The latter is a necessity, as these patients have few treatment options. However, the knowledge of tumor dormancy has revealed that MRD in solid cancers could be targeted earlier, even if DTCs are not actively proliferating[109]. Additionally, the notion that dormant DTCs co-exist with growing lesions in stage IV cancer has raised the possibility that these dormant DTCs may evade anti-proliferative treatments. Thus, strategies that combine anti-proliferative therapies with drugs that kill dormant cells may provide long-term benefit even in patients at stage IV.

However, the concepts noted above need to be tested in practice. Acceleration of the understanding of the processes that underlie cancer-cell dormancy and, consequently, ways to target it will require pairing of experimental models with human data, such as by having research scientists team up with clinicians to incorporate the measurement of endpoints related to dormancy in existing clinical trials. Such efforts are emerging; for example, NR2F1, a dormancy marker identified in experimental systems, has been used to stratify DTCs and to determine that patients with $NR2F1^{hi}$ DTCs had longer bone metastasis–free periods than those with $NR2F1^{lo}$ DTCs[57].

Notably, a proliferation marker such as Ki67 could not provide the same information, which supports the proposal that dormancy markers may provide additional insights beyond those provided by determining the snapshot proliferative status of DTCs. Such efforts, even if initiated in small populations of patients, would be key for the validation of experimental biology in patients.

The notion that dormant cancer cells activate autophagy[18,89,90,110] has also led to a phase 2 clinical trial using autophagy inhibitors such as hydroxychloroquine and/or mTOR inhibitors in combination to treat patients with breast cancer and to prevent recurrence (clinical trial identifier NCT03032406). An additional clinical trial is focused on screening for the presence of BM DTCs in patients within 5 years of having completed breast cancer therapy (clinical trial identifier NCT02732171). Patients with BM DTCs will be offered the possibility of participating in other trials targeting DTCs, such as NCT03032406.

The concept of reprogramming malignant DTCs into dormancy[46] has also led to a clinical trial testing this concept in disseminated prostate cancer that has not yet become detectable by imaging (clinical trial identifier NCT03572387). This clinical trial repurposed 5-azacytidine and all-*trans* retinoic acid (both drugs approved by the US Food and Drug Administration) to treat patients with prostate cancer after hormonal ablation. Although these studies are ongoing, they support the notion that foundational science can be used to develop innovative trials that can be executed despite potential cost issues[24]. Understanding how dormancy develops in patients may also help guide trials that were supposed to target micro-metastatic disease but failed to show therapeutic value. Preclinical data have identified RANKL (TNFSF11) as a tempting target with strong potential to prevent breast cancer bone metastasis[111,112]. A phase 3 study (D-CARE) was developed that combined a human blocking monoclonal antibody against the receptor for RANKL (denosumab) with standard-of-care adjuvant or neoadjuvant systemic therapy and locoregional treatments. However, this treatment did not improve disease-related outcomes for women with high-risk early breast cancer[113]. The reasons for this outcome may include the possibility that dosing schedules left a window for dormant DTC populations to become reactivated. There is also evidence from other studies that chemotherapy causes severe alterations of the BM microenvironment[114] with clear signs of premature aging that could actually promote the reactivation of dormant DTCs. Unfortunately, the trial did not include intermediate endpoints for assessing the numbers or phenotypes of DTCs or circulating tumor cells and thus for anticipating what might have been happening to the residual disease. The development of markers and methods for detecting the DTCs that lead to MRD in such trials will enhance the understanding of how to target these residual cells on the basis of their unique biology.

Progress in on cancer dormancy research has expanded considerably and will probably yield innovative biomedical results in the future. The findings discussed in this Perspective highlight the fact that the time is ripe to start translating the knowledge gained from experimental models to the clinic.

Received: 15 November 2019; Accepted: 28 May 2020;
Published online: 06 July 2020

References

1. Almog, N. et al. Prolonged dormancy of human liposarcoma is associated with impaired tumor angiogenesis. *FASEB J.* **20**, 947–949 (2006).
2. Folkman, J. Role of angiogenesis in tumor growth and metastasis. *Semin. Oncol.* **29**, 15–18 (2002).
3. Holmgren, L., O'Reilly, M. S. & Folkman, J. Dormancy of micrometastases: balanced proliferation and apoptosis in the presence of angiogenesis suppression. *Nat. Med.* **1**, 149–153 (1995).
4. Uhr, J. W. & Marches, R. Dormancy in a model of murine B cell lymphoma. *Semin. Cancer Biol.* **11**, 277–283 (2001).
5. Marches, R., Hsueh, R. & Uhr, J. W. Cancer dormancy and cell signaling: induction of $p21^{waf1}$ initiated by membrane IgM engagement increases survival of B lymphoma cells. *Proc. Natl Acad. Sci. USA* **96**, 8711–8715 (1999).
6. Farrar, J. D. et al. Cancer dormancy. VII. A regulatory role for $CD8^+$ T cells and IFN-γ in establishing and maintaining the tumor-dormant state. *J. Immunol.* **162**, 2842–2849 (1999).
7. Marches, R., Scheuermann, R. H. & Uhr, J. W. Cancer dormancy: role of cyclin-dependent kinase inhibitors in induction of cell cycle arrest mediated via membrane IgM. *Cancer Res.* **58**, 691–697 (1998).
8. Vitetta, E. S. et al. Tumor dormancy and cell signaling. V. Regrowth of the BCL1 tumor after dormancy is established. *Blood* **89**, 4425–4436 (1997).
9. Uhr, J. W. et al. Role of antibody signaling in inducing tumor dormancy. *Adv. Exp. Med. Biol.* **406**, 69–74 (1996).
10. Racila, E. et al. Tumor dormancy and cell signaling: anti-mu-induced apoptosis in human B-lymphoma cells is not caused by an APO-1-APO-1 ligand interaction. *Proc. Natl Acad. Sci. USA* **93**, 2165–2168 (1996).
11. Racila, E. et al. Tumor dormancy and cell signaling. II. Antibody as an agonist in inducing dormancy of a B cell lymphoma in SCID mice. *J. Exp. Med.* **181**, 1539–1550 (1995).
12. Marches, R. et al. Tumour dormancy and cell signalling-III: Role of hypercrosslinking of IgM and CD40 on the induction of cell cycle arrest and apoptosis in B lymphoma cells. *Ther. Immunol.* **2**, 125–136 (1995).
13. Koebel, C. M. et al. Adaptive immunity maintains occult cancer in an equilibrium state. *Nature* **450**, 903–907 (2007).
14. Aguirre-Ghiso, J. A., Liu, D., Mignatti, A., Kovalski, K. & Ossowski, L. Urokinase receptor and fibronectin regulate the ERK^{MAPK} to $p38^{MAPK}$ activity ratios that determine carcinoma cell proliferation or dormancy in vivo. *Mol. Biol. Cell* **12**, 863–879 (2001).
15. Aguirre Ghiso, J. A., Kovalski, K. & Ossowski, L. Tumor dormancy induced by downregulation of urokinase receptor in human carcinoma involves integrin and MAPK signaling. *J. Cell Biol.* **147**, 89–104 (1999).
16. Naumov, G. N. et al. Ineffectiveness of doxorubicin treatment on solitary dormant mammary carcinoma cells or late-developing metastases. *Breast Cancer Res. Treat.* **82**, 199–206 (2003).
17. Aguirre-Ghiso, J. A. & Sosa, M. S. Emerging topics on disseminated cancer cell dormancy and the paradigm of metastasis. *Ann. Rev. Cancer Biol.* **2**, 377–393 (2018).
18. Sosa, M. S., Bragado, P. & Aguirre-Ghiso, J. A. Mechanisms of disseminated cancer cell dormancy: an awakening field. *Nat. Rev. Cancer* **14**, 611–622 (2014).
19. Giancotti, F. G. Mechanisms governing metastatic dormancy and reactivation. *Cell* **155**, 750–764 (2013).
20. Schewe, D. M. & Aguirre-Ghiso, J. A. ATF6α-Rheb-mTOR signaling promotes survival of dormant tumor cells in vivo. *Proc. Natl Acad. Sci. USA* **105**, 10519–10524 (2008).
21. Ranganathan, A. C., Ojha, S., Kourtidis, A., Conklin, D. S. & Aguirre-Ghiso, J. A. Dual function of pancreatic endoplasmic reticulum kinase in tumor cell growth arrest and survival. *Cancer Res.* **68**, 3260–3268 (2008).
22. Ranganathan, A. C., Zhang, L., Adam, A. P. & Aguirre-Ghiso, J. A. Functional coupling of p38-induced up-regulation of BiP and activation of RNA-dependent protein kinase-like endoplasmic reticulum kinase to drug resistance of dormant carcinoma cells. *Cancer Res.* **66**, 1702–1711 (2006).
23. Carlson, P. et al. Targeting the perivascular niche sensitizes disseminated tumour cells to chemotherapy. *Nat. Cell Biol.* **21**, 238–250 (2019).
24. Ghajar, C. M. Metastasis prevention by targeting the dormant niche. *Nat. Rev. Cancer* **15**, 238–247 (2015).
25. Aguirre-Ghiso, J. A. How dormant cancer persists and reawakens. *Science* **361**, 1314–1315 (2018).
26. Aguirre-Ghiso, J. A. Models, mechanisms and clinical evidence for cancer dormancy. *Nat. Rev. Cancer* **7**, 834–846 (2007).
27. Malladi, S. et al. Metastatic latency and immune evasion through autocrine inhibition of WNT. *Cell* **165**, 45–60 (2016).
28. Aguirre-Ghiso, J. A. The problem of cancer dormancy: understanding the basic mechanisms and identifying therapeutic opportunities. *Cell Cycle* **5**, 1740–1743 (2006).
29. Linde, N., Fluegen, G. & Aguirre-Ghiso, J. A. The relationship between dormant cancer cells and their microenvironment. *Adv. Cancer Res.* **132**, 45–71 (2016).
30. Pommier, A. et al. Unresolved endoplasmic reticulum stress engenders immune-resistant, latent pancreatic cancer metastases. *Science* **360**, eaao4908 (2018).
31. Ghajar, C. M. et al. The perivascular niche regulates breast tumour dormancy. *Nat. Cell Biol.* **15**, 807–817 (2013).
32. Albrengues, J. et al. Neutrophil extracellular traps produced during inflammation awaken dormant cancer cells in mice. *Science* **361**, eaao4227 (2018).

33. Fluegen, G. et al. Phenotypic heterogeneity of disseminated tumour cells is preset by primary tumour hypoxic microenvironments. *Nat. Cell Biol.* **19**, 120–132 (2017).
34. Er, E. E. et al. Pericyte-like spreading by disseminated cancer cells activates YAP and MRTF for metastatic colonization. *Nat. Cell Biol.* **20**, 966–978 (2018).
35. Valiente, M. et al. Serpins promote cancer cell survival and vascular co-option in brain metastasis. *Cell* **156**, 1002–1016 (2014).
36. Bragado, P. et al. TGF–β2 dictates disseminated tumour cell fate in target organs through TGF-β-RIII and p38α/β signalling. *Nat. Cell Biol.* **15**, 1351–1361 (2013).
37. Pinho, S. & Frenette, P. S. Haematopoietic stem cell activity and interactions with the niche. *Nat. Rev. Mol. Cell Biol.* **20**, 303–320 (2019).
38. Goel, A. J., Rieder, M. K., Arnold, H. H., Radice, G. L. & Krauss, R. S. Niche cadherins control the quiescence-to-activation transition in muscle stem cells. *Cell Rep.* **21**, 2236–2250 (2017).
39. Grzelak, C. A. & Ghajar, C. M. Metastasis 'systems' biology: how are macro-environmental signals transmitted into microenvironmental cues for disseminated tumor cells? *Curr. Opin. Cell Biol.* **48**, 79–86 (2017).
40. Horsley, V., Aliprantis, A. O., Polak, L., Glimcher, L. H. & Fuchs, E. NFATc1 balances quiescence and proliferation of skin stem cells. *Cell* **132**, 299–310 (2008).
41. Kobielak, K., Stokes, N., de la Cruz, J., Polak, L. & Fuchs, E. Loss of a quiescent niche but not follicle stem cells in the absence of bone morphogenetic protein signaling. *Proc. Natl Acad. Sci. USA* **104**, 10063–10068 (2007).
42. Sharma, S. et al. Secreted Protein Acidic and Rich in Cysteine (SPARC) mediates metastatic dormancy of prostate cancer in bone. *J. Biol. Chem.* **291**, 19351–19363 (2016).
43. Kobayashi, A. et al. Bone morphogenetic protein 7 in dormancy and metastasis of prostate cancer stem-like cells in bone. *J. Exp. Med.* **208**, 2641–2655 (2011).
44. Gorgoulis, V. et al. Cellular senescence: defining a path forward. *Cell* **179**, 813–827 (2019).
45. Lujambio, A. et al. Non-cell-autonomous tumor suppression by p53. *Cell* **153**, 449–460 (2013).
46. Sosa, M. S. et al. NR2F1 controls tumour cell dormancy via SOX9- and RARβ-driven quiescence programmes. *Nat. Commun.* **6**, 6170 (2015).
47. Cackowski, F. C. et al. Mer tyrosine kinase regulates disseminated prostate cancer cellular dormancy. *J. Cell. Biochem.* **118**, 891–902 (2017).
48. Gao, H. et al. The BMP inhibitor Coco reactivates breast cancer cells at lung metastatic sites. *Cell* **150**, 764–779 (2012).
49. Laughney, A. M. et al. Regenerative lineages and immune-mediated pruning in lung cancer metastasis. *Nat. Med.* **26**, 259–269 (2020).
50. Metz, E. P. & Rizzino, A. Sox2 dosage: A critical determinant in the functions of Sox2 in both normal and tumor cells. *J. Cell. Physiol.* **234**, 19298–19306 (2019).
51. Jia, Q. et al. Low levels of Sox2 are required for melanoma tumor-repopulating cell dormancy. *Theranostics* **9**, 424–435 (2019).
52. Duarte, L. F. et al. Histone H3.3 and its proteolytically processed form drive a cellular senescence programme. *Nat. Commun.* **5**, 5210 (2014).
53. Kishino, E. et al. Anti-cell growth and anti-cancer stem cell activity of the CDK4/6 inhibitor palbociclib in breast cancer cells. *Breast Cancer* **27**, 415–425 (2019).
54. Sosa, M. S., Bernstein, E. & Aguirre-Ghiso, J. A. in *Tumor Dormancy and Recurrence* (eds. Wang, Y. & Crea, F.) 1–16 (Springer International Publishing, 2017).
55. Braun, S. et al. Cytokeratin-positive cells in the bone marrow and survival of patients with stage I, II, or III breast cancer. *N. Engl. J. Med.* **342**, 525–533 (2000).
56. Chéry, L. et al. Characterization of single disseminated prostate cancer cells reveals tumor cell heterogeneity and identifies dormancy associated pathways. *Oncotarget* **5**, 9939–9951 (2014).
57. Borgen, E. et al. NR2F1 stratifies dormant disseminated tumor cells in breast cancer patients. *Breast Cancer Res.* **20**, 120 (2018).
58. Naume, B. et al. Clinical outcome with correlation to disseminated tumor cell (DTC) status after DTC-guided secondary adjuvant treatment with docetaxel in early breast cancer. *J. Clin. Oncol.* **32**, 3848–3857 (2014).
59. Lawson, M. A. et al. Osteoclasts control reactivation of dormant myeloma cells by remodelling the endosteal niche. *Nat. Commun.* **6**, 8983 (2015).
60. Lu, X. et al. VCAM-1 promotes osteolytic expansion of indolent bone micrometastasis of breast cancer by engaging α4β1-positive osteoclast progenitors. *Cancer Cell* **20**, 701–714 (2011).
61. Zheng, H. et al. Therapeutic antibody targeting tumor- and osteoblastic niche-derived Jagged1 sensitizes bone metastasis to chemotherapy. *Cancer Cell* **32**, 731–747.e736 (2017).
62. Wang, H. et al. The osteogenic niche is a calcium reservoir of bone micrometastases and confers unexpected therapeutic vulnerability. *Cancer Cell* **34**, 823–839.e827 (2018).
63. Luo, X. et al. Stromal-initiated changes in the bone promote metastatic niche development. *Cell Rep.* **14**, 82–92 (2016).
64. Ghajar, C. M. et al. The perivascular niche regulates breast tumour dormancy. *Nat. Cell Biol.* **15**, 807–817 (2013).
65. Agarwal, P. et al. Mesenchymal niche-specific expression of Cxcl12 controls quiescence of treatment-resistant leukemia stem cells. *Cell Stem Cell* **24**, 769–784.e766 (2019).
66. Price, T. T. et al. Dormant breast cancer micrometastases reside in specific bone marrow niches that regulate their transit to and from bone. *Sci. Transl. Med.* **8**, 340ra73 (2016).
67. Sipkins, D. A. et al. In vivo imaging of specialized bone marrow endothelial microdomains for tumour engraftment. *Nature* **435**, 969–973 (2005).
68. Esposito, M. et al. Bone vascular niche E-selectin induces mesenchymal-epithelial transition and Wnt activation in cancer cells to promote bone metastasis. *Nat. Cell Biol.* **21**, 627–639 (2019).
69. Gawrzak, S. et al. MSK1 regulates luminal cell differentiation and metastatic dormancy in ER$^+$ breast cancer. *Nat. Cell Biol.* **20**, 211–221 (2018).
70. Goss, P. E. & Chambers, A. F. Does tumour dormancy offer a therapeutic target? *Nat. Rev. Cancer* **10**, 871–877 (2010).
71. Hong, S. P. et al. Single-cell transcriptomics reveals multi-step adaptations to endocrine therapy. *Nat. Commun.* **10**, 3840 (2019).
72. Selli, C. et al. Molecular changes during extended neoadjuvant letrozole treatment of breast cancer: distinguishing acquired resistance from dormant tumours. *Breast Cancer Res.* **21**, 2 (2019).
73. Cackowski, F. C. & Taichman, R. S. Parallels between hematopoietic stem cell and prostate cancer disseminated tumor cell regulation. *Bone* **119**, 82–86 (2019).
74. Webster, M. R. et al. Wnt5A promotes an adaptive, senescent-like stress response, while continuing to drive invasion in melanoma cells. *Pigment Cell Melanoma Res.* **28**, 184–195 (2015).
75. Park, J. et al. Cancer cells induce metastasis-supporting neutrophil extracellular DNA traps. *Sci. Transl. Med.* **8**, 361ra138 (2016).
76. Tohme, S. et al. Neutrophil extracellular traps promote the development and progression of liver metastases after surgical stress. *Cancer Res.* **76**, 1367–1380 (2016).
77. Miarka, L. et al. The hepatic microenvironment and TRAIL-R2 impact outgrowth of liver metastases in pancreatic cancer after surgical resection. *Cancers* **11**, E745 (2019).
78. Singh, A. et al. Angiocrine signals regulate quiescence and therapy resistance in bone metastasis. *JCI Insight* **4**, 125679 (2019).
79. Kaur, A. et al. Remodeling of the collagen matrix in aging skin promotes melanoma metastasis and affects immune cell motility. *Cancer Discov.* **9**, 64–81 (2019).
80. Fane, M. & Weeraratna, A. T. How the ageing microenvironment influences tumour progression. *Nat. Rev. Cancer* **20**, 89–106 (2020).
81. Ecker, B. L. et al. Age-related changes in HAPLN1 increase lymphatic permeability and affect routes of melanoma metastasis. *Cancer Discov.* **9**, 82–95 (2019).
82. Boudreau, N. & Bissell, M. J. Extracellular matrix signaling: integration of form and function in normal and malignant cells. *Curr. Opin. Cell Biol.* **10**, 640–646 (1998).
83. Weaver, V. M. et al. Reversion of the malignant phenotype of human breast cells in three-dimensional culture and in vivo by integrin blocking antibodies. *J. Cell Biol.* **137**, 231–245 (1997).
84. Postovit, L. M. et al. Human embryonic stem cell microenvironment suppresses the tumorigenic phenotype of aggressive cancer cells. *Proc. Natl Acad. Sci. USA* **105**, 4329–4334 (2008).
85. Mintz, B. & Illmensee, K. Normal genetically mosaic mice produced from malignant teratocarcinoma cells. *Proc. Natl Acad. Sci. USA* **72**, 3585–3589 (1975).
86. Saad, N. et al. Cancer reversion with oocyte extracts is mediated by cell cycle arrest and induction of tumour dormancy. *Oncotarget* **9**, 16008–16027 (2018).
87. Nobre, A. R., Entenberg, D., Wang, Y., Condeelis, J. & Aguirre-Ghiso, J. A. The different routes to metastasis via hypoxia-regulated programs. *Trends Cell Biol.* **28**, 941–956 (2018).
88. Rusu, P. et al. GPD1 specifically marks dormant glioma stem cells with a distinct metabolic profile. *Cell Stem Cell* **25**, 241–257.e248 (2019).
89. Vera-Ramirez, L., Vodnala, S. K., Nini, R., Hunter, K. W. & Green, J. E. Autophagy promotes the survival of dormant breast cancer cells and metastatic tumour recurrence. *Nat. Commun.* **9**, 1944 (2018).
90. La Belle Flynn, A. et al. Autophagy inhibition elicits emergence from metastatic dormancy by inducing and stabilizing Pfkfb3 expression. *Nat. Commun.* **10**, 3668 (2019).
91. Sosa, M. S., Bragado, P., Debnath, J. & Aguirre-Ghiso, J. A. Regulation of tumor cell dormancy by tissue microenvironments and autophagy. *Adv. Exp. Med. Biol.* **734**, 73–89 (2013).
92. Eyles, J. et al. Tumor cells disseminate early, but immunosurveillance limits metastatic outgrowth, in a mouse model of melanoma. *J. Clin. Invest.* **120**, 2030–2039 (2010).

93. Saudemont, A. & Quesnel, B. In a model of tumor dormancy, long-term persistent leukemic cells have increased B7-H1 and B7.1 expression and resist CTL-mediated lysis. *Blood* **104**, 2124–2133 (2004).
94. Agudo, J. et al. Quiescent tissue stem cells evade immune surveillance. *Immunity* **48**, 271–285.e275 (2018).
95. Piranlioglu, R. et al. Primary tumor-induced immunity eradicates disseminated tumor cells in syngeneic mouse model. *Nat. Commun.* **10**, 1430 (2019).
96. Krall, J. A. et al. The systemic response to surgery triggers the outgrowth of distant immune-controlled tumors in mouse models of dormancy. *Sci. Transl. Med.* **10**, eaan3464 (2018).
97. Johnson, R. W. et al. Induction of LIFR confers a dormancy phenotype in breast cancer cells disseminated to the bone marrow. *Nat. Cell Biol.* **18**, 1078–1089 (2016).
98. Takeishi, S. et al. Ablation of Fbxw7 eliminates leukemia-initiating cells by preventing quiescence. *Cancer Cell* **23**, 347–361 (2013).
99. Zhang, W. et al. Fbxw7 and Skp2 regulate stem cell switch between quiescence and mitotic division in lung adenocarcinoma. *BioMed Res. Int.* **2019**, 9648269 (2019).
100. Shimizu, H., Takeishi, S., Nakatsumi, H. & Nakayama, K. I. Prevention of cancer dormancy by Fbxw7 ablation eradicates disseminated tumor cells. *JCI Insight* **4**, 125138 (2019).
101. Shlush, L. I. et al. Tracing the origins of relapse in acute myeloid leukaemia to stem cells. *Nature* **547**, 104–108 (2017).
102. Giustacchini, A. et al. Single-cell transcriptomics uncovers distinct molecular signatures of stem cells in chronic myeloid leukemia. *Nat. Med.* **23**, 692–702 (2017).
103. Jeanpierre, S. et al. The quiescent fraction of chronic myeloid leukemic stem cells depends on BMPR1B, Stat3 and BMP4-niche signals to persist in patients in remission. *Haematologica* https://doi.org/10.3324/haematol.2019.232793 (2020).
104. Zhang, B. et al. Bone marrow niche trafficking of miR-126 controls the self-renewal of leukemia stem cells in chronic myelogenous leukemia. *Nat. Med.* **24**, 450–462 (2018).
105. Duarte, D. et al. Inhibition of endosteal vascular niche remodeling rescues hematopoietic stem cell loss in AML. *Cell Stem Cell* **22**, 64–77.e66 (2018).
106. Passaro, D. et al. Increased vascular permeability in the bone marrow microenvironment contributes to disease progression and drug response in acute myeloid leukemia. *Cancer Cell* **32**, 324–341.e326 (2017).
107. Abdelhamed, S. et al. Extracellular vesicles impose quiescence on residual hematopoietic stem cells in the leukemic niche. *EMBO Rep.* **20**, e47546 (2019).
108. Kumar, B. et al. Acute myeloid leukemia transforms the bone marrow niche into a leukemia-permissive microenvironment through exosome secretion. *Leukemia* **32**, 575–587 (2018).
109. Aguirre-Ghiso, J. A., Bragado, P. & Sosa, M. S. Metastasis awakening: targeting dormant cancer. *Nat. Med.* **19**, 276–277 (2013).
110. Avivar-Valderas, A., Wen, H. C. & Aguirre-Ghiso, J. A. Stress signaling and the shaping of the mammary tissue in development and cancer. *Oncogene* **33**, 5483–5490 (2014).
111. Sisay, M., Mengistu, G. & Edessa, D. The RANK/RANKL/OPG system in tumorigenesis and metastasis of cancer stem cell: potential targets for anticancer therapy. *Onco Targets Ther.* **10**, 3801–3810 (2017).
112. Esposito, M. & Kang, Y. Targeting tumor-stromal interactions in bone metastasis. *Pharmacol. Ther.* **141**, 222–233 (2014).
113. Coleman, R. et al. Adjuvant denosumab in early breast cancer (D-CARE): an international, multicentre, randomised, controlled, phase 3 trial. *Lancet Oncol.* **21**, 60–72 (2020).
114. Demaria, M. et al. Cellular senescence promotes adverse effects of chemotherapy and cancer relapse. *Cancer Discov.* **7**, 165–176 (2017).
115. Yumoto, K. et al. Axl is required for TGF-β2-induced dormancy of prostate cancer cells in the bone marrow. *Sci. Rep.* **6**, 36520 (2016).
116. Jung, Y. et al. Endogenous GAS6 and Mer receptor signaling regulate prostate cancer stem cells in bone marrow. *Oncotarget* **7**, 25698–25711 (2016).
117. Harper, K. L. et al. Mechanism of early dissemination and metastasis in Her2$^+$ mammary cancer. *Nature* **540**, 588–592 (2016).
118. Bowers, M. et al. Osteoblast ablation reduces normal long-term hematopoietic stem cell self-renewal but accelerates leukemia development. *Blood* **125**, 2678–2688 (2015).
119. Kaur, A. et al. sFRP2 in the aged microenvironment drives melanoma metastasis and therapy resistance. *Nature* **532**, 250–254 (2016).

Acknowledgements

We thank the Aguirre-Ghiso and Maguer-Satta labs for useful discussions during the preparation of this article. E.R. is supported by a doctoral fellowship from the University of Lyon, France, and by CLARA and IDEX Lyon mobility fellowships. E.R., A.R.N. and J.A.A.-G. are supported by grants CA109182, CA218024, CA216248 and CA196521 from the US National Institutes of Health; the Jimmy V Foundation; the Falk Medical Research Trust; HiberCell; and Metavivor. J.A.A.-G. is a Samuel Waxman Cancer Research Foundation Investigator. V.M.S. is supported by grants from 'Fondation de France' 2014-0047501 and 2017-00076282/Fondation Ramona Ehrman Amador, 'Association Laurette Fugain' ALF2014-03, Ligue contre le Cancer (Haute Savoie, Loire, Puy de Dôme and Rhone), 'Association ALTE-SMP' and the Institut Convergence PLASCAN.

Author contributions

All authors conceived of the article, performed literature searches, integrated the information, and wrote, discussed and edited the manuscript.

Competing interests

J.A.A.-G. is a scientific co-founder of, scientific advisory board member and equity owner in HiberCell and receives financial compensation as a consultant for HiberCell, a Mount Sinai spin-off company focused on the research and development of therapeutics that prevent or delay the recurrence of cancer.

Additional information

Correspondence should be addressed to J.A.A.-G.

APPENDIX 2

During my PhD I also had the incredible opportunity to be mentored by and collaborate with Ana Rita Nobre, another PhD student in Pr. Aguirre-Ghiso's laboratory, leading to two publications (Appendix 2 and 3).

The first project I participated in functionalized the role of TGFβ2 secretion by mesenchymal stem cells in cancer dormancy induction. I mainly contributed to this project by performing *in vivo* experiments and their analysis, and by taking charge of mice colonies maintenance.

Nobre AR, **Risson E**, Singh DK, Di Martino JS, Cheung JF, Wang J, Johnson J, Russnes HG, Bravo-Cordero JJ, Birbrair A, Bjorn Naume, Mohamad Azhar, Paul S. Frenette and Julio A. Aguirre-Ghiso: **Bone marrow NG2$^+$/Nestin$^+$ mesenchymal stem cells drive DTC dormancy via TGF-β2**. *Nature Cancer* 2021, doi:10.1038/s43018-021-00179-8.

nature cancer

ARTICLES

https://doi.org/10.1038/s43018-021-00179-8

Check for updates

Bone marrow NG2$^+$/Nestin$^+$ mesenchymal stem cells drive DTC dormancy via TGF-β2

Ana Rita Nobre[1,2], Emma Risson[1,3], Deepak K. Singh[1], Julie S. Di Martino[4], Julie F. Cheung[1], Jiapeng Wang[5], John Johnson[5], Hege G. Russnes[6,7], Jose Javier Bravo-Cordero[4], Alexander Birbrair[8,11], Bjorn Naume[9,10], Mohamad Azhar[5], Paul S. Frenette[8] and Julio A. Aguirre-Ghiso[1]✉

In the bone marrow (BM) microenvironment, where breast cancer (BC)-disseminated tumor cells (DTCs) can remain dormant for decades, NG2$^+$/Nestin$^+$ mesenchymal stem cells (MSCs) promote hematopoietic stem cell quiescence. Here we reveal that periarteriolar BM-resident NG2$^+$/Nestin$^+$ MSCs can also instruct BC DTCs to enter dormancy. NG2$^+$/Nestin$^+$ MSCs produce transforming growth factor (TGF)-β2 and bone morphogenetic protein (BMP)7 and activate a quiescence pathway dependent on TGFBRIII and BMPRII, which via p38-kinase, results in p27 induction. Genetic depletion of MSCs or conditional knockout of TGF-β2 in MSCs using an NG2-Cre^{ER} driver led to bone metastatic outgrowth of otherwise dormant p27$^+$/Ki67$^-$ DTCs. Also, patients with estrogen receptor-positive BC without systemic recurrence displayed higher frequency of TGF-β2 and BMP7 detection in the BM. Our results provide direct proof that hematopoietic stem cell dormancy niches control BC DTC dormancy and suggest that aging or extrinsic factors that affect the NG2$^+$/Nestin$^+$ MSC niche homeostasis may result in a break from dormancy and BC bone relapse.

Metastases that are derived from DTCs, are the major source of cancer-related deaths from solid cancers[1]. Post-extravasation DTCs can remain in a dormant state from prolonged periods[2] and years to decades can lapse before dormant DTCs emerge as overt lesions. We postulate that targeting dormant DTCs is the shortest path to change patient outcomes by curtailing metastatic outgrowth. However, to achieve this goal we must understand the cancer-cell-intrinsic and microenvironmental mechanisms that control DTC dormancy and reactivation.

The BM is a site where dormant DTCs are found and where metastasis can develop in various cancers after prolonged periods of clinical 'remission'[2–9]. In trying to understand how the BM microenvironment might control DTC dormancy, we[8,10] and others[2,4,11,12] found that in both humans and mice, this microenvironment is a restrictive site for metastasis initiation. This is due to the presence of several cues, such as TGF-β2 (ref. [10]), BMP7 (refs. [13,14]), GAS6 (refs. [15–17]) and leukemia inhibitory factor[12,18], which induce DTC dormancy. Studies in mostly two-dimensional or three-dimensional (3D) in vitro models, proposed that MSCs[19], vascular endothelial cells[11,20] and/or osteoblasts[16,21,22] may be the source of dormancy cues for cancer cells. However, the function of such niche cells in vivo has not been formally tested.

There is a long-standing hypothesis that the niches that control hematopoietic stem cell (HSC) dormancy may instruct DTCs to become dormant[23]. A previous study in prostate cancer has drawn a connection between the HSC niche and dormancy of DTCs[24]. While informative, these studies did not functionally dissect in depth and in vivo the role of key cell types that regulate HSC dormancy in regulating DTC quiescence. Further, the niche influence has been inferred from the analysis of cancer cells recovered from the BM or from indirect competition assays. Thus, there is still a critical need to understand the cellular components and how BM niches enforce DTC dormancy.

Dormancy of HSCs in the BM is a robust and long-lived process that, if unperturbed, results in HSCs dividing and self-renewing only four to five times in the lifetime of a mouse[25]. Such a powerful mechanism of quiescence and self-renewal cycles might explain how DTCs, if responsive to niche signals, could persist for decades in the BM of patients with BC. The HSC microenvironment in the BM is a complex multicellular network promoting HSC dormancy, self-renewal and differentiation into lineage-committed progenitors[26]. Previous studies have revealed that periarteriolar stromal cells, enriched in MSC activity, innervated by the sympathetic nervous system, and expressing the neural markers NG2 and Nestin (mesenchymal stem and progenitor cells, hereafter referred to as NG2$^+$/Nestin$^+$ MSCs for simplicity), are critical for the control of HSC quiescence and hematopoiesis[27]. Notably, aging-induced alterations causing replicative stress damage or sympathetic neuropathy from infiltrating leukemia cells, for example, eliminates the control of HSC dormancy by NG2$^+$/Nestin$^+$ MSCs and can fuel malignancy[28,29]. We and others also discovered that TGF-β2 and BMP7 in the BM milieu are key inducers of DTC dormancy in various

[1]Division of Hematology and Oncology, Department of Medicine and Department of Otolaryngology, Department of Oncological Sciences, Black Family Stem Cell Institute, The Tisch Cancer Institute, Icahn School of Medicine at Mount Sinai, New York, NY, USA. [2]Abel Salazar Biomedical Sciences Institute, University of Porto, Porto, Portugal. [3]Université de Lyon, Lyon, France. [4]Division of Hematology and Oncology, Department of Medicine, The Tisch Cancer Institute, Icahn School of Medicine at Mount Sinai, New York, NY, USA. [5]Department of Cell Biology and Anatomy, University of South Carolina School of Medicine, Columbia, SC, USA. [6]Division of Surgery and Cancer Medicine, Department of Oncology, Oslo University Hospital, Oslo, Norway. [7]Division of Laboratory Medicine, Department of Pathology, Oslo University Hospital, Oslo, Norway. [8]Ruth L. and David S. Gottesman Institute for Stem Cell and Regenerative Medicine Research, Albert Einstein College of Medicine, Bronx, NY, USA. [9]Division of Cancer Medicine, Department of Oncology, Oslo University Hospital, Oslo, Norway. [10]Institute of Clinical Medicine, University of Oslo, Oslo, Norway. [11]Present address: Department of Pathology, Federal University of Minas Gerais, Belo Horizonte, Brazil. ✉e-mail: julio.aguirre-ghiso@mssm.edu

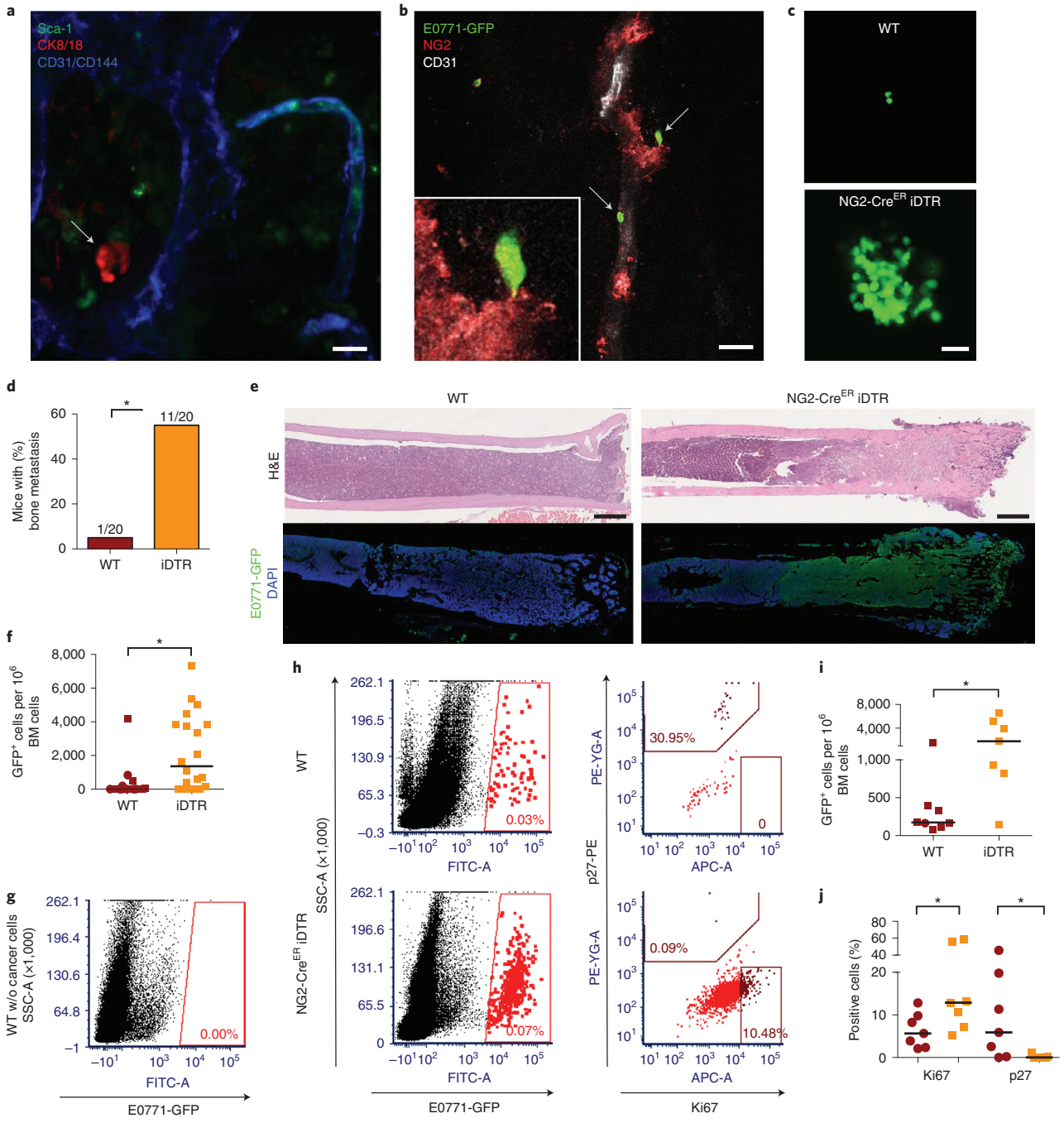

Fig. 1 | Depletion of NG2⁺/Nestin⁺ MSCs awakens dormant DTCs in the BM. a,**b**, Whole-bone imaging of MMTV-Neu (GEM model, CK8/18⁺ cancer cells, representative image of two independent experiments) and E0771-GFP (intracardiacally injected) BC cells (representative image of five independent experiments). Scale bars, 10 µm (**a**) and 20 µm (**b**). **c**–**f**, Effect of NG2⁺/Nestin⁺ MSC depletion before BM seeding by DTCs ($n = 20$ mice per condition from three independent experiments. Experimental design shown in Extended Data Fig. 1a). Representative images of E0771-GFP⁺ DTC clusters in BM flushes from WT and NG2⁺/Nestin⁺ MSC-depleted mice (NG2-Cre^{ER}iDTR) (**c**). Scale bar, 50 µm. Incidence of bone metastasis (>1,000 GFP⁺ DTCs per 10^6 BM cells) 2 weeks after cancer cell injections (two-tailed Fisher's exact test; $P = 0.001$) (**d**). Hematoxylin and eosin (H&E) and GFP staining of WT and NG2-Cre^{ER}iDTR bones (**e**). DAPI, 4,6-diamidino-2-phenylindole. Scale bars, 500 µm. Number of E0771-GFP cells per million of BM cells after BM flushing, counted manually (median, two-tailed Mann–Whitney *U*-test, $P = 0.0004$) (**f**). **g**,**h**, Representative plots and gates used in FACS for detection and characterization of E0771-GFP cells in BM flushes. **i**, Number of E0771-GFP cancer cells per million of BM cells, counted by FACS ($n = 15$ mice, median, two-tailed Mann–Whitney *U*-test, $P = 0.021$). **j**, Percentage of E0771-GFP cells Ki67^{high} and p27⁺ (FACS) ($n = 14$, median, two-tailed Mann–Whitney *U*-test, $P = 0.038$ and 0.05). $^*P \leq 0.05$ (P values indicated above).

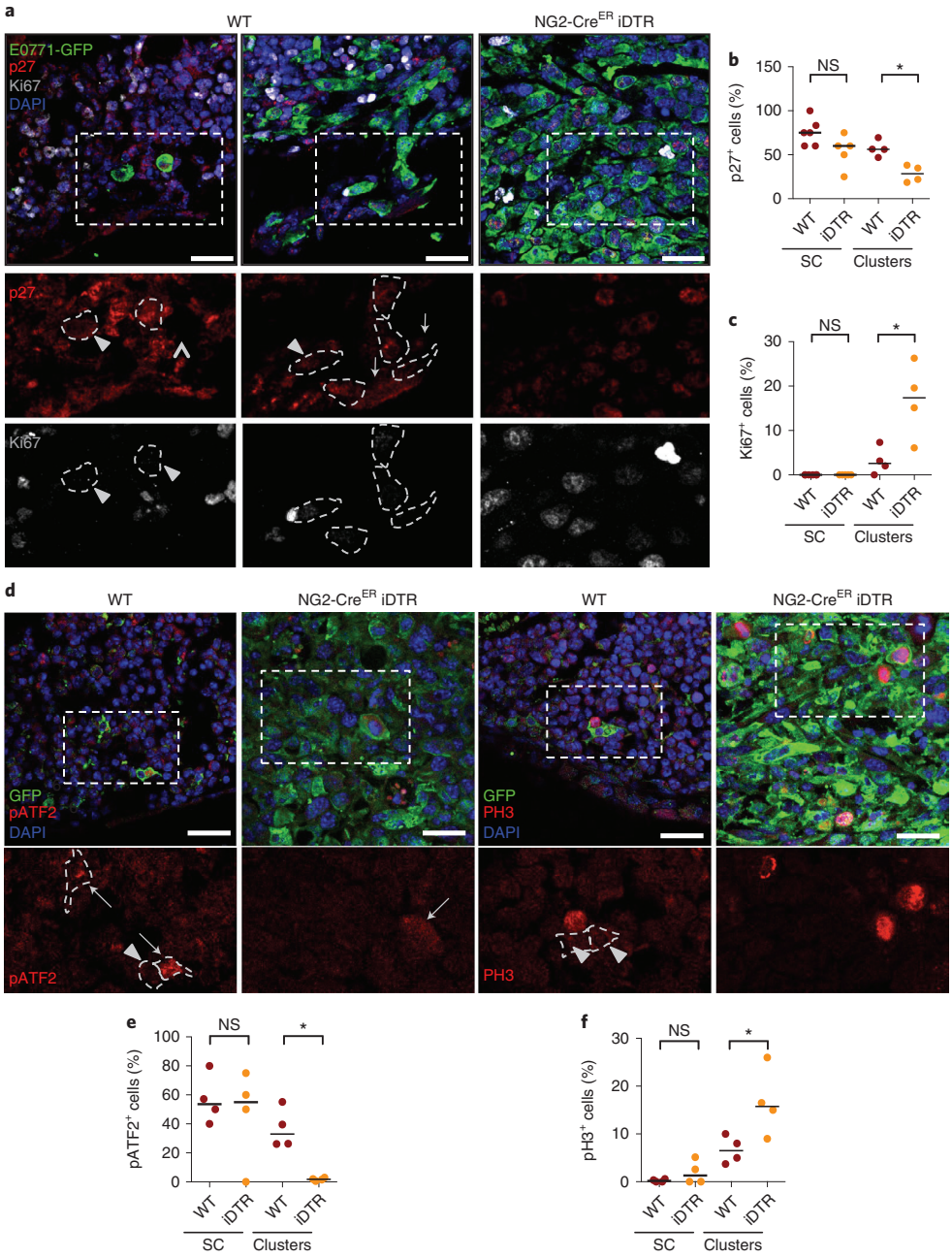

Fig. 2 | Dormant to proliferative shift of BM E0771-GFP cancer cells upon depletion of NG2$^+$/Nestin$^+$ MSCs. a, Representative images of p27 and Ki67 in E0771-GFP cells in WT and NG2-Cre^{ER}iDTR bones. Single cells and small clusters are shown in WT mice and a metastasis in NG2-Cre^{ER}iDTR. Scale bars, 25 µm; arrows, positive cells; arrowheads, negative cells; dotted lines, GFP$^+$ cell border. **b**,**c**, Percentage of p27$^+$ (**b**) and Ki67$^+$ (**c**) E0771-GFP cells detected by immunofluorescence ($n=6$ WT and 5 iDTR mice, median, two-tailed Mann–Whitney *U*-test; $P=0.029$ (**b**) and 0.05 (**c**)). SC, single cell. **d**–**f**, Representative images (**d**) (scale bars, 25 µm; arrows, positive cells; arrowheads, negative cells) and quantification of p-ATF2$^+$ (**e**) and PH3$^+$ (**f**) E0771-GFP DTCs in WT and NG2-Cre^{ER}iDTR bones ($n=4$ WT and 4 iDTR mice, two-tailed Mann–Whitney *U*-test; $P=0.03$ (**e**) and 0.05 (**f**)). *$P \leq 0.05$ (*P* values indicated above), NS, not significant.

epithelial cancers[10,27]. However, the source of these cytokines has remained elusive.

Here, we show using in vitro and in vivo assays that NG2$^+$/Nestin$^+$ MSCs are a source of TGF-β2 and BMP7 and that both niche MSCs and cytokines maintain the dormancy of different cancer cell types via TGFBRIII and BMPRII, respectively and p38 and p27 signaling. Furthermore, depletion of the NG2$^+$/Nestin$^+$ MSCs or knockout (KO) of TGF-β2 specifically from NG2$^+$/Nestin$^+$ MSCs led to metastatic outgrowth in the BM. Also in 3D organoid assays 'revitalized' but not 'aged' NG2$^+$/Nestin$^+$ MSCs can reprogram malignant cells into a dormancy-like phenotype. Last, detectable BMP7 and TGF-β2 levels were observed at higher frequency in the BM of patients with estrogen receptor positive (ER$^+$) BC without systemic recurrence compared to patients with systemic recurrence

and BMP7 presence was associated with a longer time to metastatic recurrence after therapy. Our results pinpoint a functional link between the niches that control adult HSC quiescence and DTC dormancy.

Results

Depletion of NG2$^+$/Nestin$^+$ MSCs from the BM niche reactivates dormant E0771 DTCs. The BM frequently harbors dormant DTCs in both humans and mice[2,4,8,10–12]. As observed in humans and previous models of BM DTC detection, in both spontaneous (MMTV-HER2 (ref. [30]) and Fig. 1a) and experimental metastatic BC mouse models (intracardiac- injected E0771-GFP (Fig. 1b) and MMTV-PyMT-CFP cells) we could only find few DTCs in the BM of femurs, sternum and calvaria bones (150–400 DTCs per million BM cells). In wild-type (WT) animals these DTCs were nonmetastatic or developed lesions at low frequency in the bones (~5–16%; Figs. 1d and 5d). In contrast, these mice showed 100% incidence of metastasis to the lung (data not shown), which is frequently a permissive site for metastasis[10].

Different factors and BM stromal cells were proposed to induce and maintain DTC dormancy[11,16,19–22]. However, in vivo studies functionally linking specific BM cells and dormancy-inducing factors to DTC dormancy are still missing. NG2$^+$/Nestin$^+$ MSCs are critical inducers of HSC quiescence and hematopoiesis[27]. Thus, we set out to test whether, as with dormancy of HSCs[27], the NG2$^+$/Nestin$^+$ MSCs could also induce dormancy of DTCs. To this end we took advantage of the C57BL/6 NG2-Cre^{ER} inducible diphtheria toxin receptor (iDTR) mouse model[27,31]. Treatment of mice with 2 mg of tamoxifen (TAM) for 5 d leads to Cre recombinase activation and the expression of the diphtheria toxin receptor (DTR) in periarteriolar NG2$^+$ cells, which upon 2-day treatment with 250 ng of diphtheria toxin (DT) causes a targeted depletion of NG2$^+$ cells[27,31]. This strategy reproducibly led to the depletion of ~50% of NG2$^+$/Nestin$^+$ MSCs (measured as CD45$^-$Ter119$^-$CD31$^-$PDGFRa$^+$CD51$^+$ MSCs (Extended Data Fig. 1a–c), which overlap with NG2$^+$/Nestin$^+$ MSCs[27,31]) in the BM of long bones. Twenty-four hours after DT treatment, we performed intracardiac injection of 2×10^5 E0771-GFP cells per mouse (Extended Data Fig. 1a and Supplementary Movie 1) and 2 weeks later, we measured the burden of BM DTCs. All mice had E0771-GFP$^+$ DTCs in the BM detectable by fluorescence-activated cell sorting (FACS) (Fig. 1g,h), corroborating the injection efficiency and that these cells can persist in the BM at a low burden in all injected mice. Only 5% (1 out of 20) of WT mice showed >1,000 DTCs per million BM cells (manually counted after BM flush). In contrast, 55% (11 out of 20) of NG2-Cre^{ER}iDTR mice with a deficiency of NG2$^+$/Nestin$^+$ MSCs displayed a build-up of E0771-GFP$^+$ colonies in the BM (Fig. 1c,d). Consistently, histological analysis confirmed that indeed the BM of WT animals exhibited normal histology, whereas NG2-Cre^{ER}iDTR mice revealed large areas of bone metastasis and replacement of the BM by E0771-GFP$^+$ cancer cells (Fig. 1e). Further, quantification of the DTC burden (both manual counting (Fig. 1f) and FACS assisted (Fig. 1i)) showed a striking increase in number of DTCs in the BM compartment of NG2-Cre^{ER}iDTR compared to WT mice. FACS staining of Ki67 and p27 also showed a statistically significant increase in the percentage of Ki67$^+$E0771-GFP$^+$ cells and decrease in p27$^+$ DTCs was detected in NG2-Cre^{ER}iDTR mice compared with WT mice (Fig. 1h–j). The results were reproduced using a MMTV-PyMT-CFP cell line with only 1 out of 5 (20%) control animals showing $>10^3$ cancer cells per 10^6 BM cells, whereas 3 out of 5 (60%) showed reactivation. The burden of cancer cells in the iDTR group animal that reactivated (60%) increased by tenfold and mice with a high cell burden showed a correlative increase in the percentage of Ki67$^+$ DTCs upon depletion of NG2$^+$/Nestin$^+$ MSCs (Extended Data Fig. 1d–g). We conclude that a 50% reduction in NG2$^+$/Nestin$^+$ MSCs (measured as CD45$^-$Ter119$^-$CD31$^-$PDGFRa$^+$CD51$^+$ MSCs) can cause bone-damaging metastatic reactivation of otherwise dormant DTCs.

Further characterization revealed that in WT mice, 75% of the solitary E0771$^-$GFP DTCs were positive for p27 (quiescence regulator[10]; Fig. 2a,b) and 54% were positive for p-ATF2 (p38-activated transcription factor[32]; Fig. 2d,e). In contrast, these same DTCs were 100% negative for Ki67 and phosphohistone H3 (PH3) (Fig. 2a,c,d,f), supporting a dormant phenotype (increased expression of p-ATF2 and p27 and decreased Ki67 and PH3) as reported in different cancer models[10,33,34]. In mice depleted of NG2$^+$/Nestin$^+$ MSCs, E0771-GFP$^+$ resumed proliferation as evidenced by a reduction in the percentage of p27$^+$ (28%) and p-ATF2$^+$ (2%) cells and increase of Ki67$^+$ (17%) and PH3$^+$ (16%) in DTC clusters, which are not frequent in WT animals (Fig. 2a,c,d,f) and corroborated an awakening of DTCs and shift to a proliferative state.

DT and DTR-mediated cell death can induce inflammation when certain cell types are targeted[35–37]. However, we previously reported no difference in the number of leukocytes, expression of CXCL12 and KITL (stem cell factor) and no change in vascular volume in the NG2-Cre^{ER}iDTR model[27]. Nevertheless, we performed a multiplex ELISA for pro-inflammatory cytokines in the BM supernatant of WT and iDTR mice. We found no differences between the control and iDTR mice in the abundance levels of interleukin (IL)-1β, granulocyte–macrophage colony-stimulating factor, IL-2, IL-4, IL-6, IL-10, IL-12p70, monocyte chemoattractant protein-1 or tumor necrosis factor-α levels (interferon-γ was undetectable; Extended Data Fig. 2a). Thus, reactivation of dormant DTCs upon NG2$^+$/Nestin$^+$ MSC depletion cannot be attributed to changes in the inflammatory cytokines that we measured.

To exclude that the increased DTC burden after 2 weeks was not due to differences in vascular permeability or extravasation efficiency between WT and NG2-Cre^{ER}iDTR mice, a group of animals was analyzed 24 h after intracardiac delivery of E0771-GFP cells and dextran–Texas Red injection (Extended Data Fig. 2b). No differences in the amount of 70,000 MW dextran–Texas Red extravasation in the BM was observed after NG2$^+$/Nestin$^+$ MSC depletion as determined using image analysis (Extended Data Fig. 2c), reproducing previous results[27] and suggesting no obvious alteration in vessel

Fig. 3 | NG2$^+$/Nestin$^+$ MSCs are as a source of pro-dormancy factors TGF-β2 and BMP7 in the BM. a, mRNA levels of sorted CD45$^-$CD31$^-$Nestin-GFP$^-$ and Nestin-GFP^{bright} MSCs from Nestin-GFP mice ($n=4$ independent experiments, median, two-tailed Mann–Whitney *U*-tests; $P=0.027$ (TGF-β2) and 0.031 (BMP7)). **b**, mRNA levels of sorted MSCs, OPCs and ECs (MSC population was used as reference, $n=2$ independent experiments, one-way analysis of variance with Geisser–Greenhouse correction, $P=0.034$ (TGF-β2) and 0.005 (BMP7)) **c**, TGF-β1, TGF-β2 and TGF-β3 and BMP7 levels in BM supernatant of WT and NG2-Cre^{ER}iDTR mice 2 weeks after TAM and DT treatments ($n=24$ mice from two independent experiments, median, two-tailed Mann–Whitney *U*-tests; $P<0.0001$ (TGF-β2) and 0.011 (BMP7)). **d**–**f**, Imaging of Nestin-GFP$^+$ MSCs in Nestin-GFP mice using immunofluorescence. Dormancy factors TGF-β2 (white (**d**,**e**); red (**f**)) and BMP7 (red (**d**,**e**)) are expressed near MSCs (Nestin-GFP, green (**d**–**f**); NG2, white (**f**); representative images of three independent experiments). Scale bars, 100 μm (**d**,**e**) and 25 μm (**f**). Dotted rectangles (**d**), high-magnification insert. **g**,**h**, Analysis of $n=55$ patients with ER$^+$ BC with (M1) or without (M0) evidence of systemic recurrence. Data from SATT clinical study[9] (**g**). TGF-β2 and BMP7 levels from BM plasma samples (two-tailed Fisher's exact test, $P=0.009$). Metastasis-free survival analysis of patients who did not receive any secondary chemotherapy, excluding treatment-related interpretation bias, separated by detectable BMP7 levels compared to patients with no BMP7 (**h**). $^*P\leq0.05$ (*P* values indicated above).

permeability. Further, DTC burden was quantified after expansion of E0771-GFP$^+$ cells 1 week in vitro (due to no or low detection of E0771-GFP$^+$ in fresh BM flush). Similar numbers of E0771-GFP$^+$ cells were found in WT and NG2-Cre^{ER}iDTR mice (Extended Data Fig. 2d) arguing that the differences in final metastatic burden were not due to higher vessel permeability and/or early enhanced extravasation of DTCs.

We next tested whether depletion of NG2$^+$/Nestin$^+$ MSCs affected DTC expansion once cancer cells had seeded and established a foothold within the BM niche. To this end we used the same

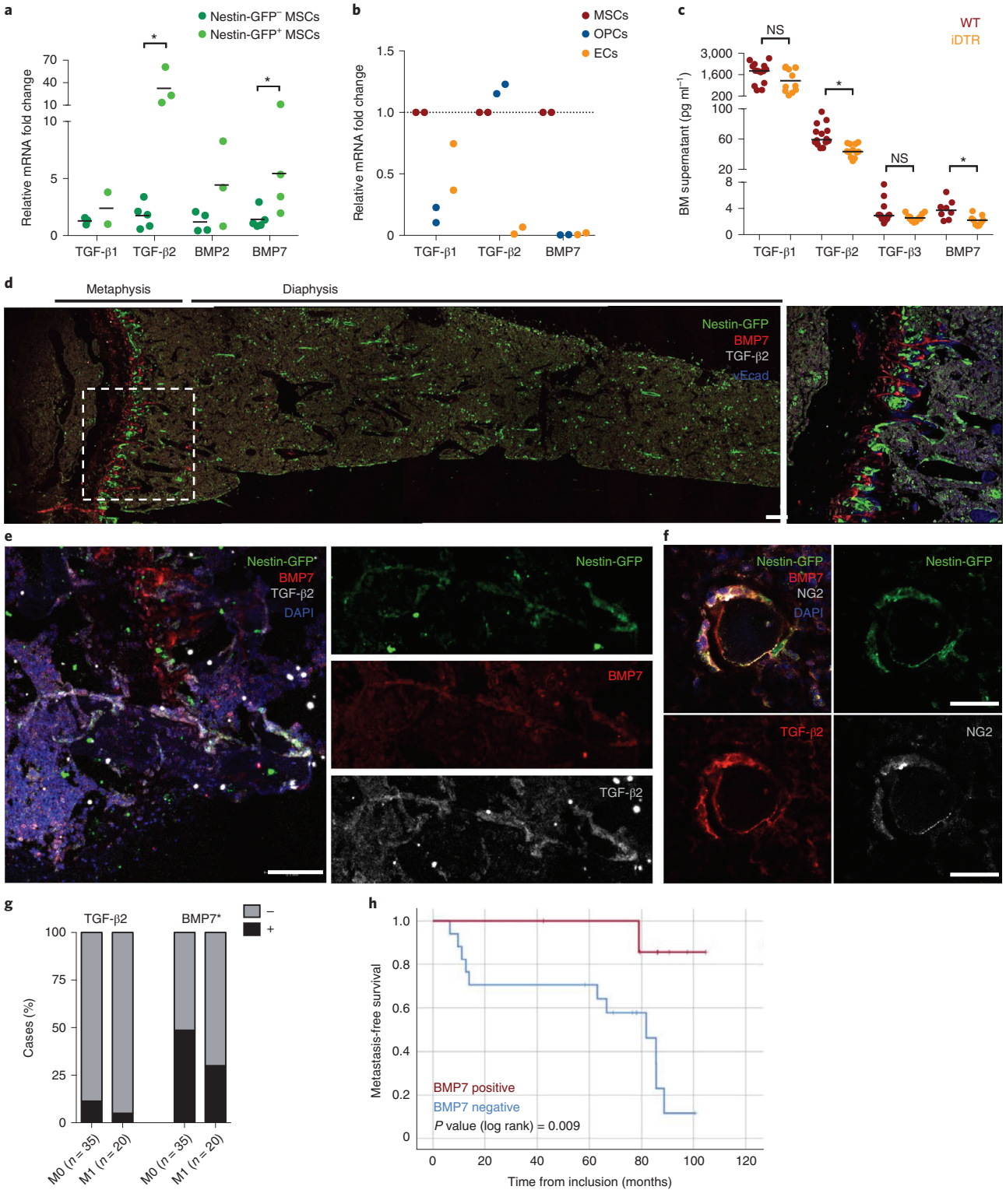

NG2-Cre^{ER}iDTR mouse model but the treatment with TAM for 5 d was followed by intracardiac injection of E0771-GFP cells, which were allowed to lodge for 72 h in unperturbed niches and only then we performed two daily treatments with DT (Extended Data Fig. 2e). Notably, depletion of NG2$^+$/Nestin$^+$ MSCs after DTCs had lodged in the BM niche also stimulated metastatic outbreak; only one-third (1 out of 6) of control WT mice displayed substantial expansion of E0771-GFP cells in the BM flushes, whereas all NG2-Cre^{ER}iDTR mice (5 out of 5) had a statistically significant increase in frequency of cancer cells per BM cells (Extended Data Fig. 2f). We conclude that NG2$^+$/Nestin$^+$ MSCs are directly or indirectly responsible for maintaining pro-dormancy niches for DTCs in the BM.

NG2$^+$/Nestin$^+$ MSCs show enhanced production of the dormancy inducers TGF-β2 and BMP7. We had shown that TGF-β2 in the BM induced DTC dormancy[10], whereas other groups identified BMP7 as an inducer of DTC dormancy[13]. However, the functional source of TGF-β2 or other factors in the BM in vivo remained unidentified. We wondered whether NG2$^+$/Nestin$^+$ MSCs may regulate dormancy by producing cues, such as TGF-β2. To address this question, we sorted BM CD31$^-$CD45$^-$Nestin-GFP^{bright} (from now on called nestin-GFP$^+$) and CD31$^-$CD45$^-$Nestin-GFP$^-$cells (from now on called Nestin-GFP$^-$) (Supplementary Fig. 1a) and measured messenger RNA levels of TGF-β1, BMP2 (involved in dormant DTC reactivation[13,34]), TGF-β2 and BMP7 (dormancy-inducing cues[10,13,34]). The Nestin-GFP$^+$ cells showed higher mRNA levels of TGF-β2 and BMP7 than Nestin-GFP$^-$ cells (Fig. 2a). In addition, because it has been shown that other niche cells have high expression of TGF-β2 (refs. [38,39]), we compared TGF-β1, TGF-β2 and BMP7 mRNA levels in MSCs, osteo-progenitor cells (OPCs) and endothelial cells (ECs). To this end, we sorted MSCs (CD45$^-$CD31$^-$Ter119$^-$PDGFR a$^+$CD51$^+$), OPCs (CD45$^-$Ter119$^-$CD31$^-$ALCAM$^+$ OPCs) and ECs (CD45$^-$Ter119$^-$CD31$^+$vEcad$^+$ ECs) from WT mice (Supplementary Fig. 1b) and we found that TGF-β1 is equally expressed by MSCs, OPCs and ECs; TGF-β2 was higher in MSCs and OPCs and BMP7 was uniquely produced by MSCs (Fig. 3b). Thus, MSCs are not an exclusive source of TGF-β2 but are the only niche cells producing both pro-dormancy TGF-β2 and BMP7 cues. Further, ELISA measurements of the BM supernatants from NG2-Cre^{ER}iDTR mice showed a statistically significant decrease in TGF-β2 and BMP7 levels but not TGF;β1 or TGF;β3 upon NG2$^+$/Nestin$^+$ MSC depletion compared with WT mice (Fig. 3c), suggesting that pro-dormancy niches established by NG2$^+$/Nestin$^+$ MSCs are a source of TGF-β2 and BMP7 in the BM but that other cells may compensate for the production and total levels of TGF-β1 and TGF-β3. Imaging of TGF-β2 and BMP7 in relation to Nestin-GFP cells revealed that BMP7 was more predominant in the growth plate (Fig. 2d) and seemed to accumulate as a secreted factor around Nestin-GFP$^+$ cells (BMP7 is an extracellular matrix-bound factor[40,41]) or colocalizing with the Nestin-GFP signal (Fig. 3d,e), whereas TGF-β2 was found homogeneously distributed across the BM. We could also find it colocalizing with the NG2 and Nestin-GFP signals supporting their production by MSCs (Fig. 3d–f). We conclude that pro-dormancy NG2$^+$/Nestin$^+$ MSCs are a source of TGF-β2 and BMP7 in the BM.

TGF-β2 and BMP7 detection in BM supernatant from patients with ER$^+$ BC. Given that the lower levels of TGF-β2 and BMP7 upon NG2$^+$/Nestin$^+$ MSC depletion were associated with reactivation of dormant DTCs leading to metastatic outgrowth (Fig. 1), we tested the hypothesis that the abundance of these two factors in the BM of patients with BC might provide some information on their progression. To this end we tested a small subset of BM plasma samples from patients with early BC with ER$^+$ disease, the BC subtype most often experiencing tumor dormancy and late recurrences in the bone, among other sites. These samples were part of a clinical study monitoring DTC status after completion of standard adjuvant anthracycline-containing chemotherapy[9]. TGF-β2 and BMP7 levels from BM plasma were detected using multiplex ELISA and revealed that patients without systemic recurrence (M0) during follow up had 2.28- and 1.62-fold higher frequency of detectable TGF-β2 and BMP7, respectively, compared to patients with systemic recurrence (M1) (Fig. 3g). Notably, metastasis-specific survival analysis of the subgroup of patients who did not receive any secondary chemotherapy, excluding treatment-related interpretation bias, pointed to markedly improved distant disease-free survival for patients with detectable BMP7 compared to patients with no BMP7 (Fig. 3h), regardless of abundance levels. Survival analysis was not possible for TGF-β2 due to the low number of patients showing detectable TGF-β2 levels. This small pilot analysis supports expanding the analysis of the association between detectable levels of factors such as TGF-β2 and BMP7 and time to metastatic recurrence in ER$^+$ patients after therapy.

NG2$^+$/Nestin$^+$ MSCs activate TGFBRIII and BMPRII signaling and a low ERK/p38 signaling ratio in cancer cells. We next tested whether NG2$^+$/Nestin$^+$ MSCs could activate key dormancy pathways downstream of TGF-β2 and BMP7 signaling in cancer cells. To this end, we optimized a co-culture system of sorted NG2$^+$/Nestin$^+$ MSCs and various human and mouse cancer cells. In this assay, CD45$^-$CD31$^-$Nestin-GFP cells sorted from BM were co-cultured (1:1 ratio) with cancer cells on top of Matrigel at low density. The co-cultures were followed for up to 4 d to ensure that the MSCs retained functionality[42]. We monitored the frequency at which single cancer cells (to mimic solitary DTC biology) remain in a solitary state or progressed to small and large cancer cell clusters, a measure of proliferative capacity (Extended Data Fig. 3a and Fig. 4a). The co-cultures revealed that the majority of control (no MSCs added) and also E0771 BC cells co-cultured with Nestin-GFP$^-$ cells progressed to large clusters; compared to control cells, Nestin-GFP$^-$ cells had some growth inhibitory effect on E0771 cells as we observed ~15% increase in the

Fig. 4 | NG2$^+$/Nestin$^+$ MSCs activate TGF-β2 and BMP7 growth inhibitory signaling in cancer cells. a, Representative images of 3D co-cultures of E0771 cells with sorted Nestin-GFP$^-$ or $^+$ MSCs for 4 d. Top left: a single cell, a doublet and cluster of cancer cells. Scale bar, 50 μm; an NG2$^+$/Nestin$^+$ MSC (PDGFR-α$^+$, red) near a cancer cell cluster (bottom left). Scale bar, 50 μm; representative images of positive cells for c-Cas-3 (apoptotic cells), phosphorylated retinoblastoma protein (p-RB) (proliferative cells), p-ATF2 (p38-pathway activation) and p27 (quiescent cells) markers (center and right). Scale bars, 10 μm (representative images of three independent experiments). PDGFR-α, platelet-derived growth factor receptor-α. **b**, Percentage of E0771 cells in a single cell ($P = 0.01$ and 0.03), doublet or cell cluster ($P = 0.04$ and 0.02) states in the indicated co-cultures ($n = 3$ independent experiments, mean and s.e.m., two-tailed Mann–Whitney *U*-tests). **c**–**f**, Percentage of E0771 cancer cells positive for c-Cas-3, p-RB, p-ATF2 and p27 in co-culture with Nestin-GFP$^-$ (dark green) or Nestin-GFP$^+$ MSCs (bright green) ($n = 2$ independent experiments, four wells per condition, mean, minimum and maximum). **g**–**j**, T-HEp3 cells with different biosensors were reverse transfected with siRNA for TGFBRIII and BMPRII followed by co-culture in Transwells with sorted Nestin-GFP$^-$ or -GFP$^+$ cells. Representative images of T-HEp3 cells with ELK-Gal4::GFP (GFP$^+$ when ERK1/2 pathway is active), p38-clover (when p38 is active the cytoplasmic signal predominates) and p27K$^-$ mVenus (mVenus signal indicates cell cycle arrest) biosensors (representative images of three independent experiments) (**g**). Scale bar, 25 μm. Quantification of T-HEp3 biosensor cell lines after transfection followed by 24-h co-culture using Transwells (**h**–**j**) ($n = 3$ independent experiments each, mean, minimum and maximum, two-tailed Mann–Whitney *U*-tests; $P = 0.05$). $^*P \leq 0.05$, *P* values indicated above.

accumulation of cells in a single-cell state; however, arrest of cancer cells in a single cell or doublet state was dramatically increased in the presence of Nestin-GFP$^+$ MSCs (Fig. 4b). Similar results were obtained with human head and neck squamous carcinoma T-HEp3 cells (Extended Data Fig. 3b) and mouse BC MMTV-PyMT-CFP cells (Extended Data Fig. 3c). Treatment of E0771 cells in these conditions with TGF-β2, BMP7 or BM-conditioned medium (BM-CM) from WT TGF-β2$^{+/+}$ mice also led to the accumulation of growth-arrested single cancer cells (Extended Data Fig. 3d,h). This effect was partially reversed when using BM-CM from mice heterozygous for TGF-β2 ($^{+/-}$) (Extended Data Fig. 3h). Thus, Nestin-GFP$^+$ MSCs, which show enhanced expression of TGF-β2 and BMP7, were able to strongly suppress proliferation of different cancer cells similarly to the purified cues or BM-CM from mice with a full gene complement of TGF-β2.

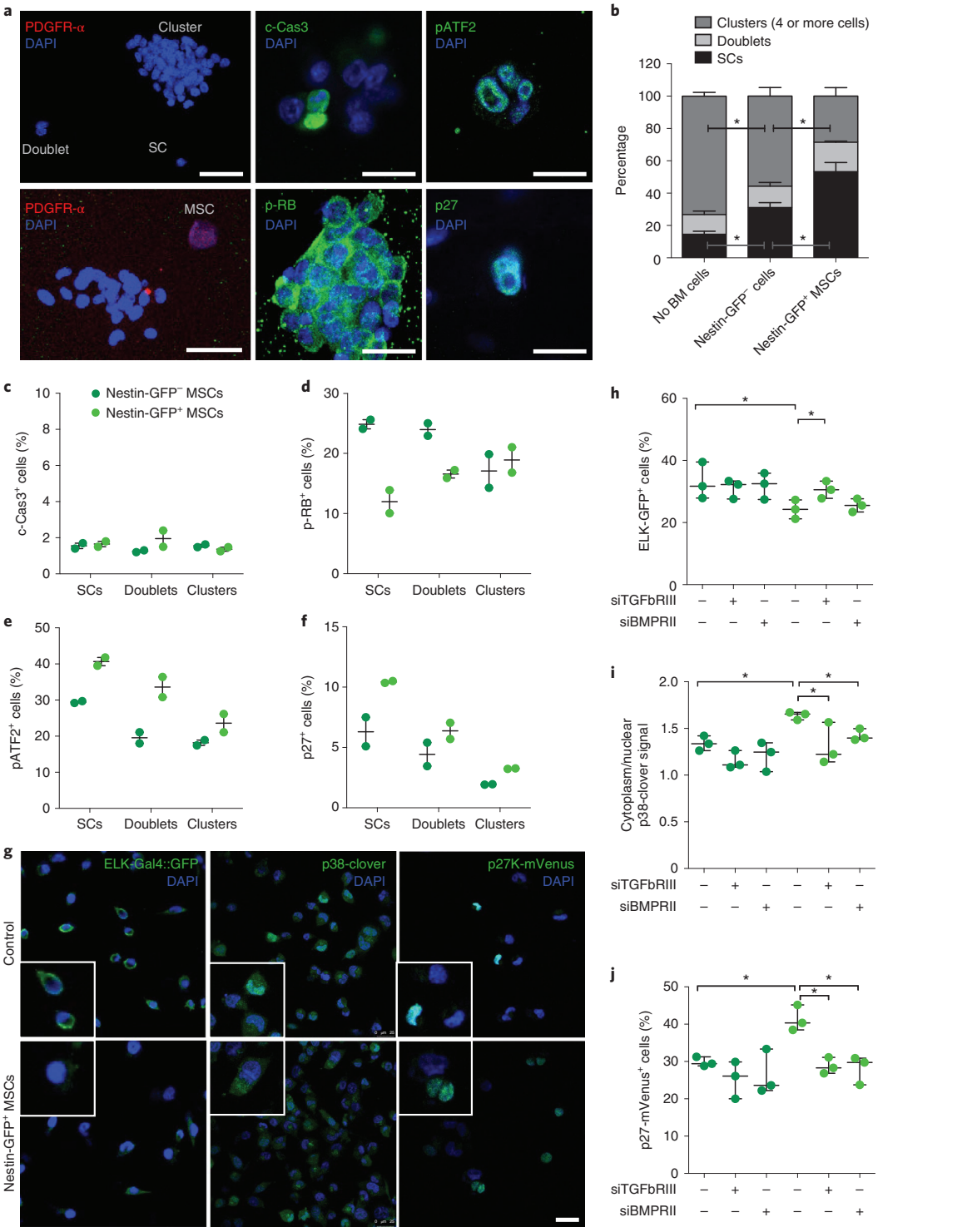

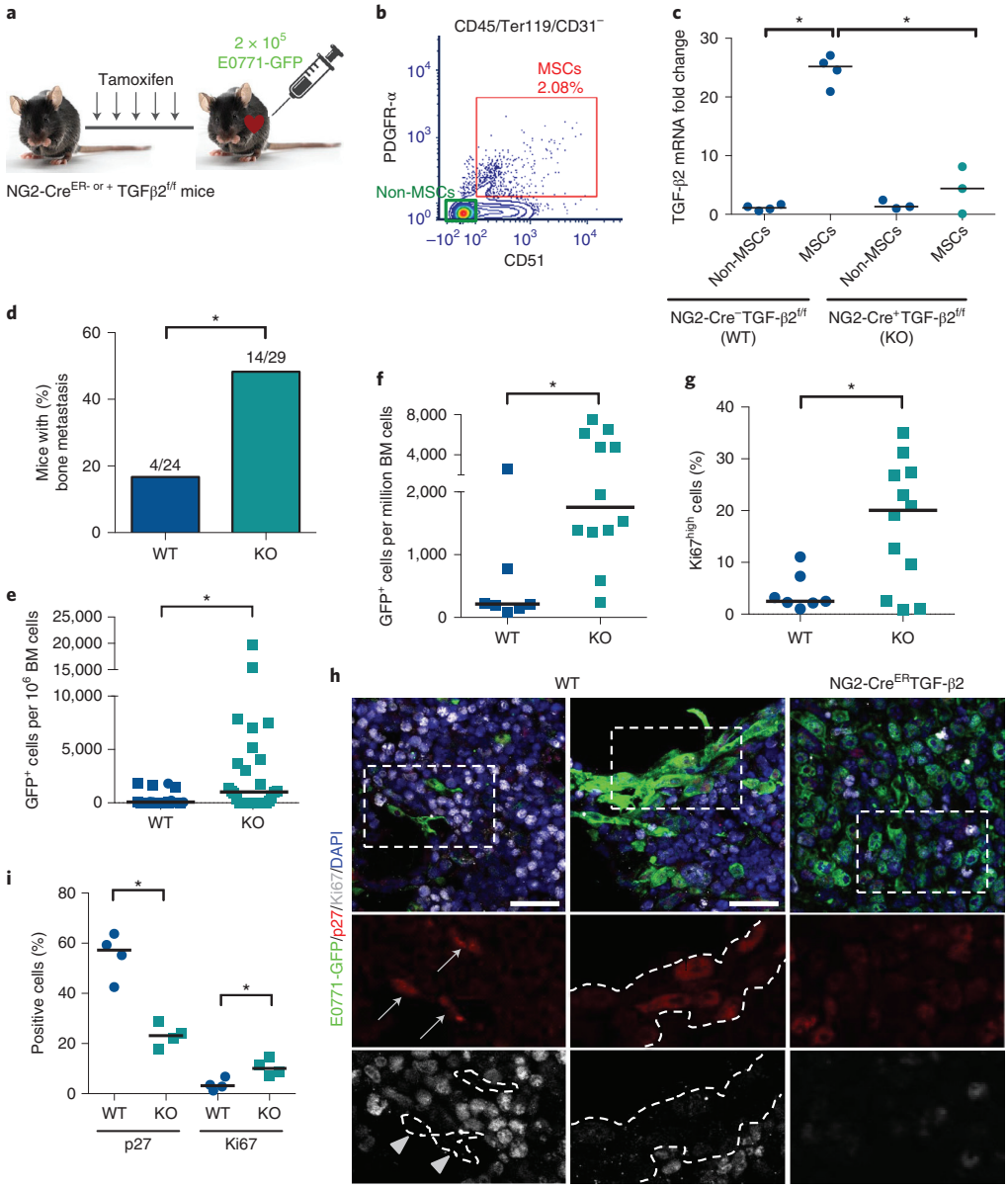

Fig. 5 | Conditional KO of TGF-β2 in NG2$^+$/Nestin$^+$ MSCs awakens dormant DTCs in the BM. a, The 7-week-old NG2-Cre^{ER-} or -Cre^{ER+} TGF-β2$^{f/f}$ mice were intraperitoneally (i.p.) treated daily with TAM for 5 d followed by intracardiac injection of 2×10^5 E0771-GFP cells. Mice were killed and organs collected 2 weeks after. **b**,**c**, Sorting strategy (**b**) and TGF-β2 mRNA levels (**c**) confirming the efficiency of TGF-β2 KO in NG2$^+$/Nestin$^+$ MSCs (sorted using CD45$^-$Ter119$^-$CD31$^-$PDGFRa$^+$CD51$^+$ markers) in NG2-Cre^{ER}TGF-β2 mice upon TAM treatments compared with WT mice ($n=4$ independent experiments, median, two-tailed Mann–Whitney *U*-tests; $P=0.014$ and 0.029). **d**, Incidence of bone metastasis (>1,000 GFP$^+$ DTCs per 10^6 BM cells) 2 weeks after cancer cell injections ($n=24$ WT and 25 KO mice from four independent experiments, two-tailed Fisher's exact test; $P=0.021$). **e**, Number of E0771-GFP cancer cells per million BM cells after BM flushing of WT and NG2-Cre^{ER}TGF-β2 mice, counted manually ($n=24$ WT and 25 KO mice from four independent experiments, median, two-tailed Mann–Whitney *U*-tests; $P=0.016$). **f**, Number of E0771-GFP cancer cells per million BM cells after BM flushing, counted by FACS ($n=7$ WT and 12 KO mice, median, two-tailed Mann–Whitney *U*-tests; $P=0.004$). **g**, Percentage of Ki67^{high} E0771-GFP cancer cells (FACS, $n=7$ and 12 mice per condition, median, two-tailed Mann–Whitney *U*-tests; $P=0.05$). **h**, Representative images of single cells and small clusters in WT and a metastasis in NG2-Cre^{ER}iDTR. Scale bars, 25 µm; arrows, positive cells; arrowheads, negative cells; dotted lines, GFP$^+$ cells border. **i**, Percentage of E0771-GFP cancer cells p27$^+$ ($P=0.029$) and Ki67$^+$ ($P=0.029$) detected by immunofluorescence ($n=4$ WT and 4 KO mice, median, two-tailed Mann–Whitney *U*-tests). $^*P\leq0.05$, *P* values indicated above.

Mechanistic analysis revealed that growth suppression was not due to apoptosis in the co-cultures (measured by cleaved caspase-3 (c-Cas3) levels), but due to a reduction in phosphorylated retinoblastoma protein levels and increase in p-ATF2 (a p38-pathway target) and p27 only observed in the cells co-cultured with Nestin-GFP$^+$ MSCs (Fig. 4c–f) or treated with TGF-β2, BMP7 or TGF-β2$^{+/+}$ BM-CM (Extended Data Fig. 3e–k). These changes were more evident in solitary E0771 cells, suggesting that in this state, cancer cells may be

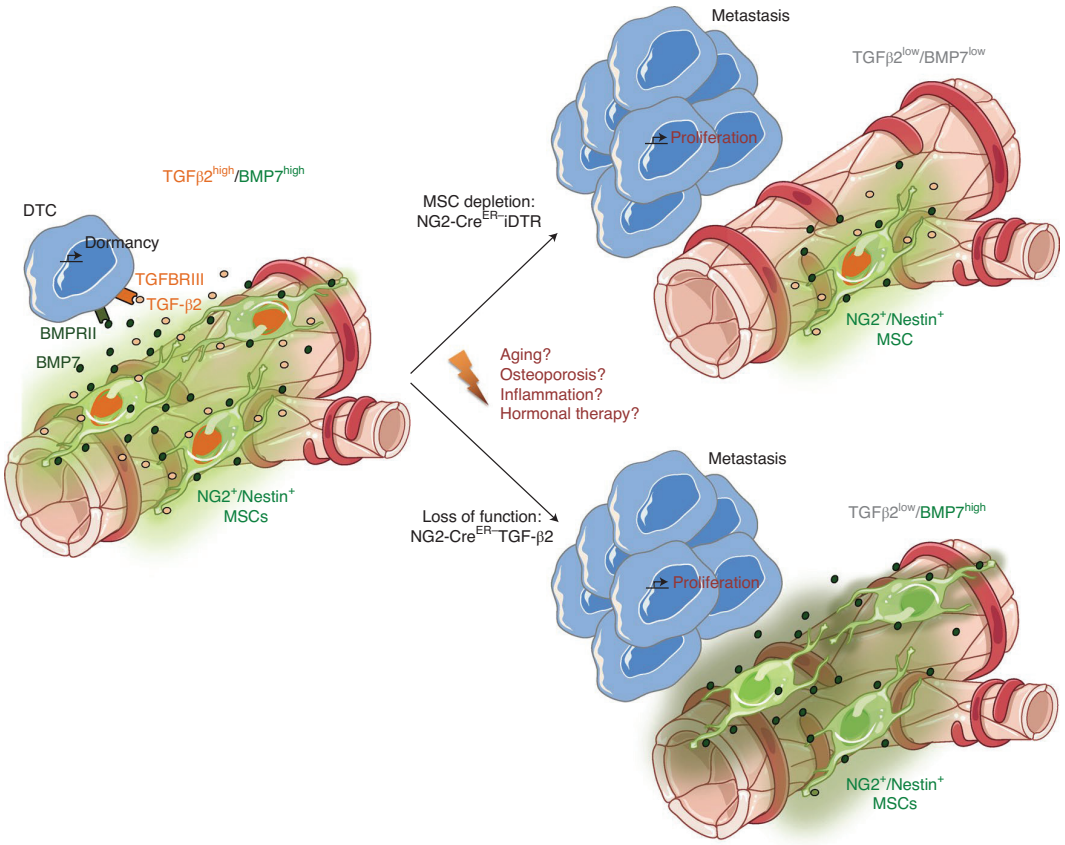

Fig. 6 | Schematic representation of the model by which HSC niches induce dormancy of BC DTCs in the BM. We propose that niches that control HSC dormancy, such as NG2$^+$/Nestin$^+$ MSCs, are responsible for producing TGF-β2 and BMP7 and inducing BC DTC dormancy in the BM (left). Upon a reduction in the number of NG2$^+$/Nestin$^+$ MSCs (top right) or in the production of TGF-β2 by MSCs (bottom right), the homeostatic control is lost, dormancy is interrupted and metastatic growth ensues. We hypothesize that perturbations of this niche caused by aging, osteoporosis or other alterations (center), may cause the niche to reduce its homeostatic control and allow for awakening of dormant DTCs in the BM. Individual elements of this original scheme were adapted from https://smart.servier.com following the terms of use and copyright license that authorize the use of their images.

more responsive to dormancy cues. Notably, TGF-β2 and BMP7 on their own could induce these molecular changes supporting that the Nestin-GFP$^+$ MSCs may be activating these pathways through those cues. These results were corroborated using biochemical approaches, which showed that in two-dimensional cultures of E0771 cells, TGF-β2 and BMP7 activated SMAD2 and SMAD1/5 phosphorylation, respectively and that both converged on the phosphorylation of ATF2 and upregulation of p27 protein levels (Extended Data Fig. 3l), required for dormancy onset[10]. BM-CM from WT TGF-β2 mice led to similar changes in p-SMAD2, p-ATF2 and p27 (Extended Data Fig. 3l) as observed in response to TGF-β2 and BMP7; however, BM-CM from mice heterozygous for TGF-β2 ($^{+/-}$) still activated these pathways suggesting that loss of one TGF-β2 allele cannot fully eliminate the immediate response on the pathway activation within a few hours, but it can reduce the proliferative response over longer periods of treatment (Extended Data Fig. 3h).

Having established that E0771 cells were responsive to TGF-β2 and BMP7 and that Nestin-GFP$^+$ MSCs produce these factors, we tested whether the MSC effect was contact dependent and if growth suppression was indeed linked to signaling downstream of these cues. To this end, we used T-HEp3 cells engineered to express an ELK–GAL4::hrGFP biosensor to monitor ERK activity[43], a p38 shuttle-clover biosensor that shows clover cytoplasmic over nuclear signal when p38 is active[44] and a p27K–mVenus reporter, where protein is stabilized and accumulated in the nucleus upon growth arrest[45]. T-HEp3-biosensor cells were transfected with short interfering (si)RNAs for TGFBRIII and BMPRII (Extended Data Fig. 4a) and then cultured in the bottom of plates while Nestin-GFP$^-$ or Nestin-GFP$^+$ cells were plated in upper level of the Transwells. These experiments showed that Nestin-GFP$^-$ cells do not lead to differences in cancer cell ERK, p38 or p27 biosensor activities and that TGFBRIII and BMPRII knockdown also do not change basal biosensors activities (Fig. 4g–j). In contrast, Nestin-GFP$^+$ MSCs led to statistically significant induction of p38 and p27 activity in cancer cells, even without being in direct contact, and these activations were completely negated by knockdown of TGFBRIII and BMPRII. Accordingly, Nestin-GFP$^+$ MSCs statistically significantly reduced ERK activity in cancer cells, which was also reversed by TGFBRIII, but not statistically significant by BMPRII knockdown (Fig. 4g–j). Both TGF-β2 and BMP7 activated the p27 and p38 biosensors while inhibiting ELK activity in cancer cells (Extended Data Fig. 4b–d), supporting that they are faithful reporters and that Nestin-GFP$^+$ MSCs can directly modulate key dormancy pathways via TGF-β2 and BMP7. In all cases, TGF-β2- or BMP7-dependent effects were reversed by knockdown of TGFBRIII in the case of TGF-β2, and BMPRII in the case of BMP7 (Extended Data Fig. 4b–d). The above results provide strong evidence supporting that NG2$^+$/Nestin$^+$ MSCs secrete TGF-β2 and BMP7 to inhibit the mitogenic (ERK1/2) pathway and activate the growth arrest (p38 and p27) pathway.

The ability of long-term cultured NG2$^+$/Nestin$^+$ MSC niche cells to maintain HSC self-renewal ex vivo is markedly diminished due to loss of the expression of niche factors in cultured MSCs[42]. The loss of these factors is also observed in MSCs passaged 3–5 times in culture[42] (MSCs Ct); however, revitalized MSCs (rMSCs) engineered to express *Klf7*, *Ostf1*, *Xbp1*, *Irf3* and *Irf7* restore the synthesis of HSC niche factors of BM-derived cultured MSCs[42]. Notably, passaged NG2$^+$/Nestin$^+$ MSCs (MSCs Ct, MSCs kept in culture for 3–5 passages that show loss of function) were not able to suppress growth of E0771 cancer cells. In contrast, rMSCs that have the ability to maintain HSC self-renewal ex vivo were able to suppress proliferation of E0771 cells (Extended Data Fig. 4e), which correlated with the specific upregulation of TGF-β2 (not TGF-β1) and BMP7 in rMSCs comparted to control MSCs (Extended Data Fig. 4f). These data further support that functional NG2$^+$/Nestin$^+$ MSCs are able to suppress cancer cell growth and that alterations of these cells may impair their dormancy-inducing function.

Conditional deletion of TGF-β2 in NG2$^+$/Nestin$^+$ MSCs triggers DTC escape from dormancy in the BM. The above experiments support strong evidence that NG2$^+$/Nestin$^+$ MSCs are critical for cancer cell dormancy onset and maintenance in the BM niche (Fig. 1). Additionally, we provide evidence that these MSCs produce abundant amounts of TGF-β2 and BMP7 (Fig. 3) and that they activate dormancy signaling pathways in cancer cells (Fig. 4). However, these experiments still do not prove that dormancy cues derived from NG2$^+$/Nestin$^+$ MSCs in the niche in vivo are required for dormancy. To address this missing link, we focused on TGF-β2 because of our knowledge on the role of this cytokine in dormancy induction and its higher levels in NG2$^+$/Nestin$^+$ MSCs (Fig. 3a and elsewhere[39]).

We crossed NG2-Cre^{ER} mice with TGF-β2^{flox} mice to generate specific conditional deletion of this cytokine in the NG2 lineage. We confirmed decreased levels of TGF-β2 in NG2$^+$/Nestin$^+$ MSCs (sorted CD45$^-$Ter119$^-$CD31$^-$PDGFRa$^+$CD51$^+$ MSCs, which contain NG2$^+$/Nestin$^+$ MSCs) from the BM of NG2-Cre^{ER}TGF-β2 mice with TAM induction (Fig. 5a–c), but no differences in TGF-β1 levels, supporting the specificity of gene disruption (Extended Data Fig. 5a). Although the NG2-Cre^{ER} driver is mainly restricted to periarteriolar Nestin-GFP$^+$ stromal cells, it can also be detected in chondrocytes, osteocytes and rarely in osteoblasts[46,47]. To determine whether the conditional KO strategy that we selected may impact TGF-β2 in those cells, we sorted MSCs, OPCs and ECs from WT and NG2-Cre^{ER}TGF-β2 (KO) mice. Only TGF-β2 levels in MSCs decreased significantly upon TAM treatment, supporting that the depletion is specific for TGF-β2 in MSCs (Extended Data Fig. 5b). To test whether disruption of TGF-β2 production in the NG2$^+$/Nestin$^+$ MSC niche in NG2-Cre^{ER}TGF-β2 mice would affect DTC behavior we injected E0771-GFP cells into the left ventricle of the heart of animals and killed them 2 weeks later. All mice had detectable E0771-GFP$^+$ DTCs in the BM by FACS (Fig. 5f), corroborating the injection efficiency. However, only ~16% (4 out of 24) of WT mice showed >1,000 DTCs per million BM cells (manually counted after BM flush), whereas 48% (14 out of 29) of NG2-Cre^{ER}TGF-β2 (KO) mice displayed a build-up of E0771-GFP$^+$ colonies in the BM (Fig. 5d). Consistently, quantification of the DTC burden (both manual counting (Fig. 5e) and by FACS (Fig. 5f)) showed an increase in number of DTCs in the BM compartment of TGF-β2 KO mice compared with WT. Additional analysis revealed that metastatic masses in TGF-β2 KO mice showed a decrease in the percentage of p27$^+$ cells (23%) and an increase in the number of Ki67$^+$cells (10%) compared to solitary DTCs and small DTC clusters in WT mice (57% p27$^+$ and 3% Ki67$^+$) (Fig. 5h,i). A similar difference was found by FACS staining of Ki67, where we found an increase in the percentage of E0771-GFP$^+$Ki67^{high} cells (Fig. 5g). We conclude that niches containing NG2$^+$/Nestin$^+$ MSCs and that produce TGF-β2 are required for BC cell dormancy induction in the BM compartment.

Discussion

Building on previous studies[11,20], we show that the BM perivascular niche plays an important role in DTC dormancy. However, here we make a leap in our understanding of this biology by revealing a specific BM cell type, namely NG2$^+$/Nestin$^+$ MSCs, which maintains both HSC[27] and DTC dormancy in this organ. We further reveal the mechanism behind this biology, where NG2$^+$/Nestin$^+$ MSCs secrete TGF-β2 and BMP7 to signal through TGFBRIII and BMPRII leading to activation of SMAD, p38 and p27 pathways and cancer dormancy. Our work provides functional evidence for the long-held notion that HSC dormancy niches support DTC dormancy. Our findings are also deeply linked to the 'seed and soil' theory of metastasis[48]. However, our findings reshape this paradigm to show that the 'seed and soil' relationship in BM is not for growth of DTCs but rather for the induction and maintenance of dormancy. In fact, our data support that when the 'soil' is negatively altered metastasis ensue. Thus, certain organs rather than being a proper 'soil' for metastasis may indeed be homeostatic and their normal function as the 'soil' is pro-dormancy; when they are altered or damaged they lose their metastasis suppressing function.

Despite our efforts, the low number of DTCs in the majority of control mice (150–400 DTCs per million BM cells) we used precluded mapping statistically their location in relation to vascular structures. Thus, we focused on a functional analysis. We now identify the active role of NG2$^+$/Nestin$^+$ MSCs in inducing and maintaining DTC dormancy in vivo. We went a step further and proved in vivo the crucial role of TGF-β2 produced by NG2$^+$/Nestin$^+$ MSCs. Future studies will test the function of BMP7 in these and other BM cells. Our data also suggest that NG2$^+$/Nestin$^+$ MSC-regulated niches are primarily pro-dormancy rather than only pro-survival, otherwise when the niche was disrupted in the NG2-Cre^{ER}iDTR model, we would see DTC clearance instead of reactivation. However, it is possible that oncogenic signaling in the E0771 cells (K-Ras (activating), MKK4 and p53 (both inactivating mutants))[49] provide absent survival signals that could be altered when we eliminate NG2$^+$/Nestin$^+$ MSCs. It is interesting that even carrying MKK4 (p38 and JNK upstream activator) and p53-inactivating mutations (and K-Ras active mutant) E0771 efficiently activated p38 signaling and CDK inhibitors expression. Perhaps TGF-β2 and BMP7 signaling is more reliant on MKK3/6 signaling for p38 activation. It also supports that niche cues can override potent oncogene signaling, further solidifying the notion that microenvironmental mechanisms may be dominant over genetics[50,51] if cancer cells can still 'read' host homeostatic signals.

We also report no major differences in vessel permeability, abundance of pro-inflammatory cytokines and DTC early seeding after NG2$^+$/Nestin$^+$ MSC depletion. Thus, the enhanced DTC growth in NG2$^+$/Nestin$^+$ MSCs depleted before or after seeding in the BM was not due to a seeding/colonization phenotype or a widespread inflammatory response. However, we cannot rule out that circumscribed and limited inflammation in the sites where the DT kills the iDTR-expressing NG2$^+$/Nestin$^+$ MSCs, could lead to tumor cell awakening. An important next question will be to define how cancer cells with different genetics and from different cancer types might affect the HSC niche to support or block a positive loop feeding dormancy of both HSC and DTCs in a homeostatic normal-like BM environment. Our results may also start to define which genetic alterations may allow cancer cells to escape microenvironmental control by NG2$^+$/Nestin$^+$ MSCs. For example, genetic alterations that affect TGFBRIII[52–54] and BMPRII[13,55] have been linked to increased bone metastasis in breast and prostate cancer, indicating that such alterations may allow DTCs to escape homeostatic control.

These genetic changes detected in DTCs may serve as biomarkers to help monitor more closely patients at risk of relapse. To this end we provide promising data that monitoring for example BMP7 presence or absence in patients with ER$^+$ BC can inform on the time to metastatic relapse. Patients that presumably had intact or functional NG2$^+$/Nestin$^+$ MSC and/or other niches and had detectable BMP7 were less prone to develop metastasis.

It is important to highlight that different cell types may produce the same or other dormancy cues, as we observed that OPCs also make TGF-β2 (Fig. 3b) and Nestin-GFP$^-$ cells slightly increase cancer cell growth arrest (Fig. 4b). Also, the driver we used, NG2-Cre^{ER}, is mainly restricted to MSCs but it can also target chondrocytes, osteocytes and few osteoblasts (data not shown and reported elsewhere[47]). However, our data from NG2-Cre^{ER}TGF-β2 mice supports that the NG2-Cre^{ER} promoter is restricted to MSCs and not OPCs or ECs. Thus, the loss of TGF-β2 in NG2$^+$/Nestin$^+$ MSCs is the main change that allows cancer cell to avoid entering dormancy in the BM. However, our experimental design did not allow testing the direct role of TGF-β2 produced by MSCs in dormancy maintenance. It is possible, as other cell types in the BM niche are also key contributors to the pro-dormancy HSC niche. To this end, it was previously described that osteoblasts are also a source of TGF-β2 (refs. [22,39]), but in our mouse models these cells do not seem to compensate for the loss of TGF-β2 in NG2$^+$/Nestin$^+$ MSCs or for the 50% loss of NG2$^+$/Nestin$^+$ MSCs after DT treatment. NG2$^+$/Nestin$^+$ MSCs may also produce additional factors to TGF-β2 and BMP7, which would explain why the penetrance of the phenotype seems greater when we compare DTC burden in the NG2-Cre^{ER}iDTR model (Fig. 1) versus NG2-Cre^{ER}TGF-β2 (Fig. 5).

It is known that aging affects the proper function of HSC niches by downregulation of niche factors by passaged MSCs[42] and that in aged mice the BM microenvironment shows lower levels of TGF-β2 and BMP7 (ref. [56]). Our results offer a new opportunity to understand how aging, inflammation and the cancer cells themselves may alter MSCs functionality leading to a disruption of the BM pro-dormancy niche, DTC awakening and bone metastasis formation (Fig. 6). Finally, a remaining question, but beyond the scope of our study, is whether the function of NG2$^+$/Nestin$^+$ MSCs as pro-dormancy niche orchestrators is limited to the BM or whether it has similar roles in other metastasis target organs. Overall, we propose that this work shifts our understanding on how homeostatic mechanisms that control adult stem cell quiescence may govern dormancy of disseminated cancer cells and control the timing of metastasis. Our work reshapes the paradigm of metastasis by revealing how the homeostatic BM microenvironment actually serves mainly as a metastasis suppressive 'soil' via dormancy induction.

Methods

Animals. Nes-GFP[57] mice were bred in and obtained from the Frenette's laboratory at the Albert Einstein Institute. B6.Cg-Tg(Cspg4-cre/Esr1*)BAkik/J (NG2-Cre^{ER}, Jackson Laboratory, stock 008538), C57BL/6-Gt(ROSA)26 Sortm1(HBEGF) Awai/J (iDTR, Jackson Laboratory, stock 007900) and TGFβ2^{flox} ([58] a gift from Mohamad Azhar's laboratory) were maintained on the C57BL/6J background and bred and crossed in our facilities. Mice were kept at 20–26 °C, 30–70% humidity, 12-h dark/light cycles, with food (LabDiet 5053 rodent diet) and water (reverse osmosis water) accessible at all times. All experimental procedures were approved by the Institutional Animal Care and Use Committee of Icahn School of Medicine at Mount Sinai. All NG2-Cre^{ER}iDTR and NG2-Cre^{ER}TGF-β2 mice were genotyped using the primers listed below, number-tagged and allocated according with their genotype. The 7–8-week-old female mice were used in all experiments. Primers were: NG2-Cre^{ER} F, TTAATCCATATTGGCAGAACGAAAACG; NG2-Cre^{ER} R, CAGGCTAAGTGCCTTCTCTACA; DTR F, ACGGAGAATGCAAATATGT GAAGGA; DTR R, ACACCTCTCTCCATGGTAACCT; ROSA WT F, TTCCCTC GTGATCTGCAACTC; ROSA WT R, CTTTAAGCCTGCCCAGAAGACT; TGFβ2$^{f/f}$ F, GCTGGCGCCGGAAC; TGFβ2$^{f/f}$ R, GCGACTATAGAGATATCAACCACTTTGT; TGFβ2 WT F, TGGCCTAGAAAGCCAGATTACAC; and TGFβ2 WT F, GGAGAGGCGAGTAAAGGAGAAG.

Induction of NG2-Cre^{ER}-mediated recombination and iDTR-mediated cell depletion. The 7–8-week-old female mice were injected i.p. with 2 mg of TAM (Sigma, T5648) dissolved in corn oil daily for 5 d to induce the Cre^{ER}-mediated recombination. In case of NG2-Cre^{ER}iDTR, mice were also injected i.p. with 250 ng of DT (Millipore, 322326) dissolved in serum chloride daily for 2 d for iDTR-mediated cell depletion.

Metastasis assays. A total of 2×10^5 E0771-GFP or MMTV-PyMT-CFP cells were intracardiac injected with echo-guidance using micro ultrasound Vevo2100, Transducer MS-250, 21 MHz and Vevo LAB 3.1.1 software (FUJIFILM VisualSonics; Supplementary Movie 1). At 24 h or 2 weeks later, mice were killed and organs were collected and processed. In a group of mice, 70,000 MW lysine fixable dextran–Texas Red (Invitrogen) was retro-orbital injected 15 min before mice were killed and perfused with PBS. BM cells were flushed from femurs and tibias, red-blood-cell lysis buffer (Lonza) was used for 2 min followed by quantification of GFP$^+$ cells and normalization to the total number of BM cells.

Flow cytometry and cell sorting. BM cells were flushed, incubated in red-blood-cell lysis buffer (Lonza) for 2 min and remaining cells were permeabilized with 0.05% Triton (when using intracellular antibodies) and stained using antibodies and dilutions described in the Nature Research Reporting Summary linked to this article for 15 min at 4 °C in the dark. In the case of host BM cell sorting (Nestin-GFP, MSCs, OPCs and ECs), 3–4 mice cells were pooled per experiment and condition. All experiments were performed using BD FACSAria II equipped with FACS Diva software (BD Biosciences). Dead cells and debris were excluded by FSC, SSC and DAPI (Thermo Fisher Scientific) staining profiles. Data were analyzed with FACS Diva (BD Biosciences) or FSC Express Cytometry 7 (De Novo) software.

Histopathology. After dissection, bones were fixed in 4% paraformaldehyde (PFA; Thermo Fisher Scientific) for 24 h. Bones were then decalcified in 14% EDTA, renewed every other day for 7–10 d at 4 °C with agitation. Bones were processed, embedded in paraffin and sections were cut. H&E and immunofluorescences were performed and slides were scanned using NanoZoomer S60 Digital slide scanner and NDP.view2 software (Hamamatsu).

Immunofluorescence. Tissue sections were submitted to hydration in xylene and a graded alcohol series, slides were steamed in 10 mM citrate buffer (pH 6) for 40 min for antigen retrieval. Fixed 3D cultures were permeabilized using 0.5% Triton X-100 in PBS for 20 min. Both sections and co-cultures were blocked with 3% bovine serum albumin (BSA; Fisher Bioreagents) and 5% normal goat serum (Gibco PCN5000) in PBS for 1 h at room temperature. Primary antibodies described in the Nature Research Reporting Summary linked to this article were incubated overnight at 4 °C, followed by washing and secondary antibodies (Invitrogen, 1:1,000 dilution) incubation at room temperature for 1 h in the dark. Slides were mounted with ProLong Gold Antifade reagent with DAPI (Invitrogen, P36931) and images were obtained using Leica Software on a Leica SPE confocal microscope. All quantifications were performed using a double-blind method (quantification of coded samples and de-codification upon completion to interpret the results across multiple animals).

Whole-mount staining. Calvaria bones were fixed overnight at 4 °C in 4% PFA, blocked overnight with agitation in 3% BSA–5% normal goat serum, followed by a 24-h incubation at 4 °C with agitation with primary antibodies and dilutions described in the Nature Research Reporting Summary linked to this article. Washing for 10 h was followed by secondary antibody (Invitrogen, 1:1,000 dilution) incubation at 4 °C, overnight with agitation and 10-h wash. Images were obtained using Leica Software on a Leica SPE confocal microscope.

Sternal bones were collected and transected with a surgical blade into 2–3 fragments, 10 min after retro-orbital injection of antibodies and dilutions described in the Nature Research Reporting Summary linked to this article. The fragments were bisected sagittally for the BM cavity to be exposed, fixed in 4% PFA and immunofluorescence staining was performed as described above. Images were acquired using a ZEISS AXIO examiner D1 microscope (Zeiss) with a confocal scanner unit, CSUX1CU (Yokogawa).

Quantitative PCR. Sorted cells were processed using Cell-to-CT 1-Step Power SYBR Green kit (Invitrogen, A25600). GAPDH was used as housekeeping control for all experiments. Primers were: mouse TGF-β1 F, CCT GAG TGG CTG TCT TTT GA; mouse TGF-β1 R, GCT GAA TCG AAA GCC CTG TA; mouse TGF-β2 F, TAA AAT CGA CAT GCC GTC CC; mouse TGF-β2 R, GAG ACA TCA AAG CGG ACG AT; mouse BMP2 F, TGG AAG TGG CCC ATT TAG AG; mouse BMP2 R, TGA CGC TTT TCT CGT TTG TG; mouse BMP7 F, GAA AAC AGC AGC AGT GAC CA; mouse BMP7 R, GGT GGC GTT CAT GTA GGA GT; mouse GAPDH F, AAC TTT GGC ATT GTG GAA GGG CTC; and mouse GAPDH R, TGG AAG AGT GGG AGT TGC TGT TGA.

Human samples. The BM plasma samples analyzed for TGF-β2 and BMP7 were 55 females selected from patients with early BC included in the SATT study[9], between 18 and 65 years old (median age 48 years). In this study the patients with early BC, who had completed adjuvant chemotherapy, were monitored for

DTCs 2–3 months (BM1) and 8–9 months (BM2) after completion of adjuvant anthracycline-containing chemotherapy. If DTC-positive at 8–9 months, the patients received secondary chemotherapy intervention with docetaxel, followed by subsequent DTC monitoring 1 (BM3) and 12 months (BM4) after docetaxel. Patients with disappearance of DTCs (80%) experienced excellent prognosis compared to the patients with DTC persistence (20%)[9]. BM aspirates (from posterior iliac crest bilaterally) collected for DTC analyses were diluted 1:1 in PBS and separated by density centrifugation using Lymphoprep (Axis-Shield) as previously described[9]. Later on in the inclusion period the plasma supernatant after density centrifugation was collected (if possible) and stored initially at −20 °C and later transferred to −80 °C. From the available BM plasma samples, we initially performed a limited analysis of plasma samples from patients being DTC-positive at either BM1 or BM2 or experiencing systemic relapse without DTC presence. Of these, 55 had ER^+ disease, including 30 patients receiving secondary intervention with docetaxel chemotherapy and 25 patients with no secondary treatment intervention. The original SATT study[9] was approved by the Research Committee at the Cancer Clinic, Oslo University Hospital and by the Regional Ethical Committee (ref. no. S-03032). Written informed consent was obtained from all patients. The study is registered in Clinical Trials Gov (registration number NCT00248703). Use and analysis of these samples in the present study is covered by these originally obtained approvals and written informed consent.

ELISA. Mouse BM supernatant was collected after BM flush centrifugation and stored at −80 °C with phosphatase and protease inhibitors (Thermo Fisher Scientific). TGF-β and pro-inflammatory ELISAs were performed by Eve Technologies using the Luminex 100 and 200 systems (Luminex), Eve Technologies' TFG-β 3-Plex Discovery Assay (MilliporeSigma) and Eve Technologies' Mouse Focused 10-Plex Discovery Assay (MilliporeSigma). BMP7 ELISA was performed using RayBio kit (RayBio, ELM-BMP7) following manufacturer's instructions.

Patient BM supernatants were analyzed for TGF-β2 and BMP7 by multiplex ELISA at Human Immune Monitoring Center at Mount Sinai. ELISA assays were performed using human TGF-β2 (R & D System, DY302) and BMP7 (R & D System, DY354) kits following manufacture's recommendation. Data were analyzed using a Four Parameter Logistic Fit method.

Cell culture. E0771 (CH3 BioSystems), E0771-GFP (a gift from John Condeelis' laboratory) and MMTV-PyMT-CFP (a gift from J. Debnath) BC cell lines were cultured in RPMI (Gibco) supplemented with 10% fetal bovine serum (Gemini), 10 mM HEPES (Corning), 100 U ml^{-1} penicillin and 100 µg ml^{-1} streptomycin (Corning). The tumorigenic HEp3 (T-HEp3)[59] head and neck squamous cell carcinoma patient-derived xenograft line and Ct MSCs and rMSCs[42] were generated and maintained as described previously.

T-HEp3 cells were engineered to express an ELK–GAL4::hrGFP[43], p38 shuttle-clover[44] and p27K–mVenus[45] biosensors. T-HEp3 cells with the biosensors were reversely transfected with siRNAs (siTGFBRIII, Invitrogen 32274204; siBMPRII, Oncogene SR300456B) using Lipofectamine RNAiMAX transfection reagent (Invitrogen) according to the manufacturer's instructions.

Transwell co-cultures were performed using permeable Transwell assays (Corning), in which transfected cells were plated in the bottom of the well and sorted by Nestin-GFP^- or -GFP^+ cells in the permeable inserts.

Low-density 3D organoid co-cultures. A total of 500–1,000 cells (E0771 only or with MSCs) were seeded in 400 µl assay medium (each cell line medium with reduced fetal bovine serum content (2–5%) plus 2% Matrigel) in eight-well chamber slides (Falcon) on top of 50 µl of growth factor-reduced Matrigel (Corning). Cultures were treated every 24 h starting at day 0 with TGF-β2 (R&D), BMP7 (R&D) or BM-CM. SCs, doublets and clusters were quantified after 4 d and the cultures were fixed with 4% PFA for 20 min.

Western blot. Samples were collected in RIPA buffer and protein concentrations were calculated using Coomassie Plus protein assay (Thermo Fisher Scientific) and a standard BSA curve. Samples were boiled for 8 min at 95 °C in sample buffer (0.04 M Tris-HCl (pH 6.8), 1% SDS, 1% β-mercaptoethanol and 10% glycerol). The 8–10% SDS–PAGE gradient gels were run in running buffer (25 mM Tris, 190 mM glycine, 0.1% SDS) and transferred to PVDF membranes in transfer buffer (25 mM Tris, 190 mM glycine, 20% methanol). Membranes were blocked in 5% milk in TBS-T (Tris-buffered saline containing Tween-20) buffer. Primary antibodies described in the Nature Research Reporting Summary linked to this article were incubated overnight at 4 °C and washed with TBS-T buffer. HRP-conjugated secondary antibodies were left at room temperature for 1 h and washed with TBS-T buffer. Western blot development was performed using Amersham ECL Western Blot Detection (GE, RPN 2106) and GE ImageQuant LAS 4010.

Statistics and reproducibility. Sample sizes were chosen empirically; no statistical method was used to predetermine sample size and no exclusion criteria were applied. The experiments were not randomized, mice were number-tagged and quantifications were performed in coded samples to reduce operator bias. Statistical analyses were conducted using Prism software and differences were considered significant if $P < 0.05$. Unless otherwise specified, three or more independent experiments were performed, all values were included and median, interquartile range and two-tailed Mann–Whitney *U*-tests, incidence and Fisher's exact test or mean and s.e.m. and two-tailed Student's *t*-tests were performed.

Reporting Summary. Further information on research design is available in the Nature Research Reporting Summary linked to this article.

Data availability

The data generated during the current study that support the reported findings are available in the manuscript, including in the provided Source Data files and from the corresponding author on reasonable request. Source data are provided with this paper.

Received: 13 October 2020; Accepted: 28 January 2021;
Published online: 11 March 2021

References

1. Chaffer, C. L. & Weinberg, R. A. A perspective on cancer cell metastasis. *Science* **331**, 1559–1564 (2011).
2. Sherry, M. M., Greco, F. A., Johnson, D. H. & Hainsworth, J. D. Metastatic breast cancer confined to the skeletal system. An indolent disease. *Am. J. Med.* **81**, 381–386 (1986).
3. Engel, J. et al. The process of metastasisation for breast cancer. *Eur. J. Cancer* **39**, 1794–1806 (2003).
4. Husemann, Y. et al. Systemic spread is an early step in breast cancer. *Cancer Cell* **13**, 58–68 (2008).
5. Sanger, N. et al. Disseminated tumor cells in the bone marrow of patients with ductal carcinoma in situ. *Int. J. Cancer* https://doi.org/10.1002/ijc.25895 (2011).
6. Braun, S. et al. Cytokeratin-positive cells in the bone marrow and survival of patients with stage I, II, or III breast cancer. *N. Engl. J. Med.* https://doi.org/10.1056/NEJM200002243420801 (2000).
7. Chéry, L. et al. Characterization of single disseminated prostate cancer cells reveals tumor cell heterogeneity and identifies dormancy associated pathways. *Oncotarget* **5**, 9939–9951 (2014).
8. Borgen, E. et al. NR2F1 stratifies dormant disseminated tumor cells in breast cancer patients. *Breast Cancer Res.* https://doi.org/10.1186/s13058-018-1049-0(2018).
9. Naume, B. et al. Clinical outcome with correlation to disseminated tumor cell (DTC) status after DTC-guided secondary adjuvant treatment with docetaxel in early breast cancer. *J. Clin. Oncol.* **32**, 3848–3857 (2014).
10. Bragado, P. et al. TGF-β2 dictates disseminated tumour cell fate in target organs through TGF-β-RIII and p38α/β signalling. *Nat. Cell Biol.* **15**, 1351–1361 (2013).
11. Carlson, P. et al. Targeting the perivascular niche sensitizes disseminated tumour cells to chemotherapy. *Nat. Cell Biol.* https://doi.org/10.1038/s41556-018-0267-0 (2019).
12. Johnson, R. W. et al. Induction of LIFR confers a dormancy phenotype in breast cancer cells disseminated to the bone marrow. *Nat. Cell Biol.* **18**, 1078–1089 (2016).
13. Kobayashi, A. et al. Bone morphogenetic protein 7 in dormancy and metastasis of prostate cancer stem-like cells in bone. *J. Exp. Med.* **208**, 2641–2655 (2011).
14. Gao, H. et al. The BMP inhibitor Coco reactivates breast cancer cells at lung metastatic sites. *Cell* **150**, 764–779 (2012).
15. Taichman, R. S. et al. GAS6 receptor status is associated with dormancy and bone metastatic tumor formation. *PLoS ONE* **8**, e61873 (2013).
16. Yumoto, K. et al. Axl is required for TGF-β2-induced dormancy of prostate cancer cells in the bone marrow. *Sci. Rep.* **6**, 36520 (2016).
17. Jung, Y. et al. Endogenous GAS6 and Mer receptor signaling regulate prostate cancer stem cells in bone marrow. *Oncotarget* **7**, 25698–25711 (2016).
18. Yue, X. et al. Leukemia inhibitory factor promotes EMT through STAT3-dependent miR-21 induction. *Oncotarget* https://doi.org/10.18632/oncotarget.6756 (2015).
19. Agarwal, P. et al. Mesenchymal niche-specific expression of Cxcl12 controls quiescence of treatment-resistant leukemia stem cells. *Cell Stem Cell* **24**, 769–784 (2019).
20. Ghajar, C. M. et al. The perivascular niche regulates breast tumour dormancy. *Nat. Cell Biol.* **15**, 807–817 (2013).
21. Lawson, M. A. et al. Osteoclasts control reactivation of dormant myeloma cells by remodelling the endosteal niche. *Nat. Commun.* https://doi.org/10.1038/ncomms9983 (2015).
22. Yu-Lee, L. Y. et al. Osteoblast-secreted factors mediate dormancy of metastatic prostate cancer in the bone via activation of the TGFbRIII–p38MAPK–pS249/ T252RB pathway. *Cancer Res.* **78**, 2911–2924 (2018).
23. Cackowski, F. C. & Taichman, R. S. Parallels between hematopoietic stem cell and prostate cancer disseminated tumor cell regulation. *Bone.* **119**, 82–86 (2019).

24. Shiozawa, Y. et al. Human prostate cancer metastases target the hematopoietic stem cell niche to establish footholds in mouse bone marrow. *J. Clin. Invest.* **121**, 1298–1312 (2011).
25. Wilson, A. et al. Hematopoietic stem cells reversibly switch from dormancy to self-renewal during homeostasis and repair. *Cell* **135**, 1118–1129 (2008).
26. Pinho, S. & Frenette, P. S. Haematopoietic stem cell activity and interactions with the niche. *Nat. Rev. Mol. Cell Biol.* **20**, 303–320 (2019).
27. Kunisaki, Y. et al. Arteriolar niches maintain haematopoietic stem cell quiescence. *Nature* **502**, 637–643 (2013).
28. Hanoun, M. et al. Acute myelogenous leukemia-induced sympathetic neuropathy promotes malignancy in an altered hematopoietic stem cell Niche. *Cell Stem Cell* (2014) https://doi.org/10.1016/j.stem.2014.06.020
29. Maryanovich, M. et al. Adrenergic nerve degeneration in bone marrow drives aging of the hematopoietic stem cell niche. *Nat. Med.* https://doi.org/10.1038/s41591-018-0030-x (2018).
30. Harper, K. L. et al. Mechanism of early dissemination and metastasis in Her2$^+$ mammary cancer. *Nature* https://doi.org/10.1038/nature20609 (2016).
31. Pinho, S. et al. PDGFR and CD51 mark human nestin$^+$ sphere-forming mesenchymal stem cells capable of hematopoietic progenitor cell expansion. *J. Exp. Med.* **210**, 1351–1367 (2013).
32. Ranganathan, A. C., Adam, A. P., Zhang, L. & Aguirre-Ghiso, J. A. Tumor cell dormancy induced by p38SAPK and ER-stress signaling: An adaptive advantage for metastatic cells? *Cancer Biol. Ther.* https://doi.org/10.4161/cbt.5.7.2968 (2006).
33. Fluegen, G. et al. Phenotypic heterogeneity of disseminated tumour cells is preset by primary tumour hypoxic microenvironments. *Nat. Cell Biol.* **19**, 120–132 (2017).
34. Sosa, M. S. et al. NR2F1 controls tumour cell dormancy via SOX9- and RARβ-driven quiescence programmes. *Nat. Commun.* **6**, 1–14 (2015).
35. Männ, L. et al. CD11c.DTR mice develop a fatal fulminant myocarditis after local or systemic treatment with diphtheria toxin. *Eur. J. Immunol.* https://doi.org/10.1002/eji.201546245 (2016).
36. Christiaansen, A. F., Boggiatto, P. M. & Varga, S. M. Limitations of Foxp3$^+$ T_{reg} depletion following viral infection in DEREG mice. *J. Immunol. Methods* https://doi.org/10.1016/j.jim.2014.03.005 (2014).
37. Bennett, C. L. et al. Inducible ablation of mouse Langerhans cells diminishes but fails to abrogate contact hypersensitivity. *J. Cell Biol.* https://doi.org/10.1083/jcb.200501071 (2005).
38. Xu, C. et al. Stem cell factor is selectively secreted by arterial endothelial cells in bone marrow. *Nat. Commun.* https://doi.org/10.1038/s41467-018-04726-3 (2018).
39. Tikhonova, A. N. et al. The bone marrow microenvironment at single-cell resolution. *Nature* https://doi.org/10.1038/s41586-019-1104-8 (2019).
40. Vukicevic, S., Latin, V., Chen, P., Batorsky, R. & Reddi, A. H. Localization of osteogenic protein-1 (bone morphogenetic protein-7) during human embryonic development: High affinity binding to basement membranes. *Biochem. Biophys. Res. Commun.* **198**, 693–700 (1994).
41. Gregory, K. E. et al. The prodomain of BMP-7 targets the BMP-7 complex to the extracellular matrix. *J. Biol. Chem.* **280**, 27970–27980 (2005).
42. Nakahara, F. et al. Engineering a haematopoietic stem cell niche by revitalizing mesenchymal stromal cells. *Nat. Cell Biol.* https://doi.org/10.1038/s41556-019-0308-3 (2019).
43. Aguirre-Ghiso, J. A., Ossowski, L. & Rosenbaum, S. K. Green fluorescent protein tagging of extracellular signal-regulated kinase and p38 pathways reveals novel dynamics of pathway activation during primary and metastatic growth. *Cancer Res.* **64**, 7336–7345 (2004).
44. Regot, S., Hughey, J. J., Bajar, B. T., Carrasco, S. & Covert, M. W. High-sensitivity measurements of multiple kinase activities in live single cells. *Cell* **157**, 1724–1734 (2014).
45. Oki, T. et al. A novel cell-cycle-indicator, mVenus-p27K. *Sci. Rep.* **4**, 4012 (2014).
46. Asada, N. et al. Differential cytokine contributions of perivascular haematopoietic stem cell niches. *Nat. Cell Biol.* https://doi.org/10.1038/ncb3475 (2017).
47. Zhou, B. O., Yue, R., Murphy, M. M., Peyer, J. G. & Morrison, S. J. Leptin-receptor-expressing mesenchymal stromal cells represent the main source of bone formed by adult bone marrow. *Cell Stem Cell* https://doi.org/10.1016/j.stem.2014.06.008 (2014).
48. Paget, S. The distribution of secondary growths in cancer of the breast. *Lancet* https://doi.org/10.1016/S0140-6736(00)49915-0 (1889).
49. Yang, Y. et al. Immunocompetent mouse allograft models for development of therapies to target breast cancer metastasis. *Oncotarget* **8**, 30621–30643 (2017).
50. Boudreau, N. & Bissell, M. J. Extracellular matrix signaling: Integration of form and function in normal and malignant cells. *Curr. Opin. Cell Biol.* **10**, 640–646 (1998).
51. Kenny, P. A. & Bissell, M. J. Tumor reversion: Correction of malignant behavior by microenvironmental cues. *Int. J. Cancer* **107**, 688–695 (2003).
52. Turley, R. S. et al. The type III transforming growth factor-β receptor as a novel tumor suppressor gene in prostate cancer. *Cancer Res.* **67**, 1090–1098 (2007).
53. Ajiboye, S., Sissung, T. M., Sharifi, N. & Fig, W. D. More than an accessory: Implications of type III transforming growth factor-β receptor loss in prostate cancer. *BJU Int.* **105**, 913–916 (2010).
54. Dong, M. et al. The type III TGF-β receptor suppresses breast cancer progression. *J. Clin. Invest.* **117**, 206–217 (2007).
55. Kim, I. Y. et al. Loss of expression of bone morphogenetic protein receptor type II in human prostate cancer cells. *Oncogene* **23**, 7651–7659 (2004).
56. Singh, A. et al. Angiocrine signals regulate quiescence and therapy resistance in bone metastasis. *JCI Insight* https://doi.org/10.1172/jci.insight.125679 (2019).
57. Mignone, J. L., Kukekov, V., Chiang, A. S., Steindler, D. & Enikolopov, G. Neural stem and progenitor cells in nestin-GFP transgenic mice. *J. Comp. Neurol.* **469**, 311–324 (2004).
58. Ishtiaq Ahmed, A. S., Bose, G. C., Huang, L. & Azhar, M. Generation of mice carrying a knockout-first and conditional-ready allele of transforming growth factor β2 gene. *Genesis* **52**, 817–826 (2014).
59. Ossowski, L. & Reich, E. Changes in malignant phenotype of a human carcinoma conditioned by growth environment. *Cell* **33**, 323–333 (1983).

Acknowledgements

We thank the Aguirre-Ghiso laboratory for helpful discussions and the assistance of the Dean's Flow Cytometry CoRE, Microscope CoRE and Small Animal Imaging CoRE at BioMedical Engineering and Imaging Institute, Icahn School of Medicine at Mount Sinai. We are grateful to C. Prophete (Frenette's laboratory) for mouse husbandry. We thank M. Rypdal, A.V. Pladsen and O.C. Lingjærde for preparing the BC DTC material and data. The BC DTC work in Oslo has received funding from the Norwegian Cancer Association and Norwegian Health Region South-East (H.G. Russnes and B. Naume). Grant support was received from the National Institutes of Health (NIH)/National Cancer Institute (NCI) CA109182, CA216248, CA218024, CA196521, The V-Foundation and the Samuel Waxman Cancer Research Foundation Tumor Dormancy Program to J.A.A.G.; HL069438, DK056638, DK116312 and DK112976 to P.S.F.; Portuguese Foundation for Science and Technology (SFRH/BD/100380/2014) to A.R.N.; MD/PhD program of the University of Lyon and the Ecole Normale Supérieure of Lyon to E.R.; Susan G. Komen Career Catalyst Research (CCR18547848), NCI Career Transition Award (K22CA196750), NIH (R01CA244780) and Tisch Cancer Institute NIH Cancer Center Grant (P30-CA196521) to J.J.B.C.; Instituto Serrapilheira/Serra-1708-15285 to A.B. and NIH (HL126705, CA218578, R01HL145064) and American Heart Association (17GRNT33650018) to M.A.

Author contributions

A.R.N. designed, planned and conducted experiments, analyzed data and wrote the manuscript; E.R., D.K.S. and J.F.C. conducted experiments; J.S.d.M. and J.J.B.C. helped with optimizing the imaging experiments; J.W., J.J. and M.A. provided necessary mouse model and samples and TGF-β2 expertise input; H.G.R. and B.N. provided human data; A.B. and P.S.F. provided mouse models and BM expertise input; P.S.F. and J.A.A.G. designed experiments, analyzed data and wrote the manuscript.

Competing interests

J.A.A.G. is a scientific co-founder of, scientific advisory board member and equity owner in HiberCell and receives financial compensation as a consultant for HiberCell, a Mount Sinai spin-off company focused on the research and development of therapeutics that prevent or delay the recurrence of cancer.

Additional information

Extended data is available for this paper at https://doi.org/10.1038/s43018-021-00179-8.

Supplementary information The online version contains supplementary material available at https://doi.org/10.1038/s43018-021-00179-8.

Correspondence and requests for materials should be addressed to J.A.A.-G.

Peer review information *Nature Cancer* thanks the anonymous reviewers for their contribution to the peer review of this work.

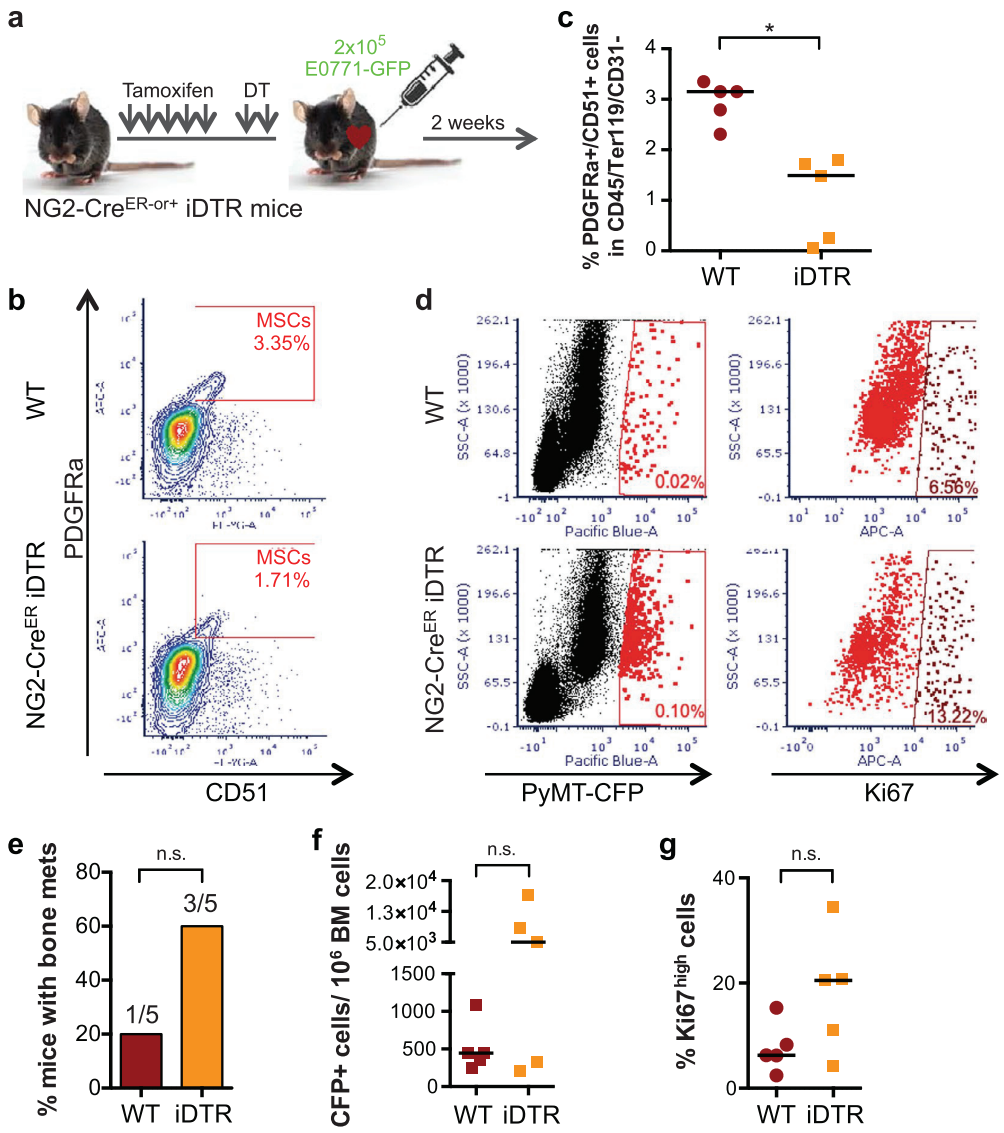

Extended Data Fig. 1 | Control of depletion of NG2+/Nestin+ MSCs and awakening of dormant PyMT-CFP DTCs in the BM.. a, 7-week old NG2-Cre^{ER}iDTR mice (NG2-Cre^{ER-or+}) were daily injected with tamoxifen for 5 days, followed by 1-day rest and 2 days with diphtheria toxin (DT). 24 h later 2×10^5 E0771-GFP cells were intra-cardiac injected and 2 weeks later mice were euthanized. **b**,**c**, FACS plots (b) and quantifications (c) confirming the depletion of NG2$^+$/Nestin$^+$ MSCs (CD45$^-$Ter119$^-$CD31$^-$PDGFRα$^+$CD51$^+$) in NG2-Cre^{ER}iDTR mice upon TAM and DT treatments compared with WT mice (n = 5 WT and 5 iDTR mice, median, 2-tailed Mann–Whitney U-test, p = 0.008). **d**-**g**, Detection and characterization of MMTV-PyMT-CFP cells in BM flushes by FACS (n = 5 WT and 5 iDTR mice). **e**, Incidence of bone metastasis (>1000 GFP+ DTCs/106 BM cells) 2 weeks after cancer cell injections (2-tailed Fisher's exact test). **f**, Number of MMTV-PyMT-CFP cancer cells per million BM cells (median, 2-tailed Mann–Whitney U-test). **g**, Percentage of Ki67^{high} E0771-GFP cancer cells (median, 2-tailed Mann–Whitney U-test). *p≤0.05 (p-values indicated above). n.s. not significant.

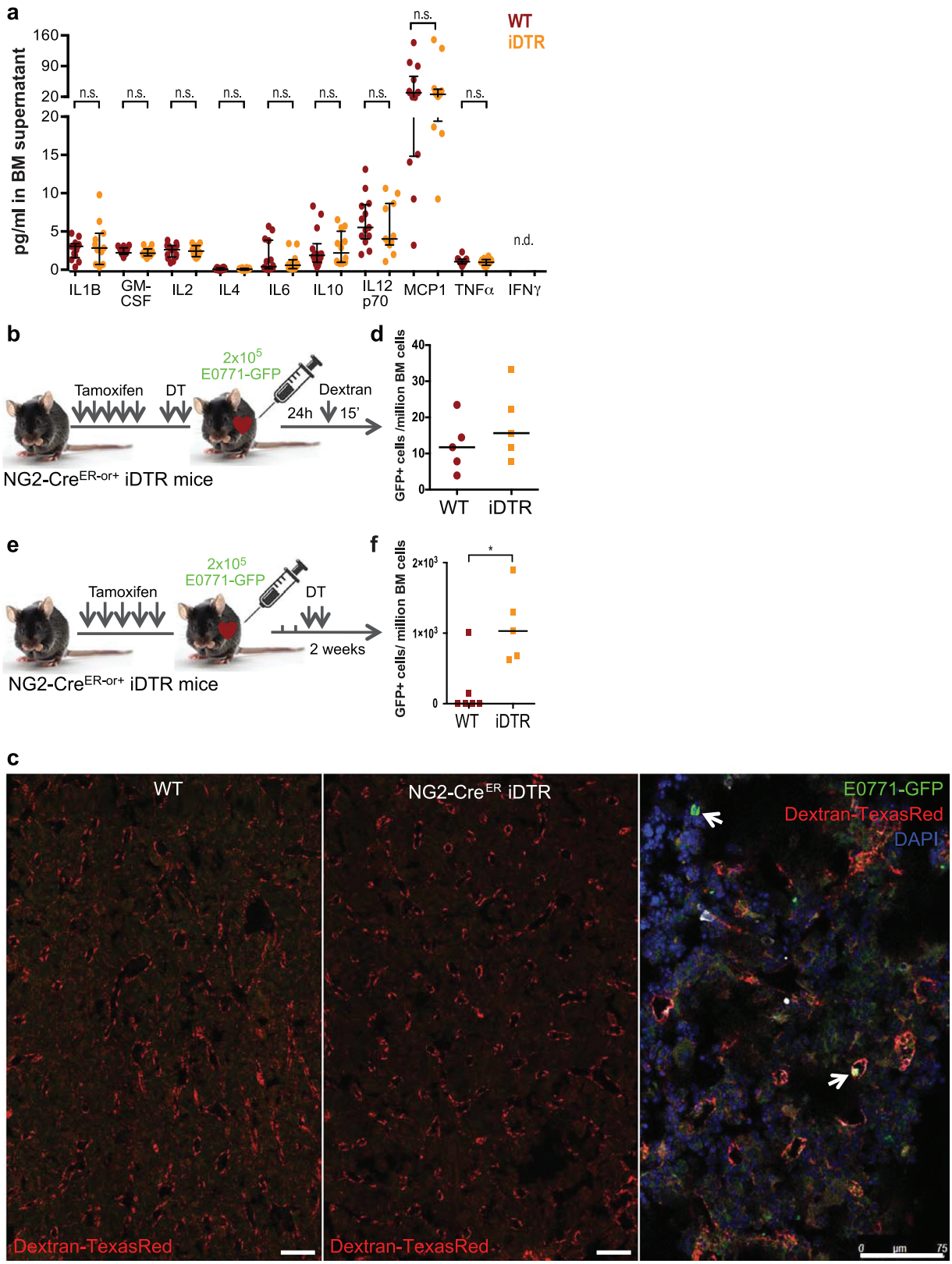

Extended Data Fig. 2 | See next page for caption.

Extended Data Fig. 2 | Pro-inflammatory cytokine status, vessel permeability and BM DTC seeding in NG2+/Nestin+ MSCs-depleted mice. a, Levels of pro-inflammatory cytokines in BM supernatant of WT and NG2-Cre^{ER}iDTR mice (n = 13 WT and 11 iDTR mice, from 2 independent experiments, median and interquartile range, 2-tailed Mann–Whitney tests, *p≤0.05, n.s. not significant, n.d. not detected). **b**-**d**, NG2-Cre^{ER}iDTR mice (NG2-Cre$^{ER-\text{ or }+}$) were daily i.p. injected with tamoxifen for 5 days followed by a rest day and 2 i.p. injections of DT. E0771-GFP cells were intra-cardiac injected and 24 h after 70 K Dextran-TexasRed was injected 15 minutes prior euthanasia. **c**, Representative images of Dextran extravasation in perfused bones. Arrows, E0771-GFP cells. **d**, Number of E0771-GFP cells detected after 1 week of *in vitro* expansion of the BM aspirates collected 24 h after injection into mice (n = 5 WT and 5 iDTR mice, median). **e**,**f**, NG2-Cre^{ER}iDTR mice (NG2-Cre$^{ER-\text{ or }+}$) were daily i.p. injected with TAM for 5 days, followed by intra-cardiac injection of E0771-GFP cancer cells. Cells were allowed to disseminate and extravasate for 72 h followed by 2 i.p. injections of DT. **f**, Number of E0771-GFP cells/million BM cells (n = 5 WT and 5 iDTR mice, median and 2-tailed Mann–Whitney tests, p=0.015). *p≤0.05 (p-values indicated above), n.s. not significant.

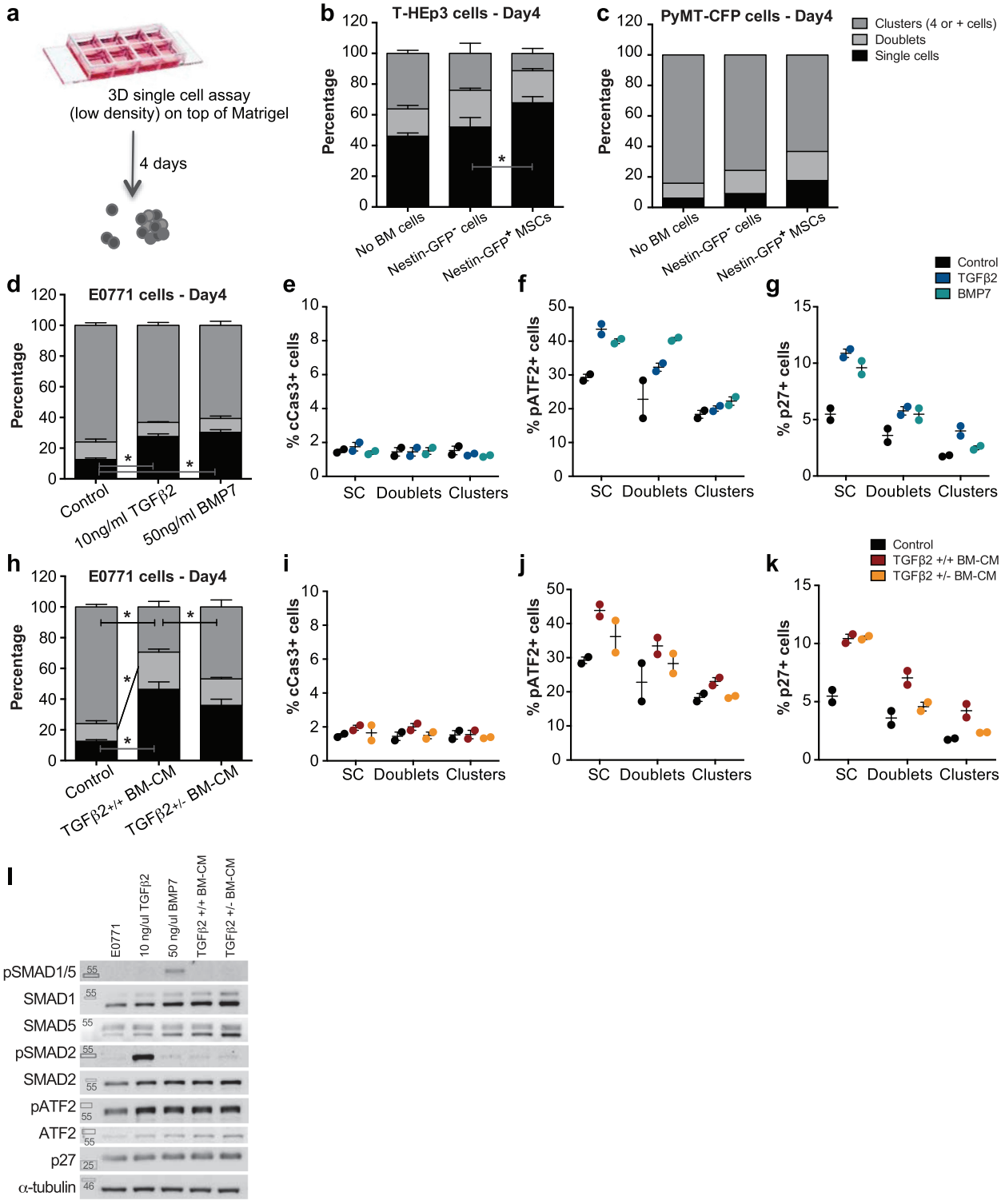

Extended Data Fig. 3 | See next page for caption.

Extended Data Fig. 3 | Effect of NG2+/Nestin+ MSCs, TGFβ2 and BMP7 on signalling pathways and growth cancer cells. a, 3D Matrigel assay used to track solitary cell to cluster growth. Single cells were plated on top of Matrigel in low density and the percentage of single cells, doublets and clusters was quantified 4 days after. **b**,**c**, Co-culture of human HNSCC PDX-derived T-HEp3 (b, n = 4 independent experiments, 4 wells per condition, mean and SEM, 2-tailed Mann–Whitney tests p=0.04) and mouse BC MMTV-PyMT (c, n = 2 independent experiments, 4 wells per condition, mean) cells with sorted Nestin-GFP- and Nestin-GFP+ MSCs for 4 days. **d**-**k**, E0771 cells were treated every day for 4 days with TGFβ2, BMP7 or bone marrow conditioned media (BM-CM) of $TGFβ2^{+/+}$ or $TGFβ2^{+/-}$ mice. d and h. Percentage of cancer cells in a single cell, doublet or cluster state with the indicated treatments (d, n = 5 independent experiments, 4 wells per condition each, mean and SEM, 2-tailed Mann–Whitney tests, p=0.03 and 0.005; h, n = 4 independent experiments, 4 wells per condition each, mean and SEM, 2-tailed Mann–Whitney tests, p=0.000005, 0.0001, 0.002 (Ct vs. $TGFβ2^{+/+}$: CS, doublets and clusters respectively) and 0.02 ($TGFβ2^{+/+}$ vs. $TGFβ2^{+/-}$ clusters)). **e**-**g** and **i**-**k**. Percentage of positive cells for c-Cas-3, p-ATF2 and p27 upon the indicated treatments (n = 2 independent experiments, 4 wells per condition each, mean, minimum and maximum). **l**, Western blots for the indicated antigens detected in E0771 cells treated for 24 h with the TGFβ2, BMP7 and different BM-CM preparations. Molecular weight markers in kDa. *$p \leq 0.05$, p-values indicated above.

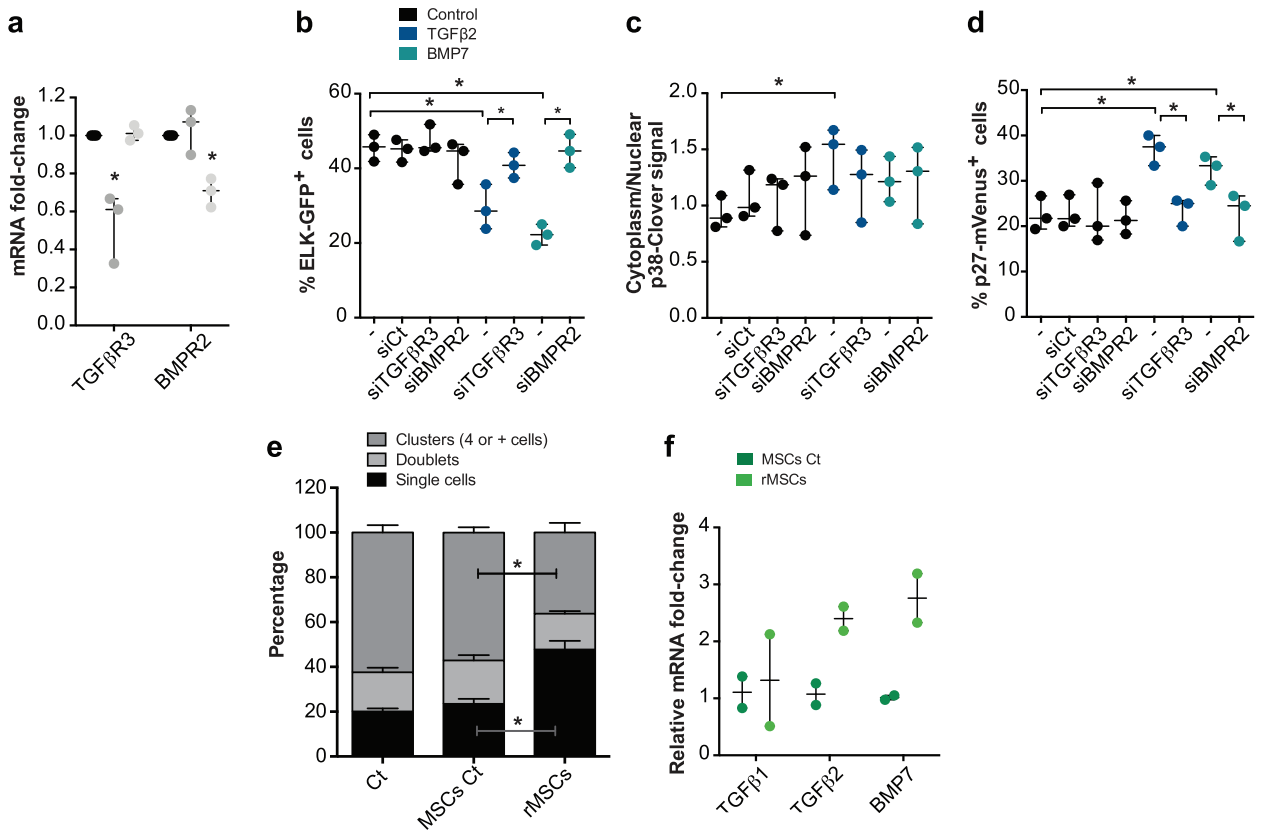

Extended Data Fig. 4 | Effect of TGFβ2 and BMP7 on signalling pathways (using ELK, p38 and p27 sensors) and MSCs in E0771 cancer cell growth. **a**-**d**, T-HEp3 cells with ERK, p38 and p27 activity biosensors were reversed transfected with control siRNA or siRNAs for TGFBRIII and BMPRII followed by 24-hour treatments with TGFβ2 and BMP7. **a**, TGFBRIII and BMPRII mRNA levels 48 h after transfection with the indicated siRNAs (n = 3 independent experiments, mean, minimum and maximum, 2-tailed Mann–Whitney tests, p=0.01 (TGFbR3) and 0.002 (BMPR2)). **b**–**d**, Quantification of the T-HEp3-biosensors activity (n = 3 independent experiments each, mean, minimum and maximum, 2-tailed Mann–Whitney tests, p=0.05). **e**, Percentage of E0771 cells in a single cell (p = 0.002), doublet or cluster (p = 0.005) state after co-culture with Control (passaged) or revitalized (r) MSCs (n = 4 independent experiments, 4 wells per condition per experiment, mean and SEM, 2-tailed Mann–Whitney tests). **f**, qPCR of TGFβ1, TGFβ2 and BMP7 from Control and rMSCs (n = 2). *p≤0.05, p-values indicated above.

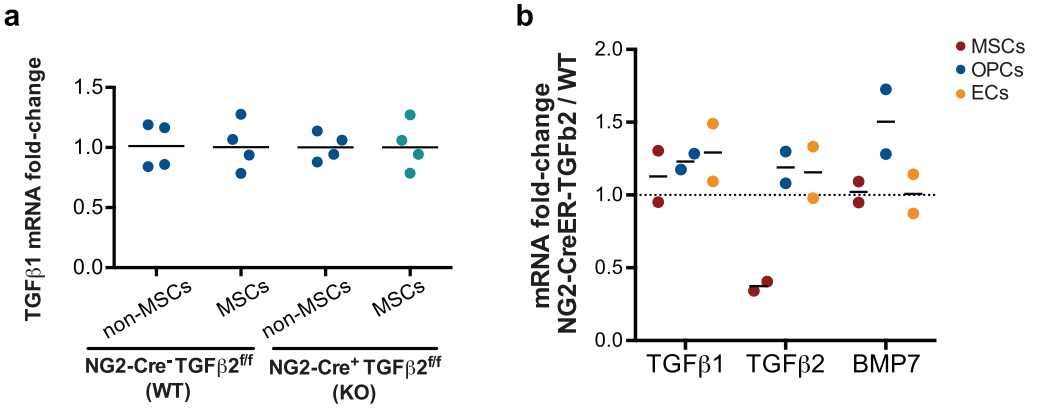

Extended Data Fig. 5 | NG2-CreERTGFβ2 mouse model controls. a, TGFβ1 mRNA levels in NG2$^+$/Nestin$^+$ MSCs (sorted using CD45$^-$Ter119$^-$CD31$^-$PDGFRα$^+$CD51$^+$ markers) in NG2-Cre^{ER}TGFβ2 mice upon TAM treatments compared with WT mice (n = 4 independent experiments). **b**, TGFβ1, TGFβ2 and BMP7 mRNA levels in MSCs (CD45$^-$CD31$^-$Ter119$^-$PDGFRα$^+$CD51$^+$), osteo-progenitor (CD45$^-$Ter119$^-$CD31$^-$ALCAM$^+$, OPCs) and endothelial (CD45$^-$Ter119$^-$CD31$^+$vEcad$^+$, ECs) cells from NG2-Cre^{ER}TGFβ2 mice upon TAM treatments compared with WT mice (n = 2 independent experiments). $^*p \leq 0.05$, p-values indicated above.

APPENDIX 3

During my PhD I also had the incredible opportunity to be mentored by and collaborate with Ana Rita Nobre, another PhD student in Pr. Aguirre-Ghiso's laboratory, leading to two publications.
The second project I participated in identified a major regulator of early disseminated tumor cell dormancy programs. I contributed to this project by initiating a discussion and collaboration with Pr. Cristina Curtis (Stanford, USA) and Dr. Jose Seoane (VHIO, Spain) to validate our findings with molecular signatures from tumors of breast cancer patients (Appendix 3).

> Nobre AR , Dalla E , Yang J , Huang X , Wullkopf L , **Risson E**, Razghandi P , Lopez-Anton M , Zheng W , Seoane JA , Curtis C , Kenigsberg E , Wang J, Aguirre-Ghiso JA : **Single-cell analysis of early disseminated cancer cells identifies ZFP281 and a mesenchymal-like dormancy program as a barrier to metastasis.**
> *Under review, Nature Cell Biology, 2022.*

This appendix will be inserted in the last version of this manuscript when the accepted and formatted paper will be available.

APPENDIX 4

I am also co-author on a publication of another ongoing project in Dr. Maguer-Satta's laboratory, which defines the role of CD10 in aggressive cancer stem cells. I participated in this project by analyzing single-cell RNAseq data.

Guyot B, Clément F, Drouet Y, **Risson E**, Schmidt X, Delay E, Treilleux I, Foy JP, Jeanpierre S, Thomas E, Kielbassa K, Tonon L, Zhu HH, Saintigny P, Gao WQ, Fouchardière A, Tirode F, Viari A, Blay JY, Maguer-Satta V: **CD10 defines stem cells features and the molecular identity of aggressive cancer cells.**
In preparation, 2022

This appendix will be inserted in the last version of this manuscript when the accepted and formatted paper will be available.

APPENDIX 5

My PhD was also affected by the ongoing SARS-CoV-2 pandemic. While New York City was in lockdown in spring 2020, I joined “The Sinai Immunology Review Project” coordinated by Miriam Merad to help review the increasing amount of pre-preprints published on MedXriv and BioXriv every day. This led to the redaction of an extremely needed review of our accumulated knowledge on SARS-CoV-2 in June 2020 (Appendix 5).

Vabret N., …, **Risson E.**, …, Merad M., Samstein R.M., The Sinai Immunology Review Project, et al. : **Immunology of COVID-19: Current State of the Science**.
Immunity 2020, doi: 10.1016/j.immuni.2020.05.002

CellPress

Immunity

Review

Immunology of COVID-19: Current State of the Science

Nicolas Vabret,[1,*] Graham J. Britton,[1] Conor Gruber,[1] Samarth Hegde,[1] Joel Kim,[1] Maria Kuksin,[1] Rachel Levantovsky,[1] Louise Malle,[1] Alvaro Moreira,[1] Matthew D. Park,[1] Luisanna Pia,[1] Emma Risson,[1] Miriam Saffern,[1] Bérengère Salomé,[1] Myvizhi Esai Selvan,[1] Matthew P. Spindler,[1] Jessica Tan,[1] Verena van der Heide,[1] Jill K. Gregory,[1] Konstantina Alexandropoulos,[1] Nina Bhardwaj,[1] Brian D. Brown,[1] Benjamin Greenbaum,[1] Zeynep H. Gümüş,[1] Dirk Homann,[1] Amir Horowitz,[1] Alice O. Kamphorst,[1] Maria A. Curotto de Lafaille,[1] Saurabh Mehandru,[1] Miriam Merad,[1,*] Robert M. Samstein,[1,*] and The Sinai Immunology Review Project

[1]Precision Immunology Institute at the Icahn School of Medicine at Mount Sinai, New York, NY, USA

*Correspondence: nicolas.vabret@mssm.edu (N.V.), miriam.merad@mssm.edu (M.M.), robert.samstein@mountsinai.org (R.M.S.)

https://doi.org/10.1016/j.immuni.2020.05.002

The coronavirus disease 2019 (COVID-19) pandemic, caused by severe acute respiratory syndrome coronavirus 2 (SARS-CoV-2) has affected millions of people worldwide, igniting an unprecedented effort from the scientific community to understand the biological underpinning of COVID19 pathophysiology. In this Review, we summarize the current state of knowledge of innate and adaptive immune responses elicited by SARS-CoV-2 infection and the immunological pathways that likely contribute to disease severity and death. We also discuss the rationale and clinical outcome of current therapeutic strategies as well as prospective clinical trials to prevent or treat SARS-CoV-2 infection.

Introduction

The recent emergence and rapid global spread of severe acute respiratory syndrome coronavirus 2 (SARS-CoV-2) and the resulting coronavirus disease 2019 (COVID-19) poses an unprecedented health crisis that was declared a pandemic by the World Health Organization (WHO) on March 11, 2020. The origin of SARS-CoV-2 was traced to the city of Wuhan in the province of Hubei, China, where a cluster of viral pneumonia cases was first detected, many in connection with the Huanan Seafood Wholesale Market. China reported this outbreak to the WHO on December 31, 2019 and soon after identified the causative pathogen as a betacoronavirus with high sequence homology to bat coronaviruses (CoVs) using angiotensin-converting enzyme 2 (ACE2) receptor as the dominant mechanism of cell entry (Lu et al., 2020a; Wan et al., 2020b). Following a likely zoonotic spillover, human-to-human transmission events were confirmed with clinical presentations ranging from no symptoms to mild fever, cough, and dyspnea to cytokine storm, respiratory failure, and death. SARS-CoV-2 is also closely related to SARS (retrospectively named SARS-CoV-1) and Middle Eastern respiratory syndrome (MERS) CoVs, causing zoonotic epidemic and local outbreaks in 2003 and 2012, respectively (de Wit et al., 2016). While SARS-CoV-2 is not as lethal as SARS-CoV-1 or MERS-CoV (Fauci et al., 2020), the considerable spread of the current pandemic has brought tremendous pressure and disastrous consequences for public health and medical systems worldwide.

The scientific response to the crisis has been extraordinary, with a plethora of COVID-19 studies posted in preprint servers in an attempt to rapidly unravel the pathogenesis of COVID-19 and potential therapeutic strategies. In response, trainees and faculty members of the Precision Immunology Institute at the Icahn School of Medicine at Mount Sinai (PrIISM) have initiated an institutional effort to critically review the preprint literature (Vabret et al., 2020), together with peer-reviewed articles published in traditional journals, and summarize the current state of science on the fast-evolving field of COVID-19 immunology. We thematically focus on the innate and adaptive immune responses to SARS-CoV-2 and related CoVs, clinical studies and prognostic laboratory correlates, current therapeutic strategies, prospective clinical trials, and vaccine approaches.

Innate Immune Sensing of SARS-CoV-2

Innate immune sensing serves as the first line of antiviral defense and is essential for immunity to viruses. To date, our understanding of the specific innate immune response to SARS-CoV-2 is extremely limited. However, the virus-host interactions involving SARS-CoV-2 are likely to recapitulate many of those involving other CoVs, given the shared sequence homology among CoVs and the conserved mechanisms of innate immune signaling. In the case of RNA viruses such as SARS-CoV-2, these pathways are initiated through the engagement of pattern-recognition receptors (PRRs) by viral single-stranded RNA (ssRNA) and double-stranded RNA (dsRNA) via cytosolic RIG-I like receptors (RLRs) and extracellular and endosomal Toll-like receptors (TLRs). Upon PRR activation, downstream signaling cascades trigger the secretion of cytokines. Among these, type I/III interferons (IFNs) are considered the most important for antiviral defense, but other cytokines, such as proinflammatory tumor necrosis factor alpha (TNF-α), and interleukin-1 (IL-1), IL-6, and IL-18 are also released. Together, they induce antiviral programs in target cells and potentiate the adaptive immune response. If present early and properly localized, IFN-I can effectively limit CoV infection (Channappanavar et al., 2016, 2019). Early evidence demonstrated that SARS-CoV-2 is sensitive to IFN-I/III pretreatment *in vitro*, perhaps to a greater degree than SARS-CoV-1 (Blanco-Melo et al., 2020; Lokugamage et al., 2020; Mantlo et al., 2020; Stanifer et al., 2020). However, the

Immunity
Review

CellPress

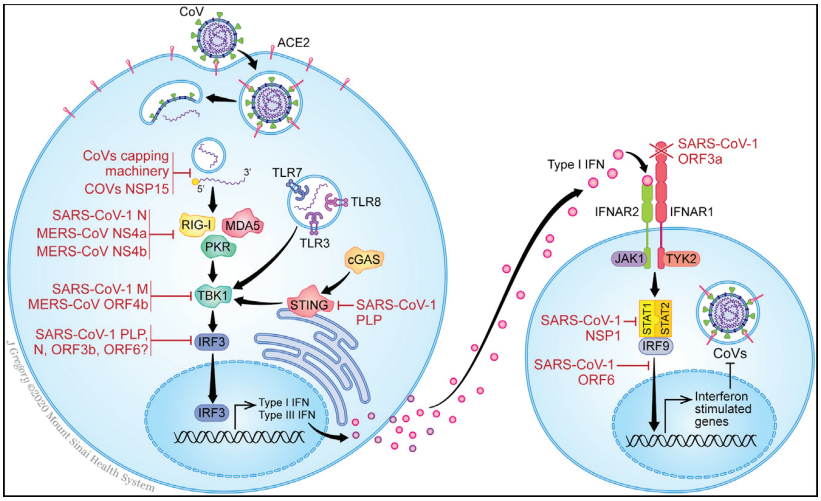

Figure 1. Mechanisms of Host Innate Immune Response and Coronaviruses Antagonism

Overview of innate immune sensing (left) and interferon signaling (right), annotated with the known mechanisms by which SARS-CoV-1 and MERS-CoV antagonize the pathways (red).

specific IFN-stimulated genes (ISGs) that mediate these protective effects are still being elucidated. Lymphocyte antigen 6 complex locus E (LY6E) has been shown to interfere with SARS-CoV-2 spike (S) protein-mediated membrane fusion (Pfaender et al., 2020; Zhao et al., 2020c). Likely, the IFN-induced transmembrane family (IFITM) proteins inhibit SARS-CoV-2 entry, as demonstrated for SARS-CoV-1 (Huang et al., 2011b), although their action in promoting infection has also been described for other CoVs (Zhao et al., 2014, 2018).

Evasion of Innate Sensing by Coronaviruses

As these cytokines represent a major barrier to viral infection, CoVs have evolved several mechanisms to inhibit IFN-I induction and signaling. Numerous studies have demonstrated that SARS-CoV-1 suppresses IFN release *in vitro* and *in vivo* (Cameron et al., 2012; Minakshi et al., 2009; Siu et al., 2009; Wathelet et al., 2007). SARS-CoV-2 likely achieves a similar effect, as suggested by the lack of robust type I/III IFN signatures from infected cell lines, primary bronchial cells, and a ferret model (Blanco-Melo et al., 2020). In fact, patients with severe COVID-19 demonstrate remarkably impaired IFN-I signatures as compared to mild or moderate cases (Hadjadj et al., 2020). As is often the case, there are multiple mechanisms of evasion for CoVs, with viral factors antagonizing each step of the pathway from PRR sensing and cytokine secretion to IFN signal transduction (Figure 1).

CoV-mediated antagonism of innate immunity begins with evasion of PRR sensing. ssRNA viruses, like CoVs, form dsRNA intermediates during their replication, which can be detected by TLR3 in the endosome and RIG-I, MDA5, and PKR in the cytosol. ssRNA may also be detected by TLR7 or TLR8 and potentially RIG-I and PKR. CoVs are known to avoid PRR activation by either avoiding recognition altogether or antagonizing PRR action (Bouvet et al., 2010; Chen et al., 2009; Deng et al., 2017; Hackbart et al., 2020; Ivanov et al., 2004; Knoops et al., 2008). To evade PRRs, dsRNA is first shielded by membrane-bound compartments that form during viral replication of SARS-CoV-1 (Knoops et al., 2008). In addition, viral RNA is guanosine-capped and methylated at the 5′ end by CoVs nonstructural proteins (NSPs) 10, 13, 14, and 16 (Bouvet et al., 2010; Chen et al., 2009; Ivanov et al., 2004), thereby resembling host mRNA to promote translation, prevent degradation, and evade RLR sensing. Finally, CoVs also encode an endoribonuclease, NSP15, that cleaves 5′ polyuridines formed during viral replication, which would otherwise be detected by MDA5 (Deng et al., 2017; Hackbart et al., 2020). CoVs have evolved additional strategies to impede activation of PRRs. SARS-CoV-1 N-protein prevents TRIM25 activation of RIG-I (Hu et al., 2017). Likewise, MERS-CoV NS4a, which itself binds dsRNA, impedes PKR activation (Comar et al., 2019; Rabouw et al., 2016) and inhibits PACT, an activator of RLRs (Niemeyer et al., 2013; Siu et al., 2014). Additionally, MERS-CoV NS4b antagonizes RNaseL, another activator of RLRs (Thornbrough et al., 2016). The role of other PRRs remains unclear. For example, SARS-CoV-1 papain-like protease (PLP) antagonizes STING, suggesting that self-DNA may also represent an important trigger (Sun et al., 2012). The extent to which SARS-CoV-2 homologs overlap in these functions is currently unknown.

Following activation, RLR and TLRs induce signaling cascades, leading to the phosphorylation of transcription factors, such as NF-kB and the interferon-regulatory factor family (IRF), ultimately leading to transcription of IFN and proinflammatory cytokines. Although no experimental studies have delineated the precise functions of SARS-CoV-2 proteins, proteomic studies have demonstrated interactions between viral proteins and PRR signaling cascades. SARS-CoV-2 ORF9b indirectly interacts with the signaling adaptor MAVS via its association with Tom70 (Gordon et al., 2020), consistent with prior reports that SARS-CoV-1 ORF9b suppresses MAVS signaling (Shi et al., 2014). Furthermore, SARS-CoV-2 NSP13 interacts with signaling intermediate TBK1, and NSP15 is associated with RNF41, an activator of TBK1 and IRF3 (Gordon et al., 2020). Similarly, SARS-CoV-1 M protein is known to inhibit the TBK1 signaling complex (Siu et al., 2009), as does MERS-CoV ORF4b (Yang et al., 2015). Other proteins, including SARS-CoV-1 PLP, N, ORF3b, and ORF6, block IRF3 phosphorylation and nuclear translocation (Devaraj et al., 2007; Kopecky-Bromberg et al., 2007). NF-kB is also inhibited by CoV proteins. These include SARS-CoV-1 PLP (Frieman et al., 2009) and MERS-CoV ORF4b and ORF5 (Canton et al., 2018; Menachery et al., 2017). Finally, SARS-CoV-1 NSP1 (Huang et al., 2011a; Kamitani et al., 2009) and MERS-CoV NSP1 (Lokugamage et al., 2015) initiate general inhibition of host transcription and translation, thus limiting antiviral defenses nonspecifically.

To prevent signaling downstream of IFN release, CoV proteins inhibit several steps of the signal transduction pathway that bridge the receptor subunits (IFNAR1 and IFNAR2) to the STAT

proteins that activate transcription. For SARS-CoV-1, these mechanisms include IFNAR1 degradation by ORF3a (Minakshi et al., 2009), decreased STAT1 phosphorylation by NSP1 (Wathelet et al., 2007), and antagonism of STAT1 nuclear translocation by ORF6 (Frieman et al., 2007; Kopecky-Bromberg et al., 2007). However, SARS-CoV-2 ORF6 shares only 69% sequence homology with SARS-CoV-1, suggesting this function may not be conserved. In support of this notion, SARS-CoV-2 infection fails to limit STAT1 phosphorylation, unlike in SARS-CoV-1 infection (Lokugamage et al., 2020).

Imbalance between Antiviral and Proinflammatory Responses

Taken together, the multiplicity of strategies developed by pathogenic CoVs to escape immune sensing, particularly the IFN-I pathway, suggests a critical role played by the dysregulation of IFN-I response in COVID-19 pathogenicity. Concordantly, animal models of SARS-CoV-1 and MERS-CoV infection indicate that failure to elicit an early IFN-I response correlates with the severity of disease (Channappanavar et al., 2016). Perhaps more importantly, these models demonstrate that timing is key, as IFN is protective early in disease but later becomes pathologic (Channappanavar et al., 2016, 2019). Perhaps interferon-induced upregulation of ACE2 in airway epithelia may contribute to this effect (Ziegler et al., 2020). Furthermore, while pathogenic CoVs block IFN signaling, they may actively promote other inflammatory pathways contributing to pathology. For instance, SARS-CoV-1 ORF3a, ORF8b, and E proteins enhance inflammasome activation (Chen et al., 2019; Nieto-Torres et al., 2015; Shi et al., 2019; Siu et al., 2019), leading to secretion of IL-1β and IL-18, which are likely to contribute to pathological inflammation. Similarly, SARS-CoV-2 NSP9 and NSP10 might induce IL-6 and IL-8 production, potentially by inhibition of NKRF, an endogenous NF-kB repressor (Li et al., 2020a). Collectively, these proinflammatory processes likely contribute to the ''cytokine storm'' observed in COVID-19 patients and substantiate a role for targeted immunosuppressive treatment regimens. Moving forward, a clear understanding of the delicate balance between antiviral and inflammatory innate immune programs will be essential to developing effective biomarkers and therapeutics for COVID-19.

Myeloid Cells

Mucosal immune responses to infectious agents are orchestrated and regulated by myeloid cells with specialized functions, which include conventional dendritic cells (cDCs), monocyte-derived DCs (moDCs), plasmacytoid DCs (pDCs), and macrophages (Guilliams et al., 2013). A growing body of evidence points to dysregulated myeloid responses that potentially drive the COVID-19 hallmark syndromes, such as acute respiratory distress syndrome (ARDS), cytokine release syndrome (CRS) and lymphopenia (Mehta et al., 2020).

Myeloid Characterization in COVID-19

Flow cytometric analyses of peripheral blood mononuclear cells (PBMCs) from symptomatic COVID-19 patients have shown a significant influx of granulocyte-macrophage colony-stimulating factor (GM-CSF)-producing, activated $CD4^+$ T cells and $CD14^+HLA\text{-}DR^{lo}$ inflammatory monocytes (IMs) (Giamarellos-Bourboulis et al., 2020; Zhang et al., 2020c; Zhou et al., 2020b). This matches single-cell transcriptomic (scRNA-seq) data demonstrating $CD14^+IL\text{-}1\beta^+$ monocytic expansion (Guo et al., 2020; Wen et al., 2020), interferon-mitogen-activated protein kinase (MAPK)-driven adaptive immune responses (Huang et al., 2020c), and IL-1β-associated inflammasome signatures (Ong et al., 2020) in peripheral blood of COVID-19 patients, although systemic levels of IL-1β detected are conspicuously low (Del Valle et al., 2020). Importantly, these immune signatures track with progression of clinical disease. scRNA-seq studies performed on pulmonary tissues of patients with severe COVID-19 disease have revealed an expansion of IMs and $Ficolin\text{-}1^+$ monocyte-derived macrophages at the expense of tissue-resident reparative alveolar macrophages (AMs) (Liao et al., 2020). The aforementioned study also observed signatures of IFN signaling and monocyte recruitment that likely contribute to the rapid decline in alveolar patency and promote ARDS. Although most of the clinical focus has been on pulmonary damage and mononuclear phagocyte (MNP) dysfunction therein, it is increasingly clear that COVID-19 likely presents systemic challenges in other organ sites, such as the ileum and kidneys. Understanding the role of non-pulmonary myeloid cells in tissue-specific pathology associated with COVID-19 will be important.

Prior Knowledge from SARS-CoV-1, MERS-CoV, and Murine Coronaviruses

While data on COVID-19 patients continues to rapidly emerge, studies of myeloid cell dysfunction in SARS-CoV-1 and MERS-CoV can provide an important roadmap to understanding COVID-19 pathogenesis (Figure 2). SARS-CoV-1 infection in mouse models results in an aberrant AM phenotype that limits DC trafficking and T cell activation (Zhao et al., 2009). Additionally, $YM1^+$ $FIZZ1^+$ alternative macrophages can increase airway hypersensitivity, thus exacerbating SARS-associated fibrosis (Page et al., 2012). Further, as described above, murine SARS-CoV-1 studies have demonstrated that delayed IFN-I signaling and inflammatory monocytes-macrophages promote lung cytokine and chemokine levels, vascular leakage, and impaired antigen-specific T cell responses, culminating in lethal disease (Channappanavar et al., 2016). The role played by prominent IFN-producing pDCs in SARS-CoV-2 control or pathogenesis warrants investigation, as they have been shown to be critical in murine CoV (MHV) control (Cervantes-Barragan et al., 2007). Longitudinal studies in SARS-CoV-2 models are awaited, but initial phenotypic studies in humanized hACE2 mice have shown the characteristic alveolar interstitial pneumonia, with infiltration of lymphocytes and monocytes and accumulation of macrophages in the alveolar lumen (Bao et al., 2020a), which recapitulates patient findings (Xu et al., 2020c). Lastly, non-human primate (NHP) studies and patient data on SARS-CoV-1 have also shown that virus spike-specific immunoglobulin G (IgG) responses can exacerbate acute lung injury due to repolarization of alveolar macrophages into proinflammatory phenotypes and enhanced recruitment of inflammatory monocyte via CCL2 and IL-8 (Clay et al., 2012; Liu et al., 2019). However, the extent to which the antibody response contributes to disease pathophysiology remains to be confirmed.

Myeloid Cells Contribution to Pathogenic Inflammation

The initial mode of viral pathogen-associated signal (PAMP) recognition by innate cells has a major impact on downstream myeloid signaling and cytokine secretion (de Marcken et al., 2019). While macrophages are somewhat susceptible to

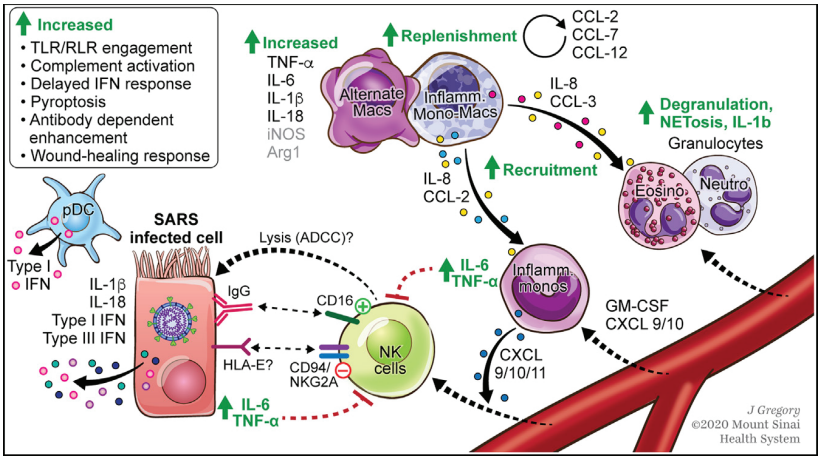

Figure 2. SARS-CoV-2 Infection Results in Myeloid Cell Activation and Changes NK Cell Function

Based on data from preliminary COVID-19 studies and earlier studies in related coronaviruses.

IL-6, IL-1β, and IFN-I/III from infected pulmonary epithelia can induce inflammatory programs in resident (alternate) macrophages while recruiting inflammatory monocytes, as well as granulocytes and lymphocytes from circulation. Sustained IL-6 and TNF-α by incoming monocytes can drive several hyperinflammation cascades. Inflammatory monocyte-derived macrophages can amplify dysfunctional responses in various ways (listed in top-left corner). The systemic CRS- and sHLH-like inflammatory response can induce neutrophilic NETosis and microthrombosis, aggravating COVID-19 severity. Other myeloid cells, such as pDCs, are purported to have an IFN-dependent role in viral control. Monocyte-derived CXCL9/10/11 might recruit NK cells from blood. Preliminary data suggest that the antiviral function of these NK cells might be regulated through crosstalk with SARS-infected cells and inflammatory monocytes.

Dashed lines indicate pathways to be confirmed. Arg1, arginase 1; iNOS, inducible-nitric oxide synthase; Inflamm., inflammatory; Mono., monocytes; Macs, macrophages; Eosino, eosinophils; Neutro, neutrophils; NETosis, neutrophil extracellular trap cell death; SHLH, secondary hemophagocytic lymphohistiocytosis.

MERS-CoV and SARS-CoV-1 infection (Perlman and Dandekar, 2005; Zhou et al., 2014), data do not suggest that they are infected by SARS-CoV-2, although one study reported ACE2 and SARS-CoV-2 nucleocapsid protein is expressed in lymph nodes and spleen-associated $CD169^{+}$ macrophages of COVID-19 patients producing IL-6 (Chen et al., 2020h). Significantly elevated systemic levels of proinflammatory cytokine IL-6 have been reported in several COVID-19 patient cohorts and shown to correlate with disease severity (Mehta et al., 2020). Increased IL-6 can also be associated with higher levels of IL-2, IL-7, IFN-ɣ, and GM-CSF, as seen in secondary hemophagocytic lymphohistiocytosis. In response to viral infections, MNPs drive IL and IFN-I and IFN-III production resulting in inflammasome activation, induction of pathogenic Th1 and Th17 cell responses, recruitment of effector immune cells, and CRS pathology (Prokunina-Olsson et al., 2020; Tanaka et al., 2016). Independently, *in vitro* studies have demonstrated SARS-CoV-1 infection can induce intracellular stress pathways, resulting in NLRP3-dependent inflammasome activation and macrophage pyroptosis (Chen et al., 2019; Shi et al., 2019). Functional studies are required to implicate these myeloid inflammasome pathways in COVID-19 lung pathology and to assess other immunogenic pathways such as RIPK1/3-dependent necroptosis (Nailwal and Chan, 2019). In conclusion, the strength and duration of myeloid ISG)signaling potentially dictate COVID-19 disease severity, but rigorous studies are warranted to confirm this.

Lastly, more work is needed to ascertain the mechanistic role played by lung-resident and recruited granulocytes in SARS-CoV-2 control and pathogenesis (Camp and Jonsson, 2017; Flores-Torres et al., 2019). In contrast to their early protective role, neutrophil NETosis and macrophage crosstalk can drive later-stage inflammatory cascades (Barnes et al., 2020), underscoring the overall pathogenic nature of damage-sensing host responses (Figure 2).

Collectively, the current knowledge of CoVs and SARS-CoV-2 infection, in particular, points to an inadvertent collusion involving myeloid cells in COVID-19 pathogenesis, despite their critical role in early sensing and antiviral responses.

Innate Lymphoid Cells

Innate lymphoid cells (ILCs) are innate immune effector cells that lack the expression of rearranged antigen receptors (T cell receptor [TCR], B cell receptor [BCR]). The ILC family is divided into two main groups: the cytotoxic natural killer (NK) cells and the non-cytotoxic helper ILCs, which include ILC1, ILC2, and ILC3 (Vivier et al., 2018). Conventional NK cells include $CD56^{bright}CD16^{-}$ NK cells and $CD56^{dim}CD16^{+}$ cells, which are specialized in cytokine production or cytotoxicity, respectively.

NK Cells Are Decreased in the Peripheral Blood of COVID-19 patients

Multiple studies have reported reduced numbers of NK cells in the peripheral blood of COVID-19 patients, which is associated with severity of the disease (Song et al., 2020; Wang et al., 2020f; Yu et al., 2020; Zheng et al., 2020b). A recent scRNA-seq analysis revealed a transcriptomic signature for NK cells that was equally represented in lungs from patients and healthy donors (Liao et al., 2020). The majority of lung NK cells are non-resident (Gasteiger et al., 2015; Marquardt et al., 2017), and CXCR3 has been shown to mediate NK cell infiltration upon influenza infection (Carlin et al., 2018). *In vitro*, CXCR3 ligands (CXCL9-11) are increased in SARS-CoV-2-infected human lung tissue (Chu et al., 2020), and CXCR3-ligand-producing monocytes are expanded in the lungs of COVID-19 patients (Liao et al., 2020). This suggests that the CXCR3 pathway might facilitate NK cell recruitment from the peripheral blood to the lungs in COVID-19 patients (Figure 2).

NK Cell Activation Pathways in Antiviral Immunity

NK cells express inhibitory and activating receptors that regulate their cytotoxicity. They are therefore able to induce the lysis of virus-infected cells that upregulate virus-derived proteins, as well as stress-inducible ligands, which are then recognized by NK-cell-activating receptors, such as NKp46 (Cerwenka and Lanier,

2001; Draghi et al., 2007; Duev-Cohen et al., 2016; Glasner et al., 2012). Future studies should investigate the expression of NK receptor ligands on SARS-CoV-2-infected cells in order to better understand the mechanisms underlying NK cell activation in COVID-19 disease. Further, secretion of IgG1 and IgG3 antibodies during SARS-CoV-2 infection (Amanat et al., 2020) may induce $CD56^{dim}$ $CD16^{+}$ NK cell activation through Fc receptor recognition of antibodies either bound to surface antigens expressed on infected cells or to extracellular virions as immune complexes (Figure 2). This interaction might trigger both cytokine production by NK cells and lysis of infected cells through antibody-mediated cellular cytotoxicity (ADCC), as shown in influenza infection (Von Holle and Moody, 2019). Emerging data highlight the capacity for NK-mediated ADCC in response to naturally isolated SARS-CoV-1 anti-S IgG that crossreacts with SARS-CoV-2 S glycoprotein when transfected into Chinese hamster ovary (CHO) cells (Pinto et al., 2020). These findings suggest that triggering NK cell activation may not only contribute to the resolution of infection, but also contribute to the cytokine storm in ARDS.

Impairment of NK Cell Function in SARS-CoV-2 Infection

Ex vivo NK cells from peripheral blood of COVID-19 patients have reduced intracellular expression of CD107a, Ksp37, granzyme B, and granulysin, suggesting an impaired cytotoxicity, as well as an impaired production of chemokines, IFN-ɣ, and TNF-α (Wilk et al., 2020; Zheng et al., 2020b). Several pathways may contribute to the dysregulation of NK cells. While influenza virus infects NK cells and induces apoptosis (Mao et al., 2009), lung NK cells do not express the entry receptor for SARS-CoV-2, ACE2, and are therefore unlikely to be directly infected by SARS-CoV-2 (Travaglini et al., 2020). The majority of NK cells found in human lung display a mature $CD16^{+}KIR^{+}CD56^{dim}$ phenotype and are able to induce cell cytotoxicity in response to loss of human leukocyte antigen (HLA) class I or through Fc receptor signaling, although to a lower extent than their peripheral blood counterpart (Marquardt et al., 2017). Killer-immunoglobulin receptors (KIRs) are acquired during NK cell development alongside CD16 (FcRγIIIA) and are essential for NK cell licensing and subsequent capacity for cytolytic function (Sivori et al., 2019). Frequencies of NK cells expressing CD16 and/or KIRs are decreased in the blood following SARS-CoV-2 and SARS-CoV-1 infection, respectively (Xia et al., 2004; Wang et al., 2020d). Collectively, the data suggest either an impaired maturation of the NK compartment or migration of the mature, circulating NK cells into the lungs or other peripheral tissues of SARS-CoV-2-infected patients.

The immune checkpoint NKG2A is increased on NK cells and CD8 T cells from COVID-19 patients (Zheng et al., 2020b). NKG2A inhibits cell cytotoxicity by binding the non-classical HLA-E molecule (Braud et al., 1998; Brooks et al., 1997), and this interaction is strongly correlated with poor control of HIV-1 infection (Ramsuran et al., 2018). Genes encoding the inhibitory receptors LAG3 and TIM3 are also upregulated in NK cells from COVID-19 patients (Wilk et al., 2020; Hadjadj et al., 2020). Thus, increased immune checkpoints on NK cells might contribute to viral escape. Additionally, COVID-19 patients have higher plasma concentrations of IL-6 (Huang et al., 2020b), which significantly correlate with lower NK cell numbers (Wang et al., 2020d, 2020f). *In vitro* stimulation by IL-6 and soluble IL-6 receptor has previously revealed impaired cytolytic functions (perforin and granzyme B production) by healthy donor NK cells, which can be restored following addition of tocilizumab (IL-6R blockade) (Cifaldi et al., 2015). TNF-α is also upregulated in the plasma of COVID-19 patients (Huang et al., 2020b), and ligand-receptor interaction analysis of peripheral blood scRNA-seq data suggests that monocyte-secreted TNF-α might bind to its receptors on NK cells (Guo et al., 2020). TNF-α is known to contribute to NK cell differentiation (Lee et al., 2009), which includes downregulation of NKp46 (Ivagnès et al., 2017), though no effect of TNF-α or IL-6 on NK cell-mediated ADCC has been reported so far. Collectively, these data suggest that crosstalk with monocytes might impair NK cell recognition and killing of SARS-CoV-2-infected cells, and antibodies targeting IL-6 and TNF-signaling may benefit enhanced NK cell functions in COVID-19 patients (Figure 2).

Relevance for Helper ILCs in SARS-CoV-2 Infection

No studies, to date, have reported ILC1, ILC2, or ILC3 functions in SARS-CoV-2 infection. All three subsets are present in healthy lung (De Grove et al., 2016; Yudanin et al., 2019). ILC2s are essential for the improvement of lung function following influenza infection in mice through amphiregulin-mediated restoration of the airway epithelium and oxygen saturation (Monticelli et al., 2011). However, ILC2s also produce IL-13, contributing to the recruitment of macrophages to the lung and influenza-induced airway hyperreactivity (Chang et al., 2011). Indeed, ILCs are involved in the polarization of alveolar macrophages, either toward a M1-like phenotype (ILC1 and ILC3) or a M2-like phenotype (ILC2) (Kim et al., 2019). Given the increased IL-13 concentrations (Huang et al., 2020b) and the dysregulation of the macrophage compartment observed in COVID-19 patients, the role played by ILCs in SARS-CoV-2 infection warrants further investigation.

T Cell Responses

T cells play a fundamental role in viral infections: CD4 T cells provide B cell help for antibody production and orchestrate the response of other immune cells, whereas CD8 T cells kill infected cells to reduce the viral burden. However, dysregulated T cell responses can result in immunopathology. To better understand the role of T cell responses in SARS-CoV-2 infection, the pursuit of two major questions is imperative: (1) what is the contribution of T cells to initial virus control and tissue damage in the context of COVID-19, and (2) how do memory T cells established thereafter contribute to protective immunity upon reinfection? Some tentative answers are beginning to emerge.

Overall Reduction of CD4 and CD8 T Cell Counts in Peripheral Blood

Similar to earlier observations about SARS-CoV-1 infection (He et al., 2005), several current reports emphasize the occurrence of lymphopenia with drastically reduced numbers of both CD4 and CD8 T cells in moderate and severe COVID-19 cases (Figure 3) (Chen et al., 2020c; Nie et al., 2020b; Wang et al., 2020d; Zeng et al., 2020; Zheng et al., 2020b). The extent of lymphopenia—most striking for CD8 T cells in patients admitted to the intensive care unit (ICU)—seemingly correlates with COVID-19-associated disease severity and mortality (Chen et al., 2020c; Diao et al., 2020; Liu et al., 2020b, 2020c; Tan et al., 2020a; Wang et al., 2020d, 2020f; Zeng et al., 2020;

Immunity
Review

CellPress

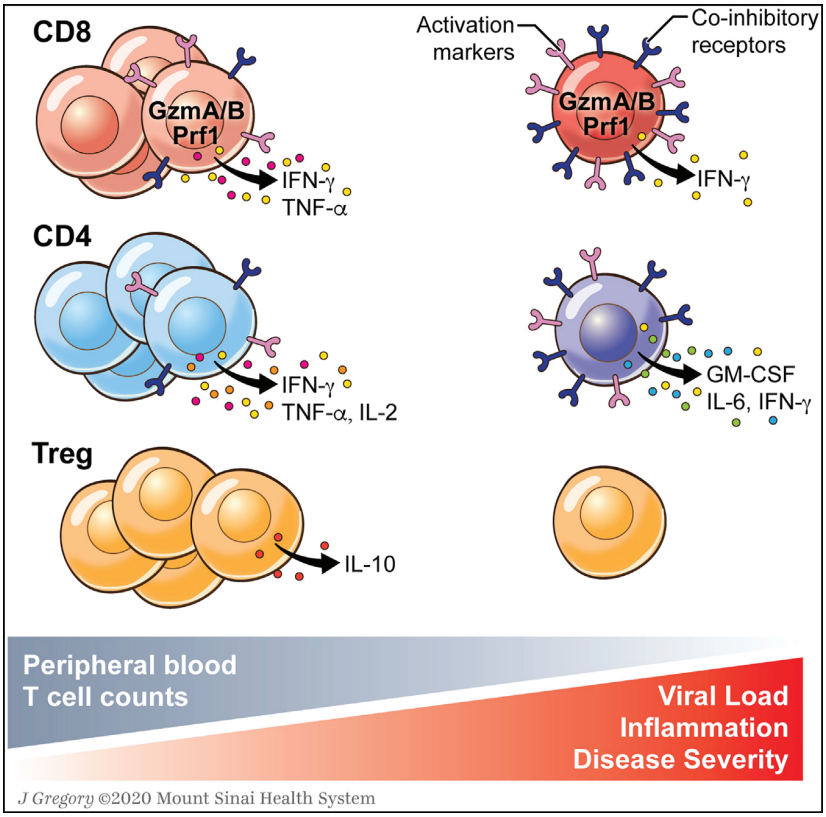

Figure 3. Working Model for T Cell Responses to SARS-CoV-2: Changes in Peripheral Blood T Cell Frequencies and Phenotype

A decrease in peripheral blood T cells associated with disease severity and inflammation is now well documented in COVID-19. Several studies report increased numbers of activated CD4 and CD8 T cells, which display a trend toward an exhausted phenotype in persistent COVID-19, based on continuous and upregulated expression of inhibitory markers as well as potential reduced polyfunctionality and cytotoxicity. In severe disease, production of specific inflammatory cytokines by CD4 T cells has also been reported. This working model needs to be confirmed and expanded on in future studies to assess virus-specific T cell responses both in peripheral blood and in tissues. In addition, larger and more defined patient cohorts with longitudinal data are required to define the relationship between disease severity and T cell phenotype.

IL, interleukin; IFN, interferon; TNF, tumor necrosis factor; GM-CSF, granulocyte-macrophage colony-stimulating factor; GzmA/B, granzyme A/granzyme B; Prf1, perforin.

Zhou et al., 2020c). Patients with mild symptoms, however, typically present with normal or slightly higher T cell counts (Liu et al., 2020a; Thevarajan et al., 2020). The cause of peripheral T cell loss in moderate to severe COVID-19, though a phenomenon also observed in other viral infections, remains elusive, and direct viral infection of T cells, in contrast to MERS-CoV (Chu et al., 2016), has not been reported.

Several mechanisms likely contribute to the reduced number of T cells in the blood, including effects from the inflammatory cytokine milieu. Indeed, lymphopenia seems to correlate with serum IL-6, IL-10, and TNF-α (Diao et al., 2020; Wan et al., 2020a), while convalescent patients were found to have restored bulk T cell frequencies paired with overall lower proinflammatory cytokine levels (Chen et al., 2020f; Diao et al., 2020; Liu et al., 2020a, 2020b; Zheng et al., 2020b). Cytokines such as IFN-I and TNF-α may inhibit T cell recirculation in blood by promoting retention in lymphoid organs and attachment to endothelium (Kamphuis et al., 2006; Shiow et al., 2006). However, in an autopsy study examining the spleens and hilar lymph nodes of six patients who succumbed to COVID-19, Chen et al. observed extensive cell death of lymphocytes and suggested potential roles for IL-6 as well as Fas-FasL interactions (Chen et al., 2020h). In support of this hypothesis, the IL-6 receptor antagonist tocilizumab was found to increase the number of circulating lymphocytes (Giamarellos-Bourboulis et al., 2020). T cell recruitment to sites of infection may also reduce their presence in the peripheral blood compartment. scRNA-seq analysis of bronchoalveolar lavage (BAL) fluid of COVID-19 patients revealed an increase in CD8 T cell infiltrate with clonal expansion (Liao et al., 2020). Likewise, post-mortem examination of a patient who succumbed to ARDS following SARS-CoV-2 infection showed extensive lymphocyte infiltration in the lungs (Xu et al., 2020c). However, another study that examined post-mortem biopsies from four COVID-19 patients only found neutrophilic infiltration (Tian et al., 2020a). Further studies are therefore needed to better determine the cause and impact of the commonly observed lymphopenia in COVID-19 patients.

Induction of Antiviral T Cell Responses

Available information about SARS-CoV-1-specific T cell immunity may serve as an orientation for further understanding of SARS-CoV-2 infection. Immunogenic T cell epitopes are distributed across several SARS-CoV-1 proteins (S, N, and M, as well as ORF3), although CD4 T cell responses were more restricted to the S protein (Li et al., 2008). In SARS-CoV-1 survivors, the magnitude and frequency of specific CD8 memory T cells exceeded that of CD4 memory T cells, and virus-specific T cells persisted for at least 6–11 years, suggesting that T cells may confer long-term immunity (Ng et al., 2016; Tang et al., 2011). Limited data from viremic SARS patients further indicated that virus-specific CD4 T cell populations might be associated with a more severe disease course, since lethal outcomes correlated with elevated Th2 cell (IL-4, IL-5, IL-10) serum cytokines (Li et al., 2008). However, the quality of CD4 T cell responses needs to be further characterized to understand associations with disease severity. Few studies have thus far characterized specific T cell immunity in SARS-CoV-2 infection. In 12 patients recovering from mild COVID-19, robust T cell responses specific for viral N, M, and S proteins were detected by IFN-γ ELISPOT, weakly correlated with neutralizing antibody concentrations (similar to convalescent SARS-CoV-1 patients; Li et al., 2008), and subsequently contracted with only N-specific T cells

detectable in about one-third of the cases post recovery (Ni et al., 2020). In a second study, PBMCs from COVID-19 patients with moderate to severe ARDS were analyzed by flow cytometry approximately 2 weeks after ICU admission (Weiskopf et al., 2020). Both virus-specific CD4 and CD8 T cells were detected in all patients at average frequencies of 1.4% and 1.3%, respectively, and very limited phenotyping according to CD45RA and CCR7 expression status characterized these cells predominantly as either CD4 Tcm (central memory) or CD8 Tem (effector memory) and Temra (effector memory RA) cells. This study is notable for the use of large complementary peptide pools comprising 1,095 SARS-Cov-2 epitopes (overlapping 15-mers for S protein as well as computationally predicted HLA-I- and -II-restricted epitopes for all other viral proteins) as antigen-specific stimuli that revealed a preferential specificity of both CD4 and CD8 T cells for S protein epitopes, with the former population modestly increasing over ~10–30 days after initial onset of symptoms. A caveat, however, pertains to the identification of specific T cells by induced CD69 and CD137 co-expression, since upregulation of CD137 by CD4 T cells, in contrast to CD154, may preferentially capture regulatory T cells (Treg) (Bacher et al., 2016). Further analyses of S protein-specific T cells by ELISA demonstrated robust induction of IFN-γ, TNF-α, and IL-2 concomitant with lower levels of IL-5, IL-13, IL-9, IL-10, and IL-22. A third report focused on S-specific CD4 T cell responses in 18 patients with mild, severe, or critical COVID-19 using overlapping peptide pools and induced CD154 and CD137 co-expression as a readout for antiviral CD4 T cells. Such cells were present in 83% of cases and presented with enhanced CD38, HLA-DR, and Ki-67 expression indicative of recent *in vivo* activation (Braun et al., 2020). Of note, the authors also detected low frequencies of S-reactive CD4 T cells in 34% of SARS-CoV-2 seronegative healthy control donors. However, these CD4 T cells lacked phenotypic markers of activation and were specific for C-terminal S protein epitopes that are highly similar to endemic human CoVs, suggesting that crossreactive CD4 memory T cells in some populations (e.g., children and younger patients that experience a higher incidence of hCoV infections) may be recruited into an amplified primary SARS-CoV-2-specific response (Braun et al., 2020). Similarly, endemic CoV-specific CD4 T cells were previously shown to recognize SARS-CoV1 determinants (Gioia et al., 2005). How previous infections with endemic CoV may affect immune responses to SARS-CoV-2 will need to be further investigated.

Finally, in general accordance with the above findings on the induction of SARS-CoV-2-specific T cells, using TCR sequencing (TCR-seq), Huang et al. and Liao et al. reported greater TCR clonality of peripheral blood (Huang et al., 2020c) as well as BAL T cells (Liao et al., 2020) in patients with mild versus severe COVID-19. Moving forward, a comprehensive identification of immunogenic SARS-CoV-2 epitopes recognized by T cells (Campbell et al., 2020), as well as further studies on convalescent patients who recovered from mild and severe disease, will be particularly important.

T Cell Contribution to COVID-19 Hyperinflammation

While the induction of robust T cell immunity is likely essential for efficient virus control, dysregulated T cell responses may cause immunopathology and contribute to disease severity in COVID-19 patients (Figure 3). This is suggested in a study by Zhou et al., which reported a significantly increased PBMC frequency of polyclonal GM-CSF$^+$ CD4 T cells capable of prodigious *ex vivo* IL-6 and IFN-γ production only in critically ill COVID-19 patients (Zhou et al., 2020c). Of note, GM-CSF$^+$ CD4 T cells have been previously implicated in inflammatory autoimmune diseases, such as multiple sclerosis or juvenile rheumatoid arthritis, and high levels of circulating GM-CSF$^+$ CD4 T cells were found to be associated with poor outcomes in sepsis (Huang et al., 2019). Additionally, two studies observed reduced frequencies of Treg cells in severe COVID-19 cases (Chen et al., 2020c; Qin et al., 2020). Since Treg cells have been shown to help resolve ARDS inflammation in mouse models (Walter et al., 2018), a loss of Tregs might facilitate the development of COVID-19 lung immunopathology. Similarly, a reduction of $\gamma\delta$-T cells, a subset of T cells with apparent protective antiviral function in influenza pneumonia (Dong et al., 2018; Zheng et al., 2013), has been reported in severely sick COVID-19 patients (Guo et al., 2020; Lei et al., 2020b).

Phenotype and Function of T Cell Subsets in COVID-19

Currently, little is known about specific phenotypical and/or functional T cell changes associated with COVID-19. In the majority of preprints and peer-reviewed studies, there are reports of increased presence of activated T cells (Figure 3) characterized by expression of HLA-DR, CD38, CD69, CD25, CD44, and Ki-67 (Braun et al., 2020; Ni et al., 2020; Guo et al., 2020; Liao et al., 2020; Thevarajan et al., 2020; Yang et al., 2020a; Zheng et al., 2020a). Generally, independent of COVID-19 disease severity, CD8 T cells seem to be more activated than CD4 T cells (Qin et al., 2020; Thevarajan et al., 2020; Yang et al., 2020a), a finding that echoes stronger CD8 than CD4 T cell responses during SARS-CoV-1 (Li et al., 2008). Furthermore, in a case study of 10 COVID-19 patients, Diao et al. showed that levels of PD-1 increased from prodromal to symptomatic stages of the disease (Diao et al., 2020). PD-1 expression is commonly associated with T cell exhaustion, but it is important to emphasize that PD-1 is primarily induced by TCR signaling; it is thus also expressed by activated effector T cells (Ahn et al., 2018).

In addition, several studies reported higher expression of various co-stimulatory and inhibitory molecules such as OX-40 and CD137 (Zhou et al., 2020c), CTLA-4 and TIGIT (Zheng et al., 2020a), and NKG2a (Zheng et al., 2020b). Reduced numbers of CD28$^+$ CD8 T cells (Qin et al., 2020) as well as larger frequencies of PD-1$^+$ TIM3$^+$ CD8 T cells in ICU patients were also reported (Zhou et al., 2020c). Expression of most of these markers was found to be higher in CD8 than in CD4 T cells, and levels tended to increase in severe versus non-severe cases, which may be due to differences in viral load. Cellular functionality was shown to be impaired in CD4 and CD8 T cells of critically ill patients, with reduced frequencies of polyfunctional T cells (producing more than one cytokine) as well as generally lower IFN-γ and TNF-α production following restimulation with phorbol myristate acetate (PMA) and ionomycin (Chen et al., 2020c; Zheng et al., 2020a, 2020b). Similarly, Zheng et al. reported that CD8 T cells in severe COVID-19 appear less cytotoxic and effector-like with reduced CD107a degranulation and granzyme B (GzmB) production (Zheng et al., 2020b). In contrast, a different study

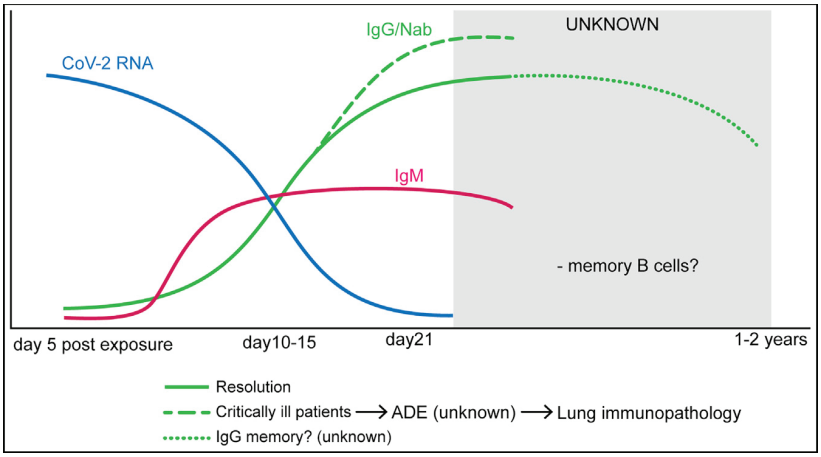

Figure 4. Antibody-Mediated Immunity in SARS-CoV-2

Virus-specific IgM and IgG are detectable in serum between 7 and 14 days after the onset of symptoms. Viral RNA is inversely correlated with neutralizing antibody titers. Higher titers have been observed in critically ill patients, but it is unknown whether antibody responses somehow contribute to pulmonary pathology. The SARS-CoV-1 humoral response is relatively short lived, and memory B cells may disappear altogether, suggesting that immunity with SARS-CoV-2 may wane 1–2 years after primary infection.

found that both GzmB and perforin were increased in CD8 T cells of severely sick patients (Zheng et al., 2020a). In accordance with the latter observation, when compared to a moderate disease group, convalescent patients with resolved severe SARS-CoV-1 infection had significantly higher frequencies of polyfunctional T cells, with CD4 T cells producing more IFN-γ, TNF-α, and IL-2 and CD8 T cells producing more IFN-γ, TNF-α, and CD107a, respectively (Li et al., 2008). However, given the vigorous dynamics of acute T cell responses and potential differences in sample timing throughout disease course, these observations are not necessarily mutually exclusive. Accordingly, RNA sequencing (RNA-seq) data by Liao et al. showed that CD8 T cells in the BAL fluid of severe COVID-19 patients express cytotoxic genes such as *GZMA*, *GZMB*, and *GZMK* at higher levels, while *KLRC1* and *XCL1* are enriched in mild cases (Liao et al., 2020).

In summary, T cells in severe COVID-19 seem to be more activated and may exhibit a trend toward exhaustion based on continuous expression of inhibitory markers such as PD-1 and TIM-3 as well as overall reduced polyfunctionality and cytotoxicity. Conversely, recovering patients were shown to have an increase in follicular helper CD4 T cells (T_{FH}) as well as decreasing levels of inhibitory markers along with enhanced levels of effector molecules such as Gzm A, GzmB, and perforin (Thevarajan et al., 2020; Yang et al., 2020a; Zheng et al., 2020b). Collectively, these studies provide a first glimpse into T cell dynamics in acute SARS-CoV-2 infection, but any conclusions have to be tempered at this stage on account of significant limitations in many of the current investigations.

B Cell Responses

Acute B Cell and Antibody Responses

The humoral immune response is critical for the clearance of cytopathic viruses and is a major part of the memory response that prevents reinfection. SARS-CoV-2 elicits a robust B cell response, as evidenced by the rapid and near-universal detection of virus-specific IgM, IgG and IgA, and neutralizing IgG antibodies (nAbs) in the days following infection. The kinetics of the antibody response to SARS-CoV-2 are now reasonably well described (Huang et al., 2020a).

Similar to SARS-CoV-1 infection (Hsueh et al., 2004), seroconversion occurs in most COVID-19 patients between 7 and 14 days after the onset of symptoms, and antibody titers persist in the weeks following virus clearance (Figure 4) (Haveri et al., 2020; Lou et al., 2020; Okba et al., 2020; Tan et al., 2020b; Wölfel et al., 2020; Wu et al., 2020b; Zhao et al., 2020a). Antibodies binding the SARS-CoV-2 internal N protein and the external S glycoprotein are commonly detected (Amanat et al., 2020; Ju et al., 2020; To et al., 2020). The receptor binding domain (RBD) of the S protein is highly immunogenic, and antibodies binding this domain can be potently neutralizing, blocking virus interactions with the host entry receptor, ACE2 (Ju et al., 2020; Wu et al., 2020b). Anti-RBD nAbs are detected in most tested patients (Ju et al., 2020; To et al., 2020; Wu et al., 2020b). Although crossreactivity to SARS-CoV-1 S and N proteins and to MERS-CoV S protein was detected in plasma from COVID-19 patients, no crossreactivity was found to the RBD from SARS-CoV-1 or MERS-CoV. In addition, plasma from COVID-19 patients did not neutralize SARS-CoV-1 or MERS-CoV (Ju et al., 2020).

RBD-specific $CD19^+IgG^+$ memory B cells were single-cell sorted from a cohort of eight COVID-19 donors between days 9 and 28 after the onset of symptoms (Ju et al., 2020). From their antibody gene sequences, 209 SARS-CoV-2-specific monoclonal antibodies were produced. The monoclonal antibodies had a diverse repertoire, relatively low or no somatic mutations, and variable binding reactivity, with dissociation constants reaching 10^{-8} to 10^{-9}, similar to antibodies isolated during acute infections. Two potent neutralizing SARS-CoV-2 RBD-specific monoclonal antibodies were characterized that did not cross-react with the RBD of SARS-CoV-1 or MERS-CoV (Ju et al., 2020). Together, these results demonstrate that antibody mediated neutralization is virus specific and likely driven by binding of epitopes within the RBD.

B Cell Memory: Development and Lifespan

The B cell response to a virus serves not only to protect from the initial challenge, but also to offer extended immunity against reinfection. Following resolution of an infection, plasma cells formed during the acute and convalescent phases continue to secrete antibodies, giving rise to serological memory. Memory B cells that are also formed during the primary infection constitute the second arm of B cell memory. Memory B cells can quickly respond to a reinfection by generating new high-affinity plasma cells. Long-term protection is achieved through the induction of long-lived plasma cells and memory B cells.

There is great interest in understanding the lifespan of B cell memory responses to SARS-CoV-2. Protection from reinfection has direct medical and social consequences as the world works to develop vaccination strategies and resume normal activities. In COVID-19 patients, evidence of near-universal seroconversion and the lack of substantial descriptions of reinfection point to a robust antibody response, which, along with the T cell memory response, would offer protection to reinfection. Indeed, a case study of a single patient described induction of $CD38^{Hi}CD27^{Hi}$ antibody-secreting cells (ASCs), concomitant with an increase in circulating follicular T helper cells (Tfh) cells (Thevarajan et al., 2020), and a scRNA-seq study of PBMCs from critically ill and recently recovered individuals revealed a plasma cell population (Guo et al., 2020). In addition, IgG memory cells specific to the RBD have been identified in the blood of COVID-19 patients (Ju et al., 2020). Consistent with the development of immunity after COVID-19 infection, a recent study of SARS-CoV-2 infection in rhesus macaques found that two macaques that had resolved the primary infection were resistant to reinfection 28 days later (Bao et al., 2020b).

Due to the timing of this outbreak, it is not yet possible to know the nature and extent of long-term memory responses, but lessons may again be learned from other human CoVs. In the case of the human CoV 229E, specific IgG and nAbs are rapidly induced but wane in some individuals around a year after infection, with some residual protection to reinfection (Callow et al., 1990; Reed, 1984). The lifespan of the humoral response following SARS-CoV-1 infection is also relatively short, with the initial specific IgG and nAb response to SARS-CoV-1 diminishing 2–3 years after infection and nearly undetectable in up to 25% of individuals (Cao et al., 2007; Liu et al., 2006). A long-term study following 34 SARS-CoV-1-infected healthcare workers over a 13-year period also found that virus-specific IgG declined after several years, but the authors observed detectable virus-specific IgG 12 years after infection (Guo et al., 2020). In the case of MERS-CoV, antibodies were detected in six of seven volunteers tested 3 years after infection (Payne et al., 2016).

IgG specific to SARS-CoV-2 trimeric spike protein was detectable in serum up to 60 days after symptom onset, but IgG titers began decreasing by 8 weeks post symptom onset (Adams et al., 2020). Long-term protection from reinfection may also be mediated by reactive memory B cells. A study that analyzed SARS-CoV-1 S protein-specific IgG memory cells at 2, 4, 6, and 8 months post infection found that S-specific IgG memory B cells decreased progressively about 90% from 2 to 8 months after infection (Traggiai et al., 2004). A further retrospective study of 23 individuals found no evidence of circulating SARS-CoV-1-specific IgG^{+} memory B cells 6 years after infection (Tang et al., 2011). This is in contrast to the memory T cell response, which was robustly detected based on induced IFN-γ production (Tang et al., 2011).

Studies of common CoVs SARS-CoV-1 and MERS-CoV indicate that virus-specific antibody responses wane over time and, in the case of common CoVs, result in only partial protection from reinfection. These data suggest that immunity to SARS-CoV-2 may diminish following a primary infection, and further studies will be required to determine the degree of long-term protection (Figure 4).

Consequences of the B Cell Response: Protection versus Enhancement

Several studies have demonstrated that high virus-specific antibody titers to SARS-CoV-2 are correlated with greater neutralization of virus *in vitro* and are inversely correlated with viral load in patients (Figure 4) (Okba et al., 2020; Wölfel et al., 2020; Zhao et al., 2020a). Despite these indications of a successful neutralizing response in the majority of individuals, higher titers are also associated with more severe clinical cases (Li et al., 2020b; Okba et al., 2020; Zhao et al., 2020a; Zhou et al., 2020a), suggesting that a robust antibody response alone is insufficient to avoid severe disease (Figure 4).

This was also observed in the previous SARS-CoV-1 epidemic, where neutralizing titers were found to be significantly higher in deceased patients compared to patients who had recovered (Zhang et al., 2006). This has led to concerns that antibody responses to these viruses may contribute to pulmonary pathology via antibody-dependent enhancement (ADE) (Figure 4). This phenomenon is observed when non-neutralizing virus-specific IgG facilitate entry of virus particles into Fc-receptor (FcR) expressing cells, particularly macrophages and monocytes, leading to inflammatory activation of these cells (Taylor et al., 2015). A study in SARS-CoV-1-infected rhesus macaques found that anti-S IgG contributed to severe acute lung injury (ALI) and massive accumulation of monocytes and macrophages in the lung (Liu et al., 2019). Furthermore, serum containing anti-S Ig from SARS-CoV-1 patients enhanced the infection of SARS-CoV-1 in human monocyte-derived macrophages *in vitro* (Yip et al., 2014). ADE was also reported with a monoclonal antibody isolated from a patient with MERS-CoV (Wan et al., 2020c). Somewhat reassuringly, there was no evidence of ADE mediated by sera from rats vaccinated with SARS-CoV-2 RBD *in vitro* (Quinlan et al., 2020) nor in macaques immunized with an inactivated SARS-CoV-2 vaccine candidate (Gao et al., 2020c).

As of now, there is no evidence that naturally developed antibodies toward SARS-CoV-2 contribute to the pathological features observed in COVID-19. However, this possibility should be considered when it comes to experimental design and development of therapeutic strategies. Importantly, in all of the descriptions of ADE as it relates to CoV, the FcR was necessary to trigger the antibody-mediated pathology. High-dose intravenous immunoglobulin (IVIg), which may blunt ADE, has been trialed in COVID-19 patients (Cao et al., 2020b; Shao et al., 2020), but further studies are needed to determine the extent to which IVIg is safe or beneficial in SARS-CoV-2 infection. Vaccine trials will need to consider the possibility of antibody-driven pathology upon antigen rechallenge; strategies using F(ab) fragments or engineered Fc monoclonal antibodies may prove particularly beneficial in this setting (Amanat and Krammer, 2020).

Predictors of COVID-19 Disease Risk and Severity

With the rapidly growing number of cases in the first few months, numerous reports on predictors of COVID-19 severity with small cohorts were released. These offered clinicians and immunologists the first understanding of the clinical course and pathological processes that are associated with the novel SARS-CoV-2 infection. This section highlights key findings from those studies, with a major focus on the immune factors associated with disease risk or severity.

Susceptibility and Risk Biomarkers

There are currently limited known risk factors for susceptibility to COVID-19, although this has been evaluated in several studies. Zhao et al. compared the ABO blood group distribution in a cohort of 2,173 COVID-19 patients to that of healthy controls from the corresponding regions (Zhao et al., 2020b). They found blood group A to be associated with a higher risk for acquiring COVID-19 when compared to non-A blood groups; blood group O had the lowest risk for the infection. Another study demonstrated an identical association (Zietz and Tatonetti, 2020), and similar results have been previously described for other viruses (Lindesmith et al., 2003), including SARS-CoV-1 (Cheng et al., 2005a).

Several large collaborative efforts are currently underway to generate, share, and analyze genetic data to understand the links between human genetic variation and COVID-19 susceptibility and severity, the most prominent of which is the COVID-19 Host Genetics Initiative (covid19hg.org). These studies are supported by previous observations on SARS-CoV-1 that followed the 2003 outbreak, which have identified significant associations between genetic variants and immune phenotypes (Chan et al., 2007; Wang et al., 2011; Zhao et al., 2011). Although identifying such polymorphisms and their associated genes and pathways for SARS-CoV-2 will require large cohorts, several studies, which remain to be tested in clinical trials, have already highlighted genetic polymorphisms that may potentially impact susceptibility. These studies have focused on genetic variants that may impact the expression or function of genes important in viral entry, namely ACE2 (SARS-CoV-2 receptor) and TMPRSS2 (spike protein activator) (Asselta et al., 2020; Cao et al., 2020c; Renieri et al., 2020; Stawiski et al., 2020). Cao et al. identified variants that are potentially expression quantitative trait loci (eQTL) of ACE2 (i.e., they may potentially alter ACE2 gene expression) and analyzed their frequencies in different populations (Cao et al., 2020c). Stawiski et al. listed variants that may be critical in ACE2 binding and thereby its function and compared the frequencies of these variants within different populations (Stawiski et al., 2020).

While there are several limitations to these studies, the major question is whether the utility of these biomarkers is replicable in large populations with COVID-19 clinical outcomes data and in targeted or large-scale genomic analyses that are currently underway. In addition, these studies will reveal the potential associations between genetic variants and susceptibility in a gene or loci agnostic fashion.

Routine Bloodwork Biomarkers

Several routine blood and serological parameters have been suggested to stratify patients who might be at higher risk for complications to aid in allocation of healthcare resources in the pandemic (Table 1). Serologic markers from routine bloodwork were reported by comparing patients with mild or moderate symptoms to those with severe symptoms. This includes different acute phase proteins, such as SAA (serum amyloid protein) and C-reactive protein (CRP) (Ji et al., 2020). Interestingly, elevations in CRP appear to be unique to COVID-19 patients when compared to other viral infections. Other consistently reported markers in non-survivors are increased procalcitonin (PCT) and IL-6 levels (Huang et al., 2020d), as well as increased serum urea, creatinine, cystatin C, direct bilirubin, and cholinesterase (Xiang et al., 2020a). Overall, inflammatory markers are common in severe cases of COVID-19 and appear to correlate with the severity of the symptoms and clinical outcome. Moreover, the extensive damage that occurs in specific organs of severe COVID-19 patients is possibly related to differences in the expression of ACE2 (Figure 5) (Du et al., 2020).

Lymphopenia is the most frequently described prognostic marker in COVID-19 (Table 1), and it appears to predict morbidity and mortality even at early stages (Fei et al., 2020). Tan et al. proposed a prognostic model based on lymphocyte counts at two time points: patients with less than 20% lymphocytes at days 10–12 from the onset of symptoms and less than 5% at days 17–19 had the worst outcomes in this study (Tan et al., 2020a). Wynants et al. compared predictors of disease severity across seven studies (>1,330 patients), highlighting CRP, neutrophil-to-lymphocyte ratio (N/L), and lactate dehydrogenase (LDH) as the most significant predictive biomarkers (Wynants et al., 2020). Furthermore, a meta-analysis of 30 COVID-19 studies with a total of 53,000 patients also attempted to identify early-stage patients with poor prognosis (Zhao et al., 2020d). The most consistent findings across the different studies were elevated levels of CRP, LDH, and D-dimer, as well as decreased blood platelet and lymphocyte counts (Yan et al., 2020b; Zhou et al., 2020d). Systemic and pulmonary thrombi have been reported with activation of the extrinsic coagulation cascade, involving dysfunctional endothelium and monocytic infiltration (Poor et al., 2020; Varga et al., 2020); thrombocytopenia and elevated D-dimer levels may be indicative of these coagulopathies in COVID-19 patients with important therapeutic implications (Fogarty et al., 2020; Poor et al., 2020).

Immunological Biomarkers in the Peripheral Blood

Immunological biomarkers are particularly important, as immunopathology has been suggested as a primary driver of morbidity and mortality with COVID-19. Several cytokines and other immunologic parameters have been correlated with COVID-19 severity (Table 1). Most notably, elevated IL-6 levels were detected in hospitalized patients, especially critically ill patients, in several studies and are associated with ICU admission, respiratory failure, and poor prognosis (Chen et al., 2020g; Huang et al., 2020b; Liu et al., 2020f). Increased IL-2R, IL-8, IL-10, and GM-CSF have been associated with disease severity as well, but studies are limited, and further studies with larger cohorts of patients are needed to indicate predictive power (Gong et al., 2020; Zhou et al., 2020b). Conflicting results regarding IL-1β and IL-4 have been reported (Fu et al., 2020; Gong et al., 2020; Wen et al., 2020). Although elevated cytokine concentrations have been widely described in COVID-19 patients, the vast majority (including IL-6, IL-10, IL-18, CTACK, and IFN-γ) do not seem to have prognostic value, because they do not always differentiate moderate cases from severe cases (Yang et al., 2020b). This stratification was possible with IP-10, MCP-3, and IL-1ra. While there are reports that levels of IL-6 at first assessment might predict respiratory failure (Herold et al., 2020), other publications with longitudinal analyses demonstrated that IL-6 increases fairly late during the disease's course, consequently compromising its prognostic value at earlier stages (Zhou et al., 2020a).

Liu et al. developed a web-based tool using k-means clustering to predict prognosis in terms of death or hospital discharge of COVID-19 patients using age, comorbidities (binary), and baseline log helper T cell count (TH), log suppressor T cell count (TS), and log TH/TS ratio (Liu et al., 2020e). Total T cell, helper T cell, and

Table 1. Routine Blood and Immunological Prognostic Biomarkers in COVID-19 Patients

	Biomarker	Purpose
Routine Bloodwork	Lymphocyte count	Predicted the disease severity and the outcomes of hospitalized patients (Tan et al., 2020a). Prognostic value was confirmed in numerous studies (Huang et al., 2020d; Liu et al., 2020b; Song et al., 2020; Wang et al., 2020f; Wynants et al., 2020; Yan et al., 2020b; Yang et al., 2020c; Zhang et al., 2020c; Zhao et al., 2020d). Decreased continuously in non-surviving patients (Wang et al., 2020b).
	N/L	Patients with N/L $\geq$3.13 were reported to be more likely to develop severe illness and to require ICU admission (Liu et al., 2020c). N/L on admission was a risk factor for short-term progression of patients with moderate pneumonia to severe pneumonia (Feng et al., 2020). Confirmed to be of prognostic value in COVID-19 in several studies (Song et al., 2020; Wynants et al., 2020; Zhou et al., 2020d).
	CRP	Proposed as an early biomarker of disease progression (Ji et al., 2020). Even in early stages, CRP levels were positively correlated with lung lesions and reflected disease severity (Wang, 2020). Confirmed in numerous studies (Fu et al., 2020; Huang et al., 2020d; Wynants et al., 2020; Yan et al., 2020b; Zhao et al., 2020d; Zhou et al., 2020b). Predicted the risk of acute myocardial injury (Liu et al., 2020g; Xu et al., 2020a).
	LDH	Higher in severe cases than in mild cases (Xiang et al., 2020a). Widely proposed to have prognostic value in COVID-19 (Huang et al., 2020d; Wynants et al., 2020; Yan et al., 2020b; Zhao et al., 2020d).
	D-dimer (and coagulation parameters)	Predicted severity independently of other variables (Zhou et al., 2020d). Elevated levels and disseminated intravascular coagulation are found in non-survivors (Wang et al., 2020b). Identified patients at risk for acute cardiac injury (Liu et al., 2020g). Other coagulation parameters, such as fibrin degradation product levels, longer prothrombin time, and activated partial thromboplastin time, were also associated with poor prognosis (Tang et al., 2020a).
	SAA	SAA was proposed to be used as an auxiliary index for diagnosis as it was elevated in 80% of the patients in a small cohort (Ji et al., 2020).
	NT-proBNP (N-terminal pro B type natriuretic peptide)	NT-proBNP was an independent risk factor of in-hospital death in patients with severe COVID-19 (Gao et al., 2020b).
	Platelet count	High platelet-to-lymphocyte ratio was associated with worse outcome (Qu et al., 2020). Thrombocytopenia was associated with poor outcome and with incidence of myocardial injury in COVID-19 (Liu et al., 2020h; Shi et al., 2020).

(*Continued on next page*)

Table 1. *Continued*

	Biomarker	Purpose
Immunological	CD4+, CD8+, and NK cell counts	Lower CD4+, CD8+, and NK cells in PBMCs correlated with severity of COVID-19 (Nie et al., 2020b). Validated by several studies (Wang et al., 2020f; Zheng et al., 2020b).
	PD-1 and Tim-3 expression on T cells	Increasing PD-1 and Tim-3 expression on T cells could be detected as patients progressed from prodromal to overtly symptomatic stages (Diao et al., 2020). Expression was higher in infected patients versus healthy controls and in ICU versus non-ICU patients in both CD4 and CD8 T cells (Zhou et al., 2020b).
	phenotypic changes in peripheral blood monocytes	The presence of a distinct population of monocytes with high forward scatter (CD11b+, CD14+, CD16+, CD68+, CD80+, CD163+, and CD206+, which secrete IL-6, IL-10, and TNF-α) was identified in patients requiring prolonged hospitalization and ICU admission (Zhang et al., 2020c). CD14+CD16+IL-6+ monocytes are increased in ICU patients (Zhou et al., 2020b).
	IP-10, MCP-3, and IL-1ra	IP-10, MCP-3, and IL-1ra were, among 48 examined cytokines, the only ones that closely associated with disease severity and outcome of COVID-19 in a study by Yang et al. (Yang et al., 2020b).
	IL-6	Associated with disease severity (hospitalization and ICU admission) and poor prognosis (Chen et al., 2020g; Huang et al., 2020b; Liu et al., 2020b, 2020f; Wang et al., 2020b). Increased levels were associated with higher risk of respiratory failure (Yao et al., 2020b).
	IL-8	Positively correlated with disease severity (Chen et al., 2020e; Gong et al., 2020), with severe cases showing the highest IL-8 levels.
	IL-10	Increased in severe or critical patients as compared to mild patients (Gong et al., 2020; Zhou et al., 2020d) without a statistically significant difference between severe and critical cases (Gong et al., 2020).
	IL-2R	Associated with disease severity in a study that, among other cytokines, also associated ferroprotein levels, PCT levels, and eosinophil counts with COVID-19 severity (Gong et al., 2020).
	IL-1β	CD14+IL-1β+ monocytes are abundant in early-recovery patients as shown in a single-cell RNA-seq analysis and thought to be associated with cytokine storm (Wen et al., 2020). IL-1β did not correlate with disease severity in a cross-sectional study with mild, severe, and critical patients (Gong et al., 2020).
	IL-4	IL-4 was associated with impaired lung lesions (Fu et al., 2020), but some reports point to a potential mediator effect (Wen et al., 2020).
	IL-18	In modeling immune cell interaction between DCs and B cells in late recovery COVID-19 patients, IL-18 was found to be important in B cell production of antibodies, which suggests its importance in recovery (Wen et al., 2020).
	GM-CSF	GM-CSF+IFN-γ+ T cells are higher in ICU than in non-ICU patients. CD14+CD16+GM-CSF+ monocytes are higher in COVID-19 patients as compared to healthy controls (Zhou et al., 2020b).
	IL-2 and IFN-γ	IL-2 and IFN-γ levels were shown to be increased in severe cases (Liu et al., 2020b).
	anti-SARS-CoV-2 antibody levels	Prolonged SARS-CoV-2 IgM positivity could be utilized as a predictive factor for poor recovery (Fu et al., 2020). Higher anti-SARS-CoV-2 IgG levels and higher N/L were more commonly found in severe cases (Zhang et al., 2020a).

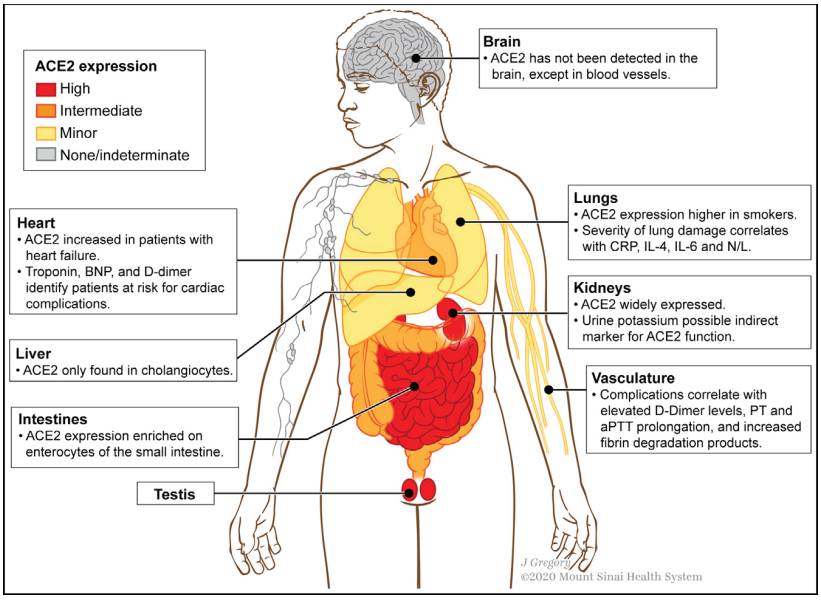

Figure 5. ACE2 Expression in Organs and Systems Most Frequently Implicated in COVID-19 Complications

The gastrointestinal tract, kidneys, and testis have the highest ACE2 expressions. In some organs, different cell types have remarkably distinct expressions; e.g., in the lungs, alveolar epithelial cells have higher ACE2 expression levels than bronchial epithelial cells; in the liver, ACE2 is not expressed in hepatocytes, Kupffer cells, or endothelial cells but is detected in cholangiocytes, which can explain liver injury to some extent. Furthermore, ACE2 expression is enriched on enterocytes of the small intestine compared to the colon.

ACE2, angiotensin-converting enzyme 2; BNP, B-type natriuretic peptide; CRP, C-reactive protein; IL, interleukin; N/L, neutrophil-to-lymphocyte ratio; PT, prothrombin time; aPTT, activated partial thromboplastin time.

suppressor T cell counts were significantly lower and the TH/TS ratio was significantly higher in patients who died from infection as compared to patients who were discharged.

Importantly, most serological and immunological changes observed in severe cases are associated with disease severity but cannot necessarily serve as predictive factors, as they may not have utility in early identification of patients at higher risk. Discovery of truly predictive biomarkers and potential drivers of hyperinflammatory processes requires comprehensive profiling of asymptomatic and mild cases and longitudinal studies that are limited to date. Confounding variables including age, gender, and comorbidities may dramatically affect associations observed. In addition, direct correlation with patient viral load will be important to provide a greater understanding of underlying causes of morbidity and mortality in COVID-19 and the contribution of viral infectivity, hyperinflammation, and host tolerance (Medzhitov et al., 2012).

In summary, lymphopenia, increases in proinflammatory markers and cytokines, and potential blood hypercoagulability characterize severe COVID-19 cases with features reminiscent of cytokine release syndromes. This correlates with a diverse clinical spectrum ranging from asymptomatic to severe and critical cases. During the incubation period and early phase of the disease, leukocyte and lymphocyte counts are normal or slightly reduced. After SARS-CoV-2 binds to ACE2 overexpressing organs, such as the gastrointestinal tracts and kidneys, increases in non-specific inflammation markers are observed. In more severe cases, a marked systemic release of inflammatory mediators and cytokines occurs, with corresponding worsening of lymphopenia and potential atrophy of lymphoid organs, impairing lymphocyte turnover (Terpos et al., 2020).

Antivirals

Antivirals are a class of small molecules that function as inhibitors of one or more stages of a virus life cycle. Because of similarities between different virus replication mechanisms, some antivirals can be repurposed against various viral infections. Currently, most of the available antiviral drugs tested against SARS-CoV-2 are small molecules previously developed against SARS-CoV-1, MERS-CoV, or other RNA and DNA viruses.

Broad-Spectrum Antivirals

A number of small molecules with known antiviral activity against other human RNA viruses are being evaluated for efficacy in treating SARS-CoV-2. The ribonucleoside analog β-D-N4-hydroxycytidine (NHC) reduced viral titers and lung injury in mice infected with SARS-CoV-2 via introduction of mutations in viral RNA (Sheahan et al., 2017). Further, an inhibitor of host DHODH, a rate-limiting enzyme in pyrimidine synthesis, was able to inhibit SARS-CoV-2 growth *in vitro* with greater efficacy than remdesivir or chloroquine (Wang et al., 2020e; Xiong et al., 2020). Merimepodib, a non-competitive inhibitor of the enzyme inosine-5′-monophosphate dehydrogenase (IMPDH), involved in host guanosine biosynthesis, is able to suppress SARS-CoV-2 replication *in vitro* (Bukreyeva et al., 2020). Finally, N-(2-hydroxypropyl)-3-trimethylammonium chitosan chloride (HTCC), which was previously shown to efficiently reduce infection by the less-pathogenic human CoV HCoV-NL63, was also found to inhibit MERS-CoV and pseudotyped SARS-CoV-2 in human airway epithelial cells (Milewska et al., 2020).

Protease Inhibitors

Much of the antiviral computational and experimental data currently available for SARS-CoV-2 focus on targeting the 3CL or Main protease (Mpro). Two prominent drug candidates targeting the SARS-CoV-2 Mpro were designed and synthesized by analyzing the substrate binding pocket of Mpro (Dai et al., 2020). The X-ray crystal structures of the novel inhibitors in complex with SARS-CoV-2 Mpro were resolved at 1.5 Å. Both compounds showed good pharmacokinetic activity *in vitro*, and one exhibited limited toxicity *in vivo* (Dai et al., 2020). Multiple studies also aimed to repurpose protease inhibitors to reduce SARS-CoV-2 titers. Nine existing HIV protease inhibitors (nelfinavir, lopinavir, ritonavir, saquinavir, atazanavir, tipranavir, amprenavir, darunavir, and indinavir) were evaluated for their

Immunity
Review

CellPress

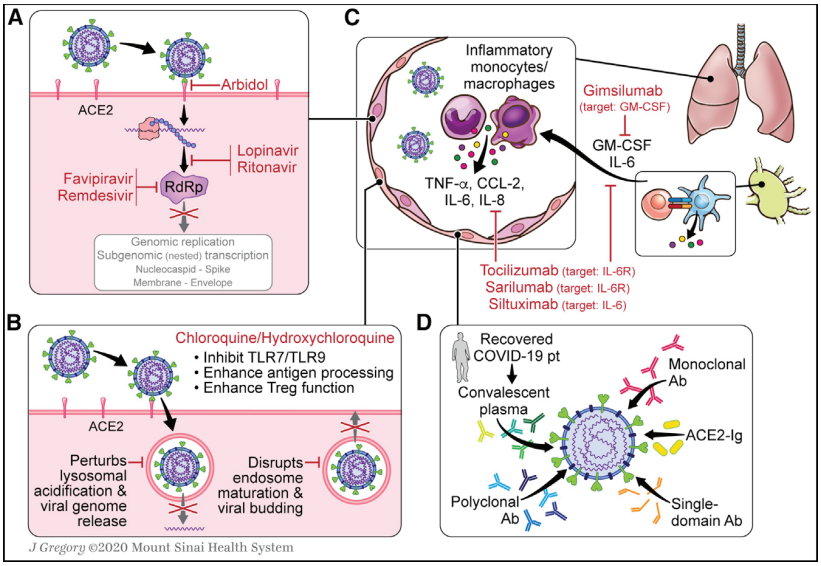

Figure 6. Available Therapeutic Options to Manage COVID-19 Immunopathology and to Deter Viral Propagation

(A) Rdrp inhibitors (remdesivir, favipiravir), protease inhibitors (lopinavir/ritonavir), and antifusion inhibitors (arbidol) are currently being investigated in their efficacy in controlling SARS-CoV-2 infections.

(B) CQ and HCQ increase the pH within lysosomes, impairing viral transit through the endolysosomal pathway. Reduced proteolytic function within lysosomes augments antigen processing for presentation on MHC complexes and increases CTLA4 expression on Tregs.

(C) Antagonism of IL-6 signaling pathway and of other cytokine-/chemokine-associated targets has been proposed to control COVID-19 CRS. These include secreted factors like GM-CSF that contribute to the recruitment of inflammatory monocytes and macrophages.

(D) Several potential sources of SARS-CoV-2 neutralizing antibodies are currently under investigation, including monoclonal antibodies, polyclonal antibodies, and convalescent plasma from recovered COVID-19 patients.

GM-CSF, granulocyte-macrophage colony-stimulating factor; CQ, chloroquine; HCQ, hydroxychloroquine; RdRp, RNA-dependent RNA polymerase.

antiviral activity in Vero cells infected with SARS-CoV-2 (Yamamoto et al., 2020), and nelfinavir was the most potent at inhibiting viral replication.

RdRp Inhibitors

The CoV RNA-dependent RNA polymerase (RdRp) catalyzes the synthesis of viral RNA (Gao et al., 2020a), making it essential for viral replication and a prime target for antiviral inhibitors. Remdesivir, an adenosine triphosphate analog, inhibits RdRp by binding to RNA strands and preventing additional nucleotides from being added, thereby terminating viral RNA transcription (Figure 6A) (Agostini et al., 2018). Remdesivir has been previously shown to be effective against MERS-CoV and SARS-CoV-1 infections in animal models (Sheahan et al., 2017; de Wit et al., 2020). Similarly, a study investigated the efficacy of remdesivir treatments on 12 rhesus macaques with SARS-CoV-2 infections (Williamson et al., 2020). Macaques treated with remdesivir showed a reduction in lung viral loads and pneumonia symptoms but no reduction in virus shedding. This study does provide evidence that if administered early enough, remdesivir may be effective at treating SARS-CoV-2 infections.

Antiviral Clinical Trials

A large number of clinical trials using experimental antiviral drugs are currently underway. A small proportion of them are aimed at repurposing existing antivirals, including arbidol (umifenovir), a broad-spectrum antiviral that blocks viral fusion; lopinavir/ritonavir (LPV/r), a combination of anti-HIV protease inhibitors; favipiravir, an RdRp inhibitor used to treat severe influenza infections (Hayden and Shindo, 2019); and remdesivir (Figure 6A). Chen et al. conducted a multicenter, randomized priority trial on 240 patients with confirmed COVID-19 infection to test favipiravir or arbidol (Chen et al., 2020b). Favipiravir was suggested to significantly improve symptom relief. However, the interpretation of this study is limited by a short clinical recovery window of 7 days, only 100 of 236 patients with confirmed COVID-19, and the lack of a control group.

LPV/r has previously shown efficacy in treating SARS-Cov-1 (Chu et al., 2004), prompting an early SARS-Cov-2 clinical trial (Li et al., 2020c). 44 patients were enrolled in a trial investigating the efficacy and safety of LPV/r (n = 21 patients), arbidol (n = 16), or control (n = 7) as treatment for mild to moderate COVID-19. At day 14 of treatment, 76.2%, 62.4%, and 71.4% of patients had a positive to negative conversion in the LPV/r, arbidol, and control groups, respectively, with no statistical significance between groups. A randomized controlled trial (RCT) with 200 severe COVID-19 patients did not observe a significant benefit of LPV/r either (Cao et al., 2020a). However, a study that looked at the impact of earlier administration of LPV/r treatment showed that when treatment of LPV/r was started within 10 days of symptom onset, a shorter duration of virus shedding was observed. Thus, timing of LPV/r administration may be critical to its efficacy (Yan et al., 2020a).

In a multicenter clinical study assessing the compassionate use of remdesivir in severe COVID-19 patients, 53 patients across several countries were treated with remdesivir for 10 days (Grein et al., 2020). 68% of the 53 patients who received remdesivir showed clinical improvement assessed through improved oxygen support or extubations. Without a proper control group, limited conclusions can be drawn with regards to the efficacy of remdesivir from this study. The measured 68% clinical improvement may be in line with average clinical improvement across patients treated with standard of care (Li et al., 2020c). A small RCT in China with 237 severe COVID-19 patients randomized 2:1 to remdesivir versus placebo demonstrated no significant benefit in time to clinical improvement (Wang et al., 2020g). Almost simultaneously, preliminary results from a larger National Institute of Allergy and Infectious Diseases (NIAID) RCT with more than 1,000 patients were announced with remdesevir to be associated with quicker time to recovery: 11 days compared with 15 days (Ledford, 2020). A non-significant benefit in mortality was also noted, and the trial was stopped early to

allow access to remdesivir in the placebo arm. Complete safety data and full publication are awaited, but this study offers encouraging results and has resulted in an FDA emergency use authorization for remdesivir in hospitalized COVID-19 patients.

Therapeutic Immunomodulation for COVID-19 Treatment

Chloroquine: Modes of Action and Immunological Impact

Chloroquine (CQ) and its derivative hydroxychloroquine (HCQ) have gained traction as possible therapeutics for COVID-19. Both drugs are used as antimalarial agents and as immunomodulatory therapies for rheumatologic diseases. However, the application of CQ and HCQ to COVID-19 stems from their past use as antivirals (Savarino et al., 2003), including for SARS-CoV-1 (Keyaerts et al., 2004; Vincent et al., 2005). CQ and HCQ interfere with lysosomal activity and have been reported to have immunomodulatory effects. CQ augments antigen processing for MHC class I and II presentation, directly inhibits endosomal TLR7 and TLR9, and enhances the activity of regulatory T cells (Garulli et al., 2008; Lo et al., 2015; Schrezenmeier and Dörner, 2020; Thomé et al., 2013a, 2013b). Early studies involving *in vitro* infection of host cells with SARS-CoV-2 demonstrated that both CQ and HCQ significantly impact endosomal maturation, resulting in increased sequestration of virion particles within endolysosomes. However, there has been conflicting evidence whether CQ is more potent than HCQ in reducing viral load (Liu et al., 2020d; Wang et al., 2020b; Yao et al., 2020a). Notably, one group reported that treatment of infected cells with HCQ before and during infection significantly reduced viral load, suggesting that combined prophylactic and therapeutic HCQ use yields maximum efficacy (Clementi et al., 2020). To better understand host immune responses to treatment, one group compared bulk transcriptomic changes in primary PBMCs treated with HCQ for 24 h to PBMCs from confirmed SARS-CoV-2 positive patients and controls, followed by a comparison of HCQ-treated primary macrophages to BAL and postmortem lung biopsies from COVID-19 patients (Corley et al., 2020). Across all comparisons, there was minimal overlap between host differential gene expression and genes altered by *in vitro* HCQ treatment. Thus, the potential mechanistic action of HCQ in the context of SARS-CoV-2 remains poorly defined.

Evaluation of HCQ Efficacy in Clinical Trials

Despite the apparent widespread use of HCQ and CQ to treat COVID-19 (Figure 6B), few controlled clinical trials have been performed so far and thus the potential benefits of these drugs for COVID-19 remains controversial. One of the earliest trials (2020-000890-25) was a single-arm, open-label trial of 600 mg daily HCQ in 20 COVID-19 patients. They reported that HCQ alone, or in combination with the antibiotic azithromycin (AZ), reduced viral load by day 6 (Gautret et al., 2020a). A follow-up trial in 80 patients treated with HCQ and AZ reported that 93% of patients had a negative PCR result on day 8 of treatment, and 81.3% were discharged within 10 days of treatment. However, it is important to note that both trials had no control arms (Gautret et al., 2020b). Rigorous statistical analyses by others that accounted for the patients excluded from the original analysis found limited evidence for HCQ monotherapy (Hulme et al., 2020; Lover, 2020). A double-blind RCT assessed HCQ monotherapy in the treatment of mild COVID-19 (ChiCTR2000029559) (Chen et al., 2020i). A total of 62 patients were enrolled; the treatment arm received 400 mg HCQ daily over 5 days. By day 6, patients who received HCQ had clinical resolution on average 1 day earlier than controls; no patients progressed to severe disease compared to four patients in the control arm. In a smaller RCT that treated 30 patients with mild COVID-19 (NCT04261517) with 400 mg HCQ for 7 days, there were no significant differences in the number of patients with negative PCR results on day 7 (all but one positive), median duration of hospitalization, time to fever resolution, or progression of disease on chest computed tomography (CT) (Chen et al., 2020d). The largest RCT to date enrolled 150 patients with mild COVID-19 across 16 centers in an open-label trial of HCQ and standard of care (ChiCTR2000029868). There were no significant differences between groups in conversion to negative SARS-CoV-2 RT-PCR result on day 28 or rate of symptom resolution; there were significantly more adverse events in the HCQ arm, though largely non-serious; they reported some evidence for faster normalization of C-reactive protein in the patients who received HCQ plus standard of care, but this finding was not significant (Tang et al., 2020b). A meta-analysis including most of the studies described here found no clinical benefits to patients receiving standard of care plus an HCQ regimen (Shamshirian et al., 2020).

Two studies have assessed HCQ efficacy in severe COVID-19. In a prospective study of 11 patients who had received 600 mg HCQ over 10 days with AZ on days 1–5, there were several patients with worsening clinical status and one death; 8 of 10 patients had a positive PCR result on day 10 (Molina et al., 2020). An ongoing double-blind RCT of patients with severe COVID-19 (NCT04323527) randomized 81 patients into high-dose HCQ (600 mg 2× per day for 10 days) or low-dose (450 mg/day for 5 days) treatment groups (Borba et al., 2020). Recruitment into the high-dose arm was halted prematurely due to poor safety outcomes. There was no significant difference in negative PCR results on day 4 or need for mechanical ventilation on day 6. Taken together, the clinical trials performed thus far to evaluate the efficacy of HCQ ± AZ for COVID-19 have not demonstrated clear evidence of clinical benefit in patients with severe disease. A search of ClinicalTrials.gov on April 27, 2020 found 140 clinical trials investigating HCQ. This number is rapidly growing, indicating the heightened interest in this therapeutic and pressing need for evidence-based recommendations.

Corticosteroids for COVID-19 Therapy

Because of their anti-inflammatory activity, corticosteroids (CSs) are an adjuvant therapy for ARDS and cytokine storm. However, the broad immunosuppression mediated by CS does raise the possibility that treatment could interfere with the development of a proper immune response against the virus. A meta-analysis of 5,270 patients with MERS-CoV, SARS-CoV-1, or SARS-CoV-2 infection found that CS treatment was associated with higher mortality rate (Yang et al., 2020c). A more recent meta-analysis of only SARS-CoV-2 infection assessed 2,636 patients and found no mortality difference associated with CS treatment, including in a subset of patients with ARDS (Gangopadhyay et al., 2020). Other studies have reported associations with delayed viral clearance and increased complications in SARS and

MERS patients (Sanders et al., 2020). In fact, the interim guidelines updated by the WHO on March 13, 2020 advise against giving systemic corticosteroids for COVID-19 (World Health Organization, 2020a). Yet, new data from COVID-19 are conflicting.

One group reported no significant difference in time to viral clearance between patients who received methylprednisolone orally (mild disease) or intravenously (i.v.) (severe) and those who did not (Fang et al., 2020). Retrospective studies from groups in China report that patients who were transferred to the ICU were less likely to have received CSs (Wang et al., 2020b) and that patients with ARDS who received methylprednisolone had reduced mortality risk (Wu et al., 2020a). In contrast, another retrospective analysis found that patients who received CSs were more likely to have either been admitted to the ICU or perished, although the CS-treated group also had significantly more comorbidities (Wang et al., 2020c). A smaller observational study of 31 patients found no association between corticosteroid treatment and time to viral clearance, length of hospital stay, or symptom duration (Zha et al., 2020). A larger study of adjuvant CSs in 244 patients with critical COVID-19 found no association with 28-day mortality; subgroup analysis of patients with ARDS found no association between treatment with CSs and clinical outcomes (Lu et al., 2020b). They also found that increased dosage was significantly associated with increased mortality risk. A retrospective review of 46 patients, of whom 26 received i.v. methylprednisolone, found that early, low-dose administration significantly improved SpO2 and chest CT, time to fever resolution, and time on supplemental oxygen therapy (Wang et al., 2020h). Others have published perspectives in support of early (Lee et al., 2020) and short-term, low-dose administration (Shang et al., 2020) based on anecdotal evidence but not clinical trials. Most of the current data on CS use in COVID-19 are from observational studies and support either modest clinical benefit or no meaningful effects. Larger RCTs are necessary to understand the risks and benefits of CSs for these patients; there are 22 trials evaluating various corticosteroids registered on ClinicalTrials.gov as of April 27, 2020.

Cytokine-Directed Therapy in COVID-19

Recombinant IFN as an Antiviral Treatment. One of the first defenses of the human body against RNA viruses like SARS-CoV-2 is the release of types I and III IFNs. It is important to note that type I IFN (IFNα/β) receptors are ubiquitously expressed, so IFNα/β signaling can result in not only antiviral effects, but also the activation of immune cells that potentially exacerbate pathogenesis. In contrast, type III IFN (also known as IFNλ) signals mainly in epithelial cells, as well as in a restricted pool of immune cells. Because type III IFNs have immunomodulatory functions, subsequent signaling could induce a potent antiviral effect without enhancing pathogenic inflammation (Andreakos et al., 2017; Prokunina-Olsson et al., 2020).

Recently, there has been a growing interest in the potential therapeutic impact of modulating the IFN response to disable COVID-19 pathogenesis. Before the current pandemic, groups have studied the role of IFNs in other betacoronavirus infections. One study of 40 patients with SARS-CoV-1 infection described unresolved elevated type I IFNs and ISGs in those with poor outcomes (Cameron et al., 2007). Others report that exogenous type I IFN does not improve outcomes when given with ribavirin in patients with MERS-CoV infection (Arabi et al., 2020), suggesting that the role of IFN as a therapeutic or prophylactic option may be strain or species specific (Sheahan et al., 2020). Interestingly, a recent study by Mount Sinai virology groups revealed that type I IFN signaling is impaired in the early response to SARS-CoV-2; *in vitro*, SARS-CoV-2 may be more susceptible to type I IFN than SARS-CoV-1 is (Blanco-Melo et al., 2020). Based on additional evidence that IFN responses to betacoronaviruses are altered as compared to other respiratory viruses (Blanco-Melo et al., 2020; Channappanavar et al., 2016; Okabayashi et al., 2006), trials of IFN-I/III administration have been initiated (NCT04343976, NCT04331899).

Cytokine Blockade. Hyperinflammatory responses and elevated levels of inflammatory cytokines, including IL-6, -8, and -10, have been shown to correlate with COVID-19 severity (Chen et al., 2020h; Diao et al., 2020; Gong et al., 2020; Moore and June, 2020; Wan et al., 2020a; Xu et al., 2020b). The drivers of this cytokine storm remain to be established, but they are likely triggered initially by a combination of viral PAMPs and host danger signals. The heterogeneous response between patients suggests other factors are involved, possibly including the SARS-CoV-2 receptor, ACE2 (Hirano and Murakami, 2020).

Several studies have begun to report the cellular programs that may contribute to the cytokine storm detected in COVID-19 patients. One group reported that in the context of generalized lymphopenia, certain subsets of CD4 T cells that express GM-CSF and IL-6 are more abundant in severe COVID-19 patients than in COVID-19 patients who do not require intensive care (Zhou et al., 2020b). Reports that other major proinflammatory cytokines (TNF-α, IFN-γ, IL-2) and chemokines (CCL2, CCL3, CCL4) are elevated underscore a potentially pathogenic $T_H1/2$ program in COVID-19 (Diao et al., 2020; Giamarellos-Bourboulis et al., 2020). Histological and single-cell analyses identified monocytes and macrophages as other potent sources of inflammatory cytokines in COVID-19 cytokine storm (Chen et al., 2020h; Giamarellos-Bourboulis et al., 2020; Law et al., 2005; Moore and June, 2020; Zhou et al., 2020b). Studies of other betacoronavirus infections, including SARS-CoV-1 and MERS-CoV, have also identified similar hyperactivation of monocytes, macrophages, and DCs as a driver of cytokine-mediated immunopathology in humans (Cheung et al., 2005; Chien et al., 2006; Huang et al., 2020c; Konig et al., 2020; Wang et al., 2005; Wong et al., 2004; Xu et al., 2020b; Zhou et al., 2020b).

Following preliminary reports of IL-6 as a critical cytokine in COVID-19-associated CRS, monoclonal antibodies that target the IL-6 signaling pathway have been proposed as therapeutic candidates (Moore and June, 2020) (Figure 6C). The commercial anti-IL-6R antibodies tocilizumab (Actemra) and sarilumab (Kevzara) and the anti-IL-6 antibody siltuximab (Sylvant) are now being tested for efficacy in managing COVID-19 CRS and pneumonia in 13 ongoing clinical trials (Table 2). To date, only one group has reported preliminary results from a cohort of 20 COVID-19 patients treated with a single administration of tocilizumab (400 mg, i.v.), along with lopinavir, methylprednisolone, and oxygen therapy (ChiCTR2000029765) (Xu et al., 2020b). The single observation study found recuperated lymphocyte counts in 10 of 19 patients and resolution of lung opacities in 19 of 20 patients on chest CT; 19 of 20 patients were discharged.

Table 2. Clinical Trials Evaluating the Efficacy of IL-6/IL-6R Blockade Therapy

Clinical Trial	Intervention
NCT04331795 (COVIDOSE) NCT04320615 (COVACTA) NCT04332913 (TOSCA) NCT04317092 (TOCOVID-19) NCT04335071 (CORON-ACT) NCT04315480 ChiCTR2000029765	tocilizumab
NCT04315298	sarilumab
NCT04310228	tocilizumab favipiravir
NCT04306705 (TACOS)	tocilizumab continuous renal replacement therapy standard of care
NCT04332094 (TOCOVID)	tocilizumab azithromycin hydroxychloroquine
NCT04341870 (CORIMUNO-VIRO)	sarilumab azithromycin hydroxychloroquine
NCT0433z638 (COV-AID)	tocilizumab siltuximab anakinra standard of care

All patients experienced an improvement in symptoms, and no subsequent pulmonary infections were reported. A second report described an association between use of tocilizumab and reduced likelihood of ICU admission and mechanical ventilation. Still, in 30 declining patients with severe COVID-19 pneumonia, this retrospective study did not report significant improvement in mortality on weighted analysis (Roumier et al., 2020). Nevertheless, these studies are encouraging, but like other treatment approaches, larger RCTs are needed.

In addition to the IL-6 signaling pathway, other cytokine- and chemokine-associated elements, including IL-1R, GM-CSF, and the chemokine receptor CCR5, have been proposed as potential targets for blockade to manage COVID-19 CRS (Figure 6C). Finally, complement activation was shown to be overactivated in lungs of COVID-19 patients. Although results from the randomized trial are not yet published, anti-C5a monoclonal antibody therapy showed benefits in two critically ill COVID-19 patients (Gao et al., 2020d).

Neutralizing Antibodies and Convalescent Plasma Therapy for COVID-19

While vaccines are being developed to educate a person's immune system to make their own nAbs against SARS-CoV-2, there is interest in using adoptive transfer of nAbs as a therapeutic approach (Figure 6D). This strategy has already proven to be effective against SARS-CoV-1 (Cao et al., 2010; Ho et al., 2005; ter Meulen et al., 2004; Park et al., 2020; Sui et al., 2004; Zhu et al., 2007) and MERS-CoV (Forni et al., 2015; Jia et al., 2019; Ying et al., 2015). In the case of SARS-CoV-2, these efforts are primarily centered on identifying nAbs made during natural infections or generating nAbs through animal vaccination approaches.

nAbs Derived from COVID-19 Patients

Patients who have recovered from SARS-CoV-2 infection are one potential source of nAbs (Chen et al., 2020a; Ju et al., 2020; Walls et al., 2020; Wölfel et al., 2020; Yuan et al., 2020). In an effort to obtain these nAbs, scientists sorted RBD-specific memory B cells and cloned their heavy and light variable regions to express recombinant forms of the corresponding antibodies (Chen et al., 2020a; Ju et al., 2020). Four of the antibodies produced in these studies (31B5, 32D4, P2C-2F6, P2C-1F11) showed high neutralizing potential *in vitro*, and all inhibited ACE2-RBD binding. Successful antibody-mediated neutralization of SARS-CoV-2 seemed to be dependent on the inhibition of ACE2/RBD binding. However, Chen et al. showed that nearly all antibodies derived from serum of 26 recovered patients bound to S1 and RBD, with only three actually inhibiting ACE2/RBD binding (Chen et al., 2020a). Of note, a SARS-CoV-1-derived neutralizing antibody (47D11) (Wang et al., 2020a) and a single-chain antibody against SARS-CoV-2 (n3130) (Wu et al., 2020c) have also been shown to neutralize SARS-CoV-2 without inhibiting ACE2/RBD binding. Thus, blocking this interaction may not be a prerequisite for an effective SARS-CoV-2 nAb. The generation of a hybridoma producing a monoclonal nAb against SARS-CoV-2 provides the potential for a therapeutic Ab that can be directly administered to patients to block ongoing infection and potentially even as a prophylactic (Figure 6D).

SARS-CoV-1 nAbs Also Neutralize SARS-CoV-2

SARS-CoV-1 and SARS-CoV-2 consensus sequences share about 80% identity (Tai et al., 2020). Thus, a wide range of SARS-CoV-1 nAbs have been tested for crossreactivity with SARS-CoV-2, as they could help speed up the development of potential COVID-19 treatments. In a recent study, antibodies were isolated from the memory B cells of an individual who recovered from SARS-CoV-1 infection. While 8 out of 25 isolated antibodies could bind SARS-CoV-2 S protein, one of them (s309; see Table 3) also neutralizes SARS-CoV-2 (Pinto et al., 2020). The combination of s309 with a weakly neutralizing antibody that could bind another RBD epitope led to enhanced neutralization potency. In addition, CR3022 (Table 3) was found to bind SARS-CoV-2 RBD (Tian et al., 2020b), but this antibody did not neutralize SARS-CoV-2 (Yuan et al., 2020). Computational simulations identified three amino acids that could be modified on CR3022 to enhance its binding affinity with SARS-CoV-2 RBD (Giron et al., 2020), potentially augmenting its neutralization potential.

nAbs Derived from Animals

Animal models represent another tool to generate nAbs against SARS-CoV-2 (Table 3). In one study, the authors developed a protocol to synthetize human nanobodies, smaller antibodies that only contain a variable heavy (VH) chain as first described in camelids (Wu et al., 2020c) (Figure 6D). Another antibody isolated from camelids immunized with SARS-CoV-1 and MERS-CoV S proteins then fused to a human Fc fragment showed neutralization potential against SARS-CoV-2 (VHH-72-Fc) (Wrapp et al., 2020). Genetically modified mice with humanized antibody genes can also be used to generate therapeutic monoclonal antibodies, as successfully experimented against Ebola

Table 3. Strategies to Isolate SARS-CoV-2 Neutralizing Antibodies

Ab Source	Clone	Target	Type of Antibody	Neutralization	Inhibition of ACE2/RBD Binding	Reference
Derived from COVID-19 patients	31B532D4	RBD	human monoclonal	yes	yes	Chen et al., 2020a
	P2C-2F6P2C-1F11	RBD	human monoclonal	yes	yes	Ju et al., 2020
Derived from SARS-CoV-1 patients	CR3022	RBD	human monoclonal	no	no	Tian et al., 2020b; Yuan et al., 2020; Giron et al., 2020
	S309	RBD	human monoclonal	yes	no	Pinto et al., 2020
Derived from SARS-CoV-1 or MERS-CoV-1 animal models	R325R302R007	S1	rabbit monoclonal	yes	no	Sun et al., 2020
	47D11	S1	recombinant human monoclonal (derived from hybridomas of immunized transgenic H2L2 mice)	yes	no	Wang et al., 2020a
	VHH-72-Fc	S	Fc-fusion derived from camelids VHH	yes	yes	Wrapp et al., 2020
		S	polyclonal mouse antibodies	yes	N/A	Walls et al., 2020; Yuan et al., 2020
Other	ACE2-Fc	RBD	ACE2-Fc fusion	yes	N/A	Lei et al., 2020a; Li et al., 2020d
	RBD-Fc	ACE2	RBD-Fc fusion	yes	N/A	Li et al., 2020d
	N3130	S1	human monoclonal single domain antibody isolated by phage display	yes	no	Wu et al., 2020c
	IVIg	N/A	polyclonal human IVIg	N/A	N/A	Díez et al., 2020; Shao et al., 2020
	$F(ab')_2$	RBD	horse polyclonal	yes	N/A	Pan et al., 2020

N/A, not assessed.

virus (Levine, 2019). Similar studies are now focused on the use of SARS-CoV-2 or derivatives to generate highly effective nAb in animal models, which can be directly given to infected patients, and efforts are already underway with estimates of clinical trials of pooled antibody cocktails beginning in early summer by Regeneron. Finally, another approach to nAb development is to fuse ACE2 protein and the Fc part of antibodies, as they would bind RBD and potentially be crossreactive among other CoVs (Figure 6D). Indeed, an ACE2-Fc (Lei et al., 2020a) and an RBD-Fc (Li et al., 2020d) have been shown to neutralize both SARS-CoV-1 and SARS-CoV-2 *in vitro*.

Convalescent Plasma Therapy

Although recombinant nAbs could provide an effective treatment, they will require a significant time investment to develop, test, and bring production to scale before becoming widely available to patients. A faster strategy consists of transferring convalescent plasma (CP) from previously infected individuals that have developed high titer nAbs that target SARS-CoV-2 (Figure 6D). Despite the current lack of appropriately controlled trials, CP therapy has been previously used and shown to be beneficial in several infectious diseases, such as the 1918 influenza pandemic (Luke et al., 2006), H1N1 influenza (Hung et al., 2011), and SARS-CoV-1 (Arabi et al., 2016). Thanks to the development of serological tests (Amanat et al., 2020; Cai et al., 2020; Xiang et al., 2020b; Zhang et al., 2020d), recovered COVID-19 patients can be screened to select plasma with high antibody titers.

Some studies and case reports on CP therapy for COVID-19 have evaluated the safety and the potential effectiveness of CP therapy in patients with severe disease (Ahn et al., 2020; Duan et al., 2020; Pei et al., 2020; Shen et al., 2020; Zhang et al., 2020b) (Table 4). These studies were neither controlled nor randomized, but they suggest that CP therapy is safe and can have a beneficial effect on the clinical course of disease. Further controlled trials are needed to determine the optimal timing and indication for CP therapy. CP therapy has also been proposed for prophylactic use in at-risk individuals, such as those with underlying health conditions or health care workers exposed to COVID-19 patients. The FDA has approved the use of CP to treat critically ill patients (Tanne, 2020). Determining when to administer the CP is also of great importance, as a study in SARS-CoV-1 patients showed that CP was much more efficient when given to patients before day 14 day of illness (Cheng et al., 2005b), as previously shown in influenza (Luke et al., 2006). This study also showed that CP therapy was more efficient in PCR-positive, seronegative patients. The amount of plasma and number of transfusions needed requires further investigation (Table 4).

Overall, CP therapy seems to be associated with improved outcomes and appears to be safe, but RCTs are needed to

Table 4. Clinical Studies of Convalescent Plasma Therapy in COVID-19 Patients

Patient Characteristics	Start of CP Therapy	Results	Reference
5 severe patients (30–70 yo)	between 10 and 22 days after hospital admission	body temperature normalized within 3 days in 4 of 5 patients	Shen et al., 2020
		clinical improvement	
		viral loads became negative within 12 days of the transfusion	
		nAb titers increased	
10 severe patients (34–78 yo)	median 16.5 dpo	disappearance of clinical symptoms after 3d	Duan et al., 2020
		chest CT improved	
		elevation of lymphocyte counts in patients with lymphocytopenia.	
		increase in SaO2 in all patients	
		resolution of SARS-CoV-2 viremia in 7 patients	
		increase in neutralizing antibody titers in 5 patients	
4 critical patients (31–73 yo)	at degradation of symptoms, between 11 and 19 days after hospital admission	clinical improvement	Zhang et al., 2020b
		reduced viral load	
		chest CT improved	
1 moderate patient, 2 critical patients	12 dpo, 27 dpo	viral detection negative 4 days after CP	Pei et al., 2020
		clinical improvement of 2 patients	
2 severe patients (67 and 71 yo)	7 dpo or 22 dpo	clinical improvement	Ahn et al., 2020
		reduced viral load	
		chest CT improved	

yo, years old; dpo, days post onset of symptoms.

confirm this. Several clinical trials are currently in progress worldwide (Belhadi et al., 2020).

Vaccine Development

The devastating effects of the pandemic spread of SARS-CoV-2 in a globally naive population has resulted in unprecedented efforts to rapidly develop, test, and disseminate a vaccine to protect against COVID-19 or to mitigate the effects of SARS-CoV-2 infection. Although vaccination has a long and successful history as an effective global health strategy, there are currently no approved vaccines to protect humans against CoVs (André, 2003). Previous work after the SARS-CoV-1 and MERS-CoV epidemics has provided a foundation on which many current efforts are currently building upon, including the importance of the S protein as a potential vaccine. Diverse vaccine platforms and preclinical animal models have been adapted to SARS-CoV-2, facilitating fast-moving and robust progress in creating and testing SARS-CoV-2 vaccine candidates. A number of vaccine candidates are already being tested in clinical trials, and more are continuing to progress toward clinical testing.

The S Protein as a Vaccine Target

Since SARS-CoV-1 first emerged, the S protein has been favored as the most promising target for vaccine development to protect against CoV infection. This particular viral protein has important roles in viral entry and in stimulating the immune response during natural infection and in vaccination studies of both SARS-CoV-1 and MERS-CoV (Du et al., 2009; Song et al., 2019; Zhou et al., 2018), which has also been confirmed for SARS-CoV-2 (Walls et al., 2020). The S protein has been found to induce robust and protective humoral and cellular immunity, including the development of nAbs and T cell-mediated immunity (Du et al., 2009). In animal models, correlates of protection against SARS-CoV-1 infection appear to be induction of nAbs against the S protein, although antibodies to other proteins have been detected, such as those against nucleoprotein (N) and ORF3a (Qiu et al., 2005; Sui et al., 2005). nAbs are also believed to protect against infection by blocking receptor binding and viral entry, which has been shown with pseudovirus-based neutralization assays (Ni et al., 2020; Nie et al., 2020a). Studies of SARS-CoV-1 indicate that T cell response against the S protein correlates with nAb titers and dominated the T cell response after natural infection, which also induced T cells active against the membrane (M) and N proteins, that memory T cell responses can persist even 11 years after infection, and that memory CD8+ T cells can protect mice from lethal challenge in the absence of memory CD4+ T cells and memory B cells (Li et al., 2008; Ng et al., 2016). RBD-specific antiviral T cell responses have also been detected in people who have recovered from COVID-19, further validating its promise as a vaccine target (Braun et al., 2020; Ni et al., 2020).

Table 5. Vaccine Candidates Currently Registered for Clinical Trials

Candidate	Design	Developer	Similar Strategy	ClinicalTrials.gov Identifier
mRNA-1273	LNP-encapsulated mRNA for full-length S protein	ModernaTX	CMV (John et al., 2018), ZKV (Pardi et al., 2017)	NCT04283461
BNT162a1, b1, b2, c2	LNP-encapsulated mRNA vaccines with different formats of RNA and targets, two for larger S sequence and two for optimized RBD	BioNTech SE and Pfizer		NCT04368728
INO-4800	DNA vaccine for full-length S protein	Inovio Pharmaceuticals	MERS-CoV (Modjarrad et al., 2019), HPV (Trimble et al., 2015)	NCT04336410
Ad5-nCoV	adenovirus type 5 encoding full-length S protein	CanSino Biologics	EBV (Zhu et al., 2015, 2017)	NCT04313127 (phase I) NCT04341389 (phase II)
ChAdOx1 nCoV-19	adenovirus encoding full-length S protein	University of Oxford	MERS-CoV (Alharbi et al., 2017), IAV (Antrobus et al., 2014)	NCT04324606
COVID-19 LV-SMENP-DC	dendritic cells infected with lentivirus expressing SMENP minigenes to express COVID-19 antigens, together with activated CTLs	Shenzhen Geno-Immune Medical Institute		NCT04276896
COVID-19 aAPCs	aAPCs infected with lentivirus expressing minigenes to express COVID-19 antigens	Shenzhen Geno-Immune Medical Institute		NCT04299724
bacTRL-Spike-1	live bacteria delivering plasmid encoding S protein	Symvivo Corporation	therapeutics reviewed (Charbonneau et al., 2020)	NCT04334980
PiCoVacc	inactivated SARS-CoV-2 vaccine	Sinovac Biotech	HAV, IAV, IBV, poliovirus, rabies virus	NCT04352608
SARS-CoV-2 rS	spike protein nanoparticle vaccine with or without Matrix-M adjuvant	Novavax		NCT04368988

aAPCs, artificial antigen-presenting cells; CMV, cytomegalovirus; EBV, Ebola virus; HAV, hepatitis A virus; HPV, human papillomavirus; IAV, influenza A virus; IBV, influenza B virus; LPN, lipid nanoparticle; ZKV, Zika virus.

Epitope Mapping

Although the antibodies targeting the RBD of the S protein have greater potential for providing cross-protective immunity, other fragments of the S protein and additional viral proteins have been investigated as target epitopes, especially for T cells. Researchers have taken advantage of the genetic similarity between SARS-CoV-2 and SARS-CoV-1 and MERS-CoV and bioinformatics approaches to rapidly identify potential B and T cell epitopes in the S and other proteins, with many studies providing data regarding antigen presentation and antibody-binding properties and one study looking into the predicted evolution of epitopes (Ahmed et al., 2020; Baruah and Bose, 2020; Bhattacharya et al., 2020; Fast et al., 2020; Grifoni et al., 2020; Lon et al., 2020; Zheng and Song, 2020). While the S protein has been found to be the most immunodominant protein in SARS-CoV-2, the M and N proteins also contain B and T cell epitopes, including some with high conservation with SARS-CoV-1 epitopes (Grifoni et al., 2020).

Vaccine Pipeline

For SARS-CoV-1 and MERS-CoV, animal studies and phase I clinical trials of potential vaccines targeting the S protein had encouraging results, with evidence of nAb induction and induction of cellular immunity (Lin et al., 2007; Martin et al., 2008; Modjarrad et al., 2019). These findings are being translated into SARS-CoV-2 vaccine development efforts, hastening the progress drastically. The WHO provided a report in April that reported 63 vaccine candidates in preclinical testing and three in clinical testing (World Health Organization, 2020b). A recent search on May 1, 2020 on ClinicalTrials.gov revealed 10 registered vaccine candidates (Table 5). The University of Pittsburgh is also looking to move their microneedle array vaccine candidate containing a codon-optimized S1 subunit protein into clinical trials (Kim et al., 2020). Sanofi and GlaxoSmithKline (GSK) have recently reported their intent to collaborate and bring together Sanofi's baculovirus expression system, which is used to produce the influenza virus vaccine, Flublok, to create an S protein vaccine adjuvanted with GSK's AS03. Sinovac Biotech will also enter testing in a clinical trial in China after it was found to protect rhesus macaques from viral challenge without signs of detectable immunopathology (Gao et al., 2020c). Although some of these vaccine candidates are based on platforms that have been used or tested for other purposes, there remain questions regarding their safety and immunogenicity, including the longevity of any induced responses, that will require continual evaluation.

Challenges

Although the development of a vaccine to protect against SARS-CoV-2 infection has progressed at an unprecedented rate and produced an impressive volume of candidates for testing,

many challenges lie ahead. The prior knowledge gained after SARS-CoV-1 was first discovered in 2003, and the subsequent emergence of MERS-CoV in 2012 provided a significant jumpstart, but the progress of SARS-CoV-2 vaccine development has already far outstripped the point of the blueprint created before COVID-19 became a pandemic. While a variety of platforms are simultaneously being innovated or adapted, they each have strengths and limitations, many of which relate to the delicate balance between safety and immunogenicity. Many shortcuts have been taken and will continue to be taken due to the urgency of the ongoing COVID-19 pandemic, but significant concerns need to be addressed. One such concern involves the accumulating data supporting the initial assessment that COVID-19 is disproportionately severe in older adults. In conjunction with the large body of work related to immune senescence, these findings indicate that vaccine design should take into consideration the impact of aging on vaccine efficacy (Nikolich-Žugich, 2018). Furthermore, questions remain regarding the possibility of antibody-dependent enhancement of COVID-19, with *in vitro* experiments, animal studies, and two studies of COVID-19 patients supporting this possibility (Cao, 2020; Tetro, 2020; Zhang et al., 2020a; Zhao et al., 2020a). Assuming vaccine candidates that can safely induce protective immune responses are identified, additional major hurdles will be the production and dissemination of a vaccine. For some types of vaccines, large-scale production will not be as much of an issue, and infrastructure already in place to produce current Good Manufacturing Practice (cGMP)-quality biologics can be repurposed, but this will only be applicable to a subset of the candidates (Thanh Le et al., 2020). In order to address the urgent need and stem the COVID-19 pandemic, regulatory agencies need to continue to support rapid testing and progression of vaccine candidates, companies need to disseminate important findings directly and openly, and researchers need to investigate correlates of protection using in-depth immune monitoring of patients with a broad range of clinical presentations and clinical trial participants. The newly announced Accelerating COVID-19 Therapeutic Interventions and Vaccines (ACTIV) is designed to bring together numerous governmental and industry entities to help address this need.

Concluding Remarks

The rapid spread of SARS-CoV-2 and the unprecedented nature of COVID-19 has demanded an urgency in both basic science and clinical research, and the scientific community has met that call with remarkable productivity. Within months, there has been a significant generation of scientific knowledge that has shed some light on the immunology of SARS-CoV-2 infections. Studies of past coronavirus outbreaks involving SARS-CoV-1 and MERS-CoV have provided a foundation for our understanding. The pathology of severe cases of COVID-19 does indeed resemble certain immunopathologies seen in SARS-CoV-1 and MERS-CoV infections, like CRS.

However, in many other ways, immune responses to SARS-CoV-2 are distinct from those seen with other coronavirus infections. The emerging epidemiological observation that significant proportions of individuals are asymptomatic despite infection not only reflects our current understanding that SARS-CoV-2 has a longer incubation period and higher rate of transmission than other coronaviruses, but also speaks to significant differences in the host immune response. Therefore, it is imperative that immune responses against SARS-CoV-2 and mechanisms of hyperinflammation-driven pathology are further elucidated to better define therapeutic strategies for COVID-19. Here, we reviewed the recent literature and highlighted hypotheses that interrogate mechanisms for viral escape from innate sensing, for hyperinflammation associated with CRS and inflammatory myeloid subpopulations, for lymphopenia marked by T cell and NK cell dysfunction, and for correlates of protection and their duration, among others. Still, additional studies are needed to address how these immune differences across patients or between different types of coronavirus infections dictate who succumbs to disease and who remains asymptomatic. Existing studies of SARS-CoV-1 and MERS-CoV and ongoing studies of SARS-CoV-2 will likely provide a robust framework to fulfill that unmet need.

CONSORTIA

The members of the Sinai Immunology Review Project are Manasi Agrawal, Mark Aleynick, Meriem Belabed, Graham Britton, Matthew Brown, Maria Casanova-Acebes, Jovani Catalan, Monica Centa, Andrew Charap, Andrew Chan, Steven T. Chen, Jonathan Chung, Cansu Cimen Bozkus, Evan Cody, Francesca Cossarini, Erica Dalla, Nicolas Fernandez, John Grout, Conor Gruber, Dan Fu Ruan, Pauline Hamon, Samarth Hegde, Etienne Humblin, Divya Jha, Maria Kuksin, Julia Kodysh, Andrew Leader, Rachel Levantovsky, Matthew Lin, Katherine Lindblad, Daniel Lozano-Ojalvo, Gabrielle Lubitz, Assaf Magen, Zafar Mahmood, Louise Malle, Gustavo Martinez-Delgado, Jaime Mateus-Tique, Elliot Meritt, Chang Moon, Alvaro Moreira, Justine Noel, Tim O'Donnell, Miyo Ota, Matthew D. Park, Luisanna Pia, Tamar Plitt, Venu Pothula, Jamie Redes, Ivan Reyes Torres, Emma Risson, Mark Roberto, Alfonso R. Sanchez-Paulete, Miriam Saffern, Bérengère Salomé, Myvizhi Esai Selvan, Joan Shang, Matthew Spindler, Alessandra Soares Schanoski, Maria Suprun, Jessica Tan, Michelle Tran, Verena van der Heide, Natalie Vaninov, C. Matthias Wilk, Julio Aguirre-Ghiso, Konstantina Alexandropoulos, Nina Bhardwaj, Dusan Bogunovic, Brian Brown, Judy Cho, Jeremiah Faith, Emilie Grasset, Zeynep H. Gümüş, Peter Heeger, Dirk Homann, Amir Horowitz, Ephraim Kenigsberg, Alice O. Kamphorst, Florian Krammer, Maria A. Curotto de Lafaille, Uri Laserson, Saurabh Mehandru, Miriam Merad, Robert Samstein, and Nicolas Vabret.

ACKNOWLEDGMENTS

We apologize to all authors whose work we could not cite due to space limitations. Trainee (PhD and MD/PhD or postdocs) and faculty contributing authors are listed in alphabetical order. Illustrations are by Jill K. Gregory and used with permission of Mount Sinai Health System. We would like to acknowledge funding sources including Fastgrant (M.M.), NCI Cancer Center Support Grant Supplement (M.M., R.M.S.) Burroughs Wellcome Fund (R.M.S.), NIH Director's Early Independence Award (R.M.S.) and NIH R01AI081848 (N.V., N.B., B.D.G.).

DECLARATION OF INTERESTS

N.B. serves as an advisor/board member for Neon, Checkpoint Sciences, Primevax, Novartis, Array BioPharma, Roche, Avidea, Boeringer Ingelheim, Rome Therapeutics, Roswell Park, and the Parker Institute for Cancer Immunotherapy. N.B. receives research support from the Parker Insitute, Novocure, Celldex, Genentech, Oncovir, and Regeneron. M.M. serves as an advisor/board member for Celsius, Pionyr, Compugen, Myeloids and Innate pharma and ad hoc for Takeda. M.M. receives research support from Regeneron, Takeda, and Genentech. A.M. has equity in Gilead Sciences and Regeneron Pharmaceuticals.

REFERENCES

Adams, E.R., Anand, R., Andersson, M.I., Auckland, K., Baillie, J.K., Barnes, E., Bell, J., Berry, T., Bibi, S., Carroll, M., et al. (2020). Evaluation of antibody

testing for SARS-Cov-2 using ELISA and lateral flow immunoassays. medRxiv. https://doi.org/10.1101/2020.04.15.20066407.

Agostini, M.L., Andres, E.L., Sims, A.C., Graham, R.L., Sheahan, T.P., Lu, X., Smith, E.C., Case, J.B., Feng, J.Y., Jordan, R., et al. (2018). Coronavirus Susceptibility to the Antiviral Remdesivir (GS-5734) Is Mediated by the Viral Polymerase and the Proofreading Exoribonuclease. MBio *9*, e00221, e18.

Ahmed, S.F., Quadeer, A.A., and McKay, M.R. (2020). Preliminary Identification of Potential Vaccine Targets for the COVID-19 Coronavirus (SARS-CoV-2) Based on SARS-CoV Immunological Studies. Viruses *12*, 254.

Ahn, E., Araki, K., Hashimoto, M., Li, W., Riley, J.L., Cheung, J., Sharpe, A.H., Freeman, G.J., Irving, B.A., and Ahmed, R. (2018). Role of PD-1 during effector CD8 T cell differentiation. Proc. Natl. Acad. Sci. USA *115*, 4749–4754.

Ahn, J.Y., Sohn, Y., Lee, S.H., Cho, Y., Hyun, J.H., Baek, Y.J., Jeong, S.J., Kim, J.H., Ku, N.S., Yeom, J.-S., et al. (2020). Use of Convalescent Plasma Therapy in Two COVID-19 Patients with Acute Respiratory Distress Syndrome in Korea. J. Korean Med. Sci. *35*, e149.

Alharbi, N.K., Padron-Regalado, E., Thompson, C.P., Kupke, A., Wells, D., Sloan, M.A., Grehan, K., Temperton, N., Lambe, T., Warimwe, G., et al. (2017). ChAdOx1 and MVA based vaccine candidates against MERS-CoV elicit neutralising antibodies and cellular immune responses in mice. Vaccine *35*, 3780–3788.

Amanat, F., and Krammer, F. (2020). SARS-CoV-2 Vaccines: Status Report. Immunity *52*, 583–589.

Amanat, F., Stadlbauer, D., Strohmeier, S., Nguyen, T.H.O., Chromikova, V., McMahon, M., Jiang, K., Asthagiri Arunkumar, G., Jurczyszak, D., Polanco, J., et al. (2020). A serological assay to detect SARS-CoV-2 seroconversion in humans. Nat. Med. Published online May 12, 2020. https://doi.org/10.1038/s41591-020-0913-5.

André, F.E. (2003). Vaccinology: Past Achievements, Present Roadblocks and Future Promises. Vaccine *21*, 593–595.

Andreakos, E., Salagianni, M., Galani, I.E., and Koltsida, O. (2017). Interferon-λs: Front-Line Guardians of Immunity and Homeostasis in the Respiratory Tract. Front. Immunol. *8*, 1232.

Antrobus, R.D., Coughlan, L., Berthoud, T.K., Dicks, M.D., Hill, A.V., Lambe, T., and Gilbert, S.C. (2014). Clinical assessment of a novel recombinant simian adenovirus ChAdOx1 as a vectored vaccine expressing conserved Influenza A antigens. Mol. Ther. *22*, 668–674.

Arabi, Y.M., Al-Enezi, F., Longuere, K.-S., Balkhy, H.H., Al-Sultan, M., Al-Omari, A., Al-Hameed, F.M., Carson, G., Shindo, N., and Fowler, R. (2016). Feasibility of a randomized controlled trial to assess treatment of Middle East Respiratory Syndrome Coronavirus (MERS-CoV) infection in Saudi Arabia: a survey of physicians. BMC Anesthesiol. *16*, 36.

Arabi, Y.M., Shalhoub, S., Mandourah, Y., Al-Hameed, F., Al-Omari, A., Al Qasim, E., Jose, J., Alraddadi, B., Almotairi, A., Al Khatib, K., et al. (2020). Ribavirin and Interferon Therapy for Critically Ill Patients With Middle East Respiratory Syndrome: A Multicenter Observational Study. Clin. Infect. Dis. *70*, 1837–1844.

Asselta, R., Paraboschi, E.M., Mantovani, A., and Duga, S. (2020). *ACE2* and *TMPRSS2* variants and expression as candidates to sex and country differences in COVID-19 severity in Italy. medRxiv. https://doi.org/10.1101/2020.03.30.20047878.

Bacher, P., Heinrich, F., Stervbo, U., Nienen, M., Vahldieck, M., Iwert, C., Vogt, K., Kollet, J., Babel, N., Sawitzki, B., et al. (2016). Regulatory T Cell Specificity Directs Tolerance versus Allergy against Aeroantigens in Humans. Cell *167*, 1067–1078.e16.

Bao, L., Deng, W., Huang, B., Gao, H., Liu, J., Ren, L., Wei, Q., Yu, P., Xu, Y., Qi, F., et al. (2020a). The Pathogenicity of SARS-CoV-2 in hACE2 Transgenic Mice. Nature. Published online May 7, 2020. https://doi.org/10.1038/s41586-020-2312-y.

Bao, L., Deng, W., Gao, H., Xiao, C., Liu, J., Xue, J., Lv, Q., Liu, J., Yu, P., Xu, Y., et al. (2020b). Reinfection could not occur in SARS-CoV-2 infected rhesus macaques. bioRxiv. https://doi.org/10.1101/2020.03.13.990226.

Barnes, B.J., Adrover, J.M., Baxter-Stoltzfus, A., Borczuk, A., Cools-Lartigue, J., Crawford, J.M., Daßler-Plenker, J., Guerci, P., Huynh, C., Knight, J.S., et al. (2020). Targeting potential drivers of COVID-19: Neutrophil extracellular traps. J. Exp. Med. *217*, e20200652.

Baruah, V., and Bose, S. (2020). Immunoinformatics-aided identification of T cell and B cell epitopes in the surface glycoprotein of 2019-nCoV. J. Med. Virol. *92*, 495–500.

Belhadi, D., Peiffer-Smadja, N., Lescure, F.-X., Yazdanpanah, Y., Mentré, F., and Laouénan, C. (2020). A brief review of antiviral drugs evaluated in registered clinical trials for COVID-19. medRxiv. https://doi.org/10.1101/2020.03.18.20038190.

Bhattacharya, M., Sharma, A.R., Patra, P., Ghosh, P., Sharma, G., Patra, B.C., Lee, S.-S., and Chakraborty, C. (2020).). Development of Epitope-Based Peptide Vaccine Against Novel Coronavirus 2019 (SARS-COV-2): Immunoinformatics Approach. J. Med. Virol. Published online February 28, 2020. https://doi.org/10.1002/jmv.25736.

Blanco-Melo, D., Nilsson-Payant, B.E., Liu, W.-C., Uhl, S., Hoagland, D., Møller, R., Jordan, T.X., Oishi, K., Panis, M., Sachs, D., et al. (2020). Imbalanced Host Response to SARS-CoV-2 Drives Development of COVID-19. Cell. Published online May 15, 2020. https://doi.org/10.1016/j.cell.2020.04.026.

Borba, M.G.S., de Almeida Val, F., Sampaio, V.S., Alexandre, M.A.A., Melo, G.C., Brito, M., Mourão, M.P.G., Brito Sousa, J.D., Baía-da-Silva, D.C., Guerra, M.V.F., et al. (2020). Effect of High vs Low Doses of Chloroquine Diphosphate as Adjunctive Therapy for Patients Hospitalized With Severe Acute Respiratory Syndrome Coronavirus 2 (SARS-CoV-2) Infection. JAMA Netw. Open *3*, e208857.

Bouvet, M., Debarnot, C., Imbert, I., Selisko, B., Snijder, E.J., Canard, B., and Decroly, E. (2010). In vitro reconstitution of SARS-coronavirus mRNA cap methylation. PLoS Pathog. *6*, e1000863.

Braud, V.M., Allan, D.S., O'Callaghan, C.A., Söderström, K., D'Andrea, A., Ogg, G.S., Lazetic, S., Young, N.T., Bell, J.I., Phillips, J.H., et al. (1998). HLA-E binds to natural killer cell receptors CD94/NKG2A, B and C. Nature *391*, 795–799.

Braun, J., Loyal, L., Frentsch, M., Wendisch, D., Georg, P., Kurth, F., Hippenstiel, S., Dingeldey, M., Kruse, B., Fauchere, F., et al. (2020). Presence of SARS-CoV-2 reactive T cells in COVID-19 patients and healthy donors. medRxiv. https://doi.org/10.1101/2020.04.17.20061440.

Brooks, A.G., Posch, P.E., Scorzelli, C.J., Borrego, F., and Coligan, J.E. (1997). NKG2A complexed with CD94 defines a novel inhibitory natural killer cell receptor. J. Exp. Med. *185*, 795–800.

Bukreyeva, N., Mantlo, E.K., Sattler, R.A., Huang, C., Paessler, S., and Zeldis, J. (2020). The IMPDH inhibitor merimepodib suppresses SARS-CoV-2 replication *in vitro*. bioRxiv. https://doi.org/10.1101/2020.04.07.028589.

Cai, X.-f., Chen, J., Hu, J.-l., Long, Q.-x., Deng, H.-j., Fan, K., Liao, P., Liu, B.-z., Wu, G.-c., Chen, Y.-k., et al. (2020). A Peptide-Based Magnetic Chemiluminescence Enzyme Immunoassay for Serological Diagnosis of Corona virus Disease 2019. J. Infect. Dis. Published online May 8, 2020. https://doi.org/10.1093/infdis/jiaa243.

Callow, K.A., Parry, H.F., Sergeant, M., and Tyrrell, D.A. (1990). The time course of the immune response to experimental coronavirus infection of man. Epidemiol. Infect. *105*, 435–446.

Cameron, M.J., Ran, L., Xu, L., Danesh, A., Bermejo-Martin, J.F., Cameron, C.M., Muller, M.P., Gold, W.L., Richardson, S.E., Poutanen, S.M., et al.; Canadian SARS Research Network (2007). Interferon-mediated immunopathological events are associated with atypical innate and adaptive immune responses in patients with severe acute respiratory syndrome. J. Virol. *81*, 8692–8706.

Cameron, M.J., Kelvin, A.A., Leon, A.J., Cameron, C.M., Ran, L., Xu, L., Chu, Y.K., Danesh, A., Fang, Y., Li, Q., et al. (2012). Lack of innate interferon responses during SARS coronavirus infection in a vaccination and reinfection ferret model. PLoS ONE *7*, e45842.

Camp, J.V., and Jonsson, C.B. (2017). A Role for Neutrophils in Viral Respiratory Disease. Front. Immunol. *8*, 550.

Campbell, K.M., Steiner, G., Wells, D.K., Ribas, A., and Kalbasi, A. (2020). Prediction of SARS-CoV-2 epitopes across 9360 HLA class I alleles. bioRxiv. https://doi.org/10.1101/2020.03.30.016931.

Canton, J., Fehr, A.R., Fernandez-Delgado, R., Gutierrez-Alvarez, F.J., Sanchez-Aparicio, M.T., García-Sastre, A., Perlman, S., Enjuanes, L., and Sola, I. (2018). MERS-CoV 4b protein interferes with the NF-κB-dependent innate immune response during infection. PLoS Pathog. *14*, e1006838.

testing for SARS-Cov-2 using ELISA and lateral flow immunoassays. medRxiv. https://doi.org/10.1101/2020.04.15.20066407.

Agostini, M.L., Andres, E.L., Sims, A.C., Graham, R.L., Sheahan, T.P., Lu, X., Smith, E.C., Case, J.B., Feng, J.Y., Jordan, R., et al. (2018). Coronavirus Susceptibility to the Antiviral Remdesivir (GS-5734) Is Mediated by the Viral Polymerase and the Proofreading Exoribonuclease. MBio *9*, e00221, e18.

Ahmed, S.F., Quadeer, A.A., and McKay, M.R. (2020). Preliminary Identification of Potential Vaccine Targets for the COVID-19 Coronavirus (SARS-CoV-2) Based on SARS-CoV Immunological Studies. Viruses *12*, 254.

Ahn, E., Araki, K., Hashimoto, M., Li, W., Riley, J.L., Cheung, J., Sharpe, A.H., Freeman, G.J., Irving, B.A., and Ahmed, R. (2018). Role of PD-1 during effector CD8 T cell differentiation. Proc. Natl. Acad. Sci. USA *115*, 4749–4754.

Ahn, J.Y., Sohn, Y., Lee, S.H., Cho, Y., Hyun, J.H., Baek, Y.J., Jeong, S.J., Kim, J.H., Ku, N.S., Yeom, J.-S., et al. (2020). Use of Convalescent Plasma Therapy in Two COVID-19 Patients with Acute Respiratory Distress Syndrome in Korea. J. Korean Med. Sci. *35*, e149.

Alharbi, N.K., Padron-Regalado, E., Thompson, C.P., Kupke, A., Wells, D., Sloan, M.A., Grehan, K., Temperton, N., Lambe, T., Warimwe, G., et al. (2017). ChAdOx1 and MVA based vaccine candidates against MERS-CoV elicit neutralising antibodies and cellular immune responses in mice. Vaccine *35*, 3780–3788.

Amanat, F., and Krammer, F. (2020). SARS-CoV-2 Vaccines: Status Report. Immunity *52*, 583–589.

Amanat, F., Stadlbauer, D., Strohmeier, S., Nguyen, T.H.O., Chromikova, V., McMahon, M., Jiang, K., Asthagiri Arunkumar, G., Jurczyszak, D., Polanco, J., et al. (2020). A serological assay to detect SARS-CoV-2 seroconversion in humans. Nat. Med. Published online May 12, 2020. https://doi.org/10.1038/s41591-020-0913-5.

André, F.E. (2003). Vaccinology: Past Achievements, Present Roadblocks and Future Promises. Vaccine *21*, 593–595.

Andreakos, E., Salagianni, M., Galani, I.E., and Koltsida, O. (2017). Interferon-λs: Front-Line Guardians of Immunity and Homeostasis in the Respiratory Tract. Front. Immunol. *8*, 1232.

Antrobus, R.D., Coughlan, L., Berthoud, T.K., Dicks, M.D., Hill, A.V., Lambe, T., and Gilbert, S.C. (2014). Clinical assessment of a novel recombinant simian adenovirus ChAdOx1 as a vectored vaccine expressing conserved Influenza A antigens. Mol. Ther. *22*, 668–674.

Arabi, Y.M., Al-Enezi, F., Longuere, K.-S., Balkhy, H.H., Al-Sultan, M., Al-Omari, A., Al-Hameed, F.M., Carson, G., Shindo, N., and Fowler, R. (2016). Feasibility of a randomized controlled trial to assess treatment of Middle East Respiratory Syndrome Coronavirus (MERS-CoV) infection in Saudi Arabia: a survey of physicians. BMC Anesthesiol. *16*, 36.

Arabi, Y.M., Shalhoub, S., Mandourah, Y., Al-Hameed, F., Al-Omari, A., Al Qasim, E., Jose, J., Alraddadi, B., Almotairi, A., Al Khatib, K., et al. (2020). Ribavirin and Interferon Therapy for Critically Ill Patients With Middle East Respiratory Syndrome: A Multicenter Observational Study. Clin. Infect. Dis. *70*, 1837–1844.

Asselta, R., Paraboschi, E.M., Mantovani, A., and Duga, S. (2020). *ACE2* and *TMPRSS2* variants and expression as candidates to sex and country differences in COVID-19 severity in Italy. medRxiv. https://doi.org/10.1101/2020.03.30.20047878.

Bacher, P., Heinrich, F., Stervbo, U., Nienen, M., Vahldieck, M., Iwert, C., Vogt, K., Kollet, J., Babel, N., Sawitzki, B., et al. (2016). Regulatory T Cell Specificity Directs Tolerance versus Allergy against Aeroantigens in Humans. Cell *167*, 1067–1078.e16.

Bao, L., Deng, W., Huang, B., Gao, H., Liu, J., Ren, L., Wei, Q., Yu, P., Xu, Y., Qi, F., et al. (2020a). The Pathogenicity of SARS-CoV-2 in hACE2 Transgenic Mice. Nature. Published online May 7, 2020. https://doi.org/10.1038/s41586-020-2312-y.

Bao, L., Deng, W., Gao, H., Xiao, C., Liu, J., Xue, J., Lv, Q., Liu, J., Yu, P., Xu, Y., et al. (2020b). Reinfection could not occur in SARS-CoV-2 infected rhesus macaques. bioRxiv. https://doi.org/10.1101/2020.03.13.990226.

Barnes, B.J., Adrover, J.M., Baxter-Stoltzfus, A., Borczuk, A., Cools-Lartigue, J., Crawford, J.M., Daßler-Plenker, J., Guerci, P., Huynh, C., Knight, J.S., et al. (2020). Targeting potential drivers of COVID-19: Neutrophil extracellular traps. J. Exp. Med. *217*, e20200652.

Baruah, V., and Bose, S. (2020). Immunoinformatics-aided identification of T cell and B cell epitopes in the surface glycoprotein of 2019-nCoV. J. Med. Virol. *92*, 495–500.

Belhadi, D., Peiffer-Smadja, N., Lescure, F.-X., Yazdanpanah, Y., Mentré, F., and Laouénan, C. (2020). A brief review of antiviral drugs evaluated in registered clinical trials for COVID-19. medRxiv. https://doi.org/10.1101/2020.03.18.20038190.

Bhattacharya, M., Sharma, A.R., Patra, P., Ghosh, P., Sharma, G., Patra, B.C., Lee, S.-S., and Chakraborty, C. (2020).). Development of Epitope-Based Peptide Vaccine Against Novel Coronavirus 2019 (SARS-COV-2): Immunoinformatics Approach. J. Med. Virol. Published online February 28, 2020. https://doi.org/10.1002/jmv.25736.

Blanco-Melo, D., Nilsson-Payant, B.E., Liu, W.-C., Uhl, S., Hoagland, D., Møller, R., Jordan, T.X., Oishi, K., Panis, M., Sachs, D., et al. (2020). Imbalanced Host Response to SARS-CoV-2 Drives Development of COVID-19. Cell. Published online May 15, 2020. https://doi.org/10.1016/j.cell.2020.04.026.

Borba, M.G.S., de Almeida Val, F., Sampaio, V.S., Alexandre, M.A.A., Melo, G.C., Brito, M., Mourão, M.P.G., Brito Sousa, J.D., Baía-da-Silva, D.C., Guerra, M.V.F., et al. (2020). Effect of High vs Low Doses of Chloroquine Diphosphate as Adjunctive Therapy for Patients Hospitalized With Severe Acute Respiratory Syndrome Coronavirus 2 (SARS-CoV-2) Infection. JAMA Netw. Open *3*, e208857.

Bouvet, M., Debarnot, C., Imbert, I., Selisko, B., Snijder, E.J., Canard, B., and Decroly, E. (2010). In vitro reconstitution of SARS-coronavirus mRNA cap methylation. PLoS Pathog. *6*, e1000863.

Braud, V.M., Allan, D.S., O'Callaghan, C.A., Söderström, K., D'Andrea, A., Ogg, G.S., Lazetic, S., Young, N.T., Bell, J.I., Phillips, J.H., et al. (1998). HLA-E binds to natural killer cell receptors CD94/NKG2A, B and C. Nature *391*, 795–799.

Braun, J., Loyal, L., Frentsch, M., Wendisch, D., Georg, P., Kurth, F., Hippenstiel, S., Dingeldey, M., Kruse, B., Fauchere, F., et al. (2020). Presence of SARS-CoV-2 reactive T cells in COVID-19 patients and healthy donors. medRxiv. https://doi.org/10.1101/2020.04.17.20061440.

Brooks, A.G., Posch, P.E., Scorzelli, C.J., Borrego, F., and Coligan, J.E. (1997). NKG2A complexed with CD94 defines a novel inhibitory natural killer cell receptor. J. Exp. Med. *185*, 795–800.

Bukreyeva, N., Mantlo, E.K., Sattler, R.A., Huang, C., Paessler, S., and Zeldis, J. (2020). The IMPDH inhibitor merimepodib suppresses SARS-CoV-2 replication *in vitro*. bioRxiv. https://doi.org/10.1101/2020.04.07.028589.

Cai, X.-f., Chen, J., Hu, J.-l., Long, Q.-x., Deng, H.-j., Fan, K., Liao, P., Liu, B.-z., Wu, G.-c., Chen, Y.-k., et al. (2020). A Peptide-Based Magnetic Chemiluminescence Enzyme Immunoassay for Serological Diagnosis of Corona virus Disease 2019. J. Infect. Dis. Published online May 8, 2020. https://doi.org/10.1093/infdis/jiaa243.

Callow, K.A., Parry, H.F., Sergeant, M., and Tyrrell, D.A. (1990). The time course of the immune response to experimental coronavirus infection of man. Epidemiol. Infect. *105*, 435–446.

Cameron, M.J., Ran, L., Xu, L., Danesh, A., Bermejo-Martin, J.F., Cameron, C.M., Muller, M.P., Gold, W.L., Richardson, S.E., Poutanen, S.M., et al.; Canadian SARS Research Network (2007). Interferon-mediated immunopathological events are associated with atypical innate and adaptive immune responses in patients with severe acute respiratory syndrome. J. Virol. *81*, 8692–8706.

Cameron, M.J., Kelvin, A.A., Leon, A.J., Cameron, C.M., Ran, L., Xu, L., Chu, Y.K., Danesh, A., Fang, Y., Li, Q., et al. (2012). Lack of innate interferon responses during SARS coronavirus infection in a vaccination and reinfection ferret model. PLoS ONE *7*, e45842.

Camp, J.V., and Jonsson, C.B. (2017). A Role for Neutrophils in Viral Respiratory Disease. Front. Immunol. *8*, 550.

Campbell, K.M., Steiner, G., Wells, D.K., Ribas, A., and Kalbasi, A. (2020). Prediction of SARS-CoV-2 epitopes across 9360 HLA class I alleles. bioRxiv. https://doi.org/10.1101/2020.03.30.016931.

Canton, J., Fehr, A.R., Fernandez-Delgado, R., Gutierrez-Alvarez, F.J., Sanchez-Aparicio, M.T., García-Sastre, A., Perlman, S., Enjuanes, L., and Sola, I. (2018). MERS-CoV 4b protein interferes with the NF-κB-dependent innate immune response during infection. PLoS Pathog. *14*, e1006838.

Cao, X. (2020). COVID-19: immunopathology and its implications for therapy. Nat. Rev. Immunol. *20*, 269–270.

Cao, W.C., Liu, W., Zhang, P.H., Zhang, F., and Richardus, J.H. (2007). Disappearance of antibodies to SARS-associated coronavirus after recovery. N. Engl. J. Med. *357*, 1162–1163.

Cao, Z., Liu, L., Du, L., Zhang, C., Jiang, S., Li, T., and He, Y. (2010). Potent and persistent antibody responses against the receptor-binding domain of SARS-CoV spike protein in recovered patients. Virol. J. *7*, 299.

Cao, B., Wang, Y., Wen, D., Liu, W., Wang, J., Fan, G., Ruan, L., Song, B., Cai, Y., Wei, M., et al. (2020a). A Trial of Lopinavir-Ritonavir in Adults Hospitalized with Severe Covid-19. N. Engl. J. Med. Published online March 18, 2020. https://doi.org/10.1056/NEJMoa2001282.

Cao, W., Liu, X., Bai, T., Fan, H., Hong, K., Song, H., Han, Y., Lin, L., Ruan, L., and Li, T. (2020b). High-Dose Intravenous Immunoglobulin as a Therapeutic Option for Deteriorating Patients With Coronavirus Disease 2019. Open Forum Infect. Dis. *7*, a102.

Cao, Y., Li, L., Feng, Z., Wan, S., Huang, P., Sun, X., Wen, F., Huang, X., Ning, G., and Wang, W. (2020c). Comparative genetic analysis of the novel coronavirus (2019-nCoV/SARS-CoV-2) receptor ACE2 in different populations. Cell Discov. *6*, 11.

Carlin, L.E., Hemann, E.A., Zacharias, Z.R., Heusel, J.W., and Legge, K.L. (2018). Natural Killer Cell Recruitment to the Lung During Influenza A Virus Infection Is Dependent on CXCR3, CCR5, and Virus Exposure Dose. Front. Immunol. *9*, 781.

Cervantes-Barragan, L., Züst, R., Weber, F., Spiegel, M., Lang, K.S., Akira, S., Thiel, V., and Ludewig, B. (2007). Control of coronavirus infection through plasmacytoid dendritic-cell-derived type I interferon. Blood *109*, 1131–1137.

Cerwenka, A., and Lanier, L.L. (2001). Natural killer cells, viruses and cancer. Nat. Rev. Immunol. *1*, 41–49.

Chan, K.Y., Ching, J.C., Xu, M.S., Cheung, A.N., Yip, S.P., Yam, L.Y., Lai, S.T., Chu, C.M., Wong, A.T., Song, Y.Q., et al. (2007). Association of ICAM3 genetic variant with severe acute respiratory syndrome. J. Infect. Dis. *196*, 271–280.

Chang, Y.J., Kim, H.Y., Albacker, L.A., Baumgarth, N., McKenzie, A.N., Smith, D.E., Dekruyff, R.H., and Umetsu, D.T. (2011). Innate lymphoid cells mediate influenza-induced airway hyper-reactivity independently of adaptive immunity. Nat. Immunol. *12*, 631–638.

Channappanavar, R., Fehr, A.R., Vijay, R., Mack, M., Zhao, J., Meyerholz, D.K., and Perlman, S. (2016). Dysregulated Type I Interferon and Inflammatory Monocyte-Macrophage Responses Cause Lethal Pneumonia in SARS-CoV-Infected Mice. Cell Host Microbe *19*, 181–193.

Channappanavar, R., Fehr, A.R., Zheng, J., Wohlford-Lenane, C., Abrahante, J.E., Mack, M., Sompallae, R., McCray, P.B., Jr., Meyerholz, D.K., and Perlman, S. (2019). IFN-I response timing relative to virus replication determines MERS coronavirus infection outcomes. J. Clin. Invest. *130*, 3625–3639.

Charbonneau, M.R., Isabella, V.M., Li, N., and Kurtz, C.B. (2020). Developing a new class of engineered live bacterial therapeutics to treat human diseases. Nat. Commun. *11*, 1738.

Chen, Y., Cai, H., Pan, J., Xiang, N., Tien, P., Ahola, T., and Guo, D. (2009). Functional screen reveals SARS coronavirus nonstructural protein nsp14 as a novel cap N7 methyltransferase. Proc. Natl. Acad. Sci. USA *106*, 3484–3489.

Chen, I.Y., Moriyama, M., Chang, M.F., and Ichinohe, T. (2019). Severe acute respiratory syndrome coronavirus viroporin 3a activates the NLRP3 inflammasome. Front. Microbiol. *10*, 50.

Chen, X., Li, R., Pan, Z., Qian, C., Yang, Y., You, R., Zhao, J., Liu, P., Gao, L., Li, Z., et al. (2020a). Human monoclonal antibodies block the binding of SARS-CoV-2 spike protein to angiotensin converting enzyme 2 receptor. Cell. Mol. Immunol. Published online April 20, 2020. https://doi.org/10.1038/s41423-020-0426-7.

Chen, C., Zhang, Y., Huang, J., Yin, P., Cheng, Z., Wu, J., Chen, S., Zhang, Y., Chen, B., Lu, M., et al. (2020b). Favipiravir versus Arbidol for COVID-19: A Randomized Clinical Trial. medRxiv. https://doi.org/10.1101/2020.03.17.20037432.

Chen, G., Wu, D., Guo, W., Cao, Y., Huang, D., Wang, H., Wang, T., Zhang, X., Chen, H., Yu, H., et al. (2020c). Clinical and immunological features of severe and moderate coronavirus disease 2019. J. Clin. Invest. Published online March 27, 2020. https://doi.org/10.1172/JCI137244.

Chen, J., Liu, D., Liu, L., Liu, P., Xu, Q., Xia, L., Ling, Y., Dan, H., Song, S., Zhang, D., et al. (2020d). A pilot study of hydroxychloroquine in treatment of patients with common coronavirus disease-19 (COVID-19). J. Zhejiang Univ. *49*.

Chen, L., Liu, H.G., Liu, W., Liu, J., Liu, K., Shang, J., Deng, Y., and Wei, S. (2020e). [Analysis of clinical features of 29 patients with 2019 novel coronavirus pneumonia]. Zhonghua Jie He He Hu Xi Za Zhi *43*, 203–208.

Chen, X., Ling, J., Mo, P., Zhang, Y., Jiang, Q., Ma, Z., Cao, Q., Hu, W., Zou, S., Chen, L., et al. (2020f). Restoration of leukomonocyte counts is associated with viral clearance in COVID-19 hospitalized patients. medRxiv. https://doi.org/10.1101/2020.03.03.20030437.

Chen, X., Zhao, B., Qu, Y., Chen, Y., Xiong, J., Feng, Y., Men, D., Huang, Q., Liu, Y., Yang, B., et al. (2020g). Detectable serum SARS-CoV-2 viral load (RNAaemia) is closely associated with drastically elevated interleukin 6 (IL-6) level in critically ill COVID-19 patients. Clin. Infect. Dis. Published online April 17, 2020. https://doi.org/10.1093/cid/ciaa449.

Chen, Y., Feng, Z., Diao, B., Wang, R., Wang, G., Wang, C., Tan, Y., Liu, L., Wang, C., Liu, Y., et al. (2020h). The Novel Severe Acute Respiratory Syndrome Coronavirus 2 (SARS-CoV-2) Directly Decimates Human Spleens and Lymph Nodes. medRxiv. https://doi.org/10.1101/2020.03.27.20045427.

Chen, Z., Hu, J., Zhang, Z., Jiang, S., Han, S., Yan, D., Zhuang, R., Hu, B., and Zhang, Z. (2020i). Efficacy of hydroxychloroquine in patients with COVID-19: results of a randomized clinical trial. medRxiv. https://doi.org/10.1101/2020.03.22.20040758.

Cheng, Y., Cheng, G., Chui, C.H., Lau, F.Y., Chan, P.K., Ng, M.H., Sung, J.J., and Wong, R.S. (2005a). ABO blood group and susceptibility to severe acute respiratory syndrome. JAMA *293*, 1450–1451.

Cheng, Y., Wong, R., Soo, Y.O.Y., Wong, W.S., Lee, C.K., Ng, M.H.L., Chan, P., Wong, K.C., Leung, C.B., and Cheng, G. (2005b). Use of convalescent plasma therapy in SARS patients in Hong Kong. Eur. J. Clin. Microbiol. Infect. Dis. *24*, 44–46.

Cheung, C.Y., Poon, L.L.M., Ng, I.H.Y., Luk, W., Sia, S.-F., Wu, M.H.S., Chan, K.-H., Yuen, K.-Y., Gordon, S., Guan, Y., and Peiris, J.S. (2005). Cytokine responses in severe acute respiratory syndrome coronavirus-infected macrophages in vitro: possible relevance to pathogenesis. J. Virol. *79*, 7819–7826.

Chien, J.-Y., Hsueh, P.-R., Cheng, W.-C., Yu, C.J., and Yang, P.-C. (2006). Temporal changes in cytokine/chemokine profiles and pulmonary involvement in severe acute respiratory syndrome. Respirology *11*, 715–722.

Chu, C.M., Cheng, V.C., Hung, I.F., Wong, M.M., Chan, K.H., Chan, K.S., Kao, R.Y., Poon, L.L., Wong, C.L., Guan, Y., et al.; HKU/UCH SARS Study Group (2004). Role of lopinavir/ritonavir in the treatment of SARS: initial virological and clinical findings. Thorax *59*, 252–256.

Chu, H., Zhou, J., Wong, B.H., Li, C., Chan, J.F., Cheng, Z.S., Yang, D., Wang, D., Lee, A.C., Li, C., et al. (2016). Middle East Respiratory Syndrome Coronavirus Efficiently Infects Human Primary T Lymphocytes and Activates the Extrinsic and Intrinsic Apoptosis Pathways. J. Infect. Dis. *213*, 904–914.

Chu, H., Chan, J.F.-W., Wang, Y., Yuen, T.T.-T., Chai, Y., Hou, Y., Shuai, H., Yang, D., Hu, B., Huang, X., et al. (2020). Comparative replication and immune activation profiles of SARS-CoV-2 and SARS-CoV in human lungs: an *ex vivo* study with implications for the pathogenesis of COVID-19. Clin. Infect. Dis. Published online April 9, 2020. https://doi.org/10.1093/cid/ciaa410.

Cifaldi, L., Prencipe, G., Caiello, I., Bracaglia, C., Locatelli, F., De Benedetti, F., and Strippoli, R. (2015). Inhibition of natural killer cell cytotoxicity by interleukin-6: implications for the pathogenesis of macrophage activation syndrome. Arthritis Rheumatol. *67*, 3037–3046.

Clay, C., Donart, N., Fomukong, N., Knight, J.B., Lei, W., Price, L., Hahn, F., Van Westrienen, J., and Harrod, K.S. (2012). Primary severe acute respiratory syndrome coronavirus infection limits replication but not lung inflammation upon homologous rechallenge. J. Virol. *86*, 4234–4244.

Clementi, N., Criscuolo, E., Diotti, R.A., Ferrarese, R., Castelli, M., Burioni, R., Clementi, M., and Mancini, N. (2020). Combined prophylactic and therapeutic use maximizes hydroxychloroquine anti-SARS-CoV-2 effects *in vitro*. bioRxiv. https://doi.org/10.1101/2020.03.29.014407.

Comar, C.E., Goldstein, S.A., Li, Y., Yount, B., Baric, R.S., and Weiss, S.R. (2019). Antagonism of dsRNA-Induced Innate Immune Pathways by NS4a and NS4b Accessory Proteins during MERS Coronavirus Infection. MBio *10*, 1–7.

Corley, M.J., Sugai, C., Schotsaert, M., Schwartz, R.E., and Ndhlovu, L.C. (2020). Comparative in vitro transcriptomic analyses of COVID-19 candidate therapy hydroxychloroquine suggest limited immunomodulatory evidence of SARS-CoV-2 host response genes. bioRxiv. https://doi.org/10.1101/2020.04.13.039263.

Dai, W., Zhang, B., Su, H., Li, J., Zhao, Y., Xie, X., Jin, Z., Liu, F., Li, C., and Li, Y. (2020). Structure-based Design of Antiviral Drug Candidates Targeting the SARS-CoV-2 Main Protease. Science. Published online April 22, 2020. https://doi.org/10.1126/science.abb4489.

De Grove, K.C., Provoost, S., Verhamme, F.M., Bracke, K.R., Joos, G.F., Maes, T., and Brusselle, G.G. (2016). Characterization and Quantification of Innate Lymphoid Cell Subsets in Human Lung. PLoS ONE *11*, e0145961.

de Marcken, M., Dhaliwal, K., Danielsen, A.C., Gautron, A.S., and Dominguez-Villar, M. (2019). TLR7 and TLR8 activate distinct pathways in monocytes during RNA virus infection. Sci. Signal. *12*, eaaw1347.

de Wit, E., van Doremalen, N., Falzarano, D., and Munster, V.J. (2016). SARS and MERS: recent insights into emerging coronaviruses. Nat. Rev. Microbiol. *14*, 523–534.

de Wit, E., Feldmann, F., Cronin, J., Jordan, R., Okumura, A., Thomas, T., Scott, D., Cihlar, T., and Feldmann, H. (2020). Prophylactic and therapeutic remdesivir (GS-5734) treatment in the rhesus macaque model of MERS-CoV infection. Proc. Natl. Acad. Sci. USA *117*, 6771–6776.

Del Valle, D.M., Kim-Schulze, S., Hsin-Hui, H., Beckmann, N.D., Nirenberg, S., Wang, B., Lavin, Y., Swartz, T., Madduri, D., Stock, A., et al. (2020). An inflammatory cytokine signature helps predict COVID-19 severity and death. medRxiv. https://doi.org/10.1101/2020.05.28.20115758.

Deng, X., Hackbart, M., Mettelman, R.C., O'Brien, A., Mielech, A.M., Yi, G., Kao, C.C., and Baker, S.C. (2017). Coronavirus nonstructural protein 15 mediates evasion of dsRNA sensors and limits apoptosis in macrophages. Proc. Natl. Acad. Sci. USA *114*, E4251–E4260.

Devaraj, S.G., Wang, N., Chen, Z., Chen, Z., Tseng, M., Barretto, N., Lin, R., Peters, C.J., Tseng, C.T.K., Baker, S.C., and Li, K. (2007). Regulation of IRF-3-dependent innate immunity by the papain-like protease domain of the severe acute respiratory syndrome coronavirus. J. Biol. Chem. *282*, 32208–32221.

Diao, B., Wang, C., Tan, Y., Chen, X., Liu, Y., Ning, L., Chen, L., Li, M., Liu, Y., Wang, G., et al. (2020). Reduction and Functional Exhaustion of T Cells in Patients with Coronavirus Disease 2019 (COVID-19). Front. Immunol. Published online May 1, 2020. https://doi.org/10.3389/fimmu.2020.00827.

Díez, J.-M., Romero, C., and Gajardo, R. (2020). Currently available intravenous immunoglobulin (Gamunex®-C and Flebogamma® DIF) contains antibodies reacting against SARS-CoV-2 antigens. bioRxiv. https://doi.org/10.1101/2020.04.07.029017.

Dong, P., Ju, X., Yan, Y., Zhang, S., Cai, M., Wang, H., Chen, H., Hu, Y., Cui, L., Zhang, J., and He, W. (2018). γδ T Cells Provide Protective Function in Highly Pathogenic Avian H5N1 Influenza A Virus Infection. Front. Immunol. *9*, 2812.

Draghi, M., Pashine, A., Sanjanwala, B., Gendzekhadze, K., Cantoni, C., Cosman, D., Moretta, A., Valiante, N.M., and Parham, P. (2007). NKp46 and NKG2D recognition of infected dendritic cells is necessary for NK cell activation in the human response to influenza infection. J. Immunol. *178*, 2688–2698.

Du, L., He, Y., Zhou, Y., Liu, S., Zheng, B.J., and Jiang, S. (2009). The spike protein of SARS-CoV–a target for vaccine and therapeutic development. Nat. Rev. Microbiol. *7*, 226–236.

Du, M., Cai, G., Chen, F., Christiani, D.C., Zhang, Z., and Wang, M. (2020). Multi-omics Evaluation of Gastrointestinal and Other Clinical Characteristics of SARS-CoV-2 and COVID-19. Gastroenterology. Published online March 28, 2020. https://doi.org/10.1053/j.gastro.2020.03.045.

Duan, K., Liu, B., Li, C., Zhang, H., Yu, T., Qu, J., Zhou, M., Chen, L., Meng, S., Hu, Y., et al. (2020). Effectiveness of convalescent plasma therapy in severe COVID-19 patients. PNAS *117*, 9490–9496.

Duev-Cohen, A., Bar-On, Y., Glasner, A., Berhani, O., Ophir, Y., Levi-Schaffer, F., Mandelboim, M., and Mandelboim, O. (2016). The human 2B4 and NTB-A receptors bind the influenza viral hemagglutinin and co-stimulate NK cell cytotoxicity. Oncotarget *7*, 13093–13105.

Fang, X., Mei, Q., Yang, T., Li, L., Wang, Y., Tong, F., Geng, S., and Pan, A. (2020). Low-dose corticosteroid therapy does not delay viral clearance in patients with COVID-19. J. Infect. Published online April 11, 2020. https://doi.org/10.1016/j.jinf.2020.03.039.

Fast, E., Altman, R.B., and Chen, B. (2020). Potential T-cell and B-cell Epitopes of 2019-nCoV. bioRxiv. https://doi.org/10.1101/2020.02.19.955484.

Fauci, A.S., Lane, H.C., and Redfield, R.R. (2020). Covid-19 - Navigating the Uncharted. N. Engl. J. Med. *382*, 1268–1269.

Fei, J., Fu, L., Li, Y., Xiang, H.-X., Xiang, Y., Li, M.-D., Liu, F.-F., Xu, D.-X., and Zhao, H. (2020). Reduction of lymphocyte at early stage elevates severity and death risk of COVID-19 patients: a hospital-based case-cohort study. medRxiv. https://doi.org/10.1101/2020.04.02.20050955.

Feng, Z., Yu, Q., Yao, S., Luo, L., Duan, J., Yan, Z., Yang, M., Tan, H., Ma, M., Li, T., et al. (2020). Early Prediction of Disease Progression in 2019 Novel Coronavirus Pneumonia Patients Outside Wuhan with CT and Clinical Characteristics. medRxiv. https://doi.org/10.1101/2020.02.19.20025296.

Flores-Torres, A.S., Salinas-Carmona, M.C., Salinas, E., and Rosas-Taraco, A.G. (2019). Eosinophils and Respiratory Viruses. Viral Immunol. *32*, 198–207.

Fogarty, H., Townsend, L., Cheallaigh, C.N., Bergin, C., Martin-Loeches, I., Browne, P., Bacon, C.L., Gaule, R., Gillett, A., Byrne, M., et al. (2020). COVID-19 Coagulopathy in Caucasian patients. Br. J. Haematol. Published online April 24, 2020. https://doi.org/10.1111/bjh.16749.

Forni, D., Filippi, G., Cagliani, R., De Gioia, L., Pozzoli, U., Al-Daghri, N., Clerici, M., and Sironi, M. (2015). The heptad repeat region is a major selection target in MERS-CoV and related coronaviruses. Sci. Rep. *5*, 14480.

Frieman, M., Yount, B., Heise, M., Kopecky-Bromberg, S.A., Palese, P., and Baric, R.S. (2007). Severe acute respiratory syndrome coronavirus ORF6 antagonizes STAT1 function by sequestering nuclear import factors on the rough endoplasmic reticulum/Golgi membrane. J. Virol. *81*, 9812–9824.

Frieman, M., Ratia, K., Johnston, R.E., Mesecar, A.D., and Baric, R.S. (2009). Severe acute respiratory syndrome coronavirus papain-like protease ubiquitin-like domain and catalytic domain regulate antagonism of IRF3 and NF-kappaB signaling. J. Virol. *83*, 6689–6705.

Fu, S., Fu, X., Song, Y., Li, M., Pan, P.-h., Tang, T., Zhang, C., Jiang, T., Tan, D., Fan, X., et al. (2020). Virologic and clinical characteristics for prognosis of severe COVID-19: a retrospective observational study in Wuhan, China. medRxiv. https://doi.org/10.1101/2020.04.03.20051763.

Gangopadhyay, K.K., Mukherjee, J.J., Sinha, B., and Ghosal, S. (2020). The role of corticosteroids in the management of critically ill patients with coronavirus disease 2019 (COVID-19): A meta-analysis. medRxiv. https://doi.org/10.1101/2020.04.17.20069773.

Gao, K., Nguyen, D.D., Wang, R., and Wei, G.-W. (2020a). Machine intelligence design of 2019-nCoV drugs. bioRxiv. https://doi.org/10.1101/2020.01.30.927889.

Gao, L., Jiang, D., Wen, X.-s., Cheng, X.-c., Sun, M., He, B., You, L.-n., Lei, P., Tan, X.-w., Qin, S., et al. (2020b). Prognostic value of NT-proBNP in patients with severe COVID-19. Respir Res. *21*, 83.

Gao, Q., Bao, L., Mao, H., Wang, L., Xu, K., Yang, M., Li, Y., Zhu, L., Wang, N., Lv, Z., et al. (2020c). Rapid development of an inactivated vaccine for SARS-CoV-2. bioRxiv. https://doi.org/10.1101/2020.04.17.046375.

Gao, T., Hu, M., Zhang, X., Li, H., Zhu, L., Liu, H., Dong, Q., Zhang, Z., Wang, Z., Hu, Y., et al. (2020d). Highly pathogenic coronavirus N protein aggravates lung injury by MASP-2-mediated complement over-activation. medRxiv. https://doi.org/10.1101/2020.03.29.20041962.

Garulli, B., Stillitano, M.G., Barnaba, V., and Castrucci, M.R. (2008). Primary CD8+ T-cell response to soluble ovalbumin is improved by chloroquine treatment in vivo. Clin. Vaccine Immunol. *15*, 1497–1504.

Gasteiger, G., Fan, X., Dikiy, S., Lee, S.Y., and Rudensky, A.Y. (2015). Tissue residency of innate lymphoid cells in lymphoid and nonlymphoid organs. Science *350*, 981–985.

Gautret, P., Lagier, J.-C., Parola, P., Hoang, V.T., Meddeb, L., Mailhe, M., Doudier, B., Courjon, J., Giordanengo, V., Vieira, V.E., et al. (2020a).

Jia, W., Channappanavar, R., Zhang, C., Li, M., Zhou, H., Zhang, S., Zhou, P., Xu, J., Shan, S., Shi, X., et al. (2019). Single intranasal immunization with chimpanzee adenovirus-based vaccine induces sustained and protective immunity against MERS-CoV infection. Emerg. Microbes Infect. *8*, 760–772.

John, S., Yuzhakov, O., Woods, A., Deterling, J., Hassett, K., Shaw, C.A., and Ciaramella, G. (2018). Multi-antigenic human cytomegalovirus mRNA vaccines that elicit potent humoral and cell-mediated immunity. Vaccine *36*, 1689–1699.

Ju, B., Zhang, Q., Ge, X., Wang, R., Sun, J., Ge, X., Yu, J., Shan, S., Zhou, B., and Song, S. (2020). Human neutralizing antibodies elicited by SARS-CoV-2 infection. Nature. Published online May 26, 2020. https://doi.org/10.1038/s41586-020-2380-z.

Kamitani, W., Huang, C., Narayanan, K., Lokugamage, K.G., and Makino, S. (2009). A two-pronged strategy to suppress host protein synthesis by SARS coronavirus Nsp1 protein. Nat. Struct. Mol. Biol. *16*, 1134–1140.

Kamphuis, E., Junt, T., Waibler, Z., Forster, R., and Kalinke, U. (2006). Type I interferons directly regulate lymphocyte recirculation and cause transient blood lymphopenia. Blood *108*, 3253–3261.

Keyaerts, E., Vijgen, L., Maes, P., Neyts, J., and Van Ranst, M. (2004). In vitro inhibition of severe acute respiratory syndrome coronavirus by chloroquine. Biochem. Biophys. Res. Commun. *323*, 264–268.

Kim, J., Chang, Y., Bae, B., Sohn, K.-H., Cho, S.-H., Chung, D.H., Kang, H.R., and Kim, H.Y. (2019). Innate immune crosstalk in asthmatic airways: Innate lymphoid cells coordinate polarization of lung macrophages. J. Allergy Clin. Immunol. *143*, 1769–1782.e11.

Kim, E., Erdos, G., Huang, S., Kenniston, T.W., Balmert, S.C., Carey, C.D., Raj, V.S., Epperly, M.W., Klimstra, W.B., Haagmans, B.L., et al. (2020). Microneedle array delivered recombinant coronavirus vaccines: Immunogenicity and rapid translational development. EBioMedicine, 102743. Published online April 2, 2020.

Knoops, K., Kikkert, M., Worm, S.H., Zevenhoven-Dobbe, J.C., van der Meer, Y., Koster, A.J., Mommaas, A.M., and Snijder, E.J. (2008). SARS-coronavirus replication is supported by a reticulovesicular network of modified endoplasmic reticulum. PLoS Biol. *6*, e226.

Konig, M.F., Powell, M., Staedtke, V., Bai, R.-Y., Thomas, D.L., Fischer, N., Huq, S., Khalafallah, A.M., Koenecke, A., Xiong, R., et al. (2020). Targeting the catecholamine-cytokine axis to prevent SARS-CoV-2 cytokine storm syndrome. medRxiv. https://doi.org/10.1101/2020.04.02.20051565.

Kopecky-Bromberg, S.A., Martínez-Sobrido, L., Frieman, M., Baric, R.A., and Palese, P. (2007). Severe acute respiratory syndrome coronavirus open reading frame (ORF) 3b, ORF 6, and nucleocapsid proteins function as interferon antagonists. J. Virol. *81*, 548–557.

Law, H.K.W., Cheung, C.Y., Ng, H.Y., Sia, S.F., Chan, Y.O., Luk, W., Nicholls, J.M., Peiris, J.S.M., and Lau, Y.L. (2005). Chemokine up-regulation in SARS-coronavirus-infected, monocyte-derived human dendritic cells. Blood *106*, 2366–2374.

Ledford, H. (2020). Hopes rise for coronavirus drug remdesivir. Nature https://www.nature.com/articles/d41586-020-01295-8.

Lee, J., Lee, S.H., Shin, N., Jeong, M., Kim, M.S., Kim, M.J., Yoon, S.R., Chung, J.W., Kim, T.D., and Choi, I. (2009). Tumor necrosis factor-alpha enhances IL-15-induced natural killer cell differentiation. Biochem. Biophys. Res. Commun. *386*, 718–723.

Lee, K.-Y., Rhim, J.-W., and Kang, J.-H. (2020). Early preemptive immunomodulators (corticosteroids) for severe pneumonia patients infected with SARS-CoV-2. Clin Exp Pediatr *63*, 117–118.

Lei, C., Fu, W., Qian, K., Li, T., Zhang, S., Fu, W., Ding, M., and Hu, S. (2020a). Neutralization of SARS-CoV-2 spike pseudotyped virus by recombinant ACE2-Ig. Nat Commun. *11*, 2070.

Lei, L., Qian, H., Yang, X., Zhou, X., Zhang, X., Zhang, D., Dai, T., Guo, R., Shi, L., Cheng, Y., et al. (2020b). The phenotypic changes of γδ T cells in COVID-19 patients. medRxiv. https://doi.org/10.1101/2020.04.05.20046433.

Levine, M.M. (2019). Monoclonal Antibody Therapy for Ebola Virus Disease. N. Engl. J. Med. *381*, 2365–2366.

Li, C.K.-F., Wu, H., Yan, H., Ma, S., Wang, L., Zhang, M., Tang, X., Temperton, N.J., Weiss, R.A., Brenchley, J.M., et al. (2008). T cell responses to whole SARS coronavirus in humans. J. Immunol. *181*, 5490–5500.

Li, J., Guo, M., Tian, X., Liu, C., Wang, X., Yang, X., Wu, P., Xiao, Z., Qu, Y., Yin, Y., et al. (2020a). Virus-host interactome and proteomic survey of PMBCs from COVID-19 patients reveal potential virulence factors influencing SARS-CoV-2 pathogenesis. bioRxiv. https://doi.org/10.1101/2020.03.31.019216.

Li, K., Chen, D., Chen, S., Feng, Y., Chang, C., Wang, Z., Wang, N., and Zhen, G. (2020b). Radiographic Findings and other Predictors in Adults with Covid-19. medRxiv. https://doi.org/10.1101/2020.03.23.20041673.

Li, Y., Xie, Z., Lin, W., Cai, W., Wen, C., Guan, Y., Mo, X., Wang, J., Wang, Y., Peng, P., et al. (2020c). An exploratory randomized controlled study on the efficacy and safety of lopinavir/ritonavir or arbidol treating adult patients hospitalized with mild/moderate COVID-19 (ELACOI). medRxiv. https://doi.org/10.1101/2020.03.19.20038984.

Li, Y., Wang, H., Tang, X., Ma, D., Du, C., Wang, Y., and Pan, H. (2020d). Potential host range of multiple SARS-like coronaviruses and an improved ACE2-Fc variant that is potent against both SARS-CoV-2 and SARS-CoV-1. bioRxiv. https://doi.org/10.1101/2020.04.10.032342.

Liao, M., Liu, Y., Yuan, J., Wen, Y., Xu, G., Zhao, J., Cheng, L., Li, J., Wang, X., Wang, F., et al. (2020). Single-cell Landscape of Bronchoalveolar Immune Cells in Patients With COVID-19. Nat. Med. Published online May 12, 2020. https://doi.org/10.1038/s41591-020-0901-9.

Lin, J.T., Zhang, J.S., Su, N., Xu, J.G., Wang, N., Chen, J.T., Chen, X., Liu, Y.X., Gao, H., Jia, Y.P., et al. (2007). Safety and immunogenicity from a phase I trial of inactivated severe acute respiratory syndrome coronavirus vaccine. Antivir. Ther. (Lond.) *12*, 1107–1113.

Lindesmith, L., Moe, C., Marionneau, S., Ruvoen, N., Jiang, X., Lindblad, L., Stewart, P., LePendu, J., and Baric, R. (2003). Human susceptibility and resistance to Norwalk virus infection. Nat. Med. *9*, 548–553.

Liu, W., Fontanet, A., Zhang, P.H., Zhan, L., Xin, Z.T., Baril, L., Tang, F., Lv, H., and Cao, W.C. (2006). Two-year prospective study of the humoral immune response of patients with severe acute respiratory syndrome. J. Infect. Dis. *193*, 792–795.

Liu, L., Wei, Q., Lin, Q., Fang, J., Wang, H., Kwok, H., Tang, H., Nishiura, K., Peng, J., Tan, Z., et al. (2019). Anti-spike IgG causes severe acute lung injury by skewing macrophage responses during acute SARS-CoV infection. JCI Insight *4*, e123158.

Liu, B., Han, J., Cheng, X., Yu, L., Zhang, L., Wang, W., Ni, L., Wei, C., Huang, Y., and Cheng, Z. (2020a). Persistent SARS-CoV-2 presence is companied with defects in adaptive immune system in non-severe COVID-19 patients. medRxiv. https://doi.org/10.1101/2020.03.26.20044768.

Liu, J., Li, S., Liu, J., Liang, B., Wang, X., Wang, H., Li, W., Tong, Q., Yi, J., Zhao, L., et al. (2020b). Longitudinal characteristics of lymphocyte responses and cytokine profiles in the peripheral blood of SARS-CoV-2 infected patients. EBioMedicine *55*, 102763.

Liu, J., Liu, Y., Xiang, P., Pu, L., Xiong, H., Li, C., Zhang, M., Tan, J., Xu, Y., Song, R., et al. (2020c). Neutrophil-to-lymphocyte ratio predicts critical illness patients with 2019 coronavirus disease in the early stage. J. Transl. Med. *18*, 206.

Liu, J., Cao, R., Xu, M., Wang, X., Zhang, H., Hu, H., Li, Y., Hu, Z., Zhong, W., and Wang, M. (2020d). Hydroxychloroquine, a less toxic derivative of chloroquine, is effective in inhibiting SARS-CoV-2 infection in vitro. Cell Discov. *6*, 16.

Liu, Q., Fang, X., Tokuno, S., Chung, U., Chen, X., Dai, X., Liu, X., Xu, F., Wang, B., and Peng, P. (2020e). Prediction of the clinical outcome of COVID-19 patients using T lymphocyte subsets with 340 cases from Wuhan, China: a retrospective cohort study and a web visualization tool. medRxiv. https://doi.org/10.1101/2020.04.06.20056127.

Liu, T., Zhang, J., Yang, Y., Ma, H., Li, Z., Zhang, J., Cheng, J., Zhang, X., Zhao, Y., Xia, Z., et al. (2020f). The role of interleukin-6 in monitoring severe case of coronavirus disease 2019. EMBO Mol. Med. Published online May 19, 2020. https://doi.org/10.15252/emmm.202012421.

Liu, Y., Li, J., Liu, D., Song, H., Chen, C., Lv, M., Pei, X., and Hu, Z. (2020g). Clinical features and outcomes of 2019 novel coronavirus-infected patients with cardiac injury. medRxiv. https://doi.org/10.1101/2020.03.11.20030957.

Liu, Y., Sun, W., Guo, Y., Chen, L., Zhang, L., Zhao, S., Long, D., and Yu, L. (2020h). Association between platelet parameters and mortality in coronavirus disease 2019: Retrospective cohort study. Platelets, 1–7. Published online April 16, 2020. https://doi.org/10.1080/09537104.2020.1754383.

Lo, B., Zhang, K., Lu, W., Zheng, L., Zhang, Q., Kanellopoulou, C., Zhang, Y., Liu, Z., Fritz, J.M., Marsh, R., et al. (2015). AUTOIMMUNE DISEASE. Patients with LRBA deficiency show CTLA4 loss and immune dysregulation responsive to abatacept therapy. Science *349*, 436–440.

Lokugamage, K.G., Narayanan, K., Nakagawa, K., Terasaki, K., Ramirez, S.I., Tseng, C.-T.K., and Makino, S. (2015). Middle East Respiratory Syndrome Coronavirus nsp1 Inhibits Host Gene Expression by Selectively Targeting mRNAs Transcribed in the Nucleus while Sparing mRNAs of Cytoplasmic Origin. J. Virol. *89*, 10970–10981.

Lokugamage, K.G., Hage, A., Schindewolf, C., Rajsbaum, R., and Menachery, V.D. (2020). SARS-CoV-2 is sensitive to type I interferon pretreatment. bioRxiv. https://doi.org/10.1101/2020.03.07.982264.

Lon, J.R., Bai, Y., Zhong, B., Cai, F., and Du, H. (2020). Prediction and Evolution of B Cell Epitopes of Surface Protein in SARS-CoV-2. bioRxiv. https://doi.org/10.1101/2020.04.03.022723.

Lou, B., Li, T., Zheng, S., Su, Y., Li, Z., Liu, W., Yu, F., Ge, S., Zou, Q., Yuan, Q., et al. (2020). Serology characteristics of SARS-CoV-2 infection since the exposure and post symptoms onset. medRxiv. https://doi.org/10.1101/2020.03.23.20041707.

Lover, A.A. (2020). Quantifying treatment effects of hydroxychloroquine and azithromycin for COVID-19: a secondary analysis of an open label non-randomized clinical trial (Gautret et al, 2020). medRxiv. https://doi.org/10.1101/2020.03.22.20040949.

Lu, R., Zhao, X., Li, J., Niu, P., Yang, B., Wu, H., Wang, W., Song, H., Huang, B., Zhu, N., et al. (2020a). Genomic characterisation and epidemiology of 2019 novel coronavirus: implications for virus origins and receptor binding. Lancet *395*, 565–574.

Lu, X., Chen, T., Wang, Y., Wang, J., Zhang, B., Li, Y., and Yan, F. (2020b). Adjuvant corticosteroid therapy for critically ill patients with COVID-19. medRxiv. https://doi.org/10.1101/2020.04.07.20056390.

Luke, T.C., Kilbane, E.M., Jackson, J.L., and Hoffman, S.L. (2006). Meta-analysis: convalescent blood products for Spanish influenza pneumonia: a future H5N1 treatment? Ann. Intern. Med. *145*, 599–609.

Mantlo, E.K., Bukreyeva, N., Maruyama, J., Paessler, S., and Huang, C. (2020). Antiviral Activities of Type I Interferons to SARS-CoV-2 Infection. Antiviral Res. Published online April 29, 2020. https://doi.org/10.1016/j.antiviral.2020.104811.

Mao, H., Tu, W., Qin, G., Law, H.K., Sia, S.F., Chan, P.L., Liu, Y., Lam, K.T., Zheng, J., Peiris, M., and Lau, Y.L. (2009). Influenza virus directly infects human natural killer cells and induces cell apoptosis. J. Virol. *83*, 9215–9222.

Marquardt, N., Kekäläinen, E., Chen, P., Kvedaraite, E., Wilson, J.N., Ivarsson, M.A., Mjösberg, J., Berglin, L., Säfholm, J., Manson, M.L., et al. (2017). Human Lung Natural Killer Cells Are Predominantly Comprised of Highly Differentiated Hypofunctional CD69 $^{-}$ CD56 ^{dim} Cells. J. Allergy Clin. Immunol. *139*, 1321–1330.

Martin, J.E., Louder, M.K., Holman, L.A., Gordon, I.J., Enama, M.E., Larkin, B.D., Andrews, C.A., Vogel, L., Koup, R.A., Roederer, M., et al.; VRC 301 Study Team (2008). A SARS DNA vaccine induces neutralizing antibody and cellular immune responses in healthy adults in a Phase I clinical trial. Vaccine *26*, 6338–6343.

Medzhitov, R., Schneider, D.S., and Soares, M.P. (2012). Disease tolerance as a defense strategy. Science *335*, 936–941.

Mehta, P., McAuley, D.F., Brown, M., Sanchez, E., Tattersall, R.S., and Manson, J.J.; HLH Across Speciality Collaboration, UK (2020). COVID-19: consider cytokine storm syndromes and immunosuppression. Lancet *395*, 1033–1034.

Menachery, V.D., Mitchell, H.D., Cockrell, A.S., Gralinski, L.E., Yount, B.L., Jr., Graham, R.L., McAnarney, E.T., Douglas, M.G., Scobey, T., Beall, A., et al. (2017). MERS-CoV accessory orfs play key role for infection and pathogenesis. MBio *8*, 1–14.

Milewska, A., Chi, Y., Szczepanski, A., Barreto-Duran, E., Liu, K., Liu, D., Guo, X., Ge, Y., Li, J., Cui, L., et al. (2020). HTCC as a highly effective polymeric inhibitor of SARS-CoV-2 and MERS-CoV. bioRxiv. https://doi.org/10.1101/2020.03.29.014183.

Minakshi, R., Padhan, K., Rani, M., Khan, N., Ahmad, F., and Jameel, S. (2009). The SARS Coronavirus 3a protein causes endoplasmic reticulum stress and induces ligand-independent downregulation of the type 1 interferon receptor. PLoS ONE *4*, e8342.

Modjarrad, K., Roberts, C.C., Mills, K.T., Castellano, A.R., Paolino, K., Muthumani, K., Reuschel, E.L., Robb, M.L., Racine, T., Oh, M.D., et al. (2019). Safety and immunogenicity of an anti-Middle East respiratory syndrome coronavirus DNA vaccine: a phase 1, open-label, single-arm, dose-escalation trial. Lancet Infect. Dis. *19*, 1013–1022.

Molina, J.M., Delaugerre, C., Le Goff, J., Mela-Lima, B., Ponscarme, D., Goldwirt, L., and de Castro, N. (2020). No evidence of rapid antiviral clearance or clinical benefit with the combination of hydroxychloroquine and azithromycin in patients with severe COVID-19 infection. Med. Mal. Infect. S0399-077X(20)30085-8. https://doi.org/10.1016/j.medmal.2020.03.006.

Monticelli, L.A., Sonnenberg, G.F., Abt, M.C., Alenghat, T., Ziegler, C.G., Doering, T.A., Angelosanto, J.M., Laidlaw, B.J., Yang, C.Y., Sathaliyawala, T., et al. (2011). Innate lymphoid cells promote lung-tissue homeostasis after infection with influenza virus. Nat. Immunol. *12*, 1045–1054.

Moore, J.B., and June, C.H. (2020). Cytokine release syndrome in severe COVID-19. Science *368*, 473–474.

Nailwal, H., and Chan, F.K. (2019). Necroptosis in anti-viral inflammation. Cell Death Differ. *26*, 4–13.

Ng, O.-W., Chia, A., Tan, A.T., Jadi, R.S., Leong, H.N., Bertoletti, A., and Tan, Y.-J. (2016). Memory T cell responses targeting the SARS coronavirus persist up to 11 years post-infection. Vaccine *34*, 2008–2014.

Ni, L., Ye, F., Chen, M.-L., Feng, Y., Deng, Y.-Q., Zhao, H., Wei, P., Ge, J., Gou, M., Li, X., et al. (2020). Detection of SARS-CoV-2-Specific Humoral and Cellular Immunity in COVID-19 Convalescent Individuals. Immunity. Published online May 3, 2020. https://doi.org/10.1016/j.immuni.2020.04.023.

Nie, J., Li, Q., Wu, J., Zhao, C., Hao, H., Liu, H., Zhang, L., Nie, L., Qin, H., Wang, M., et al. (2020a). Establishment and validation of a pseudovirus neutralization assay for SARS-CoV-2. Emerg. Microbes Infect. *9*, 680–686.

Nie, S., Zhao, X., Zhao, K., Zhang, Z., Zhang, Z., and Zhang, Z. (2020b). Metabolic disturbances and inflammatory dysfunction predict severity of coronavirus disease 2019 (COVID-19): a retrospective study. medRxiv. https://doi.org/10.1101/2020.03.24.20042283.

Niemeyer, D., Zillinger, T., Muth, D., Zielecki, F., Horvath, G., Suliman, T., Barchet, W., Weber, F., Drosten, C., and Müller, M.A. (2013). Middle East respiratory syndrome coronavirus accessory protein 4a is a type I interferon antagonist. J. Virol. *87*, 12489–12495.

Nieto-Torres, J.L., Verdiá-Báguena, C., Jimenez-Guardeño, J.M., Regla-Nava, J.A., Castaño-Rodriguez, C., Fernandez-Delgado, R., Torres, J., Aguilella, V.M., and Enjuanes, L. (2015). Severe acute respiratory syndrome coronavirus E protein transports calcium ions and activates the NLRP3 inflammasome. Virology *485*, 330–339.

Nikolich-Žugich, J. (2018). The twilight of immunity: emerging concepts in aging of the immune system. Nat. Immunol. *19*, 10–19.

Okabayashi, T., Kariwa, H., Yokota, S., Iki, S., Indoh, T., Yokosawa, N., Takashima, I., Tsutsumi, H., and Fujii, N. (2006). Cytokine regulation in SARS coronavirus infection compared to other respiratory virus infections. J. Med. Virol. *78*, 417–424.

Okba, N.M.A., Müller, M.A., Li, W., Wang, C., GeurtsvanKessel, C.H., Corman, V.M., Lamers, M.M., Sikkema, R.S., de Bruin, E., Chandler, F.D., et al. (2020). Severe Acute Respiratory Syndrome Coronavirus 2-Specific Antibody Responses in Coronavirus Disease 2019 Patients. Emerg. Infect. Dis. *26*, https://doi.org/10.3201/eid2607.200841.

Ong, E.Z., Chan, Y.F.Z., Leong, W.Y., Lee, N.M.Y., Kalimuddin, S., Haja Mohideen, S.M., Chan, K.S., Tan, A.T., Bertoletti, A., Ooi, E.E., and Low, J.G.H. (2020). A dynamic immune response shapes COVID-19 progression. Cell Host Microbe. S1931-3128(20)30185-2. Published online April 30, 2020. https://doi.org/10.1016/j.chom.2020.03.021.

Page, C., Goicochea, L., Matthews, K., Zhang, Y., Klover, P., Holtzman, M.J., Hennighausen, L., and Frieman, M. (2012). Induction of alternatively activated macrophages enhances pathogenesis during severe acute respiratory syndrome coronavirus infection. J. Virol. *86*, 13334–13349.

Pan, X., Zhou, P., Fan, T., Wu, Y., Zhang, J., Shi, X., Shang, W., Fang, L., Jiang, X., Shi, J., et al. (2020). Immunoglobulin fragment F(ab')$_2$ against RBD potently

neutralizes SARS-CoV-2 in vitro. bioRxiv. https://doi.org/10.1101/2020.04.07.029884.

Pardi, N., Hogan, M.J., Pelc, R.S., Muramatsu, H., Andersen, H., DeMaso, C.R., Dowd, K.A., Sutherland, L.L., Scearce, R.M., Parks, R., et al. (2017). Zika virus protection by a single low-dose nucleoside-modified mRNA vaccination. Nature *543*, 248–251.

Park, T., Lee, S.-Y., Kim, S., Kim, M.J., Kim, H.G., Jun, S., Kim, S.I., Kim, B.T., Park, E.C., and Park, D. (2020). Spike protein binding prediction with neutralizing antibodies of SARS-CoV-2. bioRxiv. https://doi.org/10.1101/2020.02.22.951178.

Payne, D.C., Iblan, I., Rha, B., Alqasrawi, S., Haddadin, A., Al Nsour, M., Alsanouri, T., Ali, S.S., Harcourt, J., Miao, C., et al. (2016). Persistence of Antibodies against Middle East Respiratory Syndrome Coronavirus. Emerg. Infect. Dis. *22*, 1824–1826.

Pei, S., Yuan, X., Zhang, Z., Yao, R., Xie, Y., Shen, M., Li, B., Chen, X., and Yin, M. (2020). Convalescent Plasma to Treat COVID-19: Chinese Strategy and Experiences. medRxiv. https://doi.org/10.1101/2020.04.07.20056440.

Perlman, S., and Dandekar, A.A. (2005). Immunopathogenesis of coronavirus infections: implications for SARS. Nat. Rev. Immunol. *5*, 917–927.

Pfaender, S., Mar, K.B., Michailidis, E., Kratzel, A., Hirt, D., V'kovski, P., Fan, W., Ebert, N., Stalder, H., Kleine-Weber, H., et al. (2020). LY6E impairs coronavirus fusion and confers immune control of viral disease. bioRxiv. https://doi.org/10.1101/2020.03.05.979260.

Pinto, D., Park, Y.-J., Beltramello, M., Walls, A.C., Tortorici, M.A., Bianchi, S., Jaconi, S., Culap, K., Zatta, F., De Marco, A., et al. (2020). Structural and functional analysis of a potent sarbecovirus neutralizing antibody. bioRxiv. https://doi.org/10.1101/2020.04.07.023903.

Poor, H.D., Ventetuolo, C.E., Tolbert, T., Chun, G., Serrao, G., Zeidman, A., Dangayach, N.S., Olin, J., Kohli-Seth, R., and Powell, C.A. (2020). COVID-19 Critical Illness Pathophysiology Driven by Diffuse Pulmonary Thrombi and Pulmonary Endothelial Dysfunction Responsive to Thrombolysis. medRxiv. https://doi.org/10.1101/2020.04.17.20057125.

Prokunina-Olsson, L., Alphonse, N., Dickenson, R.E., Durbin, J.E., Glenn, J.S., Hartmann, R., Kotenko, S.V., Lazear, H.M., O'Brien, T.R., Odendall, C., et al. (2020). COVID-19 and emerging viral infections: The case for interferon lambda. J. Exp. Med. *217*, e20200653.

Qin, C., Zhou, L., Hu, Z., Zhang, S., Yang, S., Tao, Y., Xie, C., Ma, K., Shang, K., Wang, W., et al. (2020). Dysregulation of Immune Response in Patients with COVID-19 in Wuhan, China. Clin. Infect. Dis. Published online March 12, 2020. https://doi.org/10.1093/cid/ciaa248.

Qiu, M., Shi, Y., Guo, Z., Chen, Z., He, R., Chen, R., Zhou, D., Dai, E., Wang, X., Si, B., et al. (2005). Antibody responses to individual proteins of SARS coronavirus and their neutralization activities. Microbes Infect. *7*, 882–889.

Qu, R., Ling, Y., Zhang, Y.-H.-Z., Wei, L.-Y., Chen, X., Li, X.-M., Liu, X.-Y., Liu, H.-M., Guo, Z., Ren, H., et al. (2020). Platelet-to-lymphocyte Ratio Is Associated With Prognosis in Patients With Coronavirus disease-19. J. Med. Virol. Published online March 17, 2020. https://doi.org/10.1002/jmv.25767.

Quinlan, B.D., Mou, H., Zhang, L., Guo, Y., He, W., Ojha, A., Parcells, M.S., Luo, G., Li, W., Zhong, G., et al. (2020). The SARS-CoV-2 receptor-binding domain elicits a potent neutralizing response without antibody-dependent enhancement. bioRxiv. https://doi.org/10.1101/2020.04.10.036418.

Rabouw, H.H., Langereis, M.A., Knaap, R.C.M., Dalebout, T.J., Canton, J., Sola, I., Enjuanes, L., Bredenbeek, P.J., Kikkert, M., de Groot, R.J., and van Kuppeveld, F.J. (2016). Middle East Respiratory Coronavirus Accessory Protein 4a Inhibits PKR-Mediated Antiviral Stress Responses. PLoS Pathog. *12*, e1005982.

Ramsuran, V., Naranbhai, V., Horowitz, A., Qi, Y., Martin, M.P., Yuki, Y., Gao, X., Walker-Sperling, V., Del Prete, G.Q., Schneider, D.K., et al. (2018). Elevated *HLA-A* expression impairs HIV control through inhibition of NKG2A-expressing cells. Science *359*, 86–90.

Reed, S.E. (1984). The behaviour of recent isolates of human respiratory coronavirus in vitro and in volunteers: evidence of heterogeneity among 229E-related strains. J. Med. Virol. *13*, 179–192.

Renieri, A., Benetti, E., Tita, R., Spiga, O., Ciolfi, A., Birolo, G., Bruselles, A., Doddato, G., Giliberti, A., Marconi, C., et al. (2020). ACE2 variants underlie interindividual variability and susceptibility to COVID-19 in Italian population. medRxiv. https://doi.org/10.1101/2020.04.03.20047977.

Roumier, M., Paule, R., Vallee, A., and Ackermann, F. (2020). Interleukin-6 blockade for severe COVID-19. medRxiv. https://doi.org/10.1101/2020.04.20.20061861.

Sanders, J.M., Monogue, M.L., Jodlowski, T.Z., and Cutrell, J.B. (2020). Pharmacologic Treatments for Coronavirus Disease 2019 (COVID-19): A Review. JAMA. Published online April 13, 2020. https://doi.org/10.1001/jama.2020.6019.

Savarino, A., Boelaert, J.R., Cassone, A., Majori, G., and Cauda, R. (2003). Effects of chloroquine on viral infections: an old drug against today's diseases? Lancet Infect. Dis. *3*, 722–727.

Schrezenmeier, E., and Dörner, T. (2020). Mechanisms of action of hydroxychloroquine and chloroquine: implications for rheumatology. Nat. Rev. Rheumatol. *16*, 155–166.

Shamshirian, A., Hessami, A., Heydari, K., Alizadeh-Navaei, R., Ebrahimzadeh, M.A., Ghasemian, R., Aboufazeli, E., Baradaran, H., Karimifar, K., Eftekhari, A., et al. (2020). Hydroxychloroquine Versus COVID-19: A Rapid Systematic Review and Meta-Analysis. medRxiv. https://doi.org/10.1101/2020.04.14.20065276.

Shang, L., Zhao, J., Hu, Y., Du, R., and Cao, B. (2020). On the use of corticosteroids for 2019-nCoV pneumonia. Lancet *395*, 683–684.

Shao, Z., Feng, Y., Zhong, L., Xie, Q., Lei, M., Liu, Z., Wang, C., Ji, J., Li, W., Liu, H., et al. (2020). Clinical Efficacy of Intravenous Immunoglobulin Therapy in Critical Patients with COVID-19: A multicenter retrospective cohort study. medRxiv. https://doi.org/10.1101/2020.04.11.20061739.

Sheahan, T.P., Sims, A.C., Graham, R.L., Menachery, V.D., Gralinski, L.E., Case, J.B., Leist, S.R., Pyrc, K., Feng, J.Y., Trantcheva, I., et al. (2017).). Broad-Spectrum Antiviral GS-5734 Inhibits Both Epidemic and Zoonotic Coronaviruses. Sci. Transl. Med. *9*, eaal3653.

Sheahan, T.P., Sims, A.C., Leist, S.R., Schäfer, A., Won, J., Brown, A.J., Montgomery, S.A., Hogg, A., Babusis, D., Clarke, M.O., et al. (2020). Comparative therapeutic efficacy of remdesivir and combination lopinavir, ritonavir, and interferon beta against MERS-CoV. Nat. Commun. *11*, 222.

Shen, C., Wang, Z., Zhao, F., Yang, Y., Li, J., Yuan, J., Wang, F., Li, D., Yang, M., Xing, L., et al. (2020). Treatment of 5 Critically Ill Patients With COVID-19 With Convalescent Plasma. JAMA *323*, 1582–1589.

Shi, C.-S., Qi, H.-Y., Boularan, C., Huang, N.-N., Abu-Asab, M., Shelhamer, J.H., and Kehrl, J.H. (2014). SARS-coronavirus open reading frame-9b suppresses innate immunity by targeting mitochondria and the MAVS/TRAF3/TRAF6 signalosome. J. Immunol. *193*, 3080–3089.

Shi, C.-S., Nabar, N.R., Huang, N.N., and Kehrl, J.H. (2019). SARS-Coronavirus Open Reading Frame-8b triggers intracellular stress pathways and activates NLRP3 inflammasomes. Cell Death Discov. *5*, 101.

Shi, S., Qin, M., Shen, B., Cai, Y., Liu, T., Yang, F., Gong, W., Liu, X., Liang, J., Zhao, Q., et al. (2020). Association of Cardiac Injury With Mortality in Hospitalized Patients With COVID-19 in Wuhan, China. JAMA Cardiol. Published online March 25, 2020. https://doi.org/10.1001/jamacardio.2020.0950.

Shiow, L.R., Rosen, D.B., Brdicková, N., Xu, Y., An, J., Lanier, L.L., Cyster, J.G., and Matloubian, M. (2006). CD69 acts downstream of interferon-alpha/beta to inhibit S1P1 and lymphocyte egress from lymphoid organs. Nature *440*, 540–544.

Siu, K.L., Kok, K.H., Ng, M.H.J., Poon, V.K.M., Yuen, K.Y., Zheng, B.J., and Jin, D.Y. (2009). Severe acute respiratory syndrome coronavirus M protein inhibits type I interferon production by impeding the formation of TRAF3.-TANK.TBK1/IKKepsilon complex. J. Biol. Chem. *284*, 16202–16209.

Siu, K.L., Yeung, M.L., Kok, K.H., Yuen, K.S., Kew, C., Lui, P.Y., Chan, C.P., Tse, H., Woo, P.C.Y., Yuen, K.Y., and Jin, D.Y. (2014). Middle east respiratory syndrome coronavirus 4a protein is a double-stranded RNA-binding protein that suppresses PACT-induced activation of RIG-I and MDA5 in the innate antiviral response. J. Virol. *88*, 4866–4876.

Siu, K.L., Yuen, K.S., Castaño-Rodriguez, C., Ye, Z.W., Yeung, M.L., Fung, S.Y., Yuan, S., Chan, C.P., Yuen, K.Y., Enjuanes, L., and Jin, D.Y. (2019). Severe acute respiratory syndrome coronavirus ORF3a protein activates the NLRP3 inflammasome by promoting TRAF3-dependent ubiquitination of ASC. FASEB J. *33*, 8865–8877.

Vivier, E., Artis, D., Colonna, M., Diefenbach, A., Di Santo, J.P., Eberl, G., Koyasu, S., Locksley, R.M., McKenzie, A.N.J., Mebius, R.E., et al. (2018). Innate Lymphoid Cells: 10 Years On. Cell *174*, 1054–1066.

Von Holle, T.A., and Moody, M.A. (2019). Influenza and Antibody-Dependent Cellular Cytotoxicity. Front. Immunol. *10*, 1457.

Walls, A.C., Park, Y.-J., Tortorici, M.A., Wall, A., McGuire, A.T., and Veesler, D. (2020). Structure, Function, and Antigenicity of the SARS-CoV-2 Spike Glycoprotein. Cell *181*, 281–292.e6.

Walter, J.M., Helmin, K.A., Abdala-Valencia, H., Wunderink, R.G., and Singer, B.D. (2018). Multidimensional assessment of alveolar T cells in critically ill patients. JCI Insight *3*, e123287.

Wan, S., Yi, Q., Fan, S., Lv, J., Zhang, X., Guo, L., Lang, C., Xiao, Q., Xiao, K., Yi, Z., et al. (2020a). Characteristics of lymphocyte subsets and cytokines in peripheral blood of 123 hospitalized patients with 2019 novel coronavirus pneumonia (NCP). medRxiv. https://doi.org/10.1101/2020.02.10.20021832.

Wan, Y., Shang, J., Graham, R., Baric, R.S., and Li, F. (2020b). Receptor Recognition by the Novel Coronavirus from Wuhan: an Analysis Based on Decade-Long Structural Studies of SARS Coronavirus. J. Virol. *94*, e00127-20, https://doi.org/10.1128/JVI.00127-20.

Wan, Y., Shang, J., Sun, S., Tai, W., Chen, J., Geng, Q., He, L., Chen, Y., Wu, J., Shi, Z., et al. (2020c). Molecular Mechanism for Antibody-Dependent Enhancement of Coronavirus Entry. J. Virol. *94*, e02015–e02019.

Wang, L. (2020). C-reactive Protein Levels in the Early Stage of COVID-19. Med. Mal. Infect. Published online March 31, 2020. https://doi.org/10.1016/j.medmal.2020.03.007.

Wang, C.-H., Liu, C.-Y., Wan, Y.-L., Chou, C.-L., Huang, K.-H., Lin, H.-C., Lin, S.-M., Lin, T.-Y., Chung, K.F., and Kuo, H.-P. (2005). Persistence of lung inflammation and lung cytokines with high-resolution CT abnormalities during recovery from SARS. Respir. Res. *6*, 42.

Wang, S.F., Chen, K.H., Chen, M., Li, W.Y., Chen, Y.J., Tsao, C.H., Yen, M.Y., Huang, J.C., and Chen, Y.M. (2011). Human-leukocyte antigen class I Cw 1502 and class II DR 0301 genotypes are associated with resistance to severe acute respiratory syndrome (SARS) infection. Viral Immunol. *24*, 421–426.

Wang, C., Li, W., Drabek, D., Okba, N.M.A., van Haperen, R., Osterhaus, A.D.M.E., van Kuppeveld, F.J.M., Haagmans, B.L., Grosveld, F., and Bosch, B.-J. (2020a). A human monoclonal antibody blocking SARS-CoV-2 infection. Nat. Commun. Published online May 4, 2020. https://doi.org/10.1038/s41467-020-16256-y.

Wang, D., Hu, B., Hu, C., Zhu, F., Liu, X., Zhang, J., Wang, B., Xiang, H., Cheng, Z., Xiong, Y., et al. (2020b). Clinical Characteristics of 138 Hospitalized Patients With 2019 Novel Coronavirus-Infected Pneumonia in Wuhan (China: JAMA).

Wang, D., Wang, J., Jiang, Q., Yang, J., Li, J., Gao, C., Jiang, H., Ge, L., and Liu, Y. (2020c). No Clear Benefit to the Use of Corticosteroid as Treatment in Adult Patients with Coronavirus Disease 2019: A Retrospective Cohort Study. medRxiv. https://doi.org/10.1101/2020.04.21.20066258.

Wang, F., Nie, J., Wang, H., Zhao, Q., Xiong, Y., Deng, L., Song, S., Ma, Z., Mo, P., and Zhang, Y. (2020d). Characteristics of peripheral lymphocyte subset alteration in COVID-19 pneumonia. J. Infect. Dis. *221*, 1762–1769, https://doi.org/10.1093/infdis/jiaa150.

Wang, M., Cao, R., Zhang, L., Yang, X., Liu, J., Xu, M., Shi, Z., Hu, Z., Zhong, W., and Xiao, G. (2020e). Remdesivir and chloroquine effectively inhibit the recently emerged novel coronavirus (2019-nCoV) in vitro. Cell Res. *30*, 269–271.

Wang, W., He, J., Lie, P., Huang, L., Wu, S., Lin, Y., and Liu, X. (2020f). The definition and risks of Cytokine Release Syndrome-Like in 11 COVID-19-Infected Pneumonia critically ill patients: Disease Characteristics and Retrospective Analysis. medRxiv. https://doi.org/10.1101/2020.02.26.20026989.

Wang, Y., Zhang, D., Du, G., Du, R., Zhao, J., Jin, Y., Fu, S., Gao, L., Cheng, Z., Lu, Q., et al. (2020g). Remdesivir in adults with severe COVID-19: a randomised, double-blind, placebo-controlled, multicentre trial. Lancet. Published online April 29, 2020. https://doi.org/10.1016/S0140-6736(20)31022-9.

Wang, Y., Jiang, W., He, Q., Wang, C., Wang, B., Zhou, P., Dong, N., and Tong, Q. (2020h). Early, low-dose and short-term application of corticosteroid treatment in patients with severe COVID-19 pneumonia: single-center experience from Wuhan, China. medRxiv. https://doi.org/10.1101/2020.03.06.20032342.

Wathelet, M.G., Orr, M., Frieman, M.B., and Baric, R.S. (2007). Severe acute respiratory syndrome coronavirus evades antiviral signaling: role of nsp1 and rational design of an attenuated strain. J. Virol. *81*, 11620–11633.

Weiskopf, D., Schmitz, K.S., Raadsen, M.P., Grifoni, A., Okba, N.M.A., Endeman, H., van den Akker, J.P.C., Molenkamp, R., Koopmans, M.P.G., van Gorp, E.C.M., et al. (2020). Phenotype of SARS-CoV-2-specific T-cells in COVID-19 patients with acute respiratory distress syndrome. medRxiv. https://doi.org/10.1101/2020.04.11.20062349.

Wen, W., Su, W., Tang, H., Le, W., Zhang, X., Zheng, Y., Liu, X., Xie, L., Li, J., Ye, J., et al. (2020). Immune cell profiling of COVID-19 patients in the recovery stage by single-cell sequencing. Cell Discov. Published online May 4, 2020. https://doi.org/10.1038/s41421-020-0168-9.

Wilk, A.J., Rustagi, A., Zhao, N.Q., Roque, J., Martinez-Colon, G.J., McKechnie, J.L., Ivison, G.T., Ranganath, T., Vergara, R., Hollis, T., et al. (2020). A single-cell atlas of the peripheral immune response to severe COVID-19. medRxiv. https://doi.org/10.1101/2020.04.17.20069930.

Williamson, B., Feldmann, F., Schwarz, B., Meade-White, K., Porter, D., Schulz, J., van Doremalen, N., Leighton, I., Yinda, C.K., Perez-Perez, L., et al. (2020). Clinical benefit of remdesivir in rhesus macaques infected with SARS-CoV-2. bioRxiv. https://doi.org/10.1101/2020.04.15.043166.

Wölfel, R., Corman, V.M., Guggemos, W., Seilmaier, M., Zange, S., Müller, M.A., Niemeyer, D., Jones, T.C., Vollmar, P., Rothe, C., et al. (2020). Virological assessment of hospitalized patients with COVID-2019. Nature. Published online April 1, 2020. https://doi.org/10.1038/s41586-020-2196-x.

Wong, C.K., Lam, C.W.K., Wu, A.K.L., Ip, W.K., Lee, N.L.S., Chan, I.H.S., Lit, L.C.W., Hui, D.S.C., Chan, M.H.M., Chung, S.S.C., and Sung, J.J. (2004). Plasma inflammatory cytokines and chemokines in severe acute respiratory syndrome. Clin. Exp. Immunol. *136*, 95–103.

World Health Organization (2020a). Clinical management of severe acute respiratory infection (SARI) when COVID-19 disease is suspected: Interim Guidance. https://www.who.int/publications-detail/clinical-management-of-severe-acute-respiratory-infection-when-novel-coronavirus-(ncov)-infection-is-suspected.

World Health Organization (2020b). Draft of the landscape of COVID-19 candidate vaccines. https://www.who.int/who-documents-detail/draft-landscape-of-covid-19-candidate-vaccines.

Wrapp, D., De Vlieger, D., Corbett, K.S., Torres, G.M., Wang, N., Van Breedam, W., Roose, K., van Schie, L., Hoffmann, M., Pöhlmann, S., et al.; VIB-CMB COVID-19 Response Team (2020). Structural Basis for Potent Neutralization of Betacoronaviruses by Single-Domain Camelid Antibodies. Cell *181*. Published online May 5, 2020. https://doi.org/10.1016/j.cell.2020.04.031.

Wu, C., Chen, X., Cai, Y., Xia, J., Zhou, X., Xu, S., Huang, H., Zhang, L., Zhou, X., Du, C., et al. (2020a). Risk Factors Associated With Acute Respiratory Distress Syndrome and Death in Patients With Coronavirus Disease 2019 Pneumonia in Wuhan, China. JAMA Intern. Med. Published online March 13, 2020. https://doi.org/10.1001/jamainternmed.2020.0994.

Wu, F., Wang, A., Liu, M., Wang, Q., Chen, J., Xia, S., Ling, Y., Zhang, Y., Xun, J., Lu, L., et al. (2020b). Neutralizing antibody responses to SARS-CoV-2 in a COVID-19 recovered patient cohort and their implications. medRxiv. https://doi.org/10.1101/2020.03.30.20047365.

Wu, Y., Li, C., Xia, S., Tian, X., Kong, Y., Wang, Z., Gu, C., Zhang, R., Tu, C., Xie, Y., et al. (2020c). Identification of Human Single-Domain Antibodies against SARS-CoV-2. Cell Host Microbe. Published online May 14, 2020. https://doi.org/10.1016/j.chom.2020.04.023.

Wynants, L., Van Calster, B., Bonten, M.M.J., Collins, G.S., Debray, T.P.A., De Vos, M., Haller, M.C., Heinze, G., Moons, K.G.M., Riley, R.D., et al. (2020). Prediction models for diagnosis and prognosis of covid-19 infection: systematic review and critical appraisal. BMJ *369*, m1328.

Xia, C.Q., Xu, L.L., Wang, Z., Qin, Z.Q., Tong, Z.H., Huang, K.W., Xiao, B., Qi, M., Jiang, B.Z., Wang, C., et al. (2004). The involvement of natural killer cells in the pathogenesis of severe acute respiratory syndrome. Am. J. Clin. Pathol. *121*, 507–511.

Xiang, J., Wen, J., Yuan, X., Xiong, S., Zhou, Xue., Liu, C., and Min, Xun. (2020a). Potential biochemical markers to identify severe cases among COVID-19 patients. medRxiv. https://doi.org/10.1101/2020.03.19.20034447.

Xiang, J., Yan, M., Li, H., Liu, T., Lin, C., Huang, S., and Shen, C. (2020b). Evaluation of Enzyme-Linked Immunoassay and Colloidal Gold- Immunochromatographic Assay Kit for Detection of Novel Coronavirus (SARS-Cov-2) Causing an Outbreak of Pneumonia (COVID-19). medRxiv. https://doi.org/10.1101/2020.02.27.20028787.

Xiong, R., Zhang, L., Li, S., Sun, Y., Ding, M., Wang, Y., Zhao, Y., Wu, Y., Shang, W., Jiang, X., et al. (2020). Novel and potent inhibitors targeting DHODH, a rate-limiting enzyme in *de novo* pyrimidine biosynthesis, are broad-spectrum antiviral against RNA viruses including newly emerged coronavirus SARS-CoV-2. bioRxiv. https://doi.org/10.1101/2020.03.11.983056.

Xu, H., Hou, K., Xu, H., Li, Z., Chen, H., Zhang, N., Xu, R., Fu, H., Sun, R., Wen, L., et al. (2020a). Acute Myocardial Injury of Patients with Coronavirus Disease 2019. medRxiv. https://doi.org/10.1101/2020.03.05.20031591.

Xu, X., Han, M., Li, T., Sun, W., Wang, D., Fu, B., Zhou, Y., Zheng, X., Yang, Y., Li, X., et al. (2020b). Effective treatment of severe COVID-19 patients with tocilizumab. Proc. Natl. Acad. Sci. USA. 202005615. Published online April 29, 2020. https://doi.org/10.1073/pnas.2005615117.

Xu, Z., Shi, L., Wang, Y., Zhang, J., Huang, L., Zhang, C., Liu, S., Zhao, P., Liu, H., Zhu, L., et al. (2020c). Pathological findings of COVID-19 associated with acute respiratory distress syndrome. Lancet Respir. Med. *8*, 420–422.

Yamamoto, N., Matsuyama, S., Hoshino, T., and Yamamoto, N. (2020). Nelfinavir inhibits replication of severe acute respiratory syndrome coronavirus 2 *in vitro*. bioRxiv. https://doi.org/10.1101/2020.04.06.026476.

Yan, D., Liu, X.-Y., Zhu, Y.-n., Huang, L., Dan, B.-t., Zhang, G.-j., and Gao, Y.-h. (2020a). Factors associated with prolonged viral shedding and impact of Lopinavir/Ritonavir treatment in patients with SARS-CoV-2 infection. Eur. Respir. J. Published online May 19, 2020. https://doi.org/10.1183/13993003.00799-2020.

Yan, L., Zhang, H.-T., Xiao, Y., Wang, M., Sun, C., Liang, J., Li, S., Zhang, M., Guo, Y., Xiao, Y., et al. (2020b). Prediction of criticality in patients with severe Covid-19 infection using three clinical features: a machine learning-based prognostic model with clinical data in Wuhan. medRxiv. https://doi.org/10.1101/2020.02.27.20028027.

Yang, Y., Ye, F., Zhu, N., Wang, W., Deng, Y., Zhao, Z., and Tan, W. (2015). Middle East respiratory syndrome coronavirus ORF4b protein inhibits type I interferon production through both cytoplasmic and nuclear targets. Sci. Rep. *5*, 17554.

Yang, X., Dai, T., Zhou, X., Qian, H., Guo, R., Lei, L., Zhang, X., Zhang, D., Shi, L., Cheng, Y., et al. (2020a). Analysis of adaptive immune cell populations and phenotypes in the patients infected by SARS-CoV-2. medRxiv. https://doi.org/10.1101/2020.03.23.20040675.

Yang, Y., Shen, C., Li, J., Yuan, J., Wei, J., Huang, F., Wang, F., Li, G., Li, Y., Xing, L., et al. (2020b). Plasma IP-10 and MCP-3 levels are highly associated with disease severity and predict the progression of COVID-19. J. Allergy Clin. Immunol. Published online April 29, 2020. https://doi.org/10.1016/j.jaci.2020.04.027.

Yang, Z., Liu, J., Zhou, Y., Zhao, X., Zhao, Q., and Liu, J. (2020c). The effect of corticosteroid treatment on patients with coronavirus infection: a systematic review and meta-analysis. J. Infect. S0163-4453(20)30191-2. https://doi.org/10.1016/j.jinf.2020.03.062.

Yao, X., Ye, F., Zhang, M., Cui, C., Huang, B., Niu, P., Liu, X., Zhao, L., Dong, E., Song, C., et al. (2020a). In Vitro Antiviral Activity and Projection of Optimized Dosing Design of Hydroxychloroquine for the Treatment of Severe Acute Respiratory Syndrome Coronavirus 2 (SARS-CoV-2). Clin. Infect. Dis. Published online March 9, 2020. https://doi.org/10.1093/cid/ciaa237.

Yao, X.H., Li, T.Y., He, Z.C., Ping, Y.F., Liu, H.W., Yu, S.C., Mou, H.M., Wang, L.H., Zhang, H.R., Fu, W.J., et al. (2020b). [A pathological report of three COVID-19 cases by minimally invasive autopsies]. Zhonghua Bing Li Xue Za Zhi *49*, E009.

Ying, T., Li, H., Lu, L., Dimitrov, D.S., and Jiang, S. (2015). Development of human neutralizing monoclonal antibodies for prevention and therapy of MERS-CoV infections. Microbes Infect. *17*, 142–148.

Yip, M.S., Leung, N.H.L., Cheung, C.Y., Li, P.H., Lee, H.H.Y., Daëron, M., Peiris, J.S.M., Bruzzone, R., and Jaume, M. (2014). Antibody-dependent infection of human macrophages by severe acute respiratory syndrome coronavirus. Virol. J. *11*, 82.

Yu, L., Tong, Y., Shen, G., Fu, A., Lai, Y., Zhou, X., and Yuan, Y. (2020).). Immunodepletion with Hypoxemia: A Potential High Risk Subtype of Coronavirus Disease 2019. medRxiv. https://doi.org/10.1101/2020.03.03.20030650.

Yuan, M., Wu, N.C., Zhu, X., Lee, C.-C.D., So, R.T.Y., Lv, H., Mok, C.K.P., and Wilson, I.A. (2020). A Highly Conserved Cryptic Epitope in the Receptor Binding Domains of SARS-CoV-2 and SARS-CoV. Science *868*, 630–633.

Yudanin, N.A., Schmitz, F., Flamar, A.-L., Thome, J.J.C., Tait Wojno, E., Moeller, J.B., Schirmer, M., Latorre, I.J., Xavier, R.J., Farber, D.L., et al. (2019). Spatial and Temporal Mapping of Human Innate Lymphoid Cells Reveals Elements of Tissue Specificity. Immunity *50*, 505–519.e4.

Zeng, Q., Li, Y.-Z., Huang, G., Wu, W., Dong, S.-Y., and Xu, Y. (2020). Mortality of COVID-19 is Associated with Cellular Immune Function Compared to Immune Function in Chinese Han Population. medRxiv. https://doi.org/10.1101/2020.03.08.20031229.

Zha, L., Li, S., Pan, L., Tefsen, B., Li, Y., French, N., Chen, L., Yang, G., and Villanueva, E.V. (2020). Corticosteroid Treatment of Patients with Coronavirus Disease 2019 (COVID-19). Med. J. Aust. Published online April 8, 2020. https://doi.org/10.5694/mja2.50577.

Zhang, L., Zhang, F., Yu, W., He, T., Yu, J., Yi, C.E., Ba, L., Li, W., Farzan, M., Chen, Z., et al. (2006). Antibody responses against SARS coronavirus are correlated with disease outcome of infected individuals. J. Med. Virol. *78*, 1–8.

Zhang, B., Zhou, X., Zhu, C., Feng, F., Qiu, Y., Feng, J., Jia, Q., Song, Q., Zhu, B., and Wang, J. (2020a). Immune phenotyping based on neutrophil-to-lymphocyte ratio and IgG predicts disease severity and outcome for patients with COVID-19. medRxiv. https://doi.org/10.1101/2020.03.12.20035048.

Zhang, B., Liu, S., Tan, T., Huang, W., Dong, Y., Chen, L., Chen, Q., Zhang, L., Zhong, Q., Zhang, X., et al. (2020b). Treatment With Convalescent Plasma for Critically Ill Patients With SARS-CoV-2 Infection. Chest. Published online March 31, 2020. https://doi.org/10.1016/j.chest.2020.03.039.

Zhang, D., Guo, R., Lei, L., Liu, H., Wang, Y., Wang, Y., Dai, T., Zhang, T., Lai, Y., Wang, J., et al. (2020c). COVID-19 infection induces readily detectable morphological and inflammation-related phenotypic changes in peripheral blood monocytes, the severity of which correlate with patient outcome. medRxiv. https://doi.org/10.1101/2020.03.24.20042655.

Zhang, J., Liu, J., Li, N., Liu, Y., Ye, R., Qin, X., and Zheng, R. (2020d). Serological detection of 2019-nCoV respond to the epidemic: A useful complement to nucleic acid testing. medRxiv. https://doi.org/10.1101/2020.03.04.20030916.

Zhao, J., Zhao, J., Van Rooijen, N., and Perlman, S. (2009). Evasion by stealth: inefficient immune activation underlies poor T cell response and severe disease in SARS-CoV-infected mice. PLoS Pathog. *5*, e1000636.

Zhao, K., Wang, H., and Wu, C. (2011). The immune responses of HLA-A*0201 restricted SARS-CoV S peptide-specific CD8$^+$ T cells are augmented in varying degrees by CpG ODN, PolyI:C and R848. Vaccine *29*, 6670–6678.

Zhao, X., Guo, F., Liu, F., Cuconati, A., Chang, J., Block, T.M., and Guo, J.-T. (2014). Interferon induction of IFITM proteins promotes infection by human coronavirus OC43. Proc. Natl. Acad. Sci. USA *111*, 6756–6761.

Zhao, X., Sehgal, M., Hou, Z., Cheng, J., Shu, S., Wu, S., Guo, F., Le Marchand, S.J., Lin, H., Chang, J., and Guo, J.T. (2018). Identification of Residues Controlling Restriction versus Enhancing Activities of IFITM Proteins on Entry of Human Coronaviruses. J. Virol. *92*, e01535-17.

Zhao, J., Yuan, Q., Wang, H., Liu, W., Liao, X., Su, Y., Wang, X., Yuan, J., Li, T., Li, J., et al. (2020a). Antibody Responses to SARS-CoV-2 in Patients of Novel Coronavirus Disease 2019. Clin. Infect. Dis. Published online March 28, 2020. https://doi.org/10.1093/cid/ciaa344.

Zhao, J., Yang, Y., Huang, H., Li, D., Gu, D., Lu, X., Zhang, Z., Liu, L., Liu, T., Liu, Y., et al. (2020b). Relationship between the ABO Blood Group and the COVID-19 Susceptibility. medRxiv. https://doi.org/10.1101/2020.03.11.20031096.

Zhao, X., Zheng, S., Chen, D., Zheng, M., Li, X., Li, G., Lin, H., Chang, J., Zeng, H., and Guo, J.-T. (2020c). LY6E Restricts the Entry of Human Coronaviruses, including the currently pandemic SARS-CoV-2. bioRxiv. https://doi.org/10.1101/2020.04.02.021469.

Zhao, X., Zhang, B., Li, P., Ma, C., Gu, J., Hou, P., Guo, Z., Wu, H., and Bai, Y. (2020d). Incidence, clinical characteristics and prognostic factor of patients with COVID-19: a systematic review and meta-analysis. medRxiv. https://doi.org/10.1101/2020.03.17.20037572.

Zheng, M., and Song, L. (2020). Novel antibody epitopes dominate the antigenicity of spike glycoprotein in SARS-CoV-2 compared to SARS-CoV. Cell. Mol. Immunol. *17*, 536–538.

Zheng, J., Liu, Y., Lau, Y.L., and Tu, W. (2013). γδ-T cells: an unpolished sword in human anti-infection immunity. Cell. Mol. Immunol. *10*, 50–57.

Zheng, H.-Y., Zhang, M., Yang, C.-X., Zhang, N., Wang, X.-C., Yang, X.-P., Dong, X.-Q., and Zheng, Y.-T. (2020a). Elevated exhaustion levels and reduced functional diversity of T cells in peripheral blood may predict severe progression in COVID-19 patients. Cell. Mol. Immunol. *17*, 541–543.

Zheng, M., Gao, Y., Wang, G., Song, G., Liu, S., Sun, D., Xu, Y., and Tian, Z. (2020b). Functional exhaustion of antiviral lymphocytes in COVID-19 patients. Cell. Mol. Immunol. *17*, 533–535.

Zhou, J., Chu, H., Li, C., Wong, B.H.-Y., Cheng, Z.-S., Poon, V.K.-M., Sun, T., Lau, C.C.-Y., Wong, K.K.-Y., Chan, J.Y.-W., et al. (2014). Active replication of Middle East respiratory syndrome coronavirus and aberrant induction of inflammatory cytokines and chemokines in human macrophages: implications for pathogenesis. J. Infect. Dis. *209*, 1331–1342.

Zhou, Y., Jiang, S., and Du, L. (2018). Prospects for a MERS-CoV spike vaccine. Expert Rev. Vaccines *17*, 677–686.

Zhou, F., Yu, T., Du, R., Fan, G., Liu, Y., Liu, Z., Xiang, J., Wang, Y., Song, B., Gu, X., et al. (2020a). Clinical course and risk factors for mortality of adult inpatients with COVID-19 in Wuhan, China: a retrospective cohort study. Lancet *395*, 1054–1062.

Zhou, Y., Fu, B., Zheng, X., Wang, D., Zhao, C., Qi, Y., Sun, R., Tian, Z., Xu, X., and Wei, H. (2020b). Aberrant pathogenic GM-CSF+ T cells and inflammatory CD14+CD16+ monocytes in severe pulmonary syndrome patients of a new coronavirus. bioRxiv. https://doi.org/10.1101/2020.02.12.945576.

Zhou, Y., Fu, B., Zheng, X., Wang, D., Zhao, C., Qi, Y., Sun, R., Tian, Z., Xu, X., and Wei, H. (2020c). Pathogenic T cells and inflammatory monocytes incite inflammatory storm in severe COVID-19 patients. Natl. Sci. Rev. Published online March 13, 2020. https://doi.org/10.1093/nsr/nwaa041.

Zhou, Y., Yang, Z., Guo, Y., Geng, S., Gao, S., Ye, S., Hu, Y., and Wang, Y. (2020d). A New Predictor of Disease Severity in Patients with COVID-19 in Wuhan, China. medRxiv. https://doi.org/10.1101/2020.03.24.20042119.

Zhu, Z., Chakraborti, S., He, Y., Roberts, A., Sheahan, T., Xiao, X., Hensley, L.E., Prabakaran, P., Rockx, B., Sidorov, I.A., et al. (2007). Potent cross-reactive neutralization of SARS coronavirus isolates by human monoclonal antibodies. Proc. Natl. Acad. Sci. USA *104*, 12123–12128.

Zhu, F.C., Hou, L.H., Li, J.X., Wu, S.P., Liu, P., Zhang, G.R., Hu, Y.M., Meng, F.Y., Xu, J.J., Tang, R., et al. (2015). Safety and immunogenicity of a novel recombinant adenovirus type-5 vector-based Ebola vaccine in healthy adults in China: preliminary report of a randomised, double-blind, placebo-controlled, phase 1 trial. Lancet *385*, 2272–2279.

Zhu, F.-C., Wurie, A.H., Hou, L.-H., Liang, Q., Li, Y.-H., Russell, J.B.W., Wu, S.-P., Li, J.-X., Hu, Y.-M., Guo, Q., et al. (2017). Safety and immunogenicity of a recombinant adenovirus type-5 vector-based Ebola vaccine in healthy adults in Sierra Leone: a single-centre, randomised, double-blind, placebo-controlled, phase 2 trial. Lancet *389*, 621–628.

Ziegler, C.J.K., Allon, S.J., Nyquist, S.K., Mbano, I.M., Miao, V.N., Tzouanas, C.N., Cao, Y., Yousif, A.S., Bals, J., Hauser, B.M., et al. (2020). SARS-CoV-2 Receptor ACE2 Is an Interferon-Stimulated Gene in Human Airway Epithelial Cells and Is Detected in Specific Cell Subsets Across Tissues. Cell. Published online April 27, 2020. https://doi.org/10.1016/j.cell.2020.04.035.

Zietz, M., and Tatonetti, N.P. (2020). Testing the association between blood type and COVID-19 infection, intubation, and death. medRxiv. https://doi.org/10.1101/2020.04.08.20058073.

APPENDIX 6

EMMA RISSON

ETUDIANTE MEDECINE-SCIENCES

3ème ANNEE DE DOCTORAT EN CANCEROLOGIE

emma.risson@gmail.com
06 02 36 55 95

PARCOURS SCIENTIFIQUE & MEDICAL

2019-2022 — Doctorat en cancérologie - **Régulation de la dormance de cellules de cancer du sein disséminées dans la moelle osseuse par TGFB2 et BMP4**
CRCL | Université de Lyon | ED BMIC | France
Mount Sinai | New York City | Etats-Unis
Sous la supervision de **Véronique Maguer-Satta** & **Julio Aguirre-Ghiso**
Collaboration internationale : 50% de la thèse au Mount Sinai Hospital, NYC

Jan-Aout 2019 — Stage M2 Recherche – **Rôle fonctionnel des cellules souches mésenchymateuses de la moelle osseuse dans la régulation de la dormance des cancers solides**
Mount Sinai Hospital | USA
Sous la supervision de **Julio Aguirre-Ghiso**

Avril-Juin 2018 — Stage M1 Recherche – **Simulation d'expérience *in silico* pour l'inférence de réseaux de régulation de gènes**
LBMC | ENS Lyon | France
Sous la supervision d'**Olivier Gandrillon**
Programmation Python, SQL, R

2016-18 — **Stages Cliniques**
Hématologie & Pneumologie médical
Hospices Civils de Lyon | France

PUBLICATIONS

Risson E, Moindrot L, ..., Aguirre-Ghiso JA, Maguer-Satta V : **Control of breast disseminated tumor cell dormancy in the bone marrow by TGFB2 and BMP4 signaling**. *In preparation*, 2022

Nobre AR , ... , **Risson E**, ..., Aguirre-Ghiso JA : **Single-cell analysis of early disseminated cancer cells identifies ZFP281 and a mesenchymal-like dormancy program as a barrier to metastasis.** *Under review, Nature Cell Biology 2022*

Nobre AR, **Risson E**, ..., Aguirre-Ghiso JA : **Bone marrow NG2+/Nestin + mesenchymal stem cells drive DTC dormancy via TGF-β2**. *Nature Cancer* 2021, doi:10.1038/s43018-021-00179-8.

Risson E, Nobre AR, Maguer-Satta V, Aguirre-Ghiso JA: **The current paradigm and challenges ahead for the dormancy of disseminated tumor cells**. *Nature Cancer* 2020, **1**:672–680. doi: 10.1038/s43018-020-0088-5

Vabret N., ..., **Risson E.**, ..., Merad M., Samstein R.M., The Sinai Immunology Review Project, et al. : **Immunology of COVID-19: Current State of the Science**. *Immunity* 2020, **52**:910–941. doi: 10.1016/j.immuni.2020.05.002

FORMATION

2017-19 — **Licence & Master Biosciences**
Ecole Normale Supérieure de Lyon
Double cursus Médecine-Sciences
Rang Master 2 : 2ème/8

Depuis 2017 — **Ecole de l'INSERM Liliane Bettencourt**
Formation scientifique précoce
Double cursus Médecine-Sciences
Rang national d'admission : 1ère/60

2015-18 — **Premier cycle études médicales**
Faculté Médecine Lyon-Est
FGSM2 & FGSM3
Concours PACES : 13ème/2000

OBTENTION FINANCEMENT

International Research Project INSERM (2022-2027) : rédaction complète du dossier de financement, 75 000€ obtenu pour la continuation de la collaboration international initiée par mon projet de thèse.
Bourse mobilité CLARA (2020)
Bourse mobilité IDEX (2020)
Bourse doctorale Université de Lyon (Contrat doctoral, 2019-2022)
Bourse double cursus médecine-sciences ENS Lyon (2017-2019)

CONGRES

Juin 2022. **28ème Congrès European Association for Cancer Research.** Séville, Espagne – Poster

Mai 2022. **4th Conference on Stem Cell, Development & Cancer.** Lyon, France – Présentation orale

Février 2022. ***5th*** **Symposium Cancer International** Lyon, France – Poster *Reporté à Novembre 2022 (COVID)*

Décembre 2021. ***6ème*** **Congrès GDR 3697 Micronit**, En ligne – Présentation orale

Juin 2021. **28ème Congrès European Association for Cancer Research** En ligne – Poster

Septembre 2020. Congrès **Systemic Effects of Metastasis** New York Academy Science – Poster *Annulation (COVID)*

Mars 2020. **Retraite du Département de Biologie du Cancer** Mount Sinai Hospital – Poster *Annulation (COVID)*

MEDIATION SCIENTIFIQUE & IMPLICATION

- CovidoErgoSum (2021) : réalisation de vidéos de vulgarisation sur la vaccination anti-COVID19 à destination du grand public (diffusion sur les réseaux sociaux)
Ex : https://bit.ly/3r9PA4J . Soutien logistique et financier de la Faculté de Médecine Lyon-Est, les Hospices Civils de Lyon, la Mairie de Lyon et le groupe Apicil. Collaboration avec étudiants de l'école Emile Cohl pour les animations

- Sinai Immunology Review Projet (2020) **:** participation à l'évaluation de la qualité des articles non vérifiés par les pairs postés sur BioRxiv et MedRxiv afin de faire avancer les connaissances scientifiques pendant la pandémie.
Publication de plus de 10 évaluations d'articles dans BioRxiv et MedRxiv
Publication d'un résumé d'article dans Nature Reviews Immunology (PMID : 32355330)

- Rédaction d'une revue sur la physiopathologie du SARS-CoV-2 (2020) **:** leader étudiante sur la partie «Anticorps monoclonaux» - Département d'immunologie Mount Sinai
Publication dans Immunity, citée plus de 1000 fois (PMID : 32505227)

- Fête de la Science (2018) **:** animation jeux de société sur la vaccination pour classes de primaire-collège

- Chargé du comité d'organisation de la "Journée de la Recherche" (2018) : Faculté de Médecine Lyon-Est, ayant pour but de mettre en relation les scientifiques et les médecins pour améliorer la prise en charge des patients.
Conférenciers invités : Alain Fischer, Yehezkel Ben-Ari et Véronique Maguer-Satta

- Élue étudiante au Département de Biologie Humaine
Université Claude Bernard Lyon 1 (2017)

ENSEIGNEMENT *Passionnée d'enseignement & de mentorat*

Chargée de TD Biostatistiques - UCBL1
L2 Science de la Vie – UCBL1 – 30 élèves (25h, 2022)

Enseignante Biostastiques - MédiPlus
Pour étudiants en PASS – 60 élèves (36h, 2021/22)

Cours de Lecture Critique d'Articles - EDILB
Pour double cursus médecine/sciences (6h, 2021)

Tutorat MEDEA - Faculté Lyon-Est
Accompagnement étudiants double cursus (depuis 2017)

Tutrice Biologie Cellulaire - Agora PACES
Pour étudiants en PACES (2016/17)

Cours particuliers Physique & Biostatistiques
Pour étudiants en PACES (depuis 2016)

ENGAGEMENT CITOYEN

Bénévole « Médecin du Monde »
sur la mission Maraude & Bus à Lyon (depuis 2021)
Formations « Premiers secours en santé mentale », « Réduction des risques pour usagers de drogues », « Orientation sociale et droits des étrangers en France »

Club Alpin Français Lyon Villeurbanne
Commission escalade

Bénévole AFS Vivre sans Frontières
Association pour séjours longs de lycéens à l'étranger dans des familles d'accueil (2013-15)
Après séjour d'un an en Argentine (Sampacho, Cordoba, 2012-13), j'ai organisé et animé des weekends de préparation au départ pour lycéens

EXPERTISE

Leadership – Management

- Formation "Managériales" – Université de Lyon
- Management de 2 ingénieures d'étude – pour mon projet de thèse : management d'équipe pour l'avancement du projet
- Encadrement de 2 étudiants : BAC+2 et BAC+4
- Formation « Science Policy & Diplomacy » - New York University

Langues

- Anglais C2 – 6 mois Angleterre 2006 (CM2, association ALLEF) + 2 ans USA (Master/Thèse)
- Espagnol B2 – 1 an Argentine 2012 (Lycée, association AFS)
- Allemand B1

Bioinformatique

Bulk & Single-Cell RNAseq – RStudio et Python
Logiciels – Inkscape, ImageJ, Prism, Flowjo

Techniques

- Manipulation de la souris : maintien de colonies, anesthésie, injections intrapéritonéales, injections mammaires
- Cytométrie en flux : analyse et tri cellulaire
- Biologie cellulaire : culture de cellules tumorales diverses, culture 3D organoïdes transduction rétrovirale, transfection
- Biologie moléculaire : WB, RT-qPCR
- Microscopie : confocal, épifluorescence

ABSTRACT

The bone marrow is one of the primary breast cancer metastatic sites, and detecting dormant cancer cells in this organ is associated with a poor prognosis. Indeed, upon awakening, dormant disseminated cancer cells underlie metastatic relapse in breast cancer patients in remission. Current treatments are developed based on primary tumor characteristics and do not target dormant disseminated cancer cells. Therefore, understanding how the bone marrow microenvironment support cancer cell dormancy is essential. The bone marrow niche is a complex microenvironment with many signals regulating hematopoietic stem cell quiescence and also controlling cancer cell dormancy. Here, we investigated the role of two major factors of the bone marrow, BMP4, and TGFβ2, in regulating cancer cell dormancy. We observed that TGFβ2 and BMP4 synergistically induce dormancy in both normal and transformed human mammary stem cells. Several assays showed that co-exposure to TGFβ2 and BMP4 had a stronger anti-proliferative effect than each ligand alone, putting cancer cells in a deep dormant stage. Moreover, functional assays revealed the heterogeneity of the G0 compartment, and single-cell RNAseq analysis identified a unique deep dormant signature. Lastly, our data suggest that the local BMP4 levels decrease with tissue aging and can therefore contribute to dormant cell awakening. These cues could be potential biomarkers to monitor the risk of awakening in patients in remission. Ultimately, our results open opportunities to prevent cancer relapse in patients by better understanding cancer dormancy regulation by TGFβ and BMP signaling in the bone marrow.

Keywords: TGFβ, BMP, Cancer, Breast, Cancer Stem Cell, Bone Marrow, Metastases, Dormancy

RÉSUMÉ

La moelle osseuse est un des lieux majeurs de métastases de cancer du sein. La détection de cellules dormantes disséminées dans cet organe est associée à un mauvais pronostic. En effet, le réveil des cellules cancéreuses engendre la rechute métastatique chez les patients en rémission. Les traitements actuels sont développés à partir des caractéristiques de la tumeur primaire, qui ne ciblent pas les cellules cancéreuses dormantes disséminées. Il est donc essentiel de mieux comprendre comment le microenvironnement de la moelle osseuse régule la dormance des cellules cancéreuses. C'est en effet un microenvironnement complexe qui régule la quiescence des cellules souches hématopoïétiques. Nous avons interrogé le rôle de deux cytokines majeurs du microenvironnement médullaire, TGFβ2 et BMP4, dans la régulation de la dormance. Nous avons observé qu'ils ont un effet synergique d'induction de dormance. En effet, nous avons démontré que la co-exposition de TGFβ2 et BMP4 avait un effet pro-quiescence beaucoup plus important que l'exposition aux cytokines seules. De plus, des expériences fonctionnelles nous ont permis de démontrer l'hétérogénéité du compartiment G0, et du séquençage transcriptomique à l'échelle de la cellule unique nous a permis d'identifier une signature spécifique aux cellules cancéreuses en dormance profonde. Nos données révèlent également que les niveaux de BMP4 diminuent avec l'âge dans les moelles osseuses normales, ce qui pourrait contribuer au réveil des cellules dormantes. Ces cytokines pourraient donc être des biomarqueurs permettant de prédire le risque de rechutes des patients. Nos résultats ouvrent donc des opportunités pour prévenir et traiter les rechutes des patients en permettant une meilleure compréhension de la régulation de la dormance des cellules cancéreuses dans la moelle osseuse par la voie TGFβ et BMP.

Mots-clés: TGFβ, BMP, Cancer, Sein, Cellule Souche Cancéreuse, Moelle osseuse, Métastases, Dormance.